SUPPRESSION OF THE T-CELL DEPENDENT HUMORAL IMMUNE RESPONSE BY Δ^9 -TETRAHYDROCANNANBINOL INVOLVES INPAIRMENT OF CD40-CD40 LIGAND INTERACTION

By

Thitirat Ngaotepprutaram

A DISSERTATION

Submitted to
Michigan State University
in partial fulfillment of the requirements
for the degree of

Pharmacology & Toxicology-Environmental Toxicology-Doctor of Philosophy

ABSTRACT

SUPPRESSION OF THE T-CELL DEPENDENT HUMORAL IMMUNE RESPONSE BY Δ^9 -TETRAHYDROCANNANBINOL INVOLVES IMPAIRMENT OF CD40-CD40 LIGAND INTERACTION

By

Thitirat Ngaotepprutaram

 Δ^9 -tetrahydrocannabinol (Δ^9 -THC), the main psychoactive congener in marijuana. modulates a variety of immunological responses, of which humoral immune responses against T cell antigens are particularly sensitive to suppression by Δ^9 -THC. Among different types of contact-mediated B cell activation, the CD40-CD40L interaction between B cells and activated CD4⁺ T cells plays an important role in all stages involved in plasma cell differentiation. Thus, the hypothesis tested in this dissertation research is that Δ^9 -THC attenuates the human T celldependent IgM antibody response by suppression of CD40L upregulation in activated CD4+ T cells and impairment of the CD40-mediated B cell activation. These studies showed that Δ^9 -THC significantly impaired the upregulation of surface CD40L on mouse splenic CD4⁺ T cells activated by anti-CD3/CD28, but not by phorbol ester plus calcium ionophore (PMA/Io). Further, suppression of anti-CD3/CD28-induced CD40L expression in mouse splenic CD4 $^+$ T cells by Δ^9 -THC likely occurred at the transcriptional level, independently of cannabinoid

receptor (CB) 1, CB2 or the glucocorticoid receptor. Mechanistically, Δ⁹-THC suppressed anti-CD3/CD28-induced DNA binding activity of NFAT and NFkB, two transcription factors critical is involved in the upregulation of CD40L in activated human CD4⁺ T cells. The inhibitory effect of Δ^9 -THC on the activation of NFAT and NFkB in primary human CD4+T cells also involved impairment of Ca²⁺ elevation without perturbation of proximal T cell receptor signaling events. Additional findings using an in vitro T cell-dependent antibody response model to induce B cell responses showed that Δ^9 -THC significantly decreased the number of IgM secreting cells, which correlated with the impairment of plasma cell differentiation as evidenced by suppression of immunoglobulin joining chain (IgJ) mRNA expression, B cell activation, and proliferation of activated B cells. Moreover, pretreatment with Δ^9 -THC was accompanied by a robust decrease of STAT3 phosphorylation, whereas the phosphorylation of p65 NFkB subunit was not affected in activated B cells. Collectively, this dissertation research demonstrated that Δ^9 -THC exhibits stimulation- and/or cell type-specific selectivity of NFkB inhibition, and identified several aspects of the multi-faceted mechanism by which Δ^9 -THC suppresses T cell-dependent humoral immunity in humans. The significance of this work is that it provides novel insights into the mechanism of cannabinoid-mediated suppression of human humoral immunity.

DEDICATION

To mother, Chunyapat Niruchajirapat, for her unwavering love. Her support, encouragement, and constant love have sustained me throughout my life. I never would be at this point in my life without you.

To my husband, Dr. Pariwate (Perry) Varnakovida, for his understanding, enduring love and support throughout all these years at graduate school. Thanks for the late-night rides when I don't know how to drive and the trips to Grand Canyon and Yellowstone.

To my bothers, Chinnachot and Porntep, and my sister, Supapich, for their encouragment and support from Thailand.

To my daughter, Primrut (Tammy), for being the source of my mental energy. You are always brightening up my world. I am enjoyed watching you learn new things and grow into an independent, strong-willed and compassionate young fellow.

ACKNOWLEDGEMENTS

First and foremost, I would like to express my deepest gratitude to my thesis advisor, Dr. Norbert Kaminski, for the opportunity of doing my Ph.D. research in his lab. Working with him has been a highly rewarding experience. He has taught me to think critically, the art of being a scientist that I will carry with me to my future carreer. I appreciated all his contributions of time, ideas to make my Ph.D. experience productive and stimulating.

I am also most grateful to my committee members, Dr. Barbara L.F. Kaplan, Dr. James Wagner and Dr. John Goudreau for their time, constructive suggestions and discussions during committee meetings. Thank you for challenging me to look at my project from different perspectives. I would like to express my special appreciation to Dr. Kaplan, who is also my co-mentor. Thanks for her time, patience and dedication in training and aissisting me in tons of experiments as well as her encouragement and expertise throughout this project.

The members of the Kaminski group have contributed immensely to my personal and professional time at MSU. The group has been a source of friendships as well as good advice and collaboration. To Bob Crawford, thanks for his patient of answering all my questions and assistance with flow cytometry. To Dr. Priya Raman, thanks for being the best officemate and the support when I has just started in the lab. To Dr. Peer Karmaus, thanks for helping with the

classes, especially PHM827. To Dr. Schuyler Pike, thanks for helping me improve my English. To Ashwini Phadnis-Moghe, thanks for helping with B cells experiments. To Natasha Kovalova and Jose Suarez Martinez, thanks for babysitting my daughter. To Weimin Chen and Kim Hambleton, thanks for listening to me when I needed to. Thank you all of you for support, wonderful conversation, game nights, parties, and dairy store trips as well as sharing the laughs and headaches about science.

My life here at MSU would have been more difficult, if it were not for the following people: Duanghatai (Noge) Wiwatratana, Tanita Suepa, and Siam Lawawirojwong. Thanks for the fun times together and I very appreciate all help, support, foods, and babysitting, especially the last couple of months after Perry went back to Thailand. I would not be able to finish all those late-night and afterhour experiments without the help from all of you.

Last but not least, I am grateful to the Royal Thai Government and the Department of Pharmacology and Toxicology for granting me the opportunity to be a part of this program. Throughout these years of training here, it has been truly inspirational and invaluable experience of research, friendship, and love.

TABLE OF CONTENTS

LIST OF	TABLES	xi
LIST OF	FIGURES	xii
LIST OF	ABBREVATIONS	xvi
LITERA	TURE REVIEW	
I. T	-cell dependent humoral immune response and plasma	
	differentiationdifferentiation	1
	A. T-cell dependent humoral immune response	1
	B. The genetic network controlling plasma cell differentiation	
II.	Signaling cascades in T cells	
	A. T cell receptor (TCR) signaling	
	B. Ca ²⁺ signaling in T cells	6
	C. NFAT	8
	D. NFκB	9
	E. GSK3	
III.	CD40-CD40 ligand (CD40L)	
	A. CD40	
	B. CD40L	
	C. Cellular response of CD40-CD40L interaction	
IV.	Regulation of CD40L expression in activated T cells	
V.	Role of CD40 in plasma cell differentiation	
	A. CD40 and T cell-dependent humoral immune response	
	B. TRAF-dependent CD40 signaling	
1/1	C. TRAF-independent CD40 signaling	17
VI.	Role of cytokines, interleukin (IL)-2, -6, and -10, in plasma	19
Cell (A. IL-2	
	B. IL-6	_
	C. IL-10	
VII.	Δ^9 -tetrahydrocannabinol (Δ^9 -THC) and cannabinoid receptors	
	A. Cannabinoids and Δ^9 -THC	
	B. Cannabinoid receptors	
	C. Signal transduction activated by CB1 and/or CB2	
	2. 2.3	

		D. Pharmacokinetics of Δ ⁹ -THC	31
		E. Pharmacodynamics of Δ^9 -THC	32
		F. Toxicity of Δ^9 -THC	34
	VIII.	Immunomodulatory properties of Δ^9 -THC	
	V 111.	A. T cells	
		B. B cells	
	IX.	Rationale	
N 4	A TED14	U O AND METHODO	
IVI		ALS AND METHODS Reagents	16
	I. II.	Plasmids	
	III.	Cell cultures	_
	IV.	Animals	
	V.	Isolation and culture of human peripheral blood mononuclear	00
		PBMCs)	50
	VI.	Isolation and culture of human peripheral blood (HPB) naïve T	
	cells		51
	VII.	Isolation and culture of HPB naïve B cells	51
	VIII.	Mouse T cell activation	52
	IX.	Human T cell activation	52
	Χ.	Flow cytometry analysis	54
	XI.	Real Time Polymerase Chain Reaction	
	XII.	Transient transfection assay	
	XIII.	Nuclear protein isolation	
	XIV.	Electrophoretic Mobility Shift Assay (EMSA)	
	XV.	Calcium determination	
	XVI.	In vitro CD40L-dependent polyclonal IgM antibody response	
	XVII.	IgM Enzyme-linked immunospot assay	
		Proliferation assay	
	XIX.	Statistical analysis	62
E	KPERIM	MENTAL RESULTS	
	I.	Effect of Δ^9 -THC on the upregulation of CD40L expression on	
	activa	ted mouse CD4 ⁺ T cells	64
		A. Expression kinetics of CD40L expression on activated T cells	
		B. Differential effects by Δ^9 -THC on CD40L upregulation in	- •
		response to different T cell activation stimuli	60
			υ υ
		C. Δ^9 -THC decreases steady-state mRNA levels of <i>CD40L</i> induced	
		hy anti-CD3/CD28	75

	D. CB1 and CB2 are not involved in suppression by Δ^9 -THC of anti-CD3/CD28-induced CD40L expression on mouse splenic CD4 ⁺ T cells	
	E. The effect of Δ^9 -THC are not mediated via GR	77
II.	Effect of Δ^9 -THC on the upregulation of CD40L on activated human	
	CD4 ⁺ T cells	
	A. Δ^9 -THC attenuates anti-CD3/CD28-induced CD40L expression	in
	activated human T cells at the transcriptional level	
	B. Δ^9 -THC impairs anti-CD3/CD28-induced DNA-binding activity NFAT and NF κ B in activated human T cells	
	C. Δ^9 -THC does not affect GSK3 β activity in activated human CD4 ⁺	
	T cells	
	D. Δ^9 -THC attenuates anti-CD3/CD28-induced elevated intracellu	lar
	Ca ²⁺ , but does not impair PLCγ activation	99
	E. Δ^9 -THC does not modulate anti-CD3/CD28-mediat	
	phosphorylation of ZAP70 or Akt in activated human CD4 ⁺) 1
III. 🗆 🗆	Effect of Δ^9 -THC on CD40L plus cytokine-induced primary loresponse by HPB B cells	
	A. Δ^9 -THC attenuates CD40L plus cytokine-induced primary lo	
	responses of HPB B cells10	
	B. Δ^9 -THC suppresses CD40L plus cytokine-induced surfa	ce
	expression of CD80, but not CD69, CD86, and ICAM1 in HPB B cells	12
	C. Δ^9 -THC impairs CD40L plus cytokine-induced proliferation of HF	
	B cells	
	D. Δ^9 -THC suppresses CD40L plus cytokine-induced mRN	NΑ
	expression of <i>IGJ</i> in HPB B cells1	
	E. Δ^9 -THC suppresses CD40L plus cytokine-induced phosphorylati	
	of STAT3, but not p65 NFκB, in HPB B cells12	21
DISCUSS	SION12	28
I.	Effect of Δ^9 -THC on the upregulation of CD40L on activated	
CD4 ⁺	T cells	
II.	Effect of Δ^9 -THC on CD40L plus cytokine-induced primary lo	
respoi	nse by HPB B cells13 Concluding remarks14	
111.	Condition of the condit	T

APPENDICES	150
APPENDIX A: Antibodies	151
APPENDIX B: TaqMan primers	153
BIBLIOGRAPHY	157

LIST OF TABLES

	Δ^9 -THC impairs CD40L plus cytokines-induced proliferation ells	120
Table 2.	List of antibodies used in this dissertation research	151
Table 3.	List of TagMan primers used in this dissertation research	153

LIST OF FIGURES

_	Schematic diagram of T cell dependent humoral immune	2
_	Schematic diagram of the cellular stages and genetic network in lifferentiation	4
	Schematic diagram of of the proposed signaling cascades and involved in transcriptional regulation in T cells	15
_	Schematic diagram of of the proposed signaling pathways ne engagement of CD40 in B cells	18
Figure 5.	Chemical structures of cannabinoid compounds	24
•	Effect of ethanol on surface expression of activation markers HPB B cells	47
•	Kinetics of PMA/Io-induced CD40L expression in mouse	65
-	Kinetics of anti-CD3/CD28-induced CD40L expression in mouse	67
	Δ^9 -THC suppresses anti-CD3/CD28-induced surface CD40L n activated mouse CD4 $^+$ T cells	70
-	Δ^9 -THC suppresses anti-CD3/CD28-induced surface CD40L n enriched mouse CD4 $^+$ T cells	72

Figure 11.	Δ^9 -THC does not suppress PMA/Io-induced surface CD40L	
expression a	ctivated mouse CD4 ⁺ T cells	73
-	Δ^9 -THC suppresses anti-CD3/CD28-induced <i>CD40L</i> mRNA activated mouse splenic T cells	76
CD40L expre	Comparison of the effect Δ ⁹ -THC on anti-CD3/CD28-inducession in splenic T cells derived from wildtype or CB1 ^{-/-} CB2 ^{-/-}	
	DEX suppresses anti-CD3/CD28-induced surface CD40L a activated mouse splenic T cells	80
_	GRE luciferase reporter activity in HEK293T cells treated with or DEX	82
-	Effect of DEX and/or Δ^9 -THC on the mRNA expression of GR-HEK293T cells	83
_	Effect of DEX and/or Δ^9 -THC on the mRNA expression of GR- n Jurkat T cells	85
•	Effect of Δ^9 -THC on anti-CD3/CD28-induced surface CD40L on activated human CD4 $^+$ T cells at different time points	88
J	Δ^9 -THC attenuates anti-CD3/CD28-induced surface CD40L n activated human CD4 $^+$ T cells	89
-	Δ^9 -THC suppresses anti-CD3/CD28-induced <i>CD40L</i> mRNA activated human T cells	92

•	Peak time of anti-CD3/CD28-induced DNA-binding activity of vated human T cells	94
-	Δ^9 -THC impairs anti-CD3/CD28-induced DNA-binding activity of F $_{\kappa}$ B in activated human T cells	95
_	Peak time of anti-CD3/CD28-induced phosphorylation of GSK3β numan CD4 ⁺ T cells	97
•	Effect of Δ^9 -THC on the GSK3 β activity in activated human	98
•	Δ^9 -THC suppresses anti-CD3/CD28-induced elevation of Ca $^{2+}$ in activated human CD4 $^+$ T cells	100
•	Effect of Δ^9 -THC on the activation of PLC $_\gamma$ in activated human	102
-	Peak time of anti-CD3/CD28-induced phosphorylation of ZAP70 numan CD4 ⁺ T cells	104
J	Peak time of anti-CD3/CD28-induced phosphorylation of Akt numan CD4 ⁺ T cells1	105
_	Effect of Δ^9 -THC on the proximal TCR signaling molecules in man CD4 $^+$ T cell	106
•	Effect of Δ^9 -THC on the phosphorylation of ZAP70 in activated T cells	108

	Effect of Δ ⁹ -THC on CD40L plus cytokine-induced IgM response lls110
	Peak time of CD40L plus cytokine-induced surface expression of CD80 on activated HPB B cells113
_	Effect of Δ^9 -THC on surface expression of activation markers HPB B cells114
	Effect of Δ ⁹ -THC on CD40L plus cytokines-induced <i>CD80</i> mRNA activated HPB B cells117
	Δ^9 -THC impairs CD40L plus cytokines-induced proliferation of B B cells
_	Effect of Δ^9 -THC on CD40L plus cytokines-induced <i>PRDM1</i> ssion in activated HPB B cells
•	Effect of Δ^9 -THC on CD40L plus cytokines-induced <i>PAX5</i> ssion in activated HPB B cells
_	Δ^9 -THC suppresses CD40L plus cytokines-induced <i>IGJ</i> mRNA activated HPB B cells
Figure 39. STAT3 in act	Effect of Δ^9 -THC on the phosphorylation of p65 NF κ B and tivated HPB B cells
	Schematic diagram summarizing the possible mechanisms involved on of T cell-dependent humoral immune response by Δ ⁹ -THC

LIST OF ABBREVATIONS

 Δ^9 -THC delta 9 -tetrahydrocannabinol

2-AG 2-arachidonyl glycerol

AF Alexa fluor

Akt protein kinase B

ANOVA analysis of variance

AP-1 activator protein 1

APC allophycocyanin

BCL-6 B-cell lymphoma

Blimp1 B lymphocytes maturation protein 1

BSA bovine serum albumin

[Ca²⁺]_i intracellular calcium concentration

cAMP cyclic adenosine monophosphate

CB1 cannabinoid receptor1

CB2 cannabinoid receptor 2

CBD cannabidiol

CBN cannabinol

CD cluster of differentitation

CD40L CD40 ligand

CD40L-L mouse fibroblast line expressing human CD40L

cDNA complementary DNA

CFSE carboxyfluorescein succinimidyl ester

CRAC calcium release activated calcium channels

CsA cyclosporin A

DMSO dimethyl sulfoxide

ELISPOT enzyme-linked immunospot

ERK extracellular signal-regulated kinase

FACS fluorescence-activated cell sorting

FITC fluorescein isothiocyanate

GSK3 β glycogen synthase kinase 3 β

HIV human immunodeficiency virus

IFN_γ interferon gamma

lg immunoglobulin

IgH immunoglobulin heavy chain

lgJ immunoglobulin joining chain

IL interleukin

IP₃ 1,4,5-inositol triphosphate

JAK Janus family kinase

JNK c-Jun N terminal kinase

LPS lipopolysaccharide

MAPK mitogen activated protein kinases

MFI mean fluorescences intensity

mRNA messenger ribonucleic acid

NA naïve or unstimulated cells

NFAT nuclear factor of activated T cells

NFκB nuclear factor kappa B

PAX5 paired box protein 5

PBMC peripheral blod mononuclear cell

PBS phosphate buffered saline

PE phycoerythrin

PI3K phosphoinositide 3-kinase

PLCγ phospholipase C γ

PPAR peroxisome proliferator activated receptors

PRDM1 PR domain zince finger protein 1

sRBC sheep erythrocyte

STAT signal transducer and activator of transcription

TCR T cell receptor

Th helper T cell

TNF tumor necrosis factor

TRAF tumor necrosis factor receptor associated factor

TRCP1 transient receptor potential cation channel, subfamily A,

member 1

TRPV transient receptor potential vanilloid

XBP-1 X-box binding protein 1

LITERATURE REVIEW

I. T-cell dependent humoral immune response and plasma cell differentiation

A. T-cell dependent humoral immune response

Humoral immunity refers to immune responses that are mediated by secreted antibodies. The main function of humoral immunity is to defend against extracellular microbes, parasites, pathogenic viruses, and foreign macromolecules. In addition, the aberrant production of antibodies is associated with many types of autoimmune diseases and hypersensitivity (reviewed in [1]). Antibodies are produced by plasma cells, which are differentiated B cells. The generation of antibody producing cells requires distinct sequential phases: B cell activation, proliferation, and differentiation. The activation phase is initiated by the binding of antigen to Ig surface receptors of B cells. However, the binding of most protein antigens, which contain only one copy of epitope per molecule, is not sufficient to initiate the response. Such molecules require accessory cells, in particular helper T cell (CD4⁺ T cells), to deliver activating signals. The presented antigen by B cells is recognized by specific T cell receptor (TCR) on the surface of CD4⁺ T cells and thereby activates T cells. Activated CD4⁺ T cells upregulate expression of many co-stimulatory molecules and secrete several cytokines important in development of plasma cells. Co-stimulatory molecules provide the contact-dependent signals requiring for B-cell activation. Cytokines

serve two principle functions in antibody response: 1) by further amplifying signaling cascades involved in B cell proliferation and differentiation and 2) by determining the type of antibodies produced by isotype switching. The activated B cells then undergo clonal expansion, isotype switching, affinity maturation in germinal center (GC) prior differentiate to plasma cells or memory cells. The antibodies that are secreted initially are predominantly of the IgM isotype (reviewed in [2]). IgM is normally secreted in the pentameric form, of which each subunit is linked by immunoglobulin joining chian (IgJ) (Figure 1).

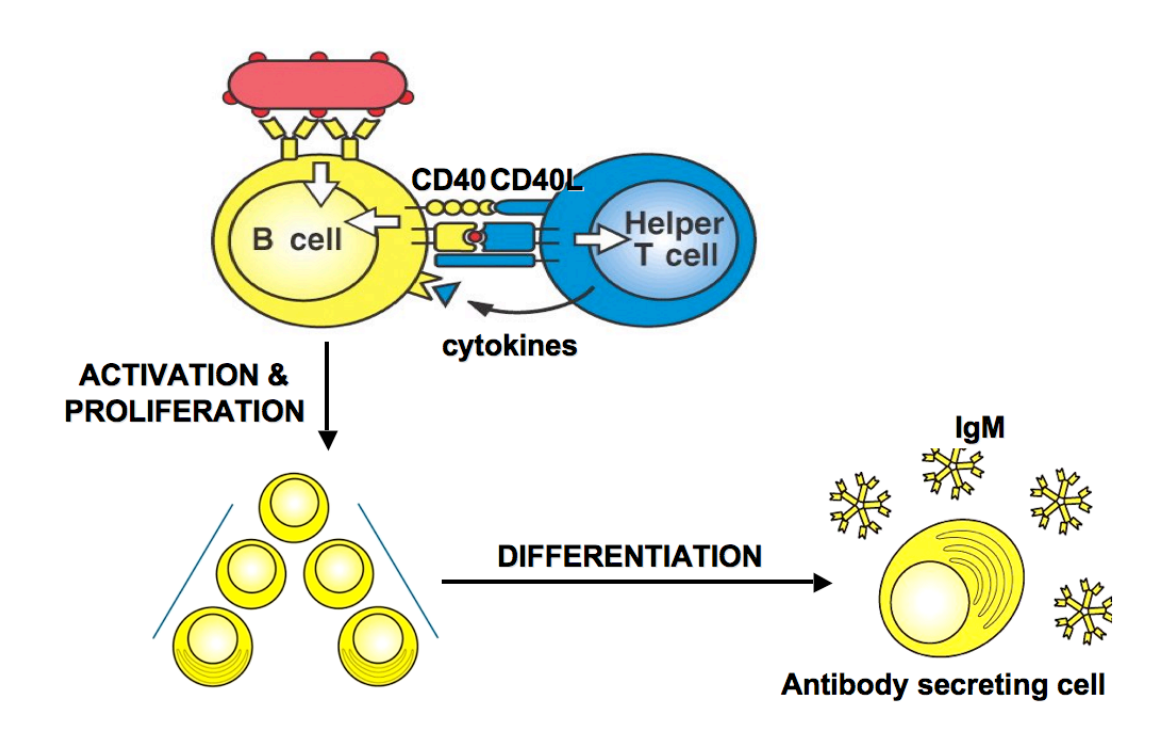


Figure 1. Schematic diagram of the T cell-dependent humoral immune response.

The interaction between B cells presenting processed antigen to specific primed helper T cells allows the primed helper T cell to delivery the activation signals that are involved in their differentiation into plasma cells. "For interpretation of the references to color in this and all other figures, the reader is referred to the electronic version of this dissertation."

B. The genetic network controlling plasma cell differentiation

The differentiation of mature B cells into plasma cells involves a complex regulatory network of transcription factors that are only partially understood. Included in this process are the down-regulation of PAX5 and Bcl-6, critical transcription factors in maintaining B cell identity and the up-regulation of IRF4, Blimp1, and XBP1, crucial transcription factors in promoting plasma cell fate (reviewed in [3]). PAX5 is essential for B cell commitment and development as its expression was found only in committed B cells beginning at the pro-B cells stage (reviewed in [4]). For instance, PAX5 controls B cell characteristics through the induction of the genes encoding for B cell receptor and co-receptor such as IgM heavy chain, CD19, CD21 [5,6], and, at the same time, repression of the genes involved in plasmacytic differentiation such as PRDM1 encoding for Blimp1 and IGJ encoding for IgJ [7]. Bcl-6 is highly expressed in GC B cells [8]. The function of Bcl-6 is to prevent premature differentiation of plasma cells by facilitating proliferation and allowing somatic hypermutation [9]. Further, both PAX5 and Bcl-6 prevent plasma cell differentiation by repressing the expression of Blimp1, often referred as the master regulator of B cell plasmacytic differentitiation (reviewed in [10]). Blimp1 can drive plasma cell differentiation by directly repressing the expression of genes important for B cell receptor signaling, germinal cell function, and proliferation, whereas allowing the expression of XBP1 [11]. XBP1 is also necessary for the effective plasma cell formation [12]; however, the underlying mechanism remains to be resolved. As

XBP1 plays an important role in unfolded protein response [13], it seems to regulate chaperones involved in handling load of the increased Ig synthesis (reviewed in [3]). IRF4 was demonstrated to induced Blimp1 expression [14]. Taken together, the mutually exclusive transcriptomes of B cells and plasma cells are maintained by the antagonistic influences of two groups of transcription factors, those that maintain the B cell program and those that promote and facilitate plasma cell differentiation (Figure 2).

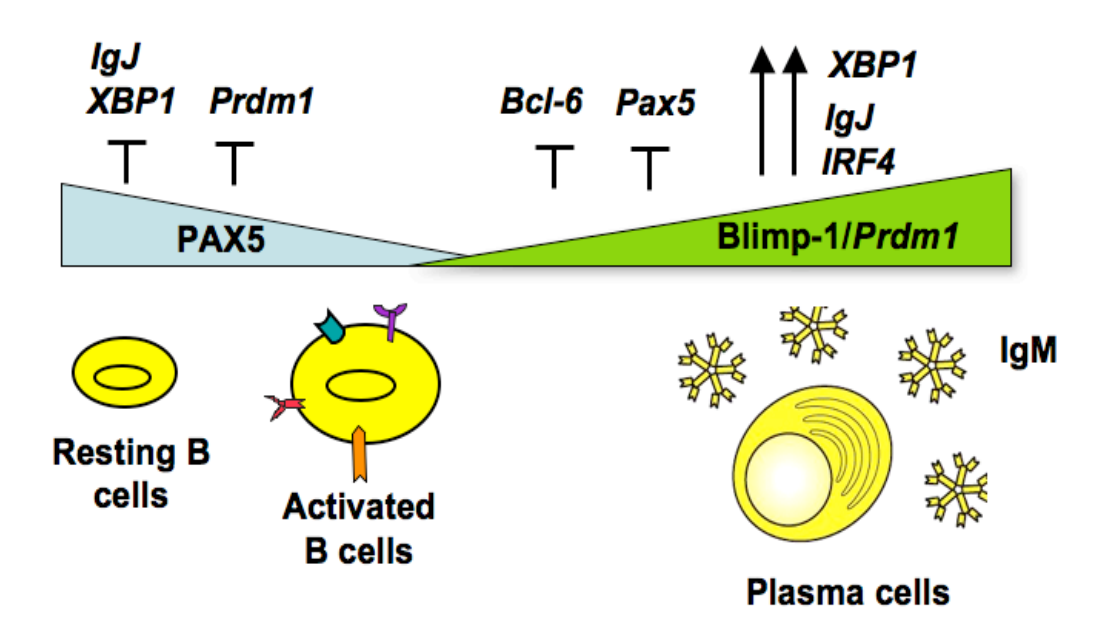


Figure 2. Schematic diagram of the cellular stages and genetic network involved in plasma cell differentiation.

The stages of cellular differentiation from a resting B cell to an antibody-secreting plasma cell are indicated, as are the relative levels of PAX5, Blimp-1 and key target genes. The pre-plasmablast stage (resting and activated B cells) is characterized by high PAX5, but low Blimp1, XBP1, and IgJ expression. Plasmablasts have intermediate Blimp1 expression, proliferate rapidly and secrete antibody. Plasma cells that secrete large quantities of antibody have high Blimp1, XBP1, and IgJ, but low PAX5 and Bcl-6. Positive influence on gene expression is indicated by (\rightarrow) and repressive activity by (\bot) .

II. Signaling cascades in T cells

A. T cell receptor signaling

T cell activation requires two independent signals; the first is antigen-specific and mediated through TCR, and the second is from costimulatory receptors, particularly CD28. Engagement of TCR along with co-stimulation through the coreceptor, CD28, leads to the activation of non-receptor protein tyrosine kinases (PTKs) of which Lck and Fyn are responsible for the phosphorylation of immunoreceptor-based tyrosine activation motifs (ITAMs) in the cytoplasmic domain of CD3 in the TCR complex (reviewed in [15]). Further, ligation of CD28 leads to activation of both phosphoinositide 3-kinase (PI3K)-dependent and independent pathways. The activation of the PI3K pathway results in the phosphorylation of protein kinase B (Akt) [16]. Phosphorylated ITAMs then serve as docking sites promoting the recruitment and the activation of many adapter proteins, including Zeta-chain-associated protein kinase 70 (ZAP70), another member of PTKs. Activation of ZAP70 by phosphorylation (pZAP70) increases both tyrosine phosphorylation and thereby catalytic activity of phospholipase C-y (PLC γ) [17]. Phosphorylated PLC γ (pPLC γ) then promotes the generation of two secondary messengers, inositol triphosphate (IP₃) and diacylglycerol (DAG) by hydrolysis of phosphatidylinositol 4,5-bisphosphate in the plasma membrane. IP₃ increases intracellular calcium concentration ([Ca²⁺]_i), which is mainly responsible for activation of NFAT, whereas DAG activates protein kinase C-

theta (PKC θ), which is mainly responsible for activation of NF κ B (reviewed in [18]).

B. Ca²⁺ signaling in T cells

Ca2+ is essential for optimal T cell activation and is regulated by two mechanisms (reviewed in [19]). The initial increase in [Ca²⁺]_i occurs in response to stimulation of TCR is mediated by release of Ca²⁺ from intracellular stores such as the endoplasmic reticulum (ER) and mitochondria. The ER is the primary source of this initial increase in [Ca²⁺]_i in T cells (reviewed in [20]). Although several intracellular messengers (IP3, cyclic ADP ribose, and nicotinic acid adenine dinucleotide phosphate) have been implicated in Ca2+ release from ER in T cells, IP3 which binds to the IP3 receptor, is the main mechanism and has been extensively characterized (reviewed in [20]). This transient elevation of [Ca²⁺]_i is necessary, but not sufficient for optimal T cell activation. Depletion of ER Ca2+ stores evokes a sustained increase in [Ca2+] through the activation of Ca²⁺ release activated Ca²⁺ (CRAC) channels located on the plasma membrane (reviewed in [21]). CRAC channels are composed of ORAI proteins, which are the pore subunits and are activated by the ER Ca2+ sensors, stromal interaction molecules (STIM) 1 and 2, (reviewed in [22]). Upon ER store depletion, STIM

forms multimers in the ER membrane and translocates to sites of ER-plasma membrane apposition where they bind to and activate ORAI channels resulting in the sustained increase in $[Ca^{2+}]_i$ [23-26].

Although IP3 is the main mechanism that controls the sustained increase in [Ca²⁺]_i, other mechanisms mediated by potassium (K⁺) channels, plasma membrane Ca²⁺ ATPase (PMCA), and mitochondria Ca²⁺ homeostasis, have been extensively studied. For example, K⁺ channels control entry of Ca²⁺ through CRAC channels by regulating the membrane potential in which depolarization decreases Ca²⁺ entry whereas hyperpolarization increases Ca²⁺ entry [27]. Voltage-dependent (Kv1.3) and Ca²⁺ activated K⁺ channels (IKCa1) are major K⁺ channels controlling the membrane potential in effector CD4⁺ T cells and upregulated during T-cell activation [28]. PMCA, the major Ca2+ clearance mechanism in T cells, regulates the amplitude of Ca2+ through its delayed upregulation, which allows larger Ca2+ rise [29]. Mitochondria are involved in the control of CRAC channel activity by reducing Ca²⁺-dependent inactivation of CRAC channels. Ca2+ entry through CRAC channels is immediately imported to the lumen of mitochondria located in the vicinity of CRAC entry, thereby increasing CRAC activity and the amplitude of Ca²⁺ signal (reviewed in [30]).

The sustained increase of Ca^{2+} through the CRAC channel is essential for the activation of transcription factors necessary for T cells to expand clonally and to acquire effector functions, for instance, through the production of cytokines and the upregulation of costimulatory molecules (reviewed in [19]). At least three transcription factors: NFAT, NF κ B, and activator protein 1 (AP1), are regulated by Ca^{2+} signaling. Among them NFAT is a pivotal target of Ca^{2+} signaling, whereas the role of Ca^{2+} may be regarded as being more indirect for NF κ B and AP1 activation (reviewed in [31]).

C. NFAT

The NFAT family consists of five members; NFAT1 (also known as NFATc2 or NFATp), NFAT2 (also known as NFATc1 or NFATc), NFAT3 (also known as NFATc4), NFAT4 (also known as NFATc3 or NFATx) and NFAT5 (also known as tonicity enhancer binding protein) (reviewed in [32]). Four NFAT proteins are expressed in T cells: NFAT1, which is constitutively expressed in resting T cells and is the predominant NFAT protein [33], NFAT2, which is inducible upon activation [33], NFAT4, which is very weakly expressed in unstimulated T cells and its expression is not inducible [33], and NFAT5, which is highly expressed in the thymus, is undetectable in mature T cells. However, the expression of NFAT5 is inducible upon activation [34].

With the exception of NFAT5, NFAT1-4 are regulated by Ca²⁺/calcineurin-dependent signaling [35]. In resting T cells, NFAT is phosphorylated by several NFAT kinases and localized in the cytosol. The sustained increase in [Ca²⁺]_i activates calmodulin, which then activates a large number of calmodulin-dependent proteins including, but not limited to, calcineurin, a serine/threonine phosphatase (reviewed in [36]). Activated calcineurin dephosphorylates NFAT resulting in nuclear translocation, stimulation of NFAT-DNA binding activity and increased transcription of NFAT-regulated genes [37,38]. Inhibition of the phosphatase activity of calcineurin by FK506 or cyclosporin A (CsA) results in relocalization of NFAT to the cytosol and loss of its DNA-binding activity (reviewed in [39]). Once the calcium-calcineurin signaling is terminated, rephosphorylation of NFAT by NFAT kinases is required for its nuclear export [40-42].

D. NF_kB

The NF κ B family consists of five genes coding for NF κ B1 (p105/p50), NF κ B2 (p100/p52), RelA (p65), RelB and c-Rel. RelA, Rel B, and cRel are synthesized as mature products that do not require proteolytic processing, whereas NF κ B1 and NF κ B2 are synthesized as large precursors that require proteolytic processing to produce the mature proteins, p50 and p52, respectively. These proteins share a common structural Rel homology domain that is important for dimerization, interaction with I κ B inhibitory proteins, and DNA binding. However only p65, RelB and c-Rel contain a transactivation domain,

therefore p50 and p52 homodimers can function as transcriptional repressors (reviewed in [43]). P50 and p65 are expressed widely in various cell types, whereas the expression of Rel B and c-Rel are restricted to lymphoid organs and haematopoitic cells (reviewed in [44]).

With a diversity of stimuli leading to the activation of NFκB, the specific biological responses are associated with different combinations of homo- and heterodimers that distinctly regulate target gene transcription. activated form of NFκB is a heterodimer of the p65 subunit associated with either a p50 or p52 subunit. In the resting state, NFκB dimers are inactive in the cytoplasm because they are bound to inhibitory IκB proteins or IκB-like proteins, such as p100 and p105. Two different pathways, canonical and non-canonical, regulate NFκB activation. The canonical pathway depends on ubiquitinationdependent degradation of $I\kappa B$ proteins. The phosphorylation of $I\kappa B$ by $I\kappa B$ kinases (IKK) upon activation promotes the rapid ubiquitination and degradation of IκB resulting in the release of active NFκB dimers. The noncanonical pathway depends on proteolytic cleavage of the precursor p100 that mainly dimerizes with RelB. The liberated NFκB dimers are transported to the nucleus and thereby activating gene expression [45]. However, to achieve the maximal NF κ B transcription response, the NFkB dimers, particularly the p65 subunit, must underao additional post-translational modification involving site-specific phosphorylation [46].

TCR ligation induces NFkB activation mainly through the canonical pathway. The activation of IKK upon T cell activation depends on the formation of the "CBM" complex, which is composed of caspase recruitment domain, CARD, membrane-associated guanylate kinase, MAGUK, protein 1 (CARMA1), B cell lymphoma 10 (BCL10) and mucosa-associated lymphoid tissue lymphoma translocation protein 1 (MALT1) (reviewed in [47]). The recruitment of CARMA1 to the constitutively interacting BCL10 and MALT1 complex is largely dependent on its phosphorylation (reviewed in [48]). PKC0 is the major kinase responsible for the phosphorylation of CARMA1 after TCR/CD28 costimulation [49]. Importantly, [Ca²⁺]_i elevation is also crucial for TCR-induced NFκB activation (reviewed in [50]). Calcineurin and calcium/calmodulin-dependent protein kinase II (CaMKII) were involved in the regulation NFκB [51]. Calcineurin was demonstrated facilitate the assembly of the CBM to complex dephosphorylation of BCL10 [52]; whereas CaMKII was identified as a BCL10 and CARMA1 kinase [53,54].

E. GSK3

GSK3 is a protein serine/theronine kinase, which is ubiquitously expressed in almost all cell types. There are two isoforms of mammalian GSK3; GSK3 α and GSK3 β [55]. Unlike most kinases, GSK3 is constitutively active and regulated by inhibitory phosphorylation at Ser21 in GSK3 α and Ser9 in GSK3 β (reviewed in [56]). In T cells, CD28 co-stimulation was found to facilitate the inactivation of GSK3 through the activation of Akt (protein kinase B), one of the

inhibitory GSK3 kinases (reviewed in [56]). GSK3 β serves as an NFAT kinase and plays an important role in regulating NFAT activity [40]. Inhibition of GSK3 β increased IL-2 production in both CD4⁺ and CD8⁺ T cells [57,58]. Although GSK3 β was also shown to regulate NF κ B activation; its role is much less established in T cells following TCR stimulation (reviewed in [59]).

III. CD40 and CD40 ligand (CD40L)

A. CD40

The CD40 receptor is a type I transmembrane glycoprotein and is a member of the tumor necrosis factor (TNF) receptor superfamily. The human *CD40* gene, located on chromosome 20, encodes for a 258 amino acid polypeptide with molecular weight of 50 kDa. CD40 is constitutively expressed on a variety of cells, both immune and non-immune cells. For example, CD40 are found on surface of B cells, activated macrophages, dendritic cells, vascular endothelial cells, astrocytes and microgial cells (reviewed in [60-62]).

B. CD40L

CD40L, also termed CD154, is a type II transmembrane protein and is a member of the TNF superfamily. The human *CD40L* gene is located on the X-chromosome and encodes for a 261 amino acid polypeptide. CD40L exists in at least two forms: the transmembrane form, which has a molecular weight of 39 kDa, and the soluble form, which has a molecular weight of 18. Similar to its receptor, CD40, CD40L can be expressed by many cell types including

eosinophils, basophils, macrophages, and natural killer cells, of which CD4⁺ T cells have the highest level of CD40L expression. In contrast to the constitutively expressed CD40, the expression of CD40L under physiological conditions is inducible and transient (reviewed in [63]).

C. Cellular response of CD40-CD40L interaction

CD40-CD40L interaction plays a crucial role in various aspects of the immune response. Ligation of CD40L on CD40⁺ cells enhances the function of the interacting effector cells. In antigen-presenting cells, the upregulation of costimulatory molecules [e.g. CD69, CD80, CD86, and Major Histocompatibility Complex (MHC)-II] as well as adhesion molecules [e.g. intercellular adhesion molecules-1 (ICAM1) and vascular cell adhesion molecules-1 (VCAM-1)] enhances antigen presentation. CD40 and/or CD40L-induced production and secretion of cytokines such as interleukin (IL)-1, IL-2, IL-6, IL-10, TNF-α, and interferon-y (IFN-y), as well as chemokines, such as monocyte chemotactic protein-1 (MCP-1), macrophage inflammatory protein 1α (MIP- 1α) and regulated on activation, normal T expressed and secreted (RANTES), involved in inflammatory response. Further, CD40-induced expression of metalloproteinases (MMPs) by endothelial cells was associated atherosclerosis (reviewed in [64,65]) and tumor metastasis in cervical cancer [66]. The implication of CD40 and/or CD40L in both physiological and pathophysiological processes emphasizes the possible targets for therapeutic intervention (reviewed in [67,68]).

IV. Regulation of CD40L expression in activated T cells

In T cells, CD40L expression is rapidly but transiently induced after T cell activation. Upon in vitro stimulation either by treatment with phorbol ester plus calcium ionophore (PMA/Io) or antibodies directed against CD3 and CD28 (anti-CD3/CD28), the level of surface CD40L on activated T cells is maximal between 6 and 8 h after activation followed by a decline over the next 12-18 h (reviewed in [69,70]). However, recent evidence suggests biphasic expression of CD40L on activated CD4+ T cells, in which the second peak occurred at 48 h post stimulation [71-74]. Interestingly, elevated expression of surface CD40L is downregulated by endocytosis upon binding to its receptor, CD40 [75]. The expression of CD40L is tightly regulated and occurs at the transcriptional, posttranscriptional, and/or post-translational level, of which the regulation at the transcriptional level is the main mechanism (reviewed in [69]). transcriptional level, NFAT is the key transcription factor found in the minimal However, optimal transcription of the CD40L gene CD40L promoter [76]. requires cooperatively binding of other transcription factors such as CD28RE, NFκB, TFE3/TFEB, EGR, AKNA, and AP1 [77]. Among them, NFκB has shown to be critically involved in the up-regulation of CD40L expression in both activated mouse and human T cells [78-80]. The signaling pathways are likely to be relevant for transcribing the CD40L gene upon T cell activation are schematically represented in Figure 3.

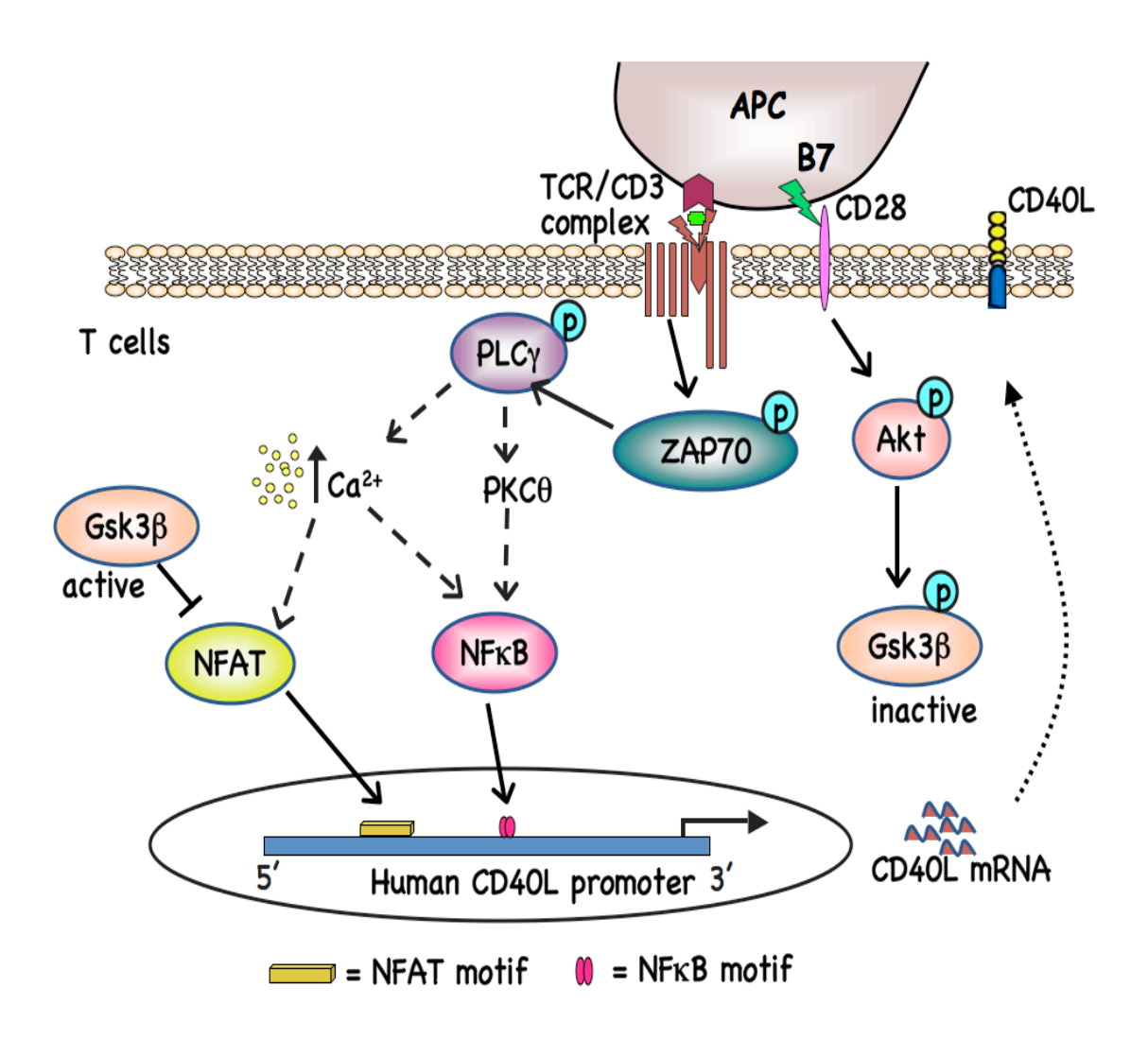


Figure 3. Schematic diagram represents the proposed signaling cascades and mechanisms involved in transcriptional regulation of CD40L promoter in T cells.

The engagement of TCR in combination with its co-receptor, CD28, leads to the activation of ZAP70 by phosphorylation. The activated ZAP70 then phosphorylates and activates PLC γ . The activation of PLC γ leads to an increase in [Ca $^{2+}$] $_i$ and activation PKC θ , which ultimately results in activation of two transcription factors, NFAT and NF κ B. The activated NFAT and NF κ B then translocate into the nucleus and binds to the CD40L promoter. *CD40L* transcripts are translated and exported to the surface. The activation of NFAT is also regulated by GSK3 β , which is constitutively active in resting T cell, but becomes inactive upon phosphorylation with Akt.

V. Role of CD40 in plasma cell differentiation

A. CD40 and T cell-dependent humoral immune response

The importance of cell-contact in T cell-induced B cell proliferation and differentiation was initially identified since plasma membrane fractions from activated T helper cells, but not cytokines, were able to reconstitute the requirement of T cell help in B cell function [81-86]. Among the different surface molecules, the engagement between CD40 and its ligand, CD40L, has been well established as a key signal for driving B cells to become plasma cells by promoting the activation, proliferation and differentiation of B cells [87,88]. Subsequently, the physiologic relevance of the CD40-CD40L interaction for normal humoral immunity was demonstrated in humans, in which mutations in the gene encoding CD40L associates with X-linked hyper-IgM syndrome. Patients suffering with X-linked hyper-IgM syndrome showed deficiencies in antibody class switching and germinal center formation [89-92]. Further, admgfyinistration of anti-CD40L antibodies to mice abrogated antibody responses against T cell-dependent, but not T cell-independent, antigens [93]. Similar results were also demonstrated in CD40L knockout mice [94].

B. TRAF-depending CD40 signaling

Upon binding to CD40L, CD40 molecules, which were once distributed evenly throughout the plasma membrane, rapidly trimerize in microdomains. The cytoplasmic tail of CD40, which lacks intrinsic enzymatic activity, delivers signals to the cells by recruitment of TNFR-associated factors (TRAFs) (reviewed in

[95]). TRAFs serve as adapter proteins, which in turn deliver signals to B cells through the activation of different signaling pathways: NFkB, Pl3K, and MAPKs (Figure 4). These signaling pathways then regulate B-cell fate in humoral immunity through the upregulation of cell adhesion molecules, co-stimulatory molecules, immunoglobulin, cytokines and lymphokines that are involved in activation, proliferation, differentiation, antibody isotype switching, as well as generation of memory B cells (reviewed in [96,97]). Among different TRAFdependent CD40 signal cascades, NFκB is the major transcription factor involved in CD40-mediated B cell proliferation [98] and IgM production [99], whereas p38 MAPK is required for CD40-induced B cell proliferation [100]. There are currently seven types of TRAFs, TRAF1 through TRAF7. All types of TRAFs, except TRAF4 and TRAF7, are directly or indirectly recruited to the cytoplasmic domain of CD40 during CD40L engagement (reviewed in [95]). The consensus binding sites for TRAF1, TRAF2, and TRAF3, are overlapping and located at the distal domain, whereas the binding site of TRAF6 is located at the proximal domain of CD40 [101]. Interestingly, TRAF2 was shown to bind to the non-canonical binding site at the carboxy-terminus of CD40, which responsible for CD40induced B-cell activation, proliferation and differentiation through the activation of NFκB [98,102].

C. TRAF-independent CD40 signaling

Janus family kinases (JAKs), in particular JAK3, is also constitutively bound to the proximal region of CD40 cytoplasmic tail [103]. To date, JAKs are

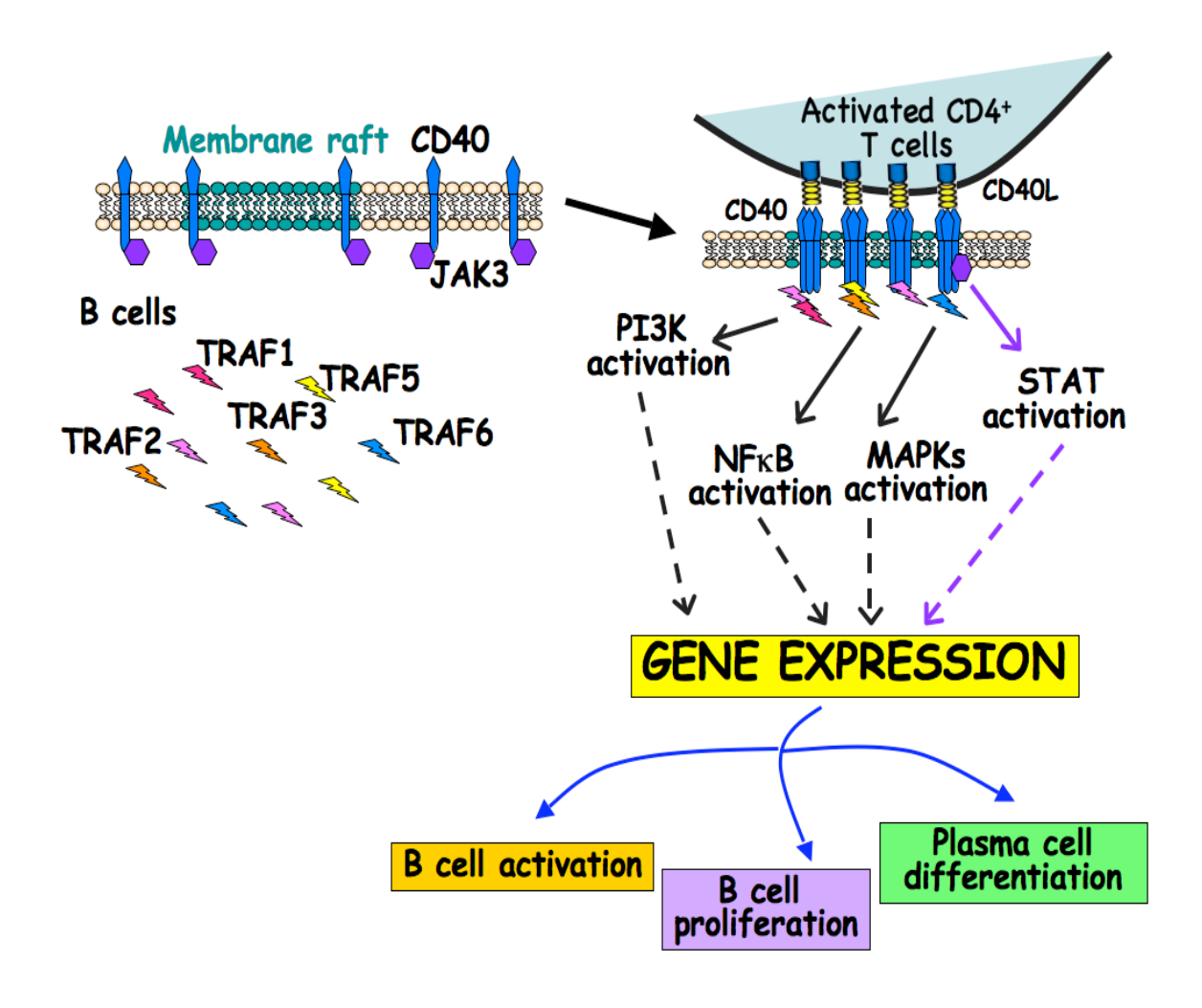


Figure 4. Schematic diagram represents the proposed downstream signaling pathways initiated by the engagement of CD40 in B cells.

The ligation of CD40 by CD40L promotes the trimerization of CD40 in the membrane raft. The trimerization of CD40 signals to B cells through two mechanisms, TRAF-dependent and -independent pathways. In TRAF-dependent pathway, the trimerized CD40 recruits the binding of TRAFs to their cytoplasmic tails. TRAFs then activate several signaling cascades such as PI3K, NF κ B, and MAPKs. In the TRAF-independent pathway, the trimerization of CD40 leads to the activation of JAKs, which are constitutively bound to their cytoplasmic tails. The activated JAKs then phosphorylate STATs. The activation of these signaling pathways regulates the expression of genes involved in B cell activation, proliferation, and differentiation.

composed of four nonreceptor tyrosine kinases (JAK1, JAK2, JAK3, and TYK2) [104,105]. Activated JAKs then phosphorylate signal transducer and activator of transcription (STAT) proteins, which then dimerize and translocate to the nucleus and regulates gene expression There are at least seven STAT proteins (STAT1, STAT2, STAT3, STAT4, STAT5A, STAT5b and STAT6) (reviewed in [106]). The ligation of CD40 induces activation of associated JAK3 leading to the phosphorylation and activation of STAT3 [103] (Figure 4). However, the role of JAK3 in CD40-mediated B cell responses is controversial. For instance, B cells transfected with mutant CD40 that lacks the bind site for JAK3 failed to induce surface expression of CD23, ICAM-1, and LT- α upon activation suggesting a critical role of JAK3 in CD40-mediated gene expression [103]. By contrast, in studies using purified B cells from JAK3-deficient patients, JAK3 is not essential for CD40-mediated B-cell proliferation, isotype switching, or upregulation of aforementioned surface molecules [107]. Further, CD40 ligation results in phosphorylation and activation of STAT6, but not STAT1, in mouse B cells [108].

VI. Role of cytokines, interleukin (IL)-2, -6, and -10, in plasma cell differentiation

Although the CD40 signaling is absolutely required for the development of T-cell dependent humoral immune response, sustained engagement of CD40 prevents the terminal differentiation of activated mature B cells into plasma cells [109,110]. Several studies demonstrated that plasma cell differentiation in

humans requires the presence of several cytokines including, but not limited to, IL-2, -6, and -10 [109,111-115]. Most cytokine receptors lack intrinsic kinase activity, and hence often employ JAKs that are associated with cytokine receptors to activate STAT proteins, which are the main downstream signaling of cytokine receptors (reviewed in [116]).

A. IL-2

IL-2 has been shown to play essential role from the initial stage of B cell activation through the final stage of B cell differentiation into plasma cells. The addition of IL-2 at the initiation of culture was able to reverse the suppression of pokeweed mitogen-induced T cell-dependent differentiation of B cells by cyclosporin A [117]. Further, exogenous IL-2 enhanced the proliferation and differentiation of B cells into antibody secreting cells after antigenic stimulation by *Staphylococcus aureus* Cowan strain I (SAC) [118,119], influenza virus [120], and hepatitis B virus in humans [121].

IL-2 receptor (IL-2R) is comprised of three subunits: IL-2R α , IL-2R β , and IL-2R γ (the common cytokine receptor γ chain). There are three classes of IL-2R, the low, intermediate, and high affinity receptors, which are defined by combinations of aforementioned subunits. The low affinity receptors contain only the IL-2R α ; intermediate affinity receptors contain IL-2R β and IL-2R γ ; high affinity receptors contain all three chains (reviewed in [122]). All three subunits of IL-2R were upregulated in human B cells and several B cell lines upon activation with different stimuli [118,123-125]. The binding of IL-2 to high affinity IL-2R

expressed on antigen activated B cells induced expression of IgJ mRNA mediated by downregulation of PAX5 mRNA, a negative regulatory motif in the *IGJ* promoter [7,126,127]. Recently, IL-2 treatment induced phosphorylation of STAT5 and ERK MAPK in primed human B cells with CD40L, CpG, and F(ab')₂ anti-Ig (IgA+IgG+IgM) [125]. However, IL-2-induced ERK signaling, but not STAT5, was responsible for plasma cell differentiation, at least in part, through the downregulation of BACH2, a transcriptional repressor of *PRDM1*, the gene that encodes Blimp1 [125].

B. IL-6

IL-6 has been identified as a B cell-differentiation-inducing factor, which is important in the terminal differentiation of B cells to antibody secreting cells [128,129]. IL-6-deficient mice were defective in the T-cell dependent IgG antibody response against vesicular stomatitis virus [130]. Consistent with the aforementioned observation, IL-6 overexpressing transgenic mice developed plasmacytosis and a massive increase in polyclonal IgG1 [131]. Further, IL-6 was shown to regulate the growth and development of plasma cell neoplasia [132].

The IL-6 receptor is comprised of two polypeptide chains, a ligand specific receptor and a common signal transducer, gp130 [133]. IL-6 treatment induced the phosphorylation of STAT3 in primary human B cells [134] and ERK MAPK in human B cell line AF10 [135] likely through the activation of gp130-associated JAKs (JAK1, JAK2, and Tyk2) [136-141]. In addition, SHP-2 has been

demonstrated to be responsible for the activation of ERK MAPK induced by IL-6 in murine pro B-cell line (BAF-B03) [142], and hepatocellular carcinoma cell line (HepG2) [143,144]. Although the molecular mechanism by which IL-6 induces plasma cell differentiation are not well established, STAT3 activation is thought to play a central role in cell survival and cell-cycle progression induced by the IL-6 family of cytokines (reviewed in [145]). STAT3 activation results in the upregulation of various genes involved in cell survival and proliferation; such as Pim-1, Bcl-2, Bcl-XL Mcl-1, cyclin D, and c-Myc [146-148]. Further, STAT3 is involved in the upregulation of Blimp1 [149].

C. IL-10

IL-10 is a potent cofactor for proliferation of human B cells activated either by anti-CD40 plus anti-IgM or CD40 cross-linking [112,150]. The effect of IL-10 on B cell survival was also demonstrated as IL-10 treatment prevented the spontaneous death of human splenic B cells in vitro [151]. IL-10 also acts as a plasma cell differentiation factor for B cells stimulated by either anti-CD40 [152], activated T cells [153] or follicular dendritic cell-like cell line [154]. Further, blocking IL-10 suppressed plasma cell differentiation and isotype switching induced by anti-CD40 plus anti-IgM by decrease IgG, IgA, and IgM production [111].

The IL-10 receptor is composed of at least two subunits, IL-10R1 or IL-10R α and IL-10R2 or IL-10R β , that are members of the interferon receptor (IFNR) family (reviewed in [155]). The IL-10/IL-10R interaction activated STAT1,

STAT3, and STAT5, most likely through the activation of JAK1 and TYK2, but not JAK2 and JAK3 in murine pro-B cell line [156,157]. In humans, IL-10 treatment resulted in the activation of several transcription factors, of which STAT1 and STAT3 in B cell chronic lymphoid lymphoma [158] and c-fos in human B cells [159]. IL-10 treatment also induces the expression of anti-apoptotic protein, bcl-2, in resting human B cells [151] or SAC-activated human B cells [160]. Further, naïve B cells derived from patients with an inactivating mutation in STAT3, but not STAT1, showed the profound defects in plasma cells differentiation induced by CD40L plus IL-10 or IL-21 through impairment of Blimp1 and XBP1 upregulation [161].

VII. Δ^9 -tetrahydrocannabinol (Δ^9 -THC) and cannabinoid receptors

A. Cannabinoids and Δ^9 -THC

The term cannabinoids originally described compounds extracted from the plant, *Cannabis sativa*. In 1964, Gaoni and Mechoulam first elucidated the chemical structure of Δ^9 -THC, the main psychoactive congener present in the cannabis plant [162]. The term cannabinoids refer to a group of compounds that are structurally related to Δ^9 -THC or that bind to cannabinoid receptors. There are three general types of cannabinoids: plant-derived, synthetic and endocannabinoids (Figure 5).

Plant-derived cannabinoids

Endocannabinoids

Synthetic cannabinoids

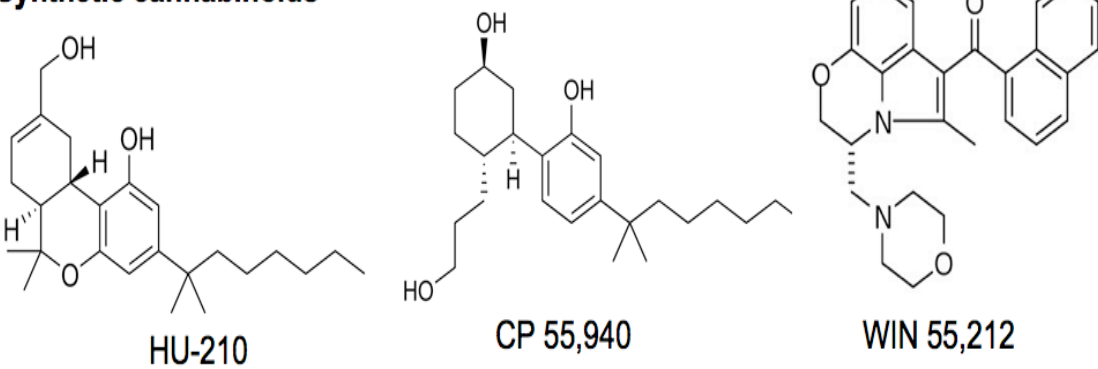


Figure 5. Chemical structures of cannabinoid compounds.

Most plant-derived cannabinoids, such as Δ^9 -THC, CBN, and CBD, contain dibenzopyran ring as a base structure. Endocannabinoids, anadamide and 2-AG, are derivatives of long-chain polyunsaturated fatty acids. Synthetic cannabinoids are classified into two groups. The first group shares structural similarity with naturally cannbinoids such as HU-210 and CP 55,940. Another group contains aminoalkylindole structure such as WIN 55,212.

There are at least 60 plant-derived cannabinoids, of which Δ^9 -THC, cannabinol (CBN), and cannabidiol (CBD) are the most abundant and most These naturally occurring plant-derived extensively characterized [163]. cannabinoids vary extensively in their biological activity, which is attributable in their respective binding affinity for cannabinoid part. to receptors. Endocannabinoids, the endogenous ligands of cannabinoid receptors, are fatty acid amides produced by humans and animals. Thus far. Narachidonoylethanolamine (anandamide) and 2-arachidonoylglycerol (2-AG) are the most extensively characterized endocannabinoids (reviewed in [164]). Synthetic cannabinoids are compounds that have structural similarity to natural cannabinoids or substances with structural features, which allow binding to one of the known cannabinoid receptors such as HU-210 and CP 55,940, which share structural similarility to Δ^9 -THC, and WIN 55,212, which has markedly different structure, but is more potent than naturally-occuring compounds [165].

For centuries, the preparations from *Cannabis sativa* such as marijuana, hashish, and hashish oil, have been used both medicinally and recreationally (reviewed in [166]). However, marijuana, hashish, and hashish oil are schedule I control substances in the U.S. since 1914 [167]. To date, marijuana is the most widely used illicit drug worldwide of which the USA is one of the countries with the highest prevalence of marijuana use (14.1%) among population aged 15 to 64 [168]. Furthermore, the Food and Drug Administration (FDA) has approved a synthetic Δ^9 -THC (Dronabinol or Marinol[®]) for treatment of chemotherapy-

induced nausea and vomiting in cancer patients as well as for treatment of weight loss in AIDS patients [169]. While marijuana is not an FDA-approvedmedicine, 18 states and the District of Columbia have currently legalized its medical use [170]. Sativex[®], a whole-plant cannabis extract, was recently approved for treatment of neuropathic pain and spasticity in multiple sclerosis in the United Kingdom, Spain, Germany, Denmark, the Czech Republic, Sweden, New Zealand and Canada. In the US, Sativex is currently in phase III trials for cancer pain treatment [171].

B. Cannabinoid receptors

The first cannabinoid receptor, now referred to as CB1, was identified and cloned from rat cerebral cortex cDNA library in 1990 [172]. Soon after, the second cannabinoid receptor, termed CB2, was cloned from the human leukemia cell line, HL-60, in 1993 [173]. Although much evidence supports the existence of non-CB1/CB2 cannabinoid receptors, only CB1 and CB2 are definitively classified as cannabinoid receptors currently (reviewed in [174,175].

Both CB1 and CB2 are members of the G protein-coupled receptor (GPCR) superfamily. Human CB1 and CB2 share an overall identity of 44% and ranging from 35% to 82% in the transmembrane regions [176]. CB1 is more conserved between species. For example, human CB1 shares 90% and 96% identity with mouse and rat, respectively; whereas human CB2 shares 82% and 56% identity to mouse and rat, respectively [177-179]. CB1 is found throughout the body, but is most abundantly expressed in the central nervous system,

especially in hippocampus, basal ganglia, and cerebellum, which correlates well with the psychotropic effects of Δ^9 -THC and have the highest expression levels [180,181]. CB2 is mainly found in peripheral tissues and is highly expressed in spleen and cells of the immune system. Human B cells have the highest level of *CNR2* mRNA, whereas CD4⁺ T cells have relative low level of *CNR2* mRNA [180]. Importantly, under certain condition and disease states, both CB1 and CB2 can be up- and down-regulated in particular cell types (reviewed in [182]). Examples include induction of *CNR1* gene transcripts (mRNA) in activated human T cells [183], down-regulation of CB1 in human colorectal cancer [184], and up-regulation of CB2 in human inflammatory bowel disease [185]. In addition, there is induction of both *CNR1* and *CNR2* mRNA in peripheral blood mononuclear cells (PBMCs) derived from chronic marijuana smokers [186].

In human populations, several reports demonstrated the divergence of the genes encoding for CB1 and CB2. To date, at least five distinct variant exonic structures were identified in human CB1 gene [187]. Both the CB1a and CB1b show altered ligand binding activity compared with CB1 [188]. The length of microsatellite (AAT)_n and single nucleotide polymorphisms at intron 2 in the *CNR1* gene was associated to susceptibility to drug abuse [26,189]. Polymorphisms in the human *CNR2* gene have been identified as well, of which 188-189 GG/GG dinucleotide polymorphism was associated to osteoporosis in several ethnic groups [190,191] and autoimmune diseases [192].

C. Signal transduction activated by CB1 and/or CB2

As members of GPCR superfamily, CB1 and CB2 were initially reported to couple to inhibitory heterotrimeric G proteins ($G\alpha_{i/o}$) since those cannabinoid-mediated responses were blocked with pertussis toxin (PTX) treatment [172,193-197]. Stimulation of CB1 and CB2 by various cannabinoids inhibited adenylyl cyclase (AC) activity resulting in decreased levels of cAMP in several cell and tissue preparations [172,193,194,196-201]. However, CB1, but not CB2, was shown to also interact with stimulatory heterotrimeric G proteins ($G\alpha_s$) resulting in activation of AC [202-207]. The differential effects of CB1-mediated AC activity could also be attributed to the specific isoform(s) of AC, of which AC types I, V, VI and VIII were inhibited, whereas types II, IV, and VII were activated following treatment with HU-210 and WIN 55,212-2 [208].

The coupling of CB1 and CB2 to mitogen-activated protein kinase (MAPK) pathway has been demonstrated in several cell types. Treatment with CP-55940, Δ^9 -THC and WIN 55212-2 activated p42/p44, the extracellular signal-regulated kinase subgroup of the mitogen-activated protein kinases (ERK MAPK), in CHO cells expressing the CB1 receptor and this effect was blocked by a CB1 antagonist or PTX [209]. Similarly, CB2 is involved in cannabinoid-mediated activation of ERK MAPK in CHO cells expressing the CB2 receptor [210] and HL-60 cells [211]. Further, CB1 and CB2 activation in human prostate epithelial PC-3 cells facilitated the phosphorylation of ERK MAPK [212]. Interestingly, WIN

55,212-2 and CBN suppressed ERK MAPK activation instimulated mouse splenocytes [213]. The differential effect of cannabinoids on the regulation of the MAPK signaling cascade may be explained by the requirement of cellular activation. Although the mechanisms underlying the regulation of MAPK signaling by cannabinoids have not been fully elucidated, MAPK activation by cannabinoids mediated, at least in part, through activation of PI3K/Akt pathway, and the subsequent activation of Raf, a MAPKKK [212,214,215]. In addition, a decrease in PKA activity as a result of cannabinoid-mediated decreases in cAMP level have shown to enhance MAPK activation in breast cancer cells (MCF-7) [216], neuroblastoma cells (N1E-115) [217], and rat hippocampal slices [218].

Voltage-gated ion channels, primarily calcium (Ca²⁺) and/or potassium (K⁺) channels, were also shown to be a target of CB1 stimulation. For instance, WIN 55,212-2 and/or CP 55,940 inhibited N-type Ca²⁺ channels in neuroblastoma cells (NG108-15 cells), CB1-transfected rat ganglion neurons, and hippocampus [196,219-222]. Anandamide inhibited P/Q-type Ca²⁺ channels in pituitary tumor cells (AtT-20) [223] and rat cerebellar brain slices [224]. WIN 55,212-2 inhibited L-type Ca²⁺ channels in cat cerebral arterial smooth cells [225] and retinal slices from larval tiger salamander [226]. Additionally, WIN 55,212-2 activated A-type, but inhibited D-type and M-type K⁺ channels in hippocampal neurons [227,228]. G protein-coupled inwardly rectifying K⁺ (GIRK) channels

were also activated by cannabinoids in a CB1-dependent manner [223,229,230]. It is noteworthy that CB2 receptors are believed not to directly modulate ion channel function, as WIN 55,212-2 did not alter the GIRK1/4 current in both AtT-20 cells and Xenopus oocytes transfected with CB2 and GIRK1/4 [229,231]. CB2 also did not modulate the activity of Q-type Ca²⁺ channels in AtT-20 cells expressing CB2 [231].

Ca²⁺ signaling has been demonstrated to be modulated by the activation of CB1 and/or CB2 in several models. CB1 coupled to $G_{\text{i/o}}$ was shown to be involved in cannabinoid-mediated increases in [Ca2+], in neuroblastoma cells (NG108-15) [232], primary culture of striatal astrocytes [233], human endothelial cells [234], canine kidney cells [235], and hamster smooth muscle cell line (DDT₁ MF-2 cells) [236]. Further, anandamide and 2-AG, acting via PTX-sensitive CB2, induced the increase of [Ca2+]; in calf pulmonary endothelial cells [237] and HL-60 cells [238], respectively. Anandamide-mediated increase in [Ca2+]; was mediated, at least in part, by the G protein-dependent activation of PLCB and thereby IP3-mediated release of Ca²⁺ from internal stores [237]. However, CB1 and CB2 were not involved in Δ^9 -THC- or CBN-induced increases in $[Ca^{2+}]_i$ in resting mouse splenic T cells and/or the human peripheral blood acute lymphoid leukemia (HPB-ALL) T cell line [239,240].

D. Pharmacokinetics of Δ^9 -THC

Inhalation through smoking a cannabis cigarette, mouth spray of Sativex, or oral administration of Marinol in capsules or baked foods or liquid are the major routes of administration and delivery of Δ^9 -THC (reviewed in [241]). Absorption through inhalation is very rapid with peak Δ^9 -THC plasma concentration of 100-200 ng/mL within first 10 minutes after smoking. However, plasma Δ^9 -THC concentrations vary depending on the potency of marijuana and the manner in which the drug is smoked [242]. With oral administration, absorption is slower with much lower (approximately 3-4 ng/mL) and peak Δ^9 -THC plasma concentration is delayed to between 1-5 hours due to extensive first pass metabolism (reviewed in [241]). Due to its lipophilicity, Δ^9 -THC immediately distributes from blood to tissues resulting in a large volume of distribution ranging from 1 to 10 L/kg [243,244]. In addition, Δ^9 -THC rapidly crosses the placenta [245] and also distributed to breast milk [246]. The Δ^9 -THC concentration in human milk was 8.4 times higher than in plasma [246].

 Δ^9 -THC is primarily metabolized by hydroxylation and oxidation via cytochrome P450 in the liver [247-249]. 11-hydroxy-THC, a monohydroxylated compound, is the major metabolite found in humans and has equipotent psychoactivity. The 11-hydroxy-THC is further oxidized to the 11-nor-9-carboxy-THC (THC-COOH), which is not psychoactive [250,251]. The acid metabolites of

 Δ^9 -THC are mainly excreted in feces (approximately 65%) [244,252], and in the urine as conjugated glucuronic acids and free THC-hydroxylated metabolites [253-255].

E. Pharmacodynamics of Δ^9 -THC

The physiological effects of Δ^9 -THC are mediated through its agonistic and antagonistic actions at the specific sites (reviewed in [241]). Δ^9 -THC binds both known cannabinoid receptors with similar K values in the nanomolar range. However, Δ^9 -THC has relatively low cannabinoid receptor efficacy with higher efficacy at CB1 than CB2, and behaves as a partial agonist to both receptors (reviewed in [256]). In addition, the binding of Δ^9 -THC to cannabinoid receptors may interfere the physiological responses mediated by endocannabinoids, the endogenous ligands of cannabinoid receptors in humans and animals (reviewed in [257]). Some effects of Δ^9 -THC have been demonstrated that are not mediated by CB1 and/or CB2, supporting the presence of cannabinoid receptor subtypes that have not yet been identified [257]. This section focuses on the effect of Δ^9 -THC on central nervous system (CNS), cardiovascular system, reproductive system, and gastrointestinal system. The effects of Δ^9 -THC on the immune system are discussed in more details in the following section.

In the CNS, Δ^9 -THC was shown to modulate the release or reuptake of neurotransmitters. For instance, Δ^9 -THC increased the CB1-mediated release of acetylcholine in rat hippocampus, of acetylcholine, glutamate and dopamine in rat

prefrontal cortex, and of dopamine in mouse and rat nucleus accumbens [258-262], but decreased gamma-aminobutyric acid uptake in the globus pallidus [263]. The release of dopamine by Δ^9 -THC most likely explains the euphoria produced by Δ^9 -THC in humans. In animal models, a characteristic "tetrad" including antinociception, hypothermia, hypomotility, and catalepsy, represents the CNS effect after *in vivo* administration of Δ^9 -THC [264]. Additional, Δ^9 -THC caused impairment in psychomotor functions including learning and memory (reviewed in [265,266]) and driving a car or piloting an aircraft [267-269].

In the cardiovascular system, single does administration of Δ^9 -THC induced tachycardia [270], increased cardiac output [271], and reduced platelet aggregation [272]. However, prolonged Δ^9 -THC ingestion significantly decreased heart rate and blood pressure [270].

In the reproductive system, Δ^9 -THC was associated with impairment of menstrual cycle and ovulation through a decrease in follicle-stimulating hormone and luteinizing hormone (reviewed in [273]). Further, testosterone synthesis from Leydig cells and sperm count was reduced by Δ^9 -THC (reviewed in [273]). In pregnant rhesus monkeys, administration of Δ^9 -THC (2.5 mg/kg/day) increased abortions, as well as produced a rapid decrease in chorionic gonadotropin and progesterone concentrations, and stillbirths [274].

In the gastrointestinal system, Δ^9 -THC was shown to prevent emesis [275,276] . Δ^9 -THC also inhibited gastrointestinal motility in both rodents [277] and humans [278]. Additionally, Δ^9 -THC at doses used for preventing chemotherapy-induced nausea and vomiting significantly delays gastric emptying [279].

F. Toxicity of Δ^9 -THC

Acute oral administration of Δ^9 -THC caused lethality only in rat at a median lethal dose of 800-900 mg/kg. In rats toxicity was characterized by severe hypothermia, and other central effects such as ataxia, muscle tremors, prostration, and rapid weight loss. Although no deaths were associated with oral administration of maximum oral Δ^9 -THC doses in dogs and monkeys, both species developed toxic signs including drowsiness, ataxia, and abnormal eating pattern [280]. Acute fatalities following cannabis use in human has been inconclusive; however, Δ^9 -THC was associated possibly with sudden death caused by myocardial infarction [281,282]. Adverse effects of marijuana use are controversial, but are mainly associated with decreased motor coordination, impaired cognitive function, and alteration in cardiovascular system including tachycardia, postural hypotension, and supine hypertension [283-286]. Chronic administration of Δ^9 -THC results in development of reversible tolerance to the

cardiovascular, psychological, skin hypothermic, and behavioral effects of Δ^9 -THC in human [252,287].

VIII. Immunomodulatory properties of Δ^9 -THC

Administration of Δ^9 -THC *in vivo* results in perturbation of host immune resistant against viral infection [288], bacterial infection [289,290], or tumor challenges [291]. These studies show that Δ^9 -THC modulates multiple immune cell populations. However, this section focuses principally on the effect of Δ^9 -THC on T cell and B cell function, which are both critical in mounting T cell-dependent humoral immune responses.

A. T cells

Many studies have shown that Δ^9 -THC has anti-inflammatory activity, partly through suppression of T cell function (reviewed in [292]). Specifically, this laboratory has identified a number of T cell-mediated responses modulated by Δ^9 -THC including proliferation, production of cytokines, expression of costimulator Τ cell molecules, and responses to specific antigens [116,288,293,294]. Importantly, the effects of Δ^9 -THC on T-cell functions depend on experimental conditions, such as concentrations of Δ^9 -THC, cell types, and specific or magnitude of immune stimuli.

Numerous laboratories have reported that lymphoproliferative responses of mouse splenocytes to T cell specific mitogens (concanavalin A, ConA; or phytohemagglutinin, PHA) were inhibited by cannabinoids, including Δ^9 -THC [295-298]. In addition, Δ^9 -THC was shown to suppresse the proliferation of mouse splenic CD4⁺ T cells stimulated by allogeneic class II histocompatibility Interestingly, Δ^9 -THC positively or negatively modulated antigens [298]. proliferation of mouse splenic CD8⁺ T cells. For example, Δ^9 -THC (< 15.9 μ M) can either enhance or suppress proliferation of mouse splenic CD8⁺ T cells stimulated by anti-CD3 antibodies or mitogens (ConA or PHA), respectively [297]. The same group also reported that CD8⁺T cells derived from lymph nodes were more resistant to the modulation by Δ^9 -THC, as demonstrated by the fact that Δ^9 -THC did not affect the proliferation of lymph node-derived T cells upon stimulation with anti-CD3 antibody or PHA [296]. Another study reported that Δ^9 -THC enhanced mitogen-induced proliferation of mouse splenocytes or human lymphocytes at low concentration (< 3.2 μ M), and was suppressive at high concentration (6.4 – 25.6 μ M) [295]. In addition, the magnitude of stimulation plays an important role in Δ^9 -THC-mediated modulation of mouse splenic T cell proliferation, in which $\Delta^9\text{-THC}$ decreased or increased the percentage of proliferating CD8⁺ T cells under condition where CD8⁺ T proliferation was high or

low, respectively [299]. CB1 and CB2 did not play a role in Δ^9 -THC-mediated suppression of PHA-induced lymphoproliferative response in mouse [294].

Activation of helper CD4⁺ T cells induces expression of many costimulatory molecules as well as cytokines [300]. Cytokines derived from helper $CD4^{+}$ T cells are classified into 2 groups, Th1 (e.g. IL-2, IFN- γ and TNF- α) or Th2 (e.g. IL-4, IL-5 and IL-10). Th1 cytokines promote and regulate cell-mediated immunity to protect the host against intracellular pathogens; whereas Th2 cytokines promote and regulate humoral immunity which confers protection against extracellular pathogens such as bacteria [300]. Disruption of the Th1/Th2 cytokine balance by Δ^9 -THC was demonstrated in both animal and human models. In vivo, a single dose or chronic treatment with Δ^9 -THC in mice resulted in lower serum concentration of IL-2 and IFN- γ [290,301]. Treatment with Δ^9 -THC decreased steady-state levels of mRNA encoding for Th1 cytokines, while increasing mRNA levels for Th2 cytokines in human T cells stimulated with allogeneic dendritic cells [302]. Interestingly, cytokine production by T cells has been shown to be positively or negatively regulated by Δ^9 -THC depending on the magnitude of stimulation. For instance, Δ^9 -THC suppressed both IL-2 and IFN-y production by mouse splenocytes induced by optimal stimulation with PMA/lo or anti-CD3/CD28 [299]. In contrast, Δ9-THC enhanced IL-2 production by mouse splenocytes induced by suboptimal stimulation with anti-CD3/CD28 [299]. CB1 and CB2 did not play a role in Δ^9 -THC-mediated suppression of PMA/Io-induced IL-2 and IFN- γ production [294]. In addition, Δ^9 -THC suppressed the expression of inducible co-stimulatory molecules (ICOS) in activated T cells regardless of the mode of cellular activation [303].

The functions of cytotoxic T lymphocytes, which are effector CD8⁺ T cells that play an important role in antiviral and antitumor immune responses, also exhibited marked sensitivity to modulation by Δ^9 -THC. For example, administration of Δ^9 -THC *in vivo* suppressed the cytolytic activity of mouse splenic cytotoxic T lymphocytes to herpes simplex virus type 1-infected cells [304,305]. Δ^9 -THC also decreased the number of CTL effector cells, but not IFN- γ production from CTL induced by *in vitro* allogenic model using tumor cells independently of CB1 and CB2 [306]. Interestingly, CTL responses directed specifically against HIVgp120 antigens were differentially modulated by Δ^9 -THC depending on the magnitude of stimulation [299].

Several contributing mechanisms responsible for immune suppression induced by cannabinoids have been demonstrated. For one, immediate (< 15 min) suppression of intracellular cAMP by Δ^9 -THC have been suggested as a mechanism responsible for cannabinoid-mediated immunosuppression [307]. In contrast, Δ^9 -THC-mediated increase of cAMP at later time points, 2 h after T cell

stimulation, decreased the dephosphorylation of Lck in response to T cell receptor activation, which is necessary for the subsequent initiation of T cell receptor signaling [308]. CB1 and CB2 were shown to be involved in Δ^9 -THCmediated impairment of proximal TCR signaling, as evidenced by attenuation of the suppressive effect of Δ^9 -THC, in the presence of CB1 and CB2 antagonists [308]. Further, cannabinoids, including Δ^9 -THC, were shown to increase $[Ca^{2+}]_i$ in resting T cells and mouse splenocytes [240,299,309] or further augment Ca²⁺ elevation in activated mouse splenocytes [299]. The elevation of [Ca2+] by cannabinoids occurred primarily via influx of extracellular calcium, which was mediated by TRPC1 [309,310]. The specific downstream signaling pathways affected by Δ^9 -THC-mediated Ca²⁺ elevation remain to be elucidated, but likely involve MAPK. Indeed, CBN, another cannabinoid sharing structural similarity to Δ^9 -THC, was shown to suppress the phosphorylation of ERK MAPK [213]. Interestingly, Δ^9 -THC increased $[{\rm Ca}^{2+}]_i$ independently of CB1 and CB2 [239], T cell activation [240] or when activated the magnitude of stimulation [299]. Additionally, impairment of transcription factors, NFAT, NFkB, and AP1, by cannabinoids was shown to be a potential mechanism responsible for suppression of both cytokine production and expression of co-stimulatory molecules by activated T cells. For instance, the differential effects of CBD on cytokine production were correlated with effects on NFAT nuclear translocation

[299]. Attenuation of ICOS expression in activated mouse T cells were mediated, at least in part, through impairment of NFAT signaling, as evidenced by decreased NFAT reporter gene activity after treatment with Δ^9 -THC [303]. Impairment of IL-2 production by CBN was attributed, at least in part, to suppression in the DNA binding activity of NF κ B, p65 and c-ReI, in mouse T cells [311].

B. B cells

In general, the majority of attention concerning immune modulation by cannabinoids has been on T cells and cells of the myeloid lineage with investigations of B cells being relatively limited. However, cannabinoids have been shown to modulate B cell function including proliferation and humoral immune response. Similar to T cells, the effect of Δ^9 -THC on B-cell function depends on the specific experimental conditions.

 Δ^9 -THC at micromolar concentrations suppressed mouse splenic B cell proliferation induced by polyclonal B cell activator, lipopolysaccharide (LPS) [312]. Interestingly, LPS-induced B cell proliferation is more sensitive to suppression by Δ^9 -THC than ConA- or PHA-induced T cell proliferation in mouse splenocytes [312]. In addition, Δ^9 -THC at nanomolar concentrations enhanced human B-cell proliferation induced by cross-linking of surface Igs or ligation of the CD40. This enhancement was not mediated by CB1, as a CB1 antagonist did not reverse the observed effect [313]. Moreover, CP 55,940 enhanced the

proliferation of both naïve and GC B cells induced by the ligation of CD40. This enhancement was blocked by the CB2 receptor antagonist, but not by the CB1 receptor antagonist supporting an involvement of CB2 receptors during B cell differentiation [314].

The effect of cannabinoids on humoral immune responses, an effector function of B cells, has been extensively characterized, of which the primary humoral immune responses against T-cell dependent antigens, sheep red blood cells (sRBC), is one of the most sensitive immune responses to suppression by cannabinoids [298,315]. These initial studies suggested that T cells are more sensitive target to modulation by cannabinoids than B cells, and are also primarily responsible for Δ^9 -THC-mediated suppression of IgM response against sRBC. Importantly, Δ^9 -THC was found not to suppress the number of IgM antibody forming cells induced either by T-cell independent antigen, DNP-Ficoll, However, subsequent study or the polyclonal B cell activator, LPS [298]. demonstrated that B cells can be modulated by Δ^9 -THC in response to ligation of CD40 in the presence of cytokines, IL-2, -6, and -10 (CD40L plus cytokine) [294]. Additionally, studies in humans emphasized that humoral immune responses, either primary or secondary, are sensitive to modulation by cannabinoids, although there is controversy concerning which immunoglobulin isotypes. The first study showed that chronic marijuana smokers had normal serum IgG, IgA, and IgM levels, although IgE levels were increased [316]. In contrast, a subsequent study showed that chronic marijuana use was associated with a

decrease in serum IgG, an increase in serum IgD, but no change in serum IgA and IgM [317]. One additional study demonstrated that oral ingestion of marijuana decreased serum IgG and IgM levels [318].

The involvement of CB1/CB2 in modulation of primary humoral immunity by Δ^9 -THC depends on the types of stimuli. Δ^9 -THC-mediated suppression of IgM responses induced by either sRBC *in vivo* or by CD40L plus cytokine *in vitro* was dependent of CB1/CB2 [294]. Interestingly, LPS-induced IgM responses were refractory to suppression by Δ^9 -THC, regardless of genotype [294]. It is noteworthy that the expression of CB2 was modulated during B cell differentiation from naïve to memory B cells. The lowest expression of CB2 at both the protein and mRNA level was observed in GC proliferating B cells [314]. Moreover, CB2-deficient mice (CB2- I_*) have defect in T cell-independent humoral immune response; however, the authors did not include T cell-dependent antigens [319]. Collectively, these findings strongly supported an involvement of CB2 during B cell differentiation.

The molecular mechanisms responsible for Δ^9 -THC-medited modulation of B-cell function remains unclear in spite of a number of signaling pathways in B cells being identified to be altered in the presence of cannabinoids. For example, Δ^9 -THC suppressed adenylate cyclase activity in B cells, which presumably is due to negative coupling of CB1 and CB2 to this membrane associated enzyme. Moreover, treatment with the membrane-permeable cAMP analogs (dibutyryl-

cAMP and 8-bromo-cAMP) reversed Δ^9 -THC-mediated suppression of the anti-sRBC IgM response. These finding suggested that suppression of T-cell dependent IgM response by Δ^9 -THC was mediated, at least in part, through impairment of adenylate cyclase [311].

IX. Rationale

In addition to the fact that marijuana is the most commonly used illegal drug in the United States, the Food and Drug Administration has approved a synthetic Δ^9 -THC (Marinol[®]) for treatment of chemotherapy-induced nausea and vomiting in cancer patients as well as for treatment of weight loss in AIDS patients [169]. This raises concerns about: 1) the human health impact as demonstrated by in vivo and in vitro studies suggesting cannabinoids can influence regulation of the immune system; and 2) undesirable immunosuppressive side effect(s) of these drugs in patients whose immune system has already been compromised.

As described earlier, Δ^9 -THC has been demonstrated to modulate a variety of immune responses, of which the primary IgM response against the T cell-dependent antigen, sheep erythrocytes (sRBC), is one the most sensitive immune response by Δ^9 -THC [294,298]. Importantly, Δ^9 -THC was found not to suppress the number of IgM antibody forming cells induced either by T cell-independent antigen, DNP-Ficoll, or the polyclonal B cell activator, LPS [298].

These initial studies suggested that T cells are a more sensitive targets to modulation by cannabinoids than B cells, and are also primarily responsible for Δ^9 -THC-mediated suppression of IgM response against sRBC. However, a subsequent study demonstrated that B cells can be modulated by Δ^9 -THC in response to ligation of CD40 in the presence of cytokines, IL-2, -6, and -10 in the absence of T cells [294]. This study suggested that B cells are also affected by Δ^9 -THC, but only under the condition that requiring CD40-CD40L interaction.

To date, there is still only a remarkably small set of studies that have assessed the effect of Δ^9 -THC on effector function of both primary human T cells and B cells. Furthermore, the molecular basis of Δ^9 -THC-mediated suppression of T cell-dependent antibody responses remains largely unknown. Therefore, this dissertation research was particularly focused on elucidating, at the molecular level, how Δ^9 -THC suppresses T cell-dependent humoral immune response in humans with emphasis on CD40-CD40L interaction. Taken together, the overarching hypothesis of this dissertation was Δ^9 -THC attenuates the human T cell-dependent IgM antibody response by suppression of CD40L upregulation in activated CD4⁺ T cells and impairment of the CD40-mediated B cell activation. To test this hypothesis, three studies were performed; of which the first two studies focused on T cells, whereas the third study focused on B cells. The first subhypothesis was Δ^9 -THC suppresses CD40L expression by activated primary mouse CD4 $^+$ T cells in CB1/CB2-dependent mechanism. The second subhypothesis was Δ^9 -THC suppresses CD40L expression in activated primary human CD4 $^+$ T cells by impairment of NFAT and NF $_K$ B activity. The third subhypothesis was attenuation of the primary IgM response by Δ^9 -THC in human is mediated by impairment of CD40-induced activation of B cells. An understanding of the mechanisms by which Δ^9 -THC affects the function of human T cells and B cells might allow its expansion for therapeutic use and also provide additional information when making risk to benefit decisions for use in immunocompromised patients.

MATERIALS AND METHODS

I. Reagents

 Δ^9 -THC dissolved in 100% ethanol was provided by the National Institute on Drug Abuse (Bethesda, MD) and was used in the studies focused on T cells. Preliminary data demonstrated that human B cells are very sensitive to ethanol (Figure 6). Therefore, Δ^9 -THC in this study was dissolved in 100% dimethyl sulfoxide (DMSO) for human B cell studies. Unless otherwise noted, all other chemicals were obtained from Sigma-Aldrich (St Louis, MO).

II. Plasmids

GRE-luciferase reporter gene plasmid (pGRE-luc) and the vector control plasmid (pTAL-luc) were purchased from Clontech (Mountain View, CA).

III. Cell culture

HEK293T were purchased from Open Biosystems and maintained in DMEM media (Gibco Invitrogen, Carlsbad, CA) supplemented with 5% Charcoal/Dextran Treated Fetal Bovine Serum (CD-FBS, Hyclone, Logan, UT), 1X HT supplement (Gibco Invitrogen), and the antibiotics Penicillin (100 units/mL)/Streptomycin (100 μ g/mL) (Gibco Invitrogen). Jurkat T cells (clone E6-1) were obtained from American Type Culture Collection (Manassas, VA) and

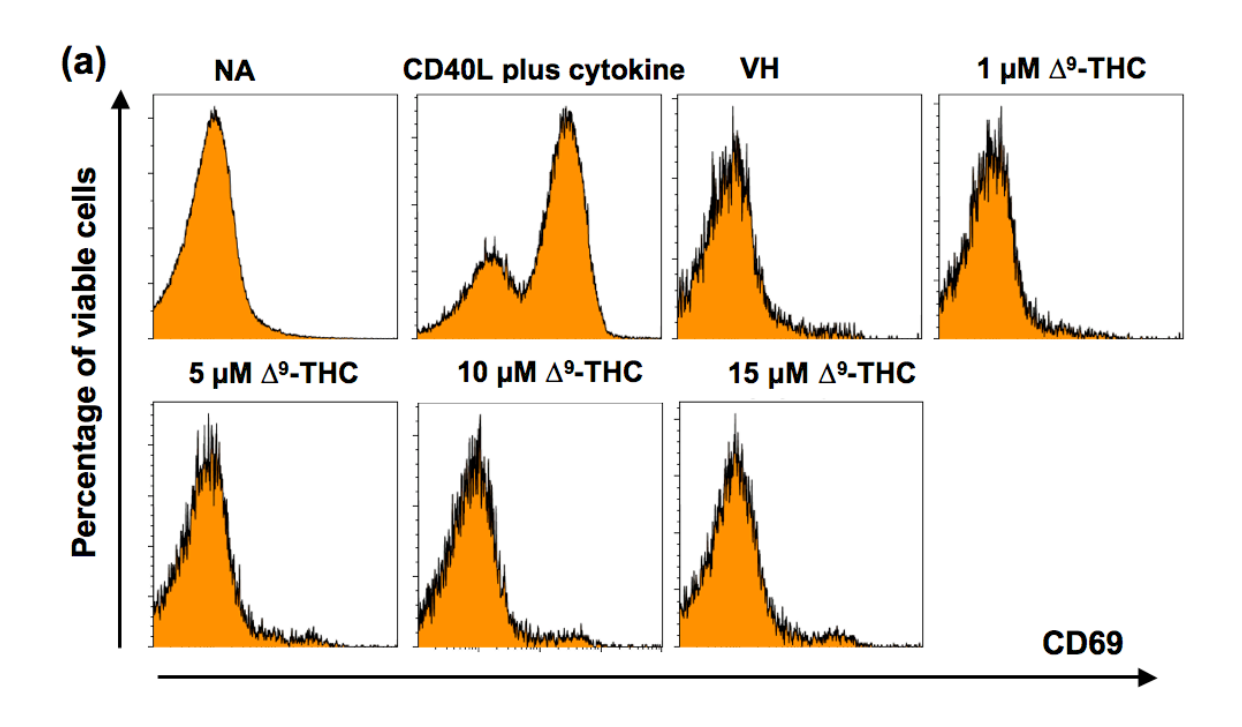
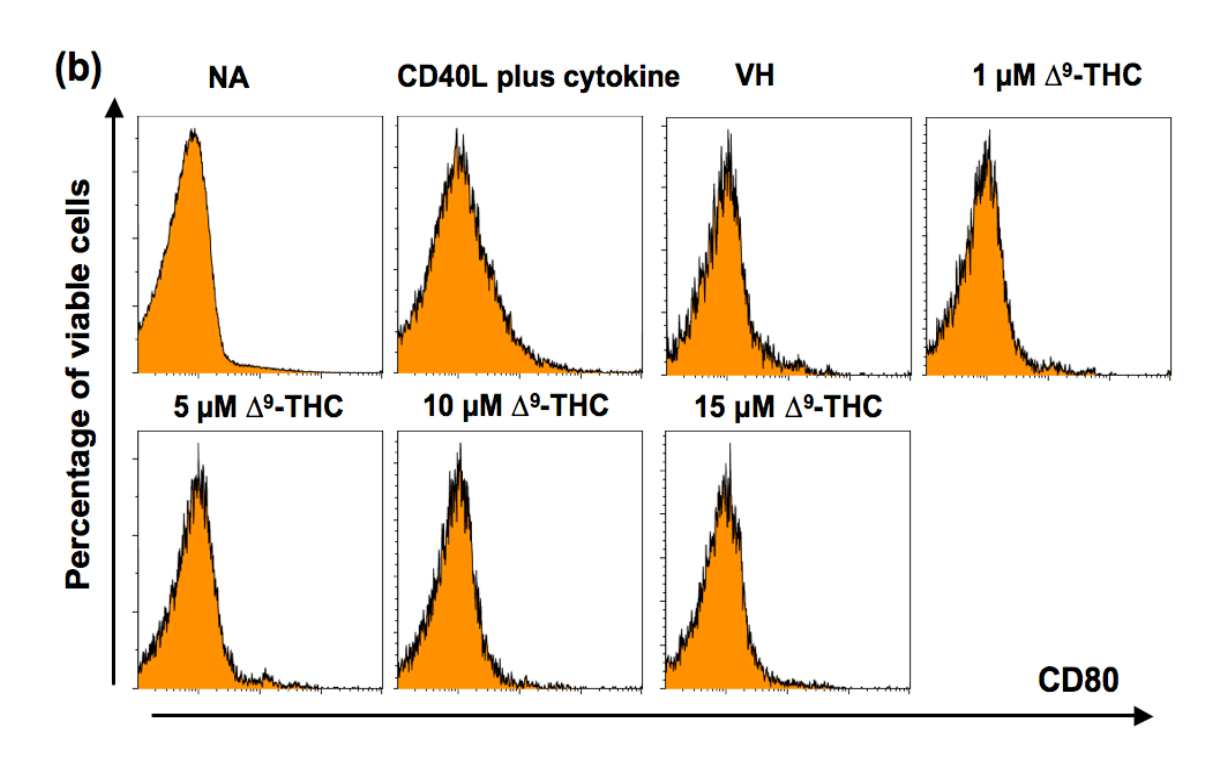
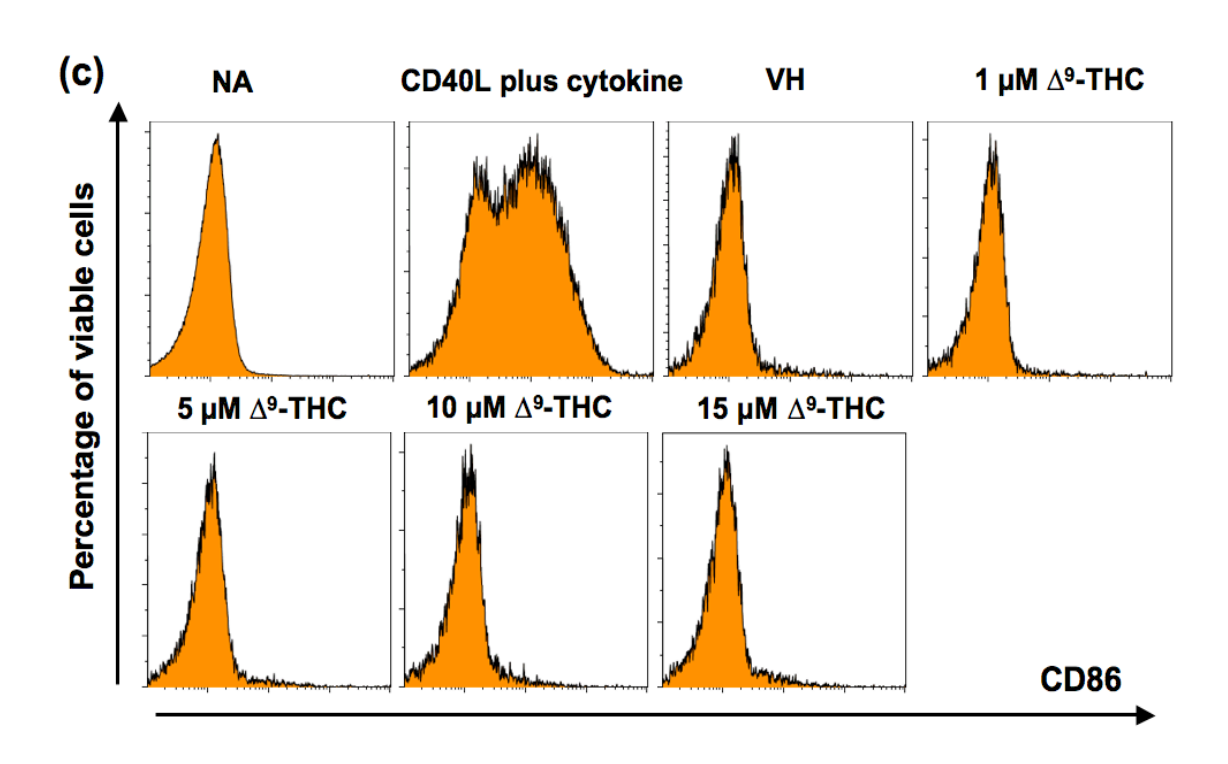


Figure 6. The demonstration that human B cells are sensitive to ethanol.

Studies characterize the effect of Δ^9 -THC demonstrated that 0.01% ethanol (VH in T cell studies) suppressed B cell activation assessed by measuring the surface expression of CD80, CD86, and CD69 (a-c). These results suggested that primary human B cells are sensitive to EtOH treatment. HPB naïve B cells (1x10⁶ cells) were treated with Δ^9 -THC at indicated concentrations or VH (0.1% Ethanol) for 30 min and then cultured with irradiated CD40L -L cells (1.5 x 10³ cells/well) in the presence of recombinant human IL-2 (10 U/mL), IL-6 (100 U/mL), and IL-10 (20 ng/mL). Surface expression of B-cell activation markers induced by CD40L plus cytokine were assessed by flow cytometric analysis on day 3 for expression of CD80, CD86, and CD69. Dead cells were identified by staining with Live/Dead near-infrared Staining Kit, and are excluded. (a) Histogram plot represents the mean fluorescent intensity of CD80. (c) Histogram plot represents the mean fluorescent intensity of CD80. (c) Histogram plot represents the mean fluorescent intensity of CD86. Results represent three different donors with three replicates per treatment group.

Figure 6 (cont'd)





maintained in RPMI media (Gibco Invitrogen, Carlsbad, CA) supplemented with 5% CD-FBS, 1X non-essential amino acids (Gibco Invitrogen), 1X sodium pyruvate (Gibco Invitrogen), and the antibiotics Penicillin (100 units/mL)/Streptomycin (100 μ g/mL). In all cases, cells were cultured at 37°C in 5% CO₂.

The stably transfected mouse fibroblast line expressing human CD40L (CD40L-L cells) was a generous gift from Dr. David Sherr (Boston University School of Public Health) and was prepared for the in vitro IgM activation model as previously described [320]. Briefly, CD40L-L cells were cultured in DMEM complete media [Dulbecco's modified Eagle Medium (Gibco Invitrogen, Carlsbad, CA) supplemented with 10% bovine calf serum (Hyclone), 50 μ M 2mercaptoethanol, 1X HT supplement, and the antibiotics Penicillin (100 units/mL)/Streptomycin (100 μ g/mL)] at 37°C in 5% CO₂ 3-4 days prior to irradiation. CD40L-L cells were trypsinized with 0.25% Trypsin-EDTA (Gibco Invitrogen) for 2-3 min at 37°C. After washing once with complete media, CD40L-L cells were resuspended in 500 μ L complete media and X-ray-irradiated at 3500 Gy (XRAD-320, Precision X-Ray, North Branford, CT). The irradiated CD40L-L cells were washed once with complete media, seeded into 96-well plate at 1.5×10^3 cells/well, and incubated at 37° C in 5% CO₂ 1 day prior to experimentation.

IV. Animals

Female C57BL/6 mice (6 weeks of age) were purchased from Charles River Laboratories (Portage, MI). CB1/CB2 null mice (CB1-/-/CB2-/-) on C57BL/6 background were a generous gift from Dr. Andreas Zimmer (University of Bonn, Germany) and were bred at Michigan State University (MSU). Mice were maintained under specific pathogen-free conditions as previously described [309]. All experimental mouse protocols were reviewed and approved by the Institutional Animal Care and Use Committee at MSU.

V. Isolation and culturing of human peripheral blood mononuclear cells (PBMCs)

Human leukocyte packs were obtained commercially from anonymous healthy donors (Gulf Coast Regional Blood Center, Houston, TX). Primary human PBMCs were isolated from buffy coats by density gradient centrifugation using Ficoll-Paque Plus (GE Healthcare, Piscataway, NJ) as previously described [320]. PBMCs were cultured at a final concentration of $1x10^6$ cells/mL in RPMI complete media [RPMI medium supplemented with 2% bovine calf serum and the antibiotics Penicillin (100 units/mL)/Streptomycin (100 μ g/mL)] at 37° C in 5% CO₂.

VI. Isolation of human peripheral blood (HPB) naïve CD4⁺ T cells

Negative selection was used to isolate human naïve CD4⁺ T cells from PBMCs using MACS Naïve Human CD4⁺ T Cells Isolation Kits per the manufacturer's protocol (Miltenyl Biotec, Auburn, CA) with some modifications. RPMI medium was used instead of EDTA-containing MACS buffer to minimize perturbation of intracellular Ca²⁺ during the isolation of naïve CD4⁺ T cells. Briefly, primary human PBMC were isolated and resuspended in RPMI medium before incubating with the antibody cocktail. The cell suspension was then applied onto the magnetic column. Unlabeled naïve CD4⁺ T cells were eluted from the column, collected and maintained in RPMI complete media at 37°C in 5% CO₂.

VII. Isolation of HPB naïve B cells

Negative selection of human naïve B cells were isolated from human PBMCs using MACS Naïve Human B Cells Isolation Kits following the manufacturer's protocol (Miltenyl Biotec, Auburn, CA) and have been described previously [320]. HPB naïve B cells were maintained in RPMI complete media [RPMI medium supplemented with 10% heat inactivated bovine calf serum (Hyclone), and the antibiotics Penicillin (100 units/mL)/Streptomycin (100 μ g/mL)] at 37°C in 5% CO₂.

VIII. Mouse T cell activation

Spleens were aseptically isolated and made into single-cell suspensions in RPMI media (Gibco Invitrogen, Carlsbad, CA) supplemented with either 2% bovine calf serum or 5% CD-FBS, 50 μ M 2-mercaptoethanol, and the antibiotics Penicillin (100 units/mL)/Streptomycin (100 µg/mL). Splenocytes, 5x10⁶ cells/mL, were cultured in 48-well plates at 37°C in 5% CO₂. Cells were stimulated with 40 nM PMA plus 0.5 μ M ionomycin (PMA/Io) or with 1 μ g/mL immobilized anti-mouse CD3 (clone 145-2C11; BD Pharmingen, San Diego, CA) plus 1 μ g/mL soluble anti-mouse CD28 (clone 37.51; BD Pharmingen) antibodies (anti-CD3/CD28) in the presence or absence of Δ^9 -THC. The immobilized CD3 was obtained by precoated 48-well plates (100 μ L/well) with 1 μ g/mL anti-mouse CD3 overnight at 4°C. Before addition of the cells, plates were washed twice with 1X RPMI followed by addition of 10 μ g/mL anti-CD28 (100 μ L/well). Stock solutions of Δ^9 -THC, 0.1 μ M cyclosporin A (CsA) and 0.5 μ M dexamethasone (DEX) were used at a final EtOH concentration of 0.1% and were added 30 min before T cell stimulation. 0.1% EtOH was used as a vehicle control (VH).

IX. Human TCR activation

Cells were subjected to either short-term (5 min) or prolonged (16 to 48 h) stimulation. For short-term stimulation, TCR stimulation was performed by anti-CD3/CD28 crosslinking. PBMCs. 1x10⁶ cells, were first incubated with anti-CD3

(clone UCHT1; BD Pharmingen, San Diego, CA) and anti-CD28 (clone 28.2; BD Pharmingen, San Diego, CA), 10 µg/mL each, for 15 min on ice. Subsequently, cells were washed once with cold 1X Hank's Balanced Salt Solution (HBSS, Invitrogen) and centrifuged at 350xg for 5 min at 4°C. After discarding the supernatant, cells were resuspended in complete media followed by incubation with 10 µg/mL lqG crosslinker (purified polyclonal goat anti-mouse lqG, BD Pharmingen, San Diego, CA) for another 15 min on ice. TCR-mediated signaling cascades were activated by transferring the tubes to a 37°C water bath and incubating for respective time periods as indicated in the results. For prolonged stimulation, PBMCs, 2x10⁵ cells, were stimulated with immobilized anti-CD3 plus soluble anti-CD28. 96-well plates were precoated with 100 μ L/well of anti-CD3 (5 μ g/mL) overnight at 4°C. Before addition of the cells, plates were washed twice with 1X RPMI followed by addition of 5 μ g/mL anti-CD28 (20 μ L/well). Cells were activated in the presence or absence of Δ^9 -THC. Stock solutions of Δ^9 -THC were used at a final EtOH concentration of 0.1% and were added 30 min before TCR stimulation. 0.1% EtOH was used as a vehicle control (VH). Δ^9 -THC or VH were present throughout the course of incubation process by adding them back to the culture after performing a washing step in the case of short-term stimulation.

X. Flow cytometry analysis

At the indicated time points, 0.5 to 1x10⁶ cells were harvested and washed once with FACS buffer [1X HBSS containing 1% bovine serum albumin (Calbiochem, San Diego, CA) and 0.1% sodium azide, pH 7.4-7.6]. necessary, dead cells were detected by staining with Live/Dead Fixable Dead Cell Stain Kit (near-infrared dye, Invitrogen). Briefly, cells were washed once with 1X Hank's Balanced Salt Solution (HBSS, Gibco Invitrogen) following by incubation with near-infrared dye for 20 min at 4°C per manufacturer's protocol. Prior staining with respective antibodies (Appendix A), Fcy III/II receptors on mouse cells were blocked using purified anti-mouse CD16/CD32; whereas Fc receptors on human cells were blocked by incubating with 20% human AB serum (Invitrogen) for 15 min at 4°C. The amount of antibodies used varied in staining for each specific antigen based on preliminary antibody titration and were typically pre-diluted in FACS buffer at appropriate amounts prior to addition to the cells. Staining for phosphorylated kinases was conducted on the same day and immediately followed by flow cytometry analysis. In all cases, stained cells were analyzed using a FACSCanto II cell analyzer (BD Biosciences). Data were analyzed using Kaluza (Bechman Coulter, Miami, FL) or FlowJo software (TreeStar, Ashland, OR).

Cell surface expression of CD40L on mouse CD4⁺ T cells was assessed by simultaneously staining with APC-anti-CD40L and FITC-anti-CD4; whereas cell surface expression of CD40L on human CD4⁺ T cells was assessed by

simultaneously staining with PE-anti-CD40L and PerCP-Cy5.5-anti-CD4 for 30 min at 4°C in the dark. Unbound antibodies were removed by washing once with FACS buffer. Cells were fixed with BD CytoFixTM Buffer (BD Biosciences) for 10 min at 4°C in the dark, followed by washing once with FACS buffer. Stained cells were then resuspended in FACS buffer for analysis.

For staining of intracellular phosphorylated kinases in CD4⁺ T cells, PBMCs or splenocytes were equilibrated at 37°C in 5% CO₂ for 3 h to normalize baseline kinase activation prior to pretreatment with Δ^9 -THC or VH. stimulation was performed at 37 °C in a water bath. Cells were fixed in 1.5% formaldehyde by direct dilution in cell culture from 32% stock (electron microscopy grade, Electron Microscopy Sciences, Hartfield, PA) for 10 min at 37°C followed by centrifugation at 600xg for 6 min at 4°C. Cells were then permeabilized by drop-wise addition of ice-cold 100% methanol while vortex mixing at medium speed. Cells were stored in methanol at -80°C until staining with indicated antibodies. Cells were washed 3 times with FACS buffer. The unbound IgG crosslinker in human samples were blocked by incubating with 15 μ g/mL mouse IgG (Invitrogen). The level of phosphorylated kinases in CD4⁺ T cells was assessed by simultaneously staining with V450 anti-CD4 and antibodies specific for phosphorylated epitopes on Zap70, Akt, and GSK3ß or with V450 anti-CD4 and antibodies specific for phosphorylated epitopes on PLCγ1/2 for 60 min at room temperature in the dark. Unbound antibodies were removed by washing twice with FACS buffer. Stained cells were then resuspended in FACS buffer for analysis.

For staining of intracellular phosphorylated kinases in B cells, HPB naïve B cells were equilibrated at 37°C in 5% CO₂ for 3 h to normalize baseline kinase activity. Cells were then pretreated with VH or Δ^9 -THC for 30 min, followed by activation with recombinant CD40L (Enzo Life Sciences, Inc., Farmingdale, NY) plus IL-2, -6, and -10 for 10 min at 37°C in a water bath. Cells were fixed in 1.5% formaldehyde by directly diluting in cell culture from 32% stock (electron microscopy grade, Electron Microscopy Sciences, Hartfield, PA) for 10 min at 37°C followed by centrifugation at 600xg for 6 min at 4°C. Cells were then permeabilized by drop-wise adding ice-cold 100% methanol while vortex mixing at medium speed and were stored in methanol at -80°C until ready to stain with indicated antibodies. Cells were washed 3 times with FACS buffer. The level of phosphorylated STAT3 (pSTAT3), and phosphorylated p65 (pp65) was assessed by simultaneously staining with Alexa Fluor 647 Mouse Anti-STAT3 and Alexa Fluor 647 Mouse Anti-NFkB p65 for 60 min at room temperature in the dark. Unbound antibodies were removed by washing twice with FACS buffer. Stained cells were then resuspended in FACS buffer for analysis.

XI. Real Time Polymerase Chain Reaction

Total RNA was isolated from activated mouse splenocytes using TRI Reagent, and isolated from activated human PBMC or activated human B cells

using RNeasy Kit (Qiagen, Valencia, CA). RNA was quantified using a Nanodrop 1000 (Thermo Scientific, Wilmington, DE). Total RNA was reverse-transcribed into cDNA using random primers with the High Capacity cDNA Reverse Transcription Kit (Applied Biosystems, Foster City, CA). TaqMan[®] Gene Expression Assay primers for target genes were purchased from Applied Biosystems (Appendix B). The relative steady-state levels of target mRNA were determined using ABI PRISM[®] 7900HT Sequence Detection System (Applied Biosystems). The fold change value of relative steady-state mRNA levels of target gene were calculated using the $\Delta\Delta$ -Ct method as described previously [321] and normalized to the endogenous reference, 18s rRNA.

XII. Transient transfection assay

HEK293T, $1x10^6$ cells, were cultured in 6-well plates at 37° C in 5% CO₂ overnight before transfection. Cells were incubated with transfection reagents [1 μ g of plasmid and 10 μ L of Lipofectamine 2000 (Invitrogen)] for 3 h. The transfected HEK293T cells were treated with either Δ^9 -THC or DEX alone and the combination of Δ^9 -THC and DEX. 24 h after treatment, luciferase activity was assayed using the Promega luciferase assay system according to the manufacturer's protocol (Promega). Fluorescence was measured using the BioTek SynergyTM HT autoreader. Data were analyzed using KC4 software (BioTek Instruments, Highland Park, VT) and presented as count per second

(CPS) normalized to total protein. Protein determinations were performed using a Bicinchoninic Acid Assay.

XIII. Nuclear protein isolation

Human PBMCs (approximately 2x10⁷ cells/mL) were stimulated with anti-CD3/CD28 in the presence or absence of Δ^9 -THC for 16 h. PBMCs were collected and washed once with PBS. Nuclear proteins was isolated as previously described with some modifications [213]. Briefly, cells were lysed with HB buffer (10 mM HEPES and 1.5 mM MgCl₂), containing protease inhibitors (1 mM DTT, 0.1 mM phenylmethylsulfonyl fluoride, 0.2 μ g/mL aprotinin, and 0.2 μ g/mL leupeptin) for 15 min on ice. Nuclei were pelleted by centrifugation at 1000xq for 5 min. The supernatant containing cytoplasmic protein was discarded. The nuclear pellet was washed twice with MDHN buffer (25 mM HEPES, 3 mM MgCl₂, and 100 mM NaCl) containing proteinase inhibitors. Nuclei were lysed using a hypertonic buffer (30 mM HEPES, 1.5 mM MgCl₂, 450 mM NaCl, 0.3 mM EDTA, and 0.1% Igepal) plus protease inhibitors by rocking for 30 min on ice. The nuclear fraction in supernatant was separated by centrifugation at 17500xg for 15 min. The salt concentration was reduced by adding equal amount of a hypotonic buffer (30 mM HEPES, 1.5 mM MgCl₂, 0.3 mM EDTA and 10%

glycerol). Protein concentrations were determined using the bicinchoninic acid assay.

XIV. Electrophoretic Mobility Shift Assay (EMSA)

Nuclear extracts (1 μ g) were incubated with 0.25 μ g poly(dI-dC) in binding buffer (100 mM NaCl, 30 mM HEPES, 1.5 mM MgCl₂, 0.3 mM EDTA, 10% glycerol, 1 mM DTT, 0.1 mM phenylmethylsulfonyl fluoride, 0.2 μ g/mL aprotinin, and 0.2 μ g/mL leupeptin) for 10 min on ice. The corresponding ³²P-labeled probe (30,000 count per minute) was added, followed by incubation at room temperature for 30 min. Samples were resolved on a 5% polyacrylamide gel in 1X TBE buffer (89 mM Tris, 89 mM boric acid, and 2 mM EDTA) as previously described [322]. Unlabeled probes were added in 100-fold molar excess to detect the specificity of DNA-protein complexes. After electrophoresis, gels were dried and analyzed by standard autoradiograph. The sequences of the oligonucleotide probes used are: NFAT 5'-AAGCACATTTTCCAGGA -3' [323] and NFκB probe. 5'-TGAGGTAGGGATTTCCACAGCTG-3' [80]. The corresponding binding site for each transcription factor is underlined.

XV. Calcium determination

Purified naïve $\mathrm{CD4}^+$ T cells (1x10 6 cells/mL, 15 mL) were allowed to equilibrate at 37 $^\circ\mathrm{C}$ in 5% CO_2 for 3 h. Naïve $\mathrm{CD4}^+$ T cells were then labeled with

the Ca^{2+} indicator dyes (Invitrogen), Fura-3 (2 μ M) and Fluo-red (5 μ M), for 60 min at room temperature prior to pretreatment with Δ^9 -THC or VH (2x10⁶ cells per treatment group). T cells were activated by incubation with anti-CD3 and anti-CD28 for 15 min on ice (10 μ g/mL each). Excess antibodies against CD3 and CD28 were removed by washing once with complete RPMI. Cells were then resuspended in complete media containing Ca^{2+} dyes and Δ^{9} -THC or VH. The intracellular Ca²⁺ measurement was then acquired by using the time parameter on the FACScan flow cytometer (Becton Dickinson, Mountain View, CA) and analyzed for Fura-Red (FL1) and Fluro-3 (FL3) fluorescence. Following 60 sec of data acquisition, cells were activated by adding IgG crosslinker (10 μ g) to crosslink the anti-CD3/CD28. Cells were analyzed for a total of 300 seconds. Post-collection analysis was performed using FlowJo software (TreeStar, Ashland, OR). The ratio of FL1/FL3 was derived and plotted over time. Kinetic plots are expressed as median of the FL1:FL3 ratio. Data are presented in arbitrary units as a function of fluorescence (relative intracellular Ca²⁺) versus time.

XVI. In vitro CD40L-dependent polyclonal IgM antibody response

HPB naïve B cells $(1x10^6 \text{ cells/mL})$ were pretreated with Δ^9 -THC or vehicle (0.02% DMSO) for 30 min prior inducting primary IgM response *in vitro* as

previously described [320]. Briefly, pretreated HPB naïve B cells (1.5x10⁵ cells) were co-cultured with irradiated CD40L-L cells preseeded in 96-well plate. The culture was supplemented with 10 U/mL of recombinant human IL-2 (Roche Applied Science, Indianapolis, IN, USA), 100 U/mL of recombinant human IL-6 (Roche Applied Science, Indianapolis, IN, USA), and 20 ng/mL of recombinant IL-10 (BioVision, Inc., Milpitas, CA). After 4 days of culture, B cells were transferred to a new 96-well plate without CD40L-L cells, and were cultured for an additional 3 days. The cells were harvested for IgM ELISPOT. The cell viability was determined by the pronase activity assay as described previously [298].

XVII. IgM ELISPOT

The number of IqM secreting cells were determined by IqM ELISPOT as previously described [320]. Briefly, ELISPOT wells were coated with purified anti-human IgM antibody (BD Biosciences) overnight at 4°C. Plates were washed with phosphate buffered saline (PBS) containing 0.1% Tween-20 and water. ELISPOT wells were then blocked with PBS containing 5% bovine serum albumin (BSA; Calbiochem, San Diego, CA) for 30 min at 37°C. Harvested cells were washed, diluted to the appropriate density, and incubated in the ELISPOT wells for 16-20 h at 37°C in 5% CO₂. Cells were removed from the wells and plates were washed with PBS containing 0.1% Tween-20 and water. For Biotin-conjugated anti-human IgM antibody detection. and streptavidinhorseradish peroxidase were added to the wells. The spots were developed with the aminoethylcarbazole staining kit. Data were collected and analyzed using the CTL ImmunoSpot system (Cellular Technology Ltd, Shaker Heights, OH).

XVIII. Proliferation assay

The B cell proliferation studies were conducted as described previously [320]. In brief, HPB naïve B cells were labeled by incubation with 5 μ M of carboxyfluorescein succinimidyl ester (CFSE) (CellTrace Cell Proliferation Kits, Invitrogen) at 5x10⁶ cells/mL following manufacturer's protocols. The labeled cells were washed in complete medium, and then adjusted to the desired cell density prior to pretreatment with Δ^9 -THC or vehicle (0.02% DMSO) for 30 min. Cells were then co-cultured with irradiated CD40L-L cells plus IL-2, -6, and -10. After 4 days of culture, B cells were transferred to a new 96-well plate without CD40L-L cells, and were cultured for an additional 3 days. The cells were harvested on day 7 for flow cytometric analysis.

XIX. Statistical analysis

GraphPad Prism 4.00 (Graphpad Software, San Diego, CA) was used for all statistical analysis. Data acquired as percentages from flow cytometry were transformed into log scale before performing statistical analysis. In the case of mRNA data, the transformed fold-change values were used in statistical analysis. For comparisons among treatment groups, one-way ANOVA was used. Dunnett's

post-hoc test was used to test for significance between treatment groups and control. The outliers were eliminated using the Grubb's test and only one outlier was allowed per treatment group. A value of p < 0.05 was considered significant.

RESULTS

I. Effect of Δ^9 -THC on the upregulation of CD40L on activated mouse CD4 † T cells

A. Expression kinetics of CD40L on activated T cells

Expression of CD40L is readily induced on T cells upon activation both in vivo and in vitro [324-329]. Here the peak time of CD40L expression in response to two different T cell activation stimuli, PMA/lo and anti-CD3/CD28, was defined at both the protein (cell surface expression) and mRNA level in splenic T cells. As shown in figure 7a and 7b, upregulation of surface CD40L by PMA/loactivated CD4⁺ T cells was detectable as early as 4 h (23.0±4.8%), maximal at 8 h (30.0±3.0%), and was declining by 18 h (19.2±1.3%). In concordance with surface expression, induction of steady-state CD40L mRNA levels by PMA/lo was rapid (as early as 2 h post activation), but transient, as evidenced by a decrease as early as 4 h after activation (Figure 7c). Although the kinetic profiles of surface CD40L expression induced by either anti-CD3/CD28 or PMA/lo were similar, the proportion of CD4⁺CD40L⁺ cells induced by PMA/lo was greater than with anti-CD3/CD28. As shown in Figure 8a and 8b, the upregulation of cell surface CD40L on activated CD4⁺ T cells by anti-CD3/CD28 was detectable at 4 h (10.0±0.3%), maximal at 8 h (15.2±0.9%), and decreased by 18 h (9.8±0.3%) after activation. By contrast, the induction of steady-state CD40L mRNA levels

by anti-CD3/CD28 had a different profile in which it peaked at 4 h post stimulation and then reached a plateau (Figure 8c).

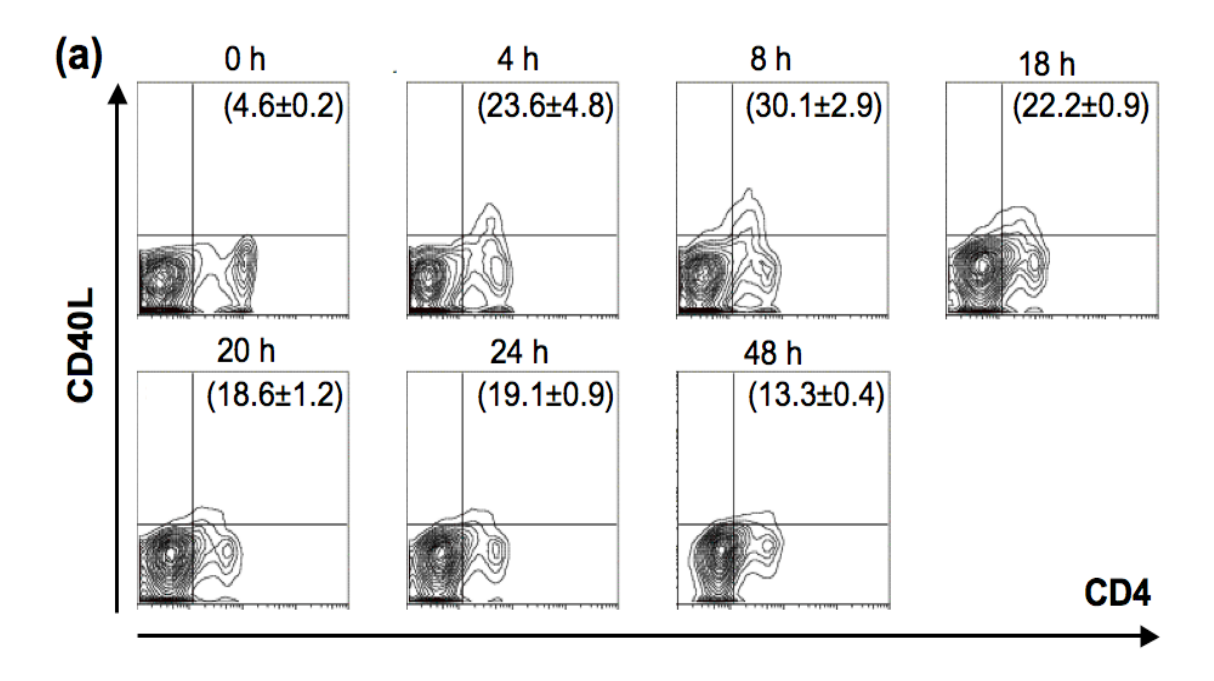
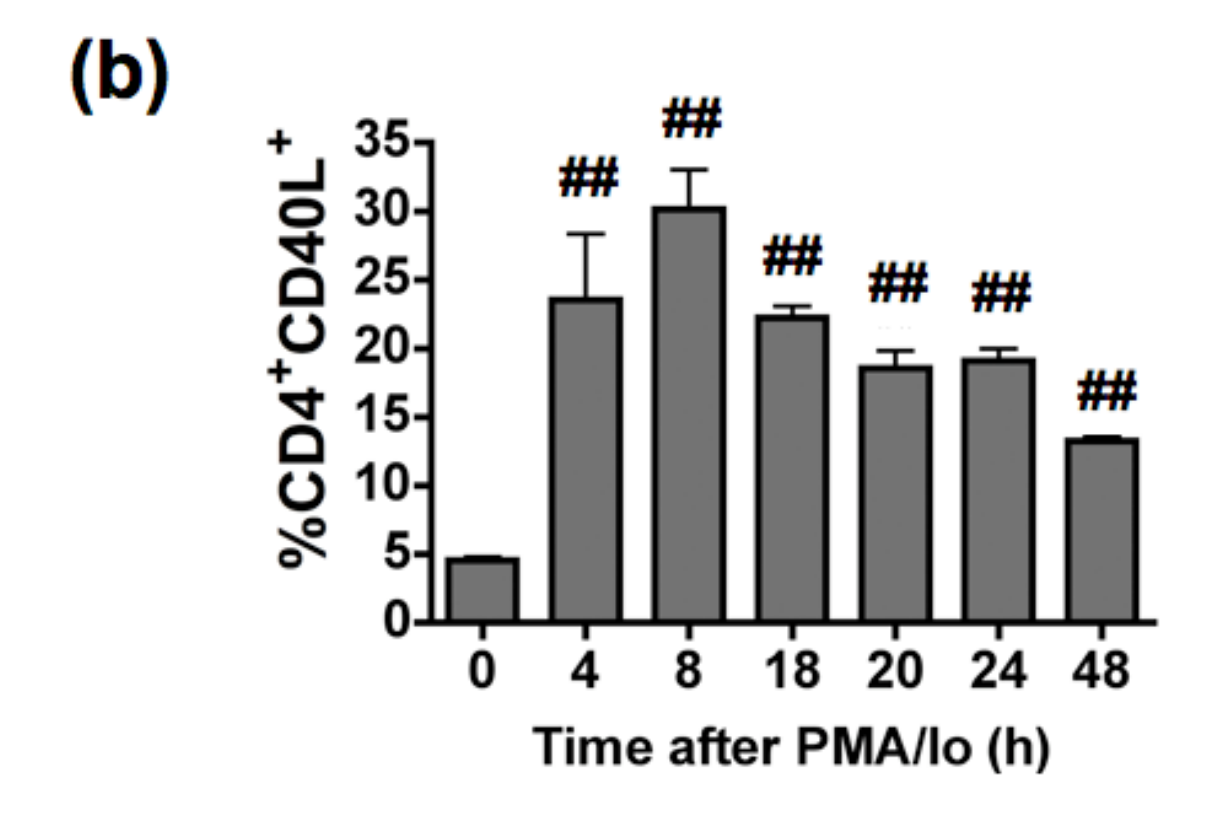
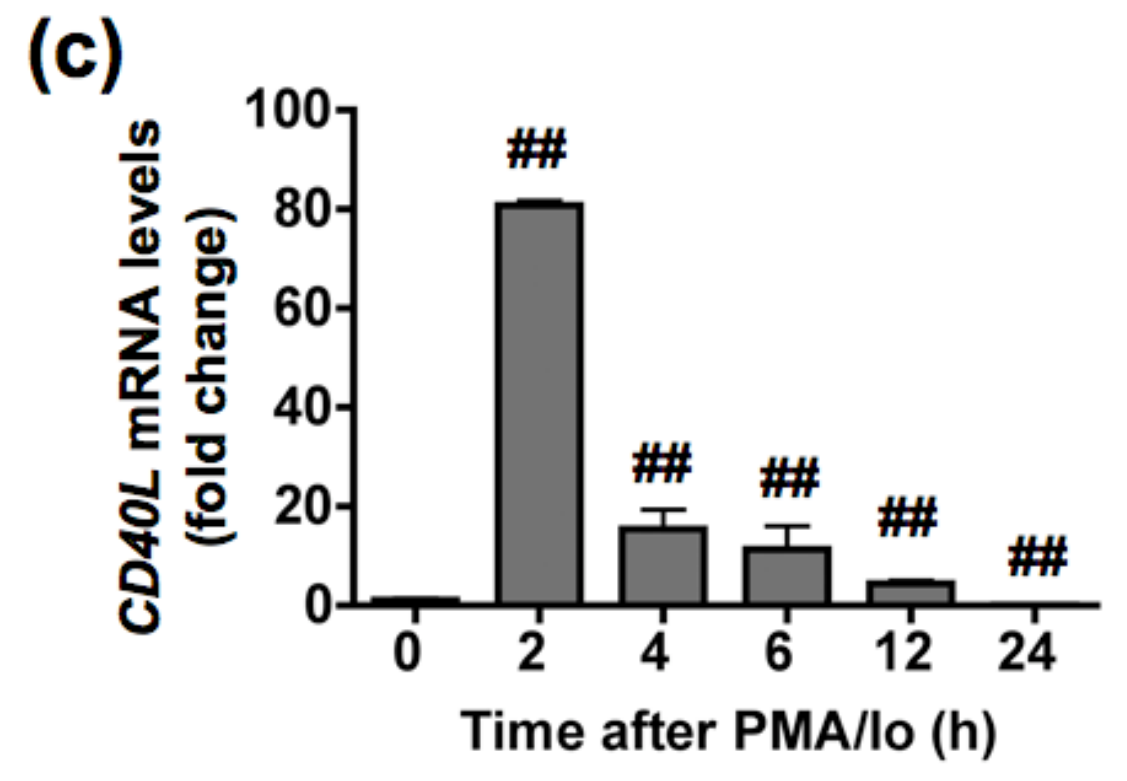


Figure 7. Kinetics of PMA/lo-induced CD40L expression in mouse splenocytes.

Splenocytes $(5x10^6 \text{ cells})$ were stimulated with 40 nM PMA plus 0.5 μ M ionomycin. (a) Cell surface CD40L on activated CD4⁺T cells was determined at indicated time points by flow cytometry. Numbers in parentheses represent the percentage of CD4⁺CD40L⁺ cell population±SEM from triplicates. (b) Bar graph is a representation of data in (a). (c) Steady-state expression of *CD40L* mRNA was determined at indicated time points by real-time PCR. The fold difference of *CD40L* mRNA molecules relative to nonactivated resting cells (naïve, NA at day 0) was normalized using the endogenous reference, 18s rRNA. Results are the mean of triplicates per time point. The ## = p \leq 0.01 compared to unstimulated cells. Results represent two separate experiments.

Figure 7 (cont'd)





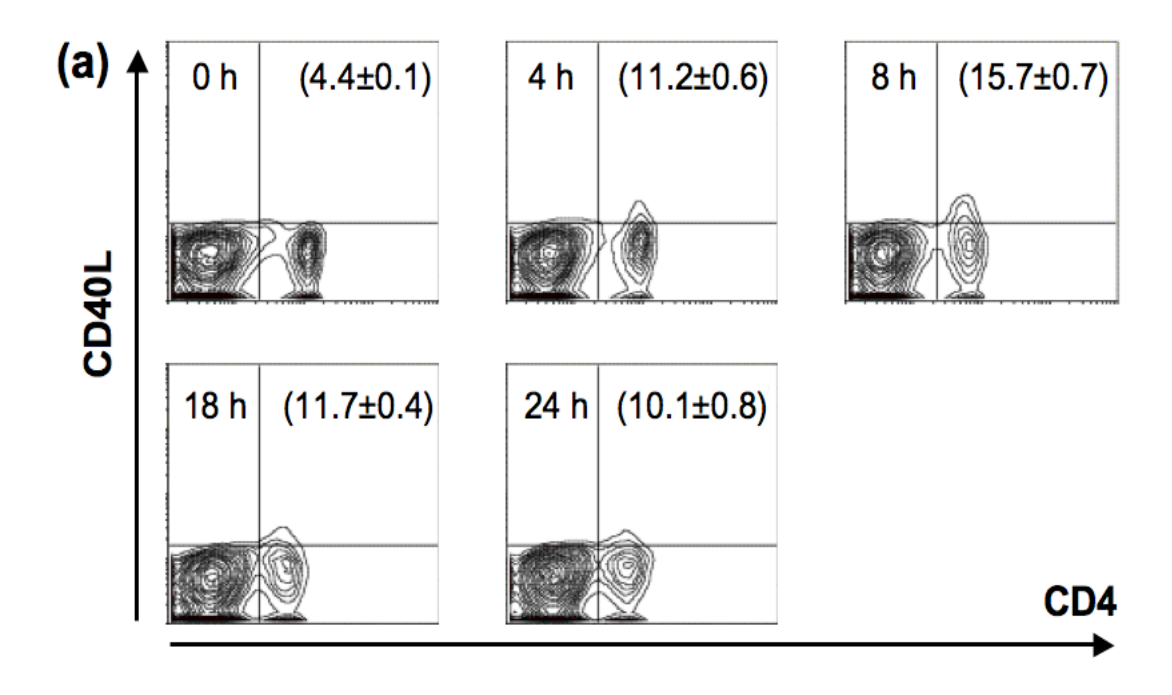
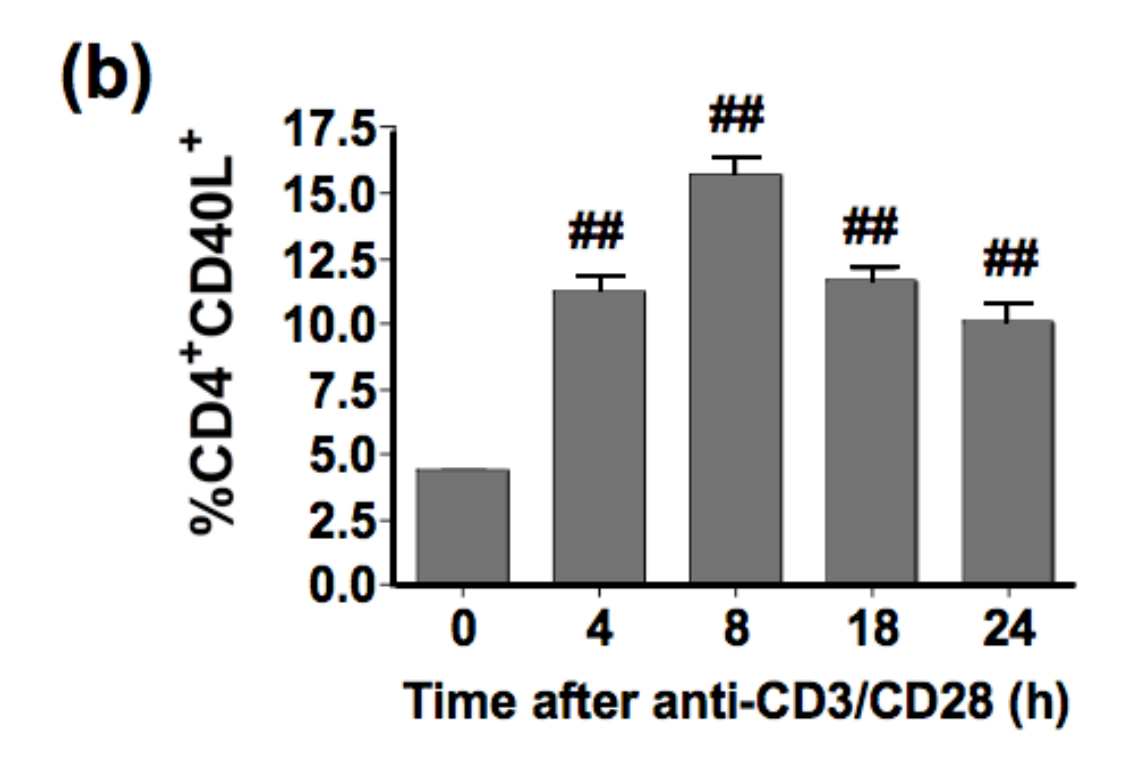
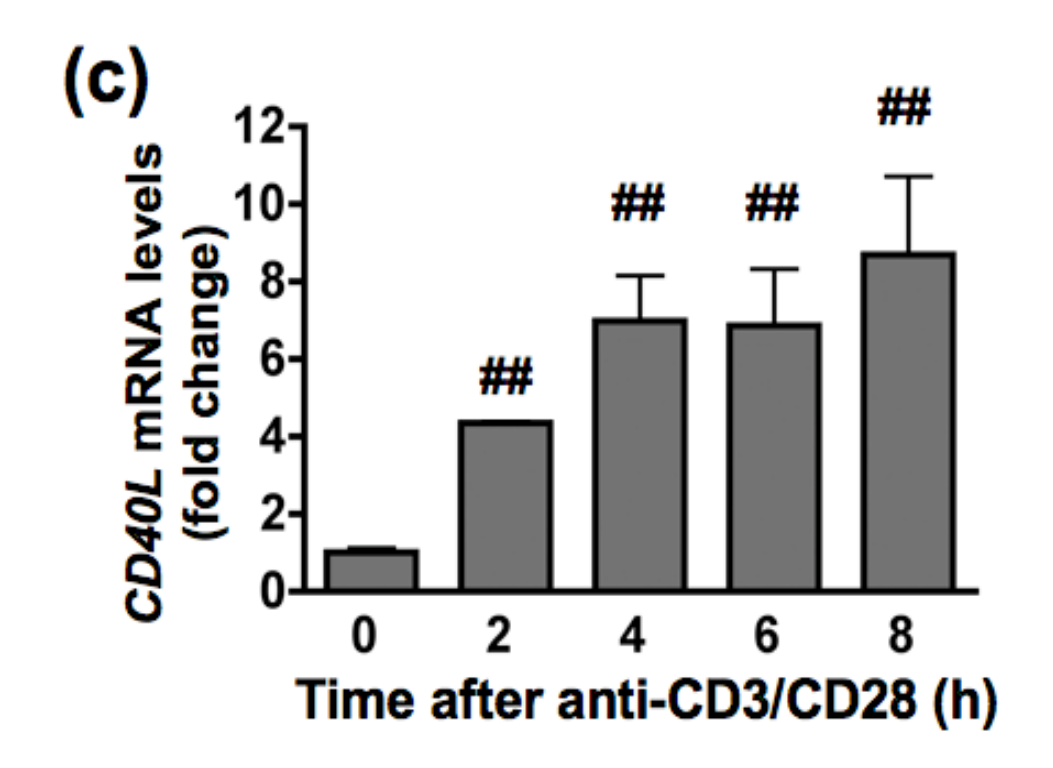


Figure 8. Kinetics of anti-CD3/CD28-induced CD40L expression in mouse splenocytes.

Splenocytes ($5x10^6$ cells) were stimulated with immobilized anti-CD3 plus soluble anti-CD28 antibodies, 1 μ g/ml each. (**a**) Cell surface CD40L on activated CD4⁺T cells was determined at indicated time points by flow cytometry. Numbers in parentheses represent the percentage of CD4⁺CD40L⁺ cell population±SEM from triplicates. (**b**) Bar graph is a representation of data in (**a**). (**c**) Steady-state expression of *CD40L* mRNA was determined at indicated time points by real-time PCR. The fold difference of *CD40L* mRNA molecules relative to nonactivated resting cells (naïve, NA at day 0) was normalized using the endogenous reference, 18s rRNA. Results are the mean of triplicates per time point. The ## = p \leq 0.01 compared to unstimulated cells. Results represent two separate experiments.

Figure 8 (cont'd)





B. Differential effects by $\Delta^9\text{-THC}$ on CD40L upregulation in response to different T cell activation stimuli

Based on the above kinetic studies, the effects of Δ^9 -THC on CD40L expression levels by CD4⁺ T cells activated with either anti-CD3/CD28 or PMA/lo was investigated at 8 h. CsA was included as a positive control for suppression of T cell activation. As shown in figure 9, Δ^9 -THC suppressed anti-CD3/CD28induced CD40L surface expression by reducing the number of CD4⁺ T cells expressing CD40L (Figure 9a and 9b), but not the expression level of CD40L on each CD4⁺ T cell (no differences in MFI between treatment groups, Figure 10c). Significant suppression by Δ^9 -THC of CD4⁺CD40L⁺ double positive cells occurred in a concentration-dependent manner and was most pronounced at 10 and 15 μ M Δ^9 -THC. Although splenocytes were used as a source of T cells, we found that enrichment of T cells did not further increase the magnitude of anti-CD3/CD28-induced CD40L surface expression nor affect the sensitivity to Δ^9 -THC (Figure 10). Conversely, Δ^9 -THC treatment did not suppress PMA/loinduced upregulation of CD40L surface expression on CD4⁺ T cells (Figure 11).

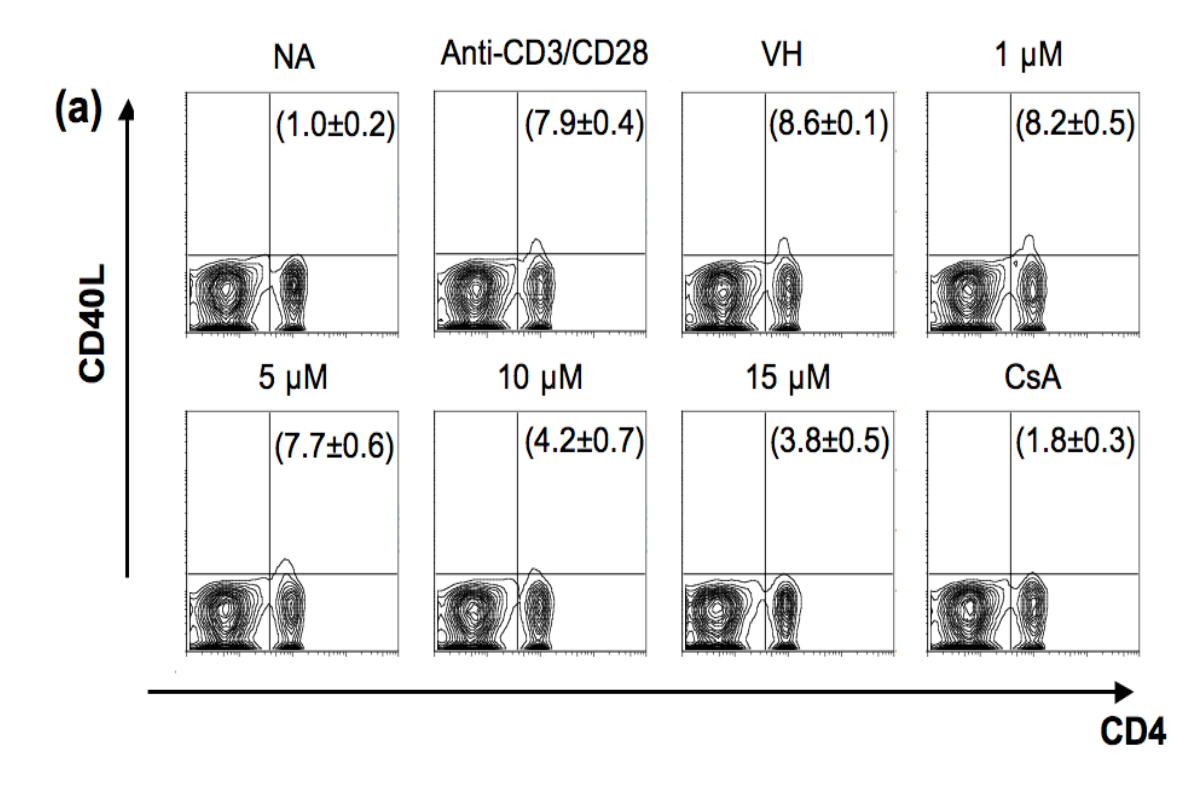
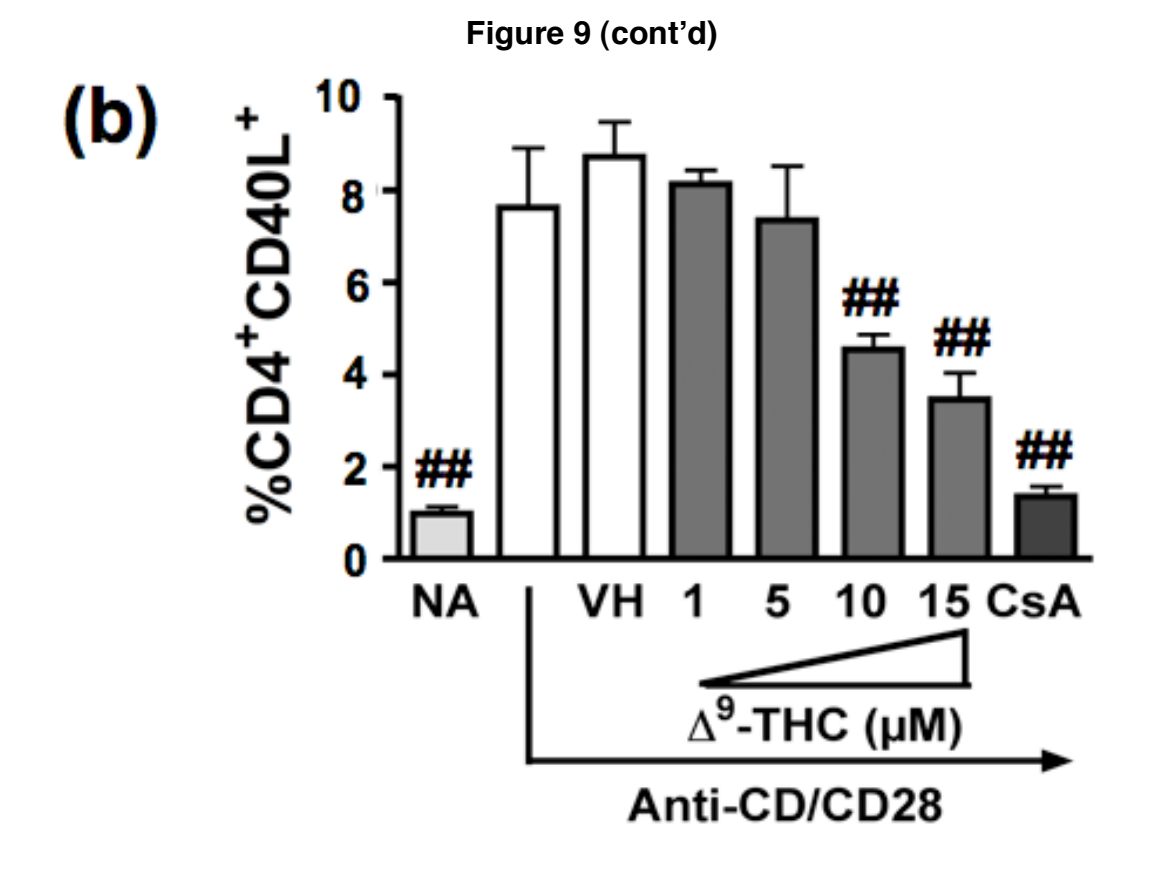
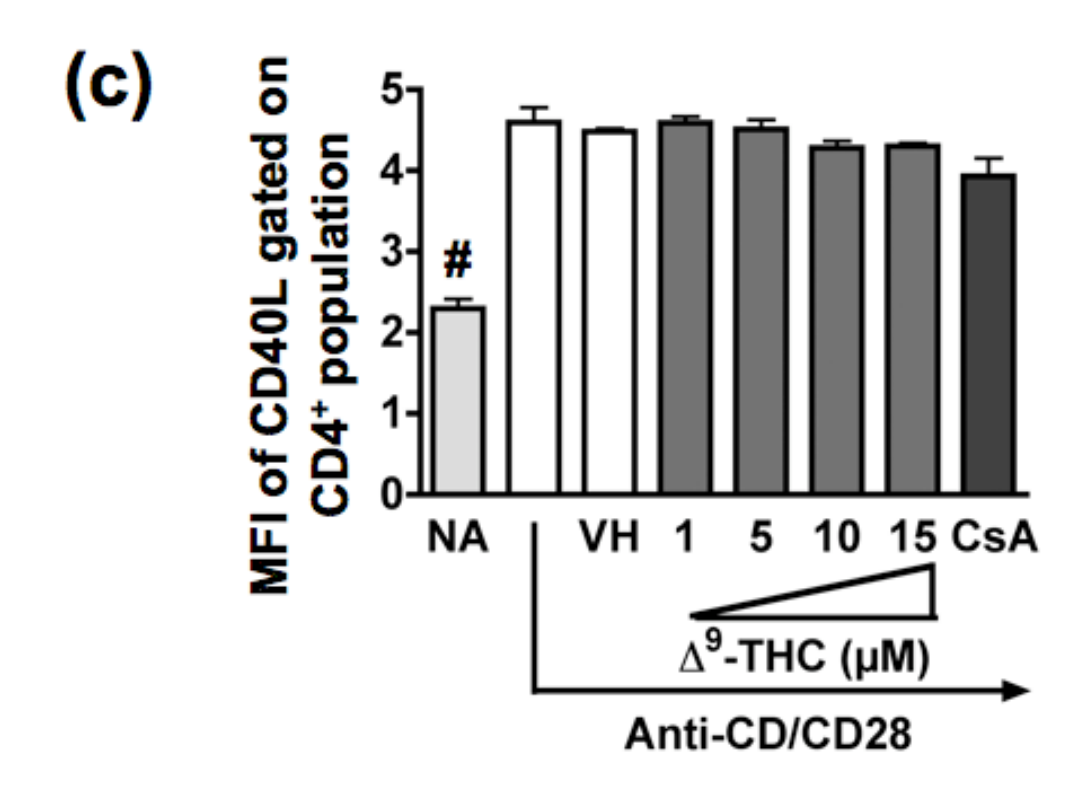


Figure 9. Δ^9 -THC suppresses anti-CD3/CD28-induced surface CD40L expression on activated mouse CD4⁺ T cells.

Splenocytes $(5x10^6 \text{ cells})$ were treated with various concentrations of Δ^9 -THC (1, 5, 10, and 15 μ M) for 30 min and then stimulated with immobilized anti-CD3 plus soluble anti-CD28 antibodies (1 μ g/ml each). (a) Cell surface CD40L expression on activated CD4⁺ was determined by flow cytometry 8 h after stimulation. Numbers in parentheses represent the percentage of CD4⁺CD40L⁺ cell population±SEM from triplicates. (b) Bar graph is a representation of data in (a). (c) Bar graph represents MFI of CD40L gated on CD4⁺ T cells. The # or ## indicates significant effect compared to vehicle control (VH = 0.1% EtOH), at p ≤ 0.05 or p ≤ 0.01, respectively. 0.1 μ M CsA was used as the positive control. Results represent two separate experiments with three replicates per treatment group.





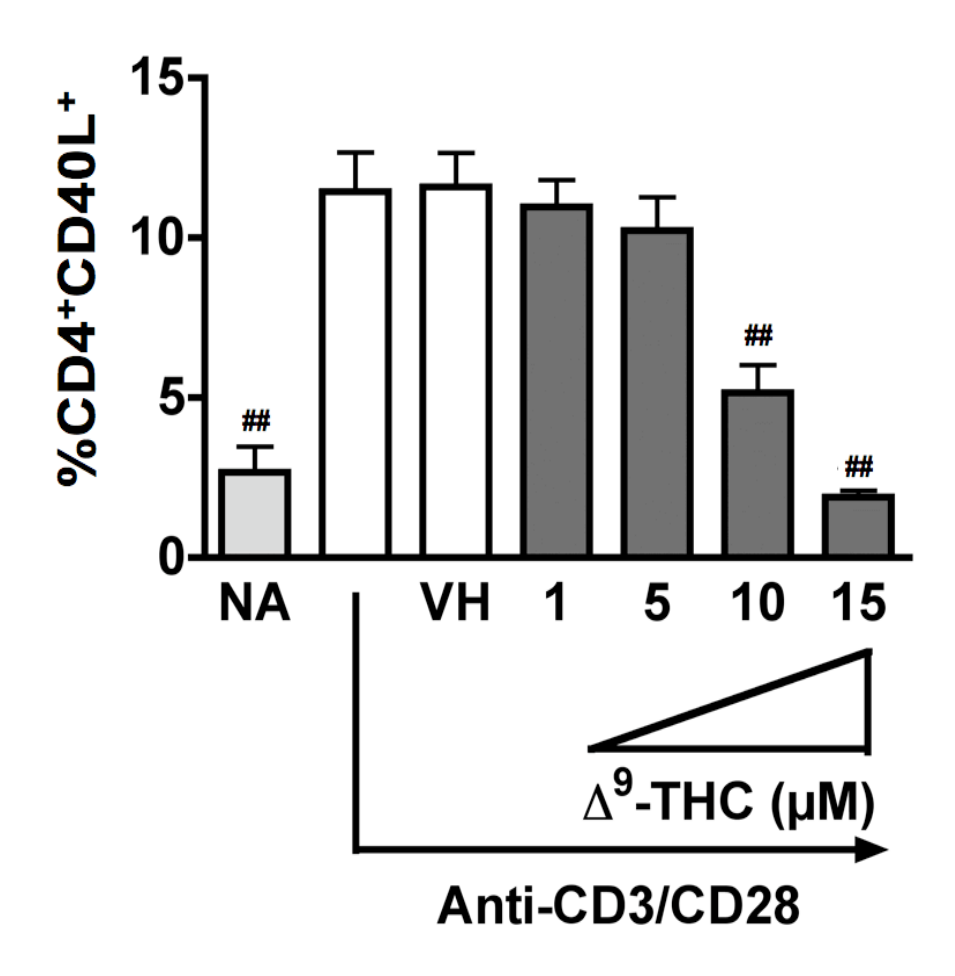


Figure 10. Δ^9 -THC suppresses anti-CD3/CD28-induced surface CD40L expression on enriched mouse CD4⁺ T cells.

Enriched CD4⁺ T cells (1x10⁶ cells) were treated with various concentrations of Δ^9 -THC (1, 5, 10, and 15 μ M) for 30 min and then stimulated with immobilized anti-CD3 plus soluble anti-CD28 antibodies (1 μ g/ml each). Cell surface CD40L expression on activated CD4⁺ was determined by flow cytometry 8 h after stimulation. Each bar represents mean of the percentage of CD4⁺CD40L⁺ cell population+SEM from triplicates. The # or ## indicates significant effect compared to vehicle control (VH = 0.1% EtOH), at p < 0.05 or p < 0.01, respectively. Results represent two separate experiments with threee replicates per treatment group.

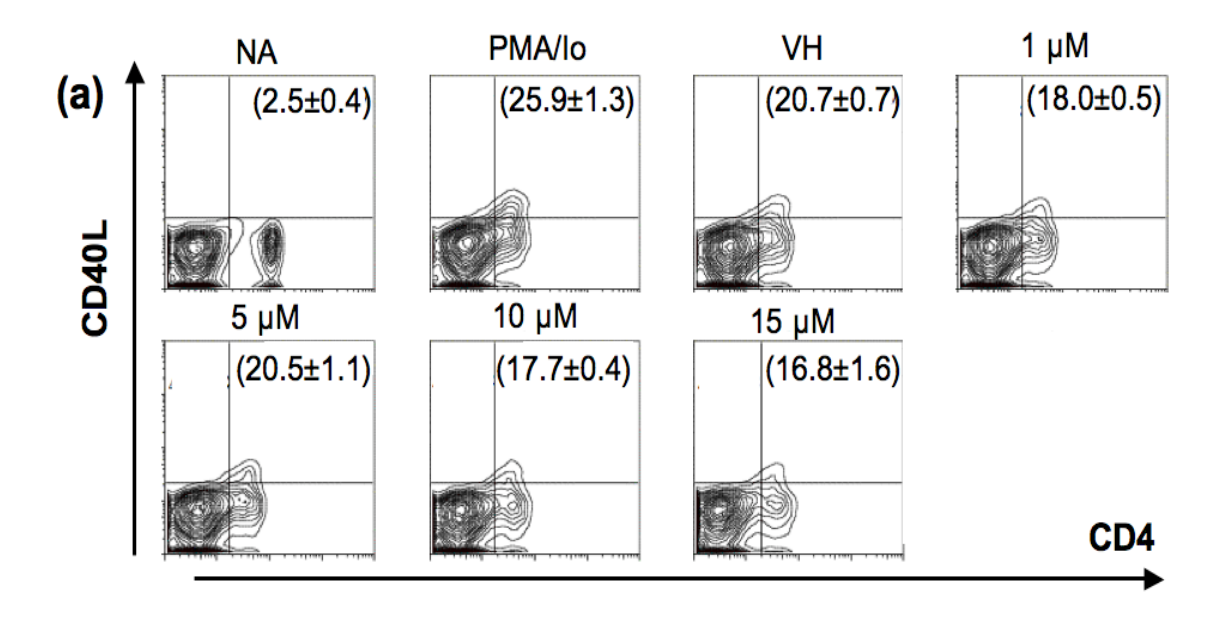
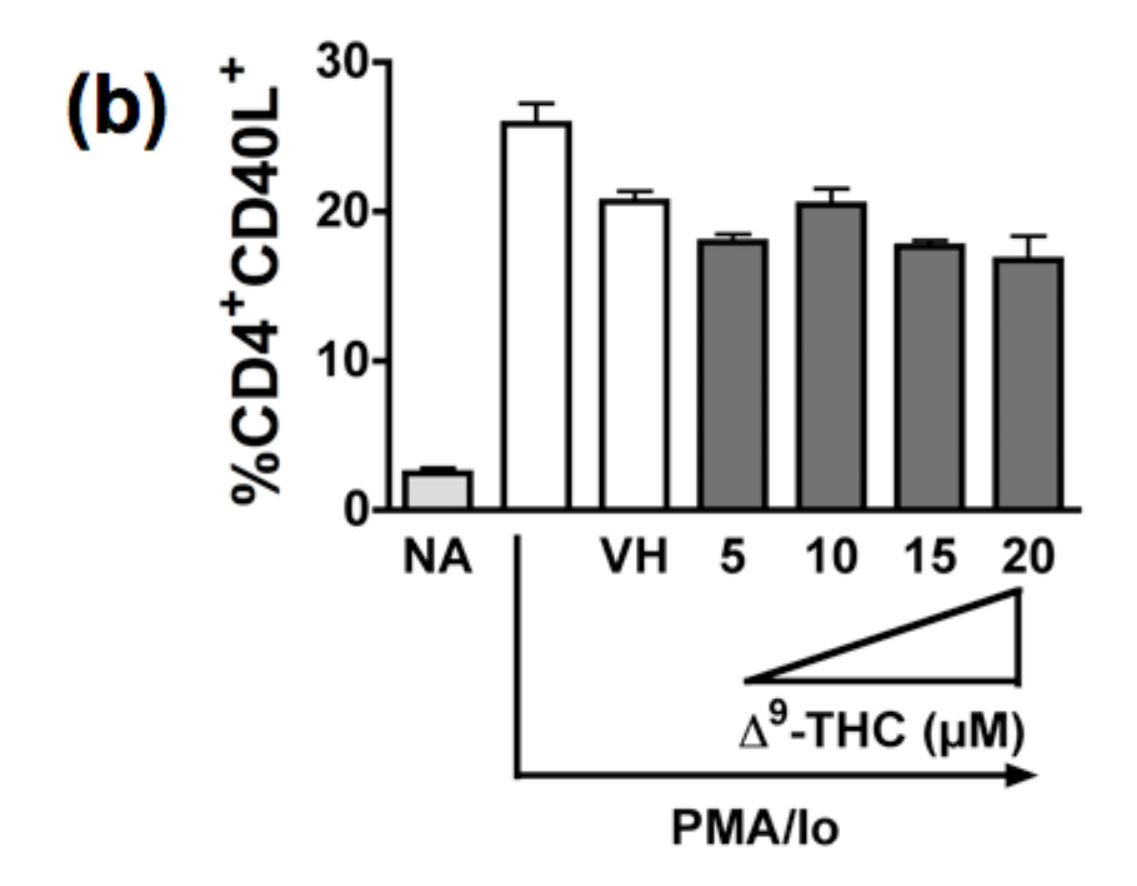


Figure 11. Δ^9 -THC does not suppress PMA/Io-induced surface CD40L expression on activated mouse CD4⁺ T cells.

Splenocytes (5x10⁶ cells) were treated with various concentrations of Δ^9 -THC (5, 10, 15, and 20 μ M) for 30 min and then stimulated with 40 nM PMA plus 0.5 μ M ionomycin for 8 h. (a) Cell surface CD40L expression on activated CD4⁺ was determined by flow cytometry. Number in parentheses represents the percentage of CD4⁺CD40L⁺ cell population±SEM. (b) Bar graph is a representation of data in (a). Results represent two separate experiments with three replicates per treatment group.

Figure 11 (cont'd)



C. Δ^9 -THC decreases steady-state mRNA levels of *CD40L* induced by anti-CD3/CD28.

The expression of surface CD40L on activated T cells is tightly controlled and occurs at the transcriptional, post-transcriptional, and/or post-translational level However, it appears to be primarily controlled at the level of transcription and post-transcription (reviewed in [62,69,330]). Therefore the effect of Δ^9 -THC was investigated on the steady-state mRNA levels of *CD40L* induced by anti-CD3/CD28. Splenocytes were treated with increasing concentrations of Δ^9 -THC followed by anti-CD3/CD28 activation for 4 h, the peak time induction of CD40L mRNA. Δ^9 -THC suppressed the induction of *CD40L* mRNA levels by anti-CD3/CD28 in a concentration-dependent manner (Figure 12).

D. CB1 and /or CB2 are not involved in suppression by Δ^9 -THC of anti-CD3/CD28-induced CD40L expression on mouse splenic CD4⁺ T cells.

CB1 and/or CB2 -dependent and -independent mechanisms have been suggested to account for cannabinoid-mediated effects on immune function [294,309]. To investigate the involvement of CB1 and/or CB2 on Δ^9 -THC-mediated suppression of anti-CD3/CD28-induced CD40L expression, comparative studies were performed using splenocytes from C57BL/6 wild type and CB1-/-CB2-/- mice. As shown in figure 13, the absence of CB1 and CB2 did not affect Δ^9 -THC-mediated suppression of either anti-CD3/CD28-induced

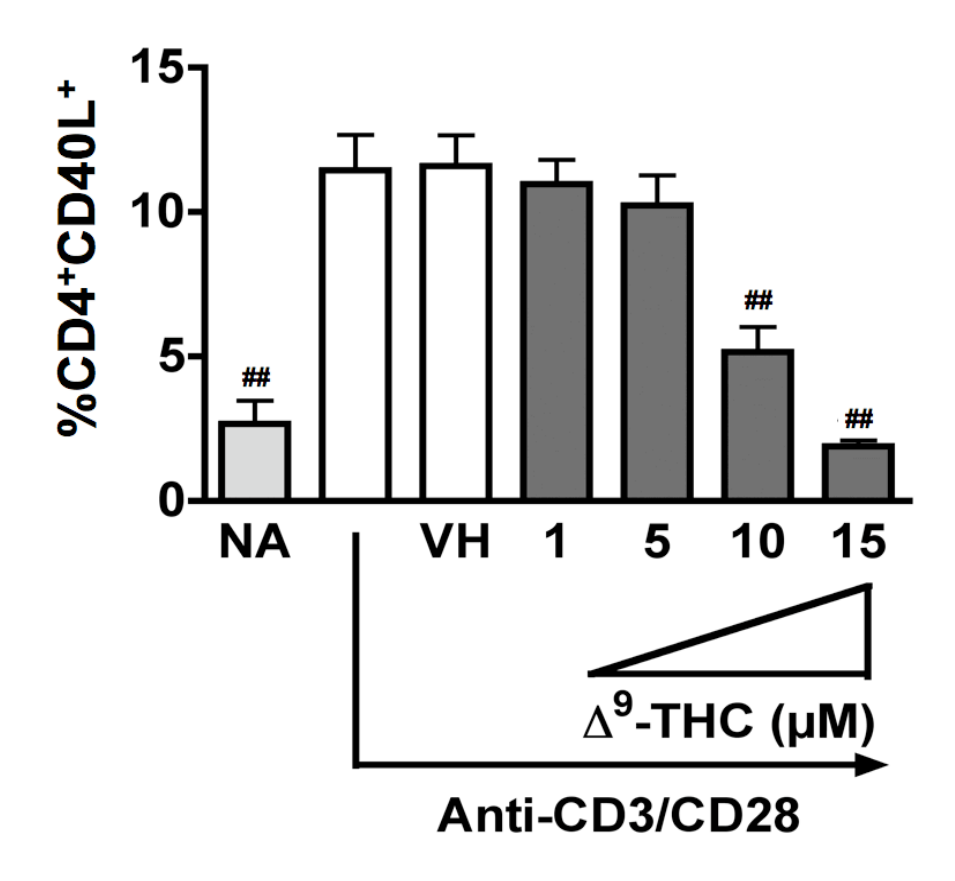


Figure 12. Δ^9 -THC suppresses anti-CD3/CD28-induced *CD40L* mRNA expression in mouse splenocytes.

Splenocytes ($5x10^6$ cells) were treated with various concentrations of Δ^9 -THC (1, 5, 10, and 15 μ M) for 30 min and then stimulated with immobilized anti-CD3 plus soluble anti-CD28 antibodies, 1 μ g/ml each. Steady-state expression of *CD40L* mRNA was determined by real-time PCR at 4 h after stimulation. The fold difference of *CD40L* mRNA molecules relative to unstimulated cells (naïve, NA) was normalized using the endogenous reference, 18s rRNA and results are the average of triplicates at various concentrations of Δ^9 -THC. The # or ## indicates significant effect compared to vehicle control (VH = 0.1% EtOH) at p \leq 0.05 or p \leq 0.01, respectively. 0.1 μ M CsA was used as the positive control. Results represent two separate experiments with three replicates per treatment group.

surface CD40L expression in CD4⁺ T cells (Figure 13a) or steady-state *CD40L* mRNA levels (Figure 13b). Although there was an increase of *CD40L* mRNA expression in CD4⁺ T cells derived from C57BL/6 at 5 μ M Δ^9 -THC (Figure 13b), it was not consistent across the experiments.

E. The effects of Δ^9 -THC are not mediated via GR

With the demonstration that Δ^9 -THC-mediated suppression of CD40L protein and mRNA expression was not mediated though CB1 or CB2, subsequent experiments were designed to identify an alternative receptor. One possibility is the GR since it was demonstrated that Δ^9 -THC specifically bound rat hippocampal GR *in vivo* and *in vitro* [331] and activation of GR is well known to be immune suppressive (reviewed in [332]). The initial study focused on the role of GR on CD40L expression. As shown in figure 14, the activation of GR using DEX, a potent GR agonist, suppressed CD40L expression-induced by anti-CD3/CD28. Next the interaction between Δ^9 -THC and GR using a GRE-luc reporter assay in HEK293T cells was investigated. However, treatment with Δ^9 -THC did not affect basal or DEX-induced luciferase activity (Figure 15). In addition, Δ^9 -THC did not affect the expression of *GILZ* or *IkB* mRNA, which are GRE-dependent genes, in both HEK293T (Figure 16a and 16b) and Jurkat T cells (Figure 17a and 17b).

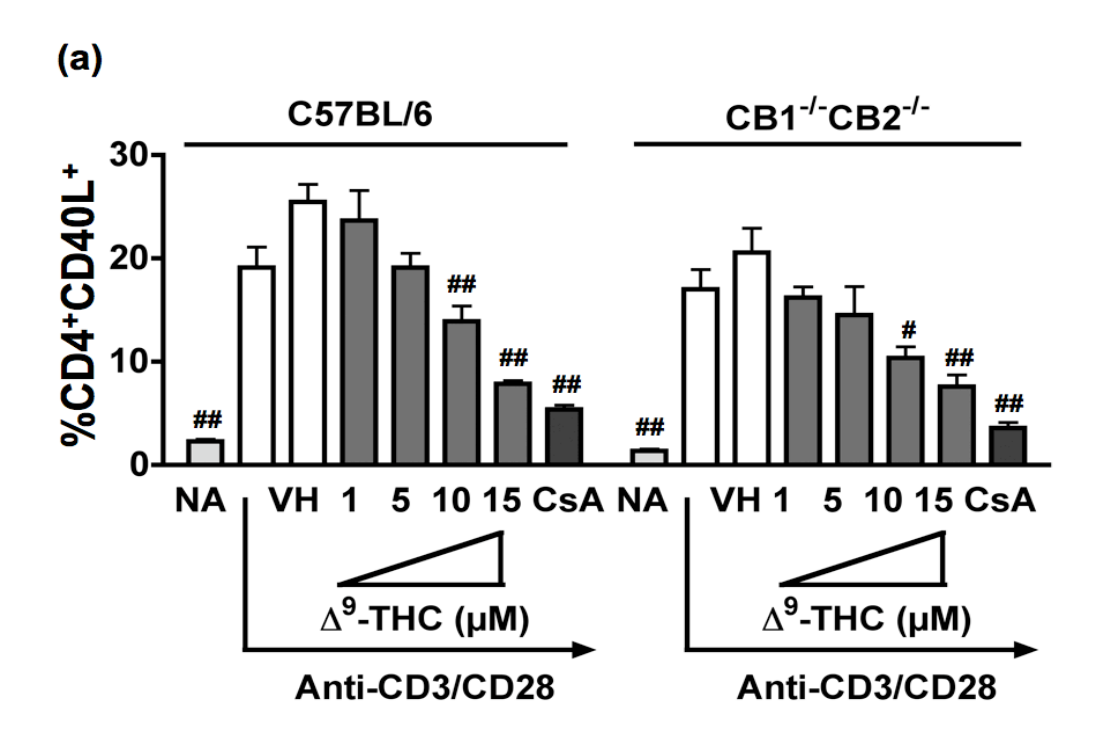
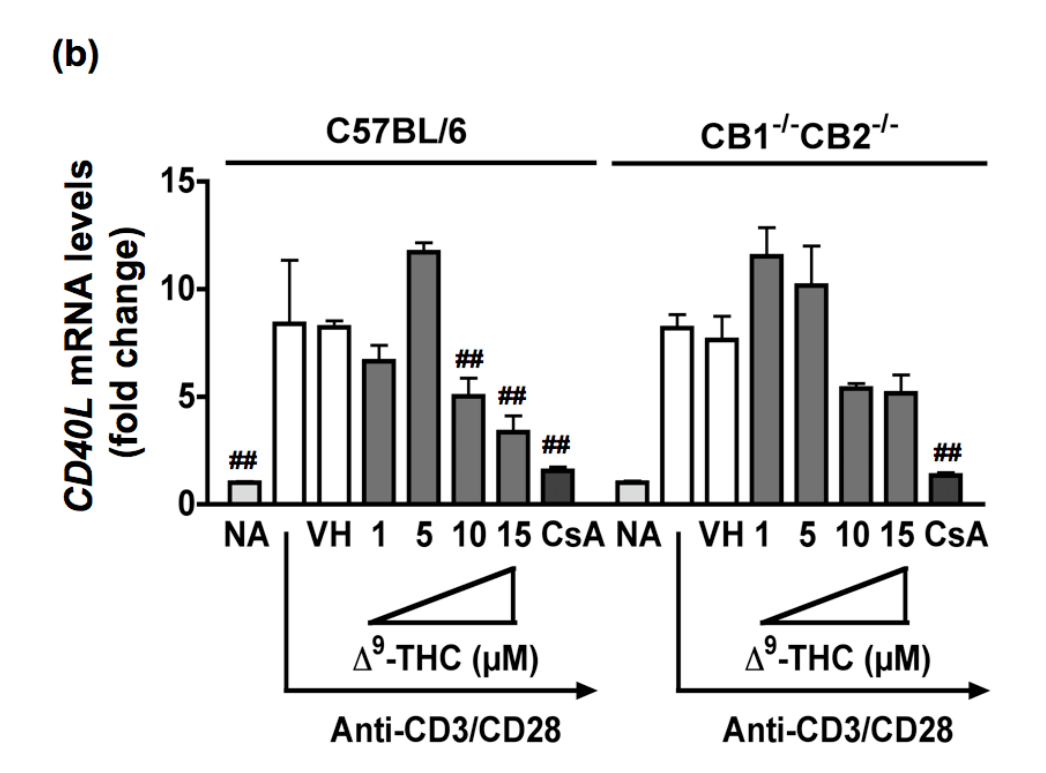


Figure 13. Comparison of the effect of Δ^9 -THC on anti-CD3/CD28-induced CD40L expression in splenic T cells derived from wildtype or CB1^{-/-}CB2^{-/-}mice.

Splenocytes $(5x10^6 \text{ cells})$ from wildtype or CB1^{-/-}CB2^{-/-} mice were treated with various concentrations of Δ^9 -THC (1, 5, 10, and 15 μ M) for 30 min and then stimulated with immobilized anti-CD3 plus soluble anti-CD28 antibodies (1 μ g/ml each). (a) Cell surface CD40L expression on activated CD4⁺ was determined by flow cytometry at 8 h after stimulation. The bar graph represents the percentage of CD4⁺CD40L⁺ cell population+SEM. (b) Steady-state expression of *CD40L* mRNA was determined by real-time PCR at 4 h after stimulation. The fold difference of *CD40L* mRNA molecules relative to unstimulated cells (naïve, NA) was normalized using the endogenous reference, 18s rRNA and results are the average of triplicates at various concentrations of Δ^9 -THC. The # or ## indicates significant effect compared to vehicle control (VH = 0.1% EtOH), at p ≤ 0.05 or p ≤ 0.01, respectively. 0.1 μ M CsA was used as the positive control. Results represent two separate experiments with three replicates per treatment group.

Figure 13 (cont'd)



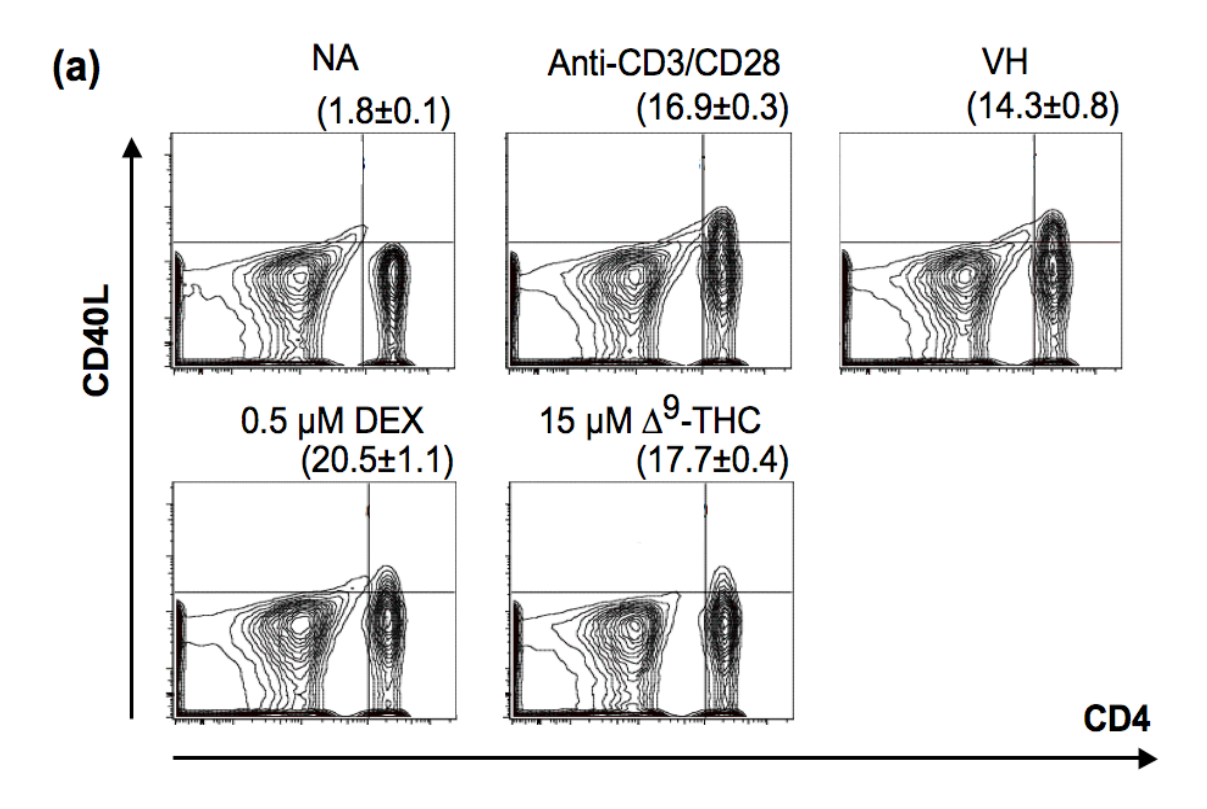
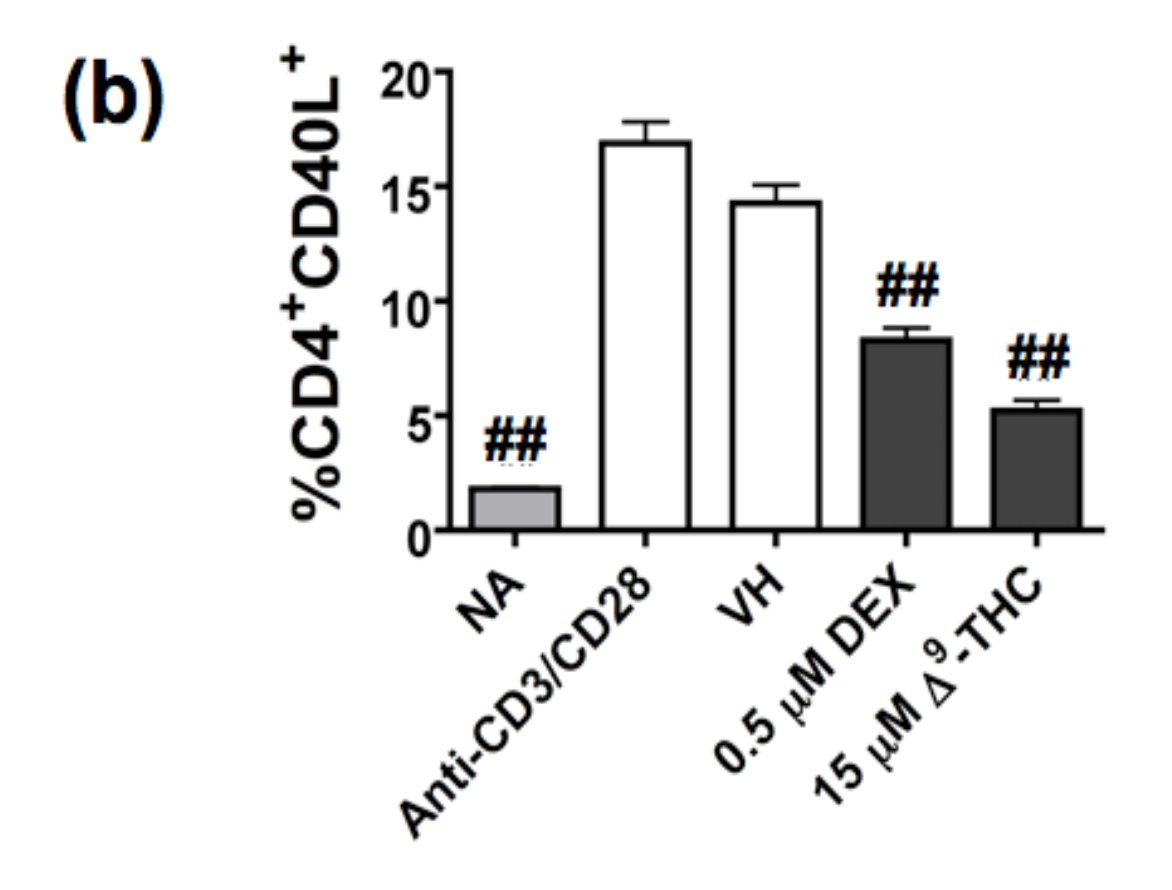


Figure 14. DEX suppresses anti-CD3/CD28-induced surface CD40L expression on activated mouse CD4⁺ T cells.

Splenocytes ($5x10^6$ cells) were treated with 0.5 μ M DEX or 15 μ M Δ^9 -THC for 30 min and then stimulated with immobilized anti-CD3 plus soluble anti-CD28 antibodies (1 μ g/ml each). (**a**) Cell surface CD40L expression on activated CD4⁺ was determined by flow cytometry at 8 h after stimulation. Number in parentheses represents the percentage of CD4⁺CD40L⁺ cell population+SEM. (**b**) Bar graph is a representation of data in (**a**). The ## indicates significant effect compared to vehicle control (VH = 0.1% EtOH), at p \leq 0.01. Results represent two separate experiments with three replicates per treatment group.

Figure 14 (cont'd)



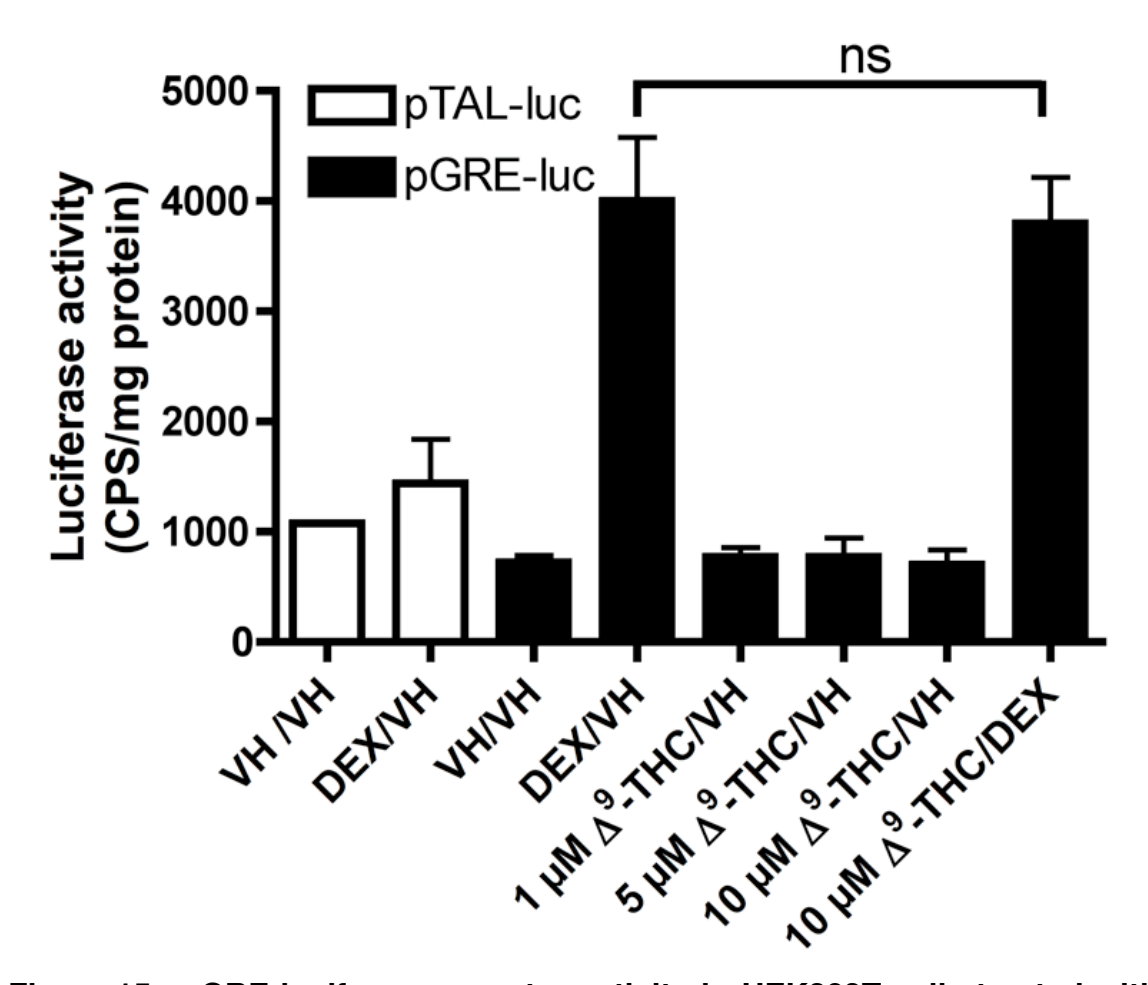


Figure 15. GRE luciferase reporter activity in HEK293T cells treated with Δ^9 -THC and/or DEX.

HEK293T cells ($5x10^6$ cells) were preseded in a 6 well plate in growth medium overnight. The cells were then transiently transfected with pGRE-luc or pTAL-luc (vector control plasmid). After transfection, the cells were treated with 0.1% EtOH (VH), 0.5 μ M DEX, different concentration of Δ^9 -THC (1, 5, and 10 μ M), or the combination of 0.5 μ M DEX plus 10 μ M Δ^9 -THC. 24 h after transfection, the luciferase activity was quantified in CPS and normalized to total protein (μ g). The results are the mean+SEM. The "ns" indicates no significant difference. Results represent two separate experiments with three replicates per treatment group.

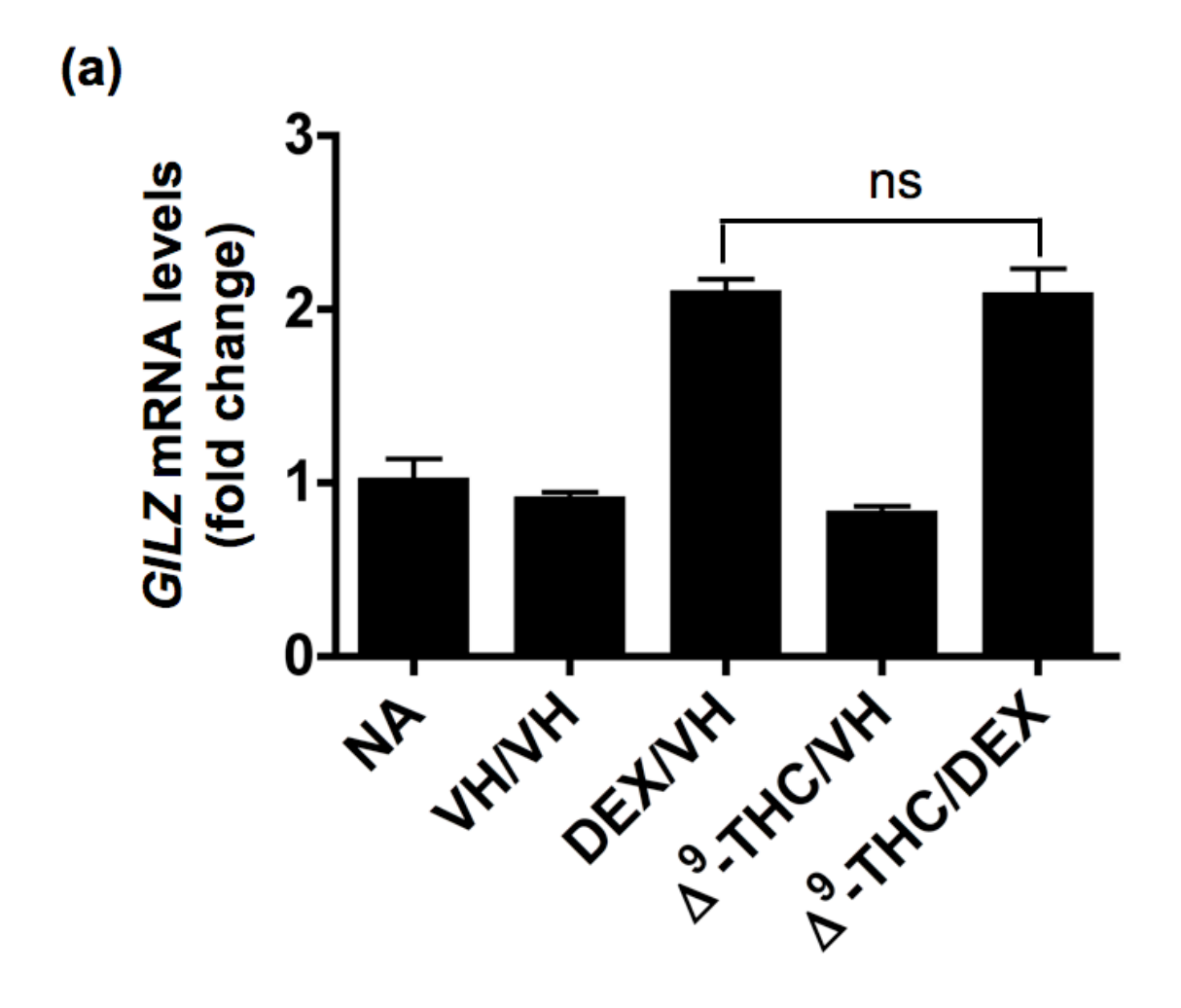
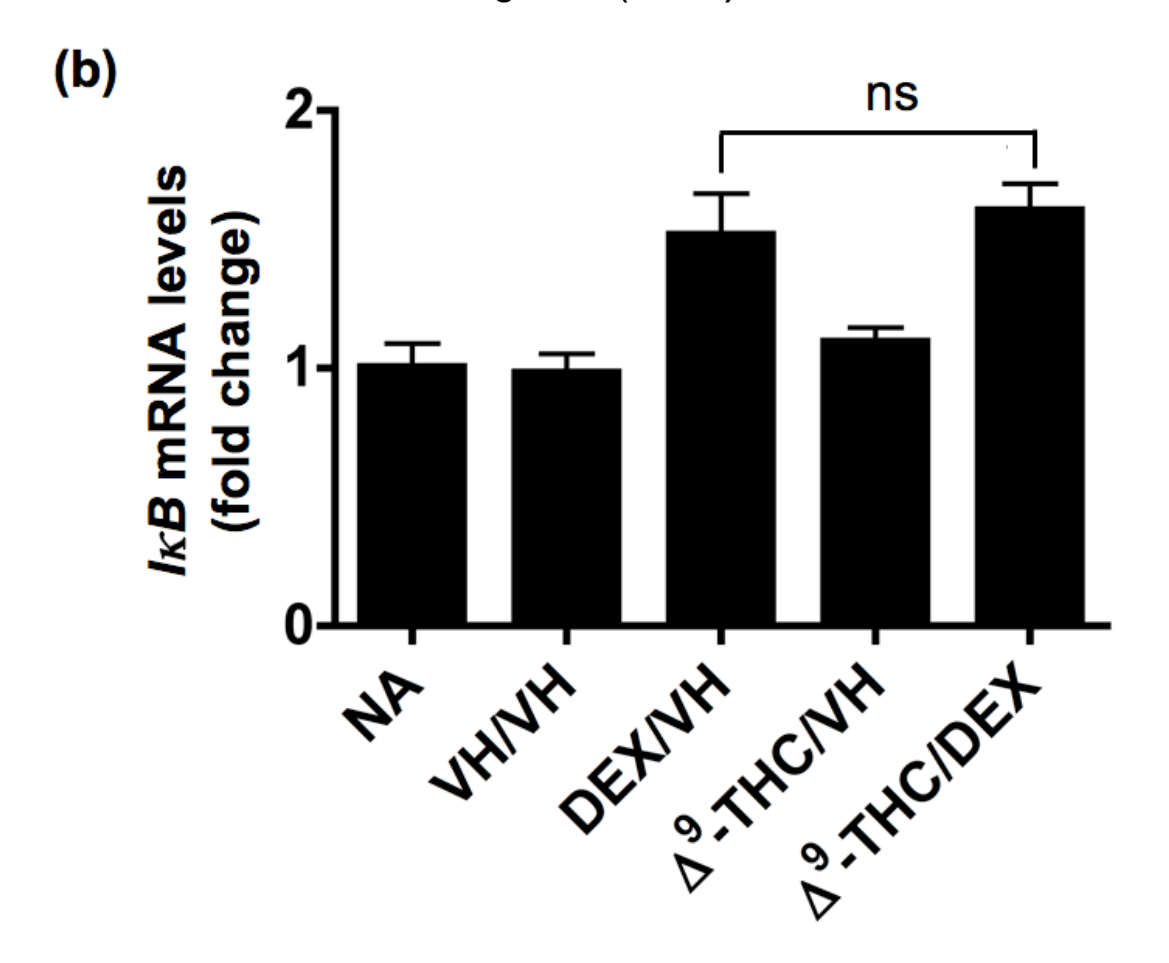


Figure 16. Effect of DEX and/or Δ^9 -THC on the mRNA expression of GR-dependent genes in HEK293T cells.

HEK293T cells (1x10⁶ cells) were preseded in a 6 well plate in growth medium overnight, followed by treatment with 0.1% EtOH (VH), 0.5 μ M DEX, 5 μ M Δ^9 -THC, or the combination of 0.5 μ M DEX plus 5 μ M Δ^9 -THC. Steady-state expression of GILZ or $I\kappa B$ mRNA were determined by real-time PCR at 6 h after treatment. The fold difference of GILZ or $I\kappa B$ mRNA molecules relative to unstimulated cells (naïve, NA) was normalized using the endogenous reference, 18s rRNA and results are the average of triplicates. The "ns" indicates no significant difference. Results represent two separate experiments with three replicates per treatment group.

Figure 16 (cont'd)



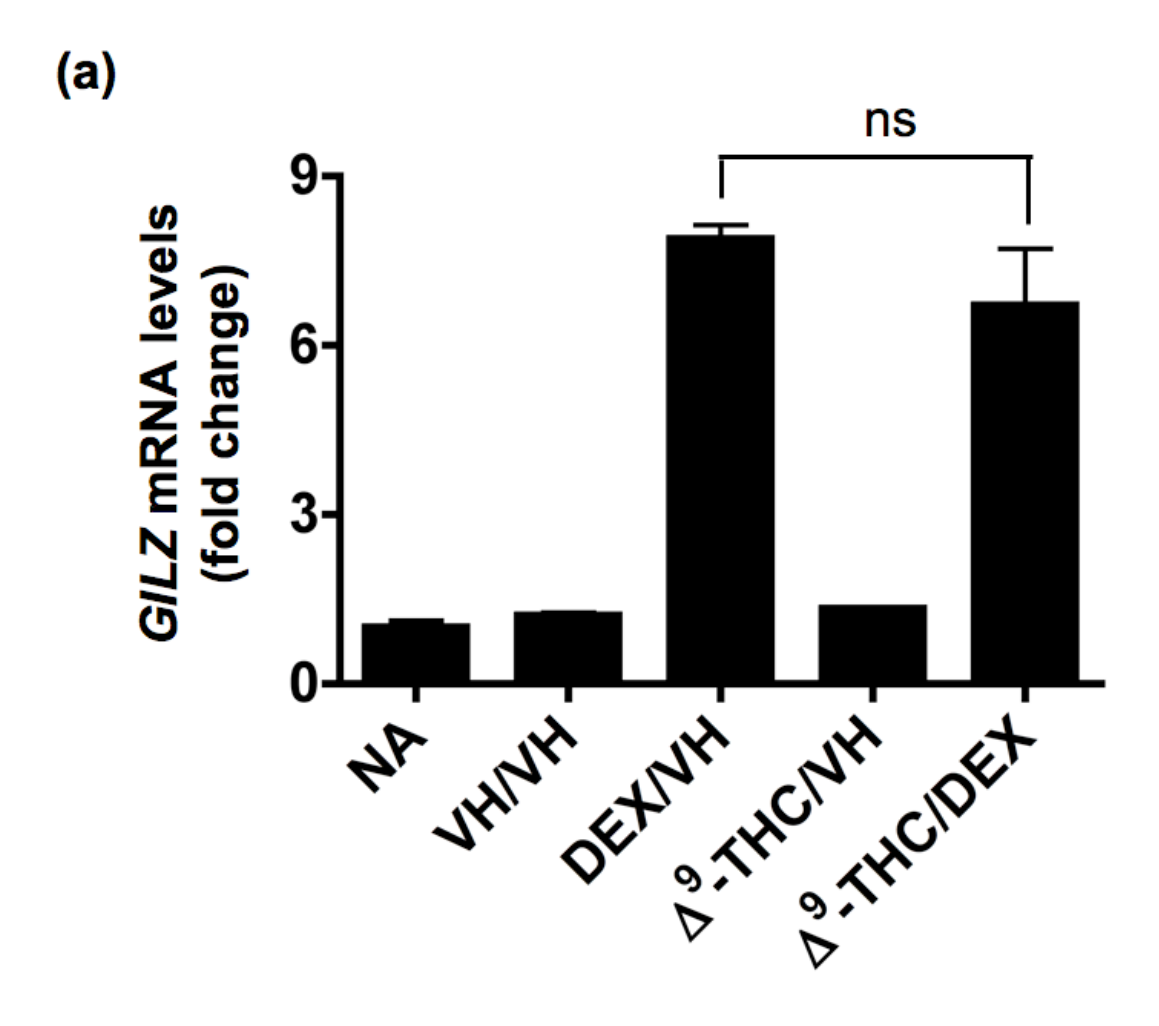
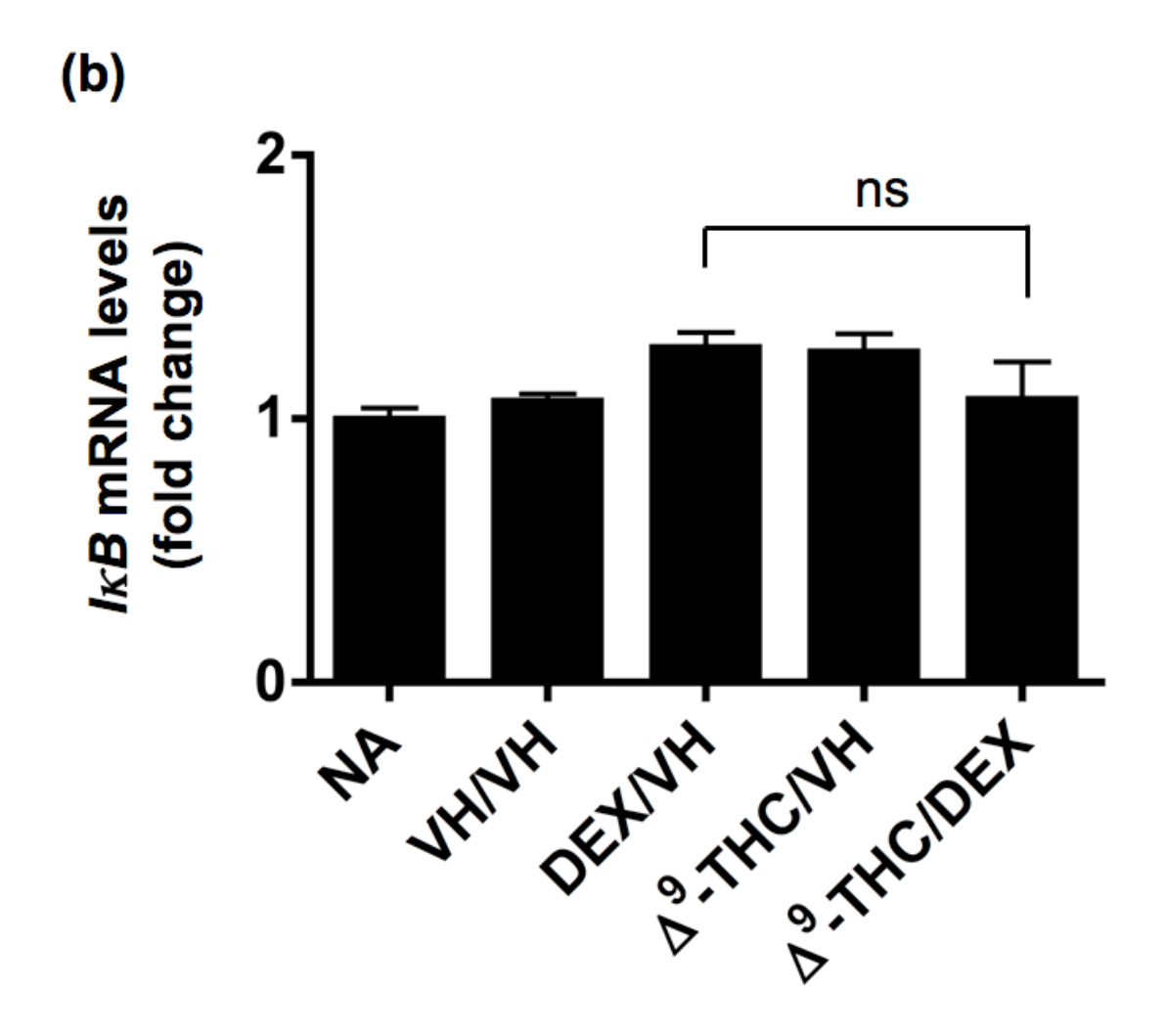


Figure 17. Effect of DEX and/or Δ^9 -THC on the mRNA expression of GR-dependent genes in Jurkat T cells.

Jurkat cells $(5x10^6 \text{ cells})$ were presended in a 6 well plate in growth medium overnight, followed by treatment with 0.1% EtOH (VH), 0.5 μ M DEX, 5 μ M Δ^9 -THC, or the combination of 0.5 μ M DEX plus 5 μ M Δ^9 -THC. Steady-state expression of GILZ or $I\kappa B$ mRNA were determined by real-time PCR at 6 h after treatment. The fold difference of GILZ or $I\kappa B$ mRNA molecules relative to unstimulated cells (naïve, NA) was normalized using the endogenous reference, 18s rRNA and results are the average of triplicates. The "ns" indicates no significant difference. Results represent two separate experiments with three replicates per treatment group.

Figure 17 (cont'd)



- II. Effect of Δ^9 -THC on the upregulation of CD40L on activated human ${\rm CD4}^+{\rm T}$ cells
- A. Δ^9 -THC attenuates anti-CD3/CD28-induced CD40L expression in activated human T cells at the transcriptional level.

Based on our previous finding that Δ^9 -THC attenuated the upregulation of CD40L expression in activated mouse splenic T cells [333], the effect of Δ^9 -THC on anti-CD3/CD28-induced CD40L expression in activated primary human T cells was investigated. Human PBMCs were stimulated with anti-CD3/CD28 in the presence or absence of Δ^9 -THC. The expression of surface CD40L was determined by flow cytometry at the indicated time points. As shown in figure 19, upregulation of surface CD40L on activated human CD4⁺ cells was detectable at 8 h, peaked at 32 h, and was declining by 72 h. Further, pretreatment with 15 μ M Δ^9 -THC attenuated the upregulation of surface CD40L expression on activated human CD4+ cells at all time points assessed (Figure 18). The concentration response studies were performed at 32 h post activation. Again, pretreatment with Δ^9 -THC significantly suppressed the percentage of double positive cells, CD4⁺CD40L⁺ cells in a concentration-dependent manner (Figure 19a and 19b). In addition, the MFI corresponding to total expression of surface CD40L on each activated CD4⁺ T cell was significantly attenuated in the

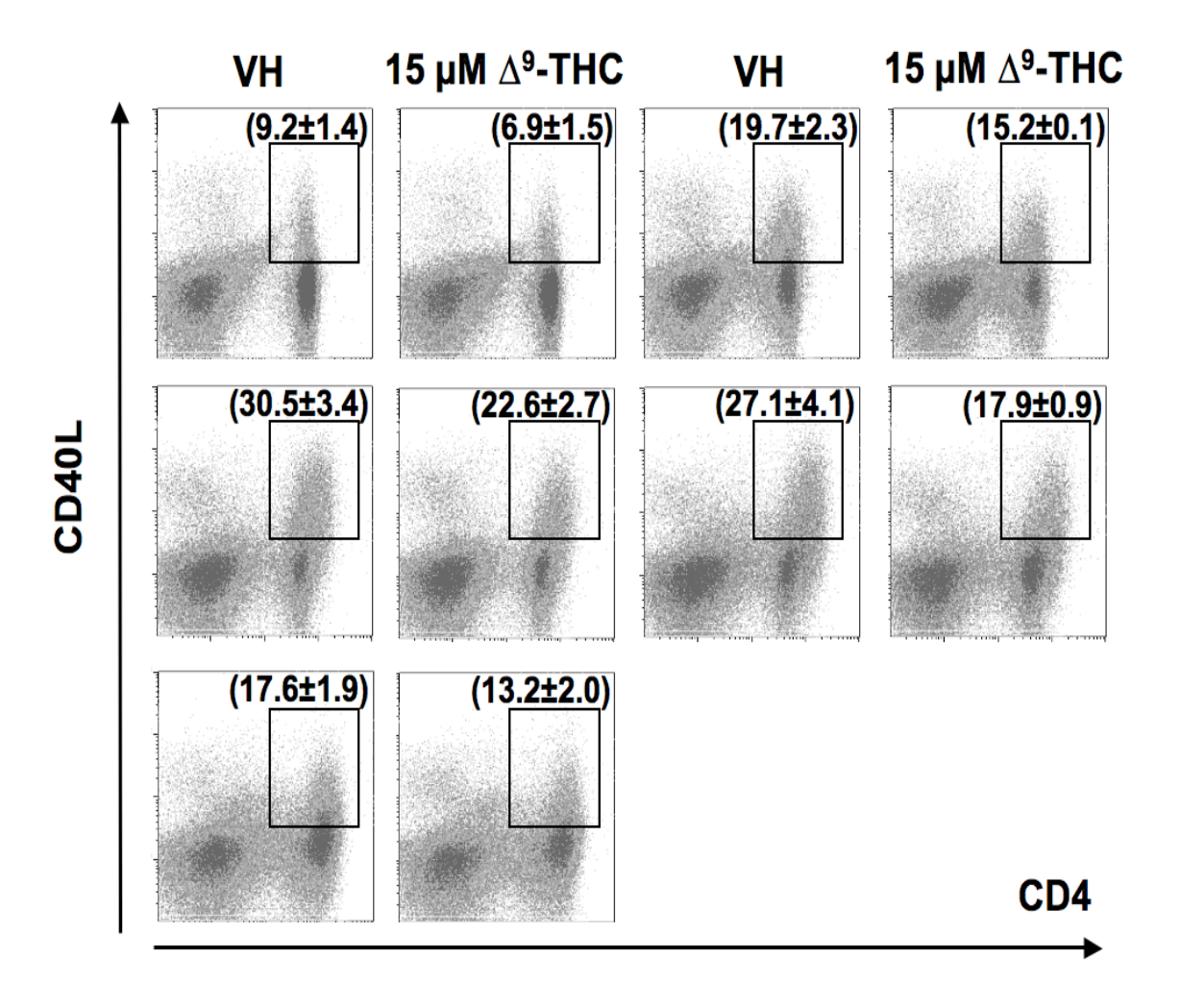


Figure 18. Effect of Δ^9 -THC on antiCD3/CD28-induced CD40L expression on activated human CD4⁺ T cells.

PBMC (1x10⁶ cells) were treated with VH (0.1% EtOH) or 15 μ M Δ^9 -THC for 30 min and then activated with anti-CD3/CD28. (Cell surface CD40L expression on activated CD4⁺ was determined at indicated time points by flow cytometry. Numbers in parentheses represent the percentage of CD4⁺CD40L⁺ cell population±SEM from triplicates. Results represent two different donors with three replicates per treatment group.

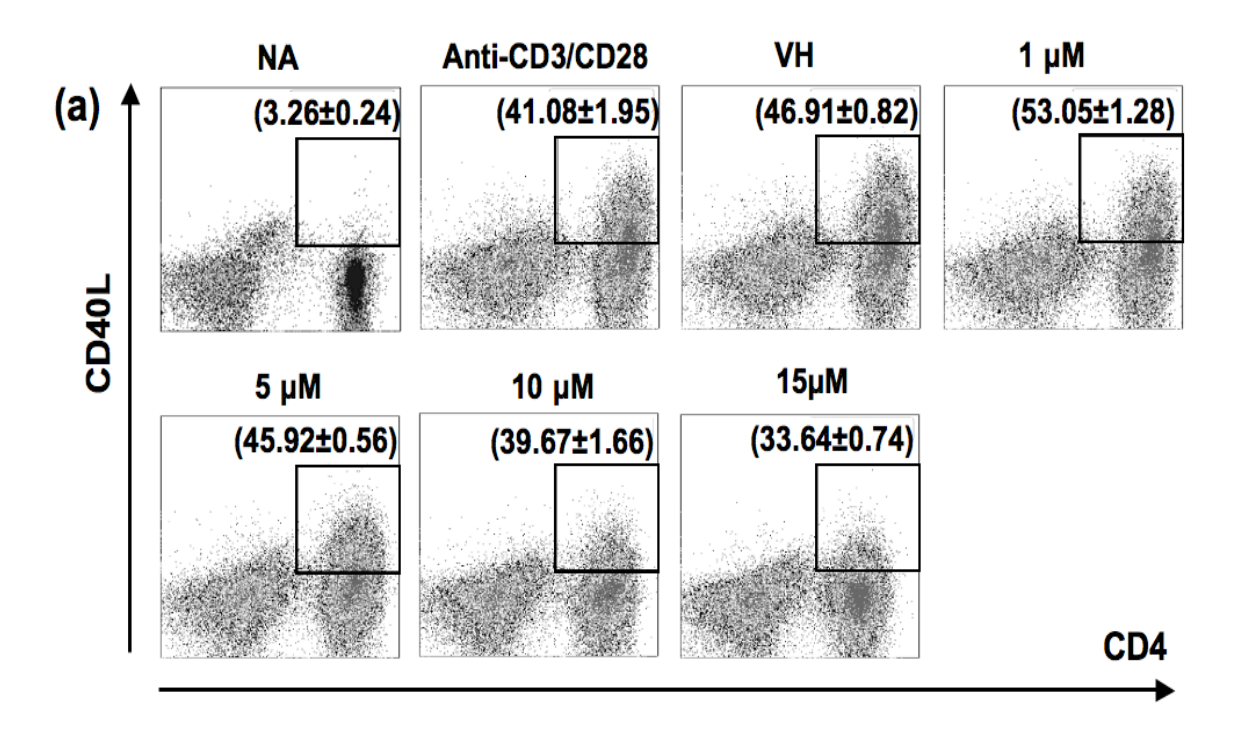
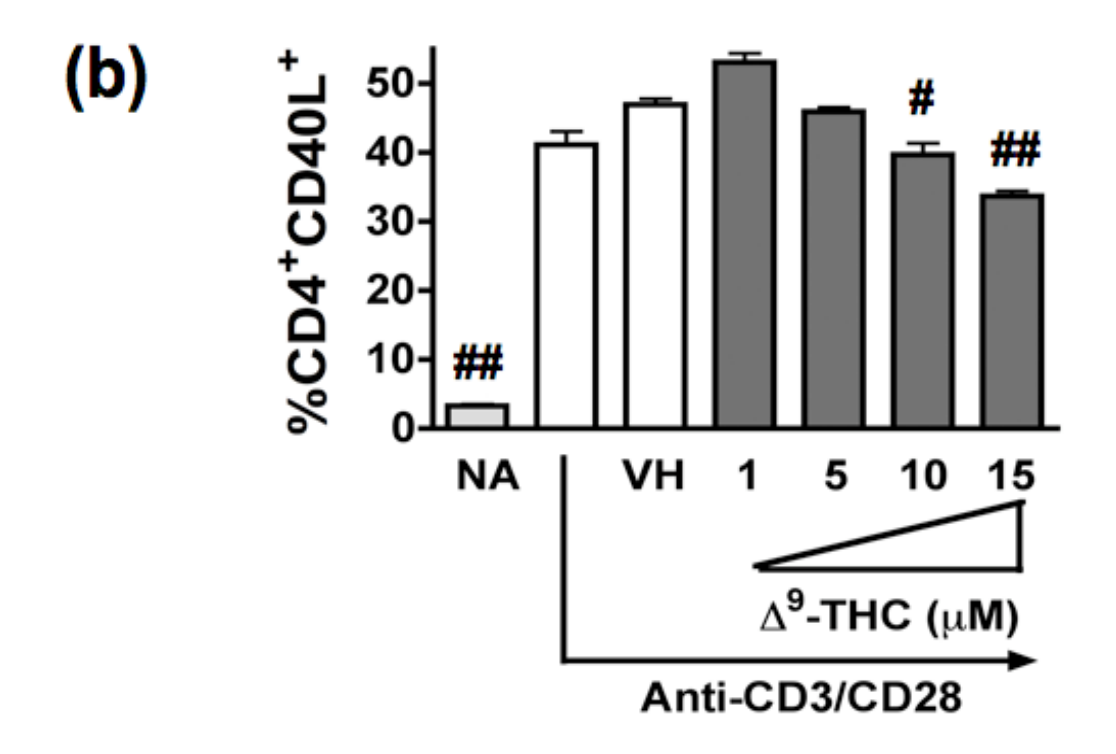
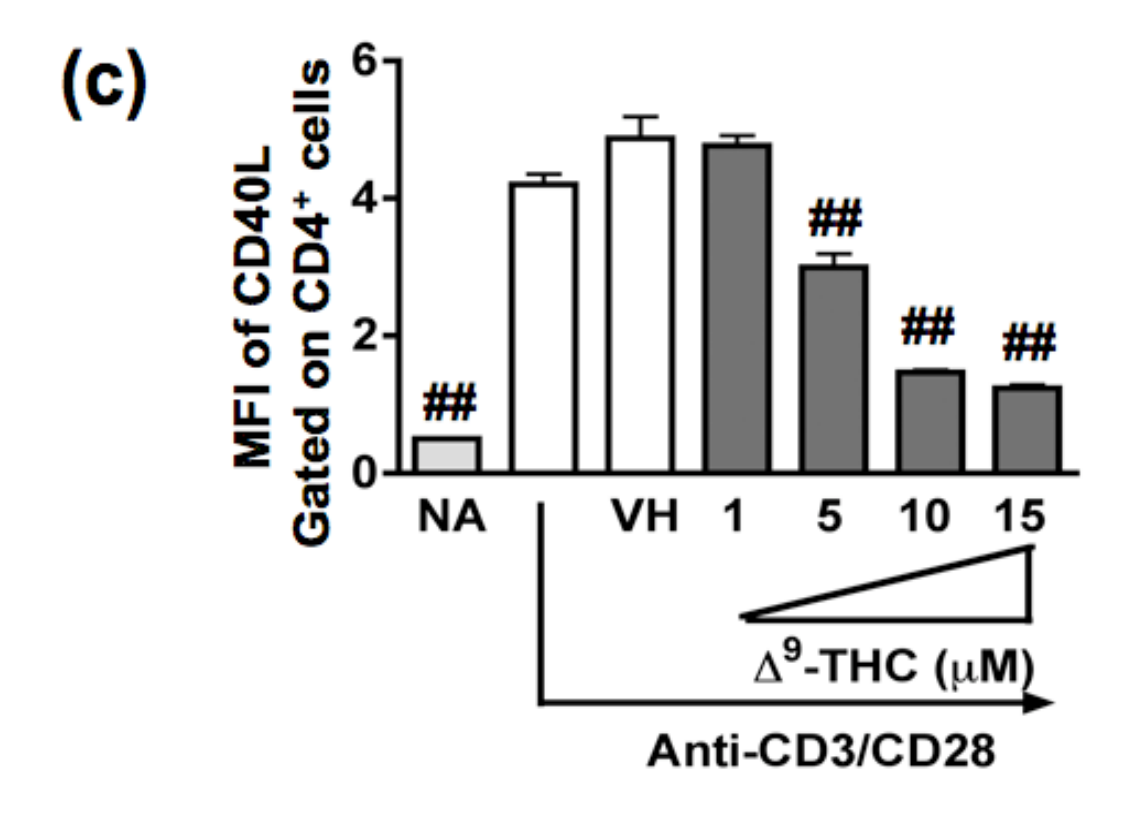


Figure 19. Δ^9 -THC attenuates TCR-induced surface CD40L expression on activated human CD4⁺T cells.

PBMC (1x10⁶ cells) were treated with Δ^9 -THC (1, 5, 10, and 15 μ M) for 30 min and then activated with anti-CD3/CD28. (a) Cell surface CD40L expression on activated CD4⁺ was determined by flow cytometry 48 h after activation. Numbers in parentheses represent the percentage of CD4⁺CD40L⁺ cell population ± SEM from triplicates. (b) Bar graph is a representation of percentage of CD4⁺CD40L⁺ cells. (c) Bar graph represents MFI of CD40L gated on CD4⁺ T cells. The * or ** indicates significant effect compared to vehicle control (VH = 0.1% EtOH), at p ≤ 0.05 or p ≤ 0.01, respectively. Results represent five different donors with three replicates per treatment group.

Figure 19 (cont'd)





presence of Δ^9 -THC (Figure 19c). The concomitant decrease in both percentage of double positive cells and MFI of CD40L clearly indicates that Δ^9 -THC impaired the upregulation of surface CD40L expression on activated human CD4⁺ T cells. It is well established that CD40L expression is almost exclusively regulated at the level of transcription (reviewed in [69]). Therefore, the steady-state level of CD40L mRNA was assessed by quantitative real time PCR in the presence or absence of Δ^9 -THC at 24 h post stimulation. As shown in figure 20, Δ^9 -THC significantly attenuated anti-CD3/CD28-induced CD40L mRNA expression in activated human T cells. The suppression of CD40L mRNA expression by Δ^9 -THC also occurred in a concentration-dependent manner, which corresponds to its effect on the protein level.

B. Δ^9 -THC impairs anti-CD3/CD28-induced DNA-binding activity of NFAT and NF $_K$ B in activated human T cells.

The transactivation of the *CD40L* gene is tightly regulated by several transcription factors (NFAT, CD28RE, NF κ B, TFE3/TFEB, EGR, AKNA, and AP1) that bind in the promoter region [77]. Although NFAT is the key transcription factor found in the minimal CD40L promoter [76], several reports demonstrated significant involvement of NF κ B in the upregulation of CD40L expression in both activated mouse and human T cells [78-80]. Previous studies from our laboratory demonstrated that cannabinoids suppressed T cell function, partly though the

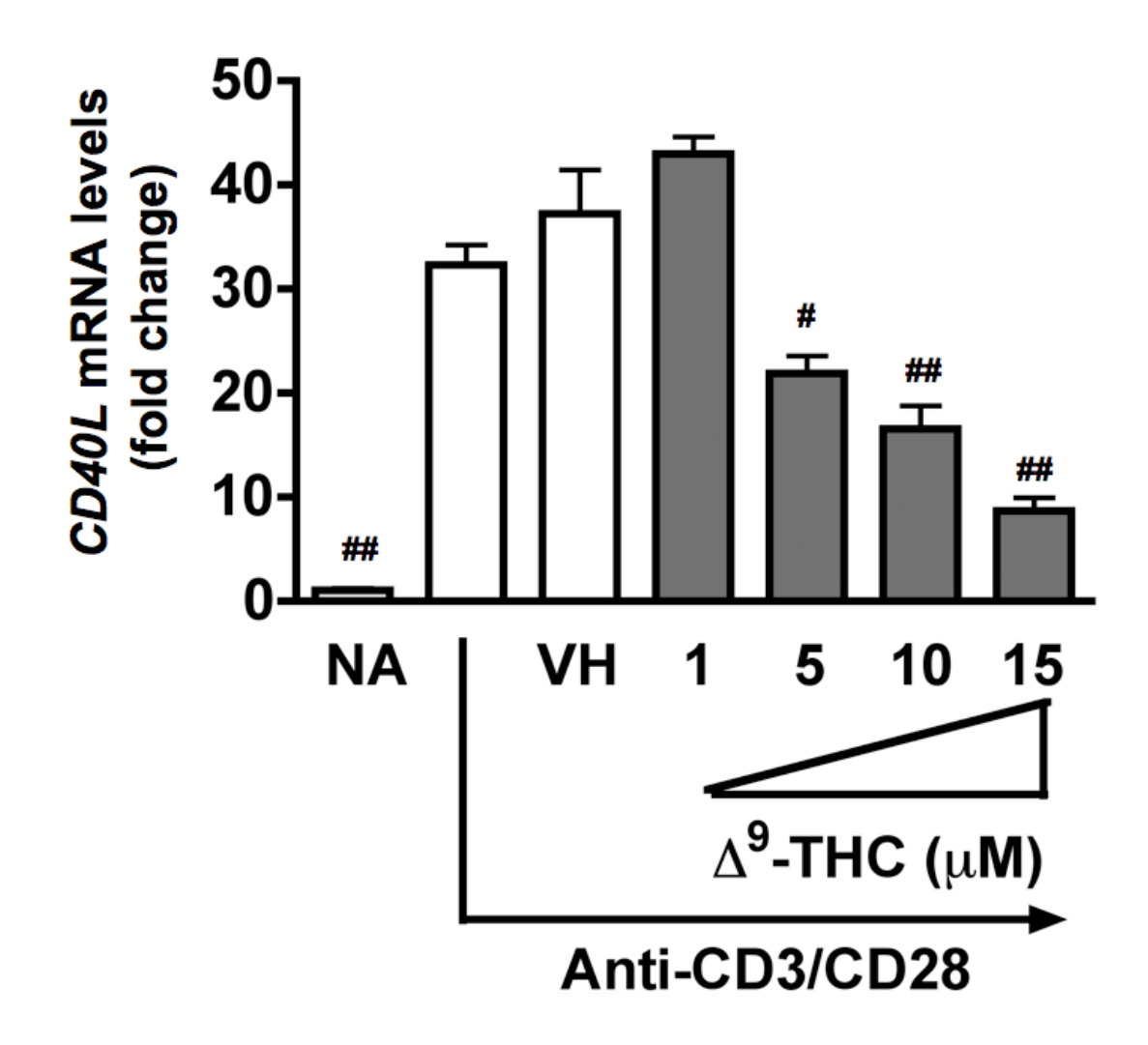


Figure 20. Δ^9 -THC suppressed TCR-induced CD40L mRNA expression in activated human CD4⁺ T cells.

PBMC (1x10⁶ cells) were treated with Δ^9 -THC (1, 5, 10, and 15 μ M) for 30 min and then activated with anti-CD3/CD28. Steady-state expression of CD40L mRNA was determined by real-time PCR 24 h after activation. The fold difference of CD40L mRNA molecules relative to nonactivated resting cells (naïve, NA) was normalized using the endogenous reference, 18s rRNA. The * or ** indicates significant effect compared to vehicle control (VH = 0.1% EtOH) at p \leq 0.05 or p \leq 0.01, respectively. Results represent three different donors with four replicates per treatment group.

impairment of NFAT and NFkB activation [303,311]. In light of the above, the effect of Δ9-THC on anti-CD3/CD28-induced DNA binding activity of NFAT and NFκB to the CD40L promoter was investigated by EMSA. Both NFAT and NFκB oligonucleotide probes containing the respective binding sites were derived from the human CD40L promoter [80,323]. Human PBMCs were activated with anti-CD3/CD28 in the presence or absence of Δ^9 -THC for 16 h, which was the time of the highest magnitude of DNA-binding activity of NFAT (Figure 21). specificity of NFAT-DNA complexes (as indicated by arrows) was determined by adding 100-fold molar excess of unlabelled probe (Figure 22a, lane 9). Upon T cell activation, there was an increase in DNA binding activity of specific NFAT-DNA complexes (lane 3) compared to the nuclear protein from nonactivated PBMCs (NA) (lane 2). Pretreatment with Δ^9 -THC (1, 5, 10, and 15 μ M – lane 5-8) followed by stimulation with anti-CD3/CD28 decreased the intensity of specific NFAT-DNA complexes, thereby indicating a decrease in NFAT-DNA binding activity. For NFkB, only one complex, indicated by an arrow, was competed completely in the presence of 100-fold molar excess of unlabelled probe (Figure 22b, lane 9). Upon activation, there was an increase in NFκB-DNA binding activity (lane 3) when compared to the nuclear protein from NA cells. Pretreatment with Δ^9 -THC (1, 5, 10, and 15 μ M - lane 5-8) followed by anti-CD3/CD28 activation decreased the intensity of specific NFkB-DNA complexes, thereby indicating a decrease in NFκB-DNA binding activity. These results suggest that $\Delta^9\text{-THC}$ impaired both NFAT- and NF κ B-DNA binding activity in activated human T cells.

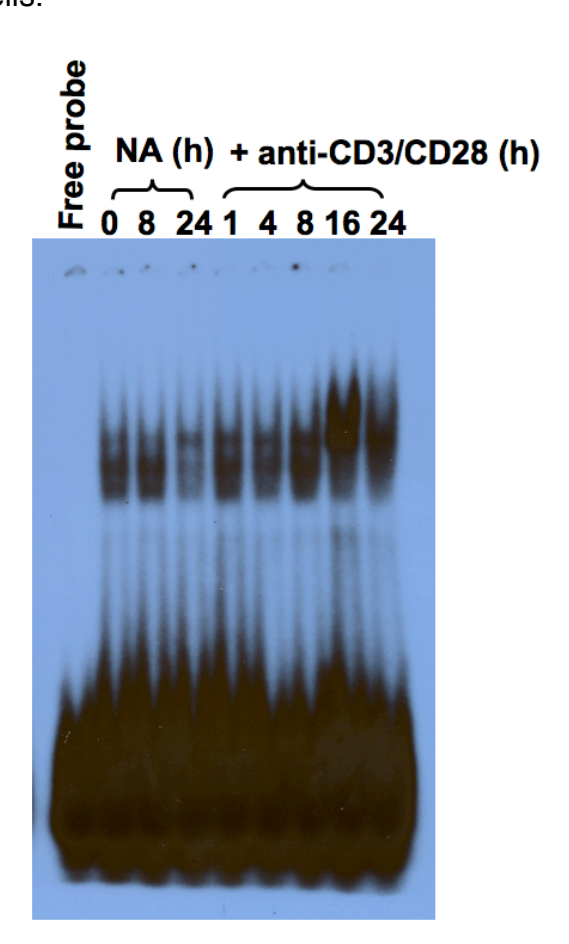


Figure 21. Peak time of anti-CD3/CD28-induced DNA-binding activity of NFAT in activated human T cells.

PBMC ($2x10^7$ cells) were activated with anti-CD3/CD28 at indicated time points. The nuclear proteins (1 μ g) were incubated with oligonucleotide probes derived from human CD40L promoter containing NFAT. The DNA-binding complexes were resolved by gel electrophoresis. The basal DNA binding activity was measured in nonactivated cells (NA) at 0, 8, and 24 h (lane 2-4). The induction of NFAT-protein complexes in activated T cells was measured at various time points (lane 5-9). Lane 1 is radiolabeled probe alone. Arrows indicate the specific DNA-protein complexes. The data are representative of two independent experiments from different donors.

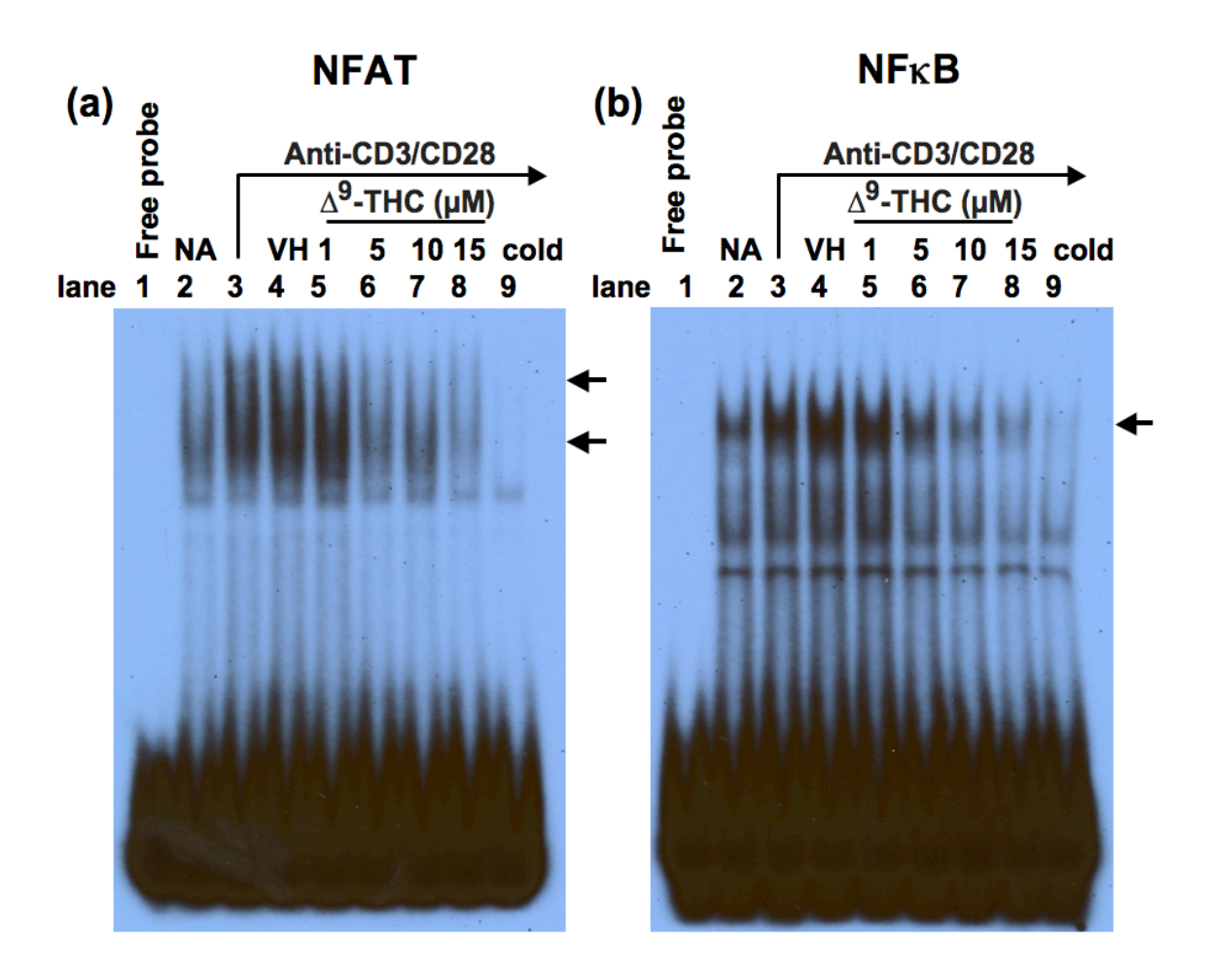


Figure 22. Δ^9 -THC impaires TCR-induced DNA binding activity of NFAT and NF_KB in activated human T cells.

PBMC (2x10⁷ cells) were treated with VH (lane 4) or Δ^9 -THC (1, 5, 10, and 15 μ M; lane 5, 6, 7, 8) for 30 min and then activated with anti-CD3/CD28, for 16 h. The basal DNA binding activity was measured in nonactivated cells (lane 2), whereas the formation of NFAT- or NFκB-DNA complexes was measured in TCR-activated cells (lane 3). The specificity of either NFAT- or NFκB-DNA complexes was determined by adding 100-fold molar excess of the unlabeled probes using the same protein as loaded in lane 3 (lane 9). Lane 1 is radiolabeled probe alone. The nuclear proteins (1 μ g) were incubated with oligonucleotide probes derived from human CD40L promoter containing either NFAT or NFκB binding site. The DNA-binding complexes were resolved by gel electrophoresis. (a) EMSA analysis of NFAT binding to the CD40L promoter. (b) EMSA analysis of NFκB binding to the CD40L promoter. Arrows indicate the specific DNA-protein complexes. The data are representative of three independent experiments from different donors.

C. Δ^9 -THC does not affect GSK3 β activity in activated human CD4 $^+$ T cells

GSK3β, a serine/theonine protein kinase, has been shown to act as a negative regulator to limit the activation of many transcription factors, particularly NFAT. The phosphorylation of NFAT by GSK3\beta inhibits NFAT activation by retaining NFAT in the cytoplasm as well as promoting the export from the nucleus (reviewed in [59]). GSK3β is constitutively active in resting cells and becomes inactive upon stimulation though TCR by phosphorylation at serine residue 9 (pGSK3 β) (reviewed in [59]). To further elucidate the mechanism by which Δ^9 -THC suppresses NFAT-DNA binding activity, the effect of Δ^9 -THC pretreatment on the activity of GSK3β in activated T cells was investigated. Human PBMCs were activated using anti-CD3/CD28 crosslinking. The peak level of pGSK3β, which corresponds to its inactive state, was assessed by flow cytometry at indicated time points post activation. As shown in Figure 23, there was an increase in the amount of pGSK3β in activated human CD4+ T cells as demonstrating by the increase of MFI, as early as 2 min, maximal at 5 min, and was declining back to the background level by 15 min. Pretreatment with Δ^9 -THC did not affect the level of pGSK3 β suggesting that Δ^9 -THC did not perturb anti-CD3/CD28-induced GSK3β inactivation in human CD4⁺ T cells (Figure 24).

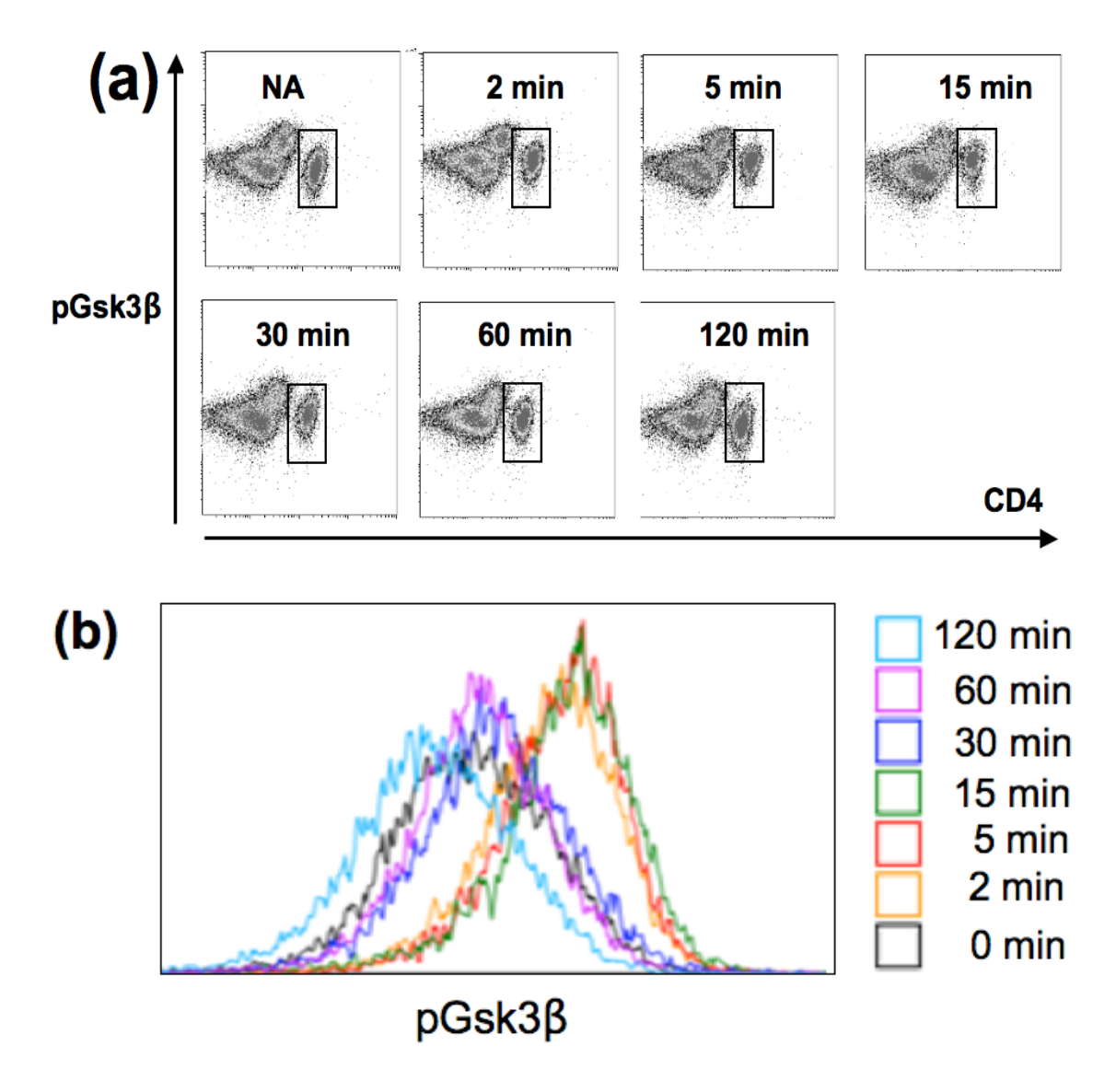


Figure 23. Peak time of anti-CD3/CD28-induced phosphorylation of $GSK3\beta$ in activated human T cells.

PBMC (1x10⁶ cells/100 μ L) were equilibrated at 37°C in 5% CO₂ for 3 h, followed by incubation with anti-CD3, anti-CD28, and IgG crosslinker on ice. T cell activation was initiated by transferring to 37°C water bath. Cells were fixed with 1.5% formaldehyde at indicated time points. Cells were permeabilized with ice-cold 100% methanol, followed by staining with anti-CD4 and anti-pGSK3 β . The intracellular expression of pGSK3 β in CD4⁺ T cells was assessed by flow cytometry. (a) Dot plot represents CD4⁺pGSK3 β ⁺ cell population at various time points (b) Histogram plot represents MFI of pGSK3 β gated on CD4⁺ T cells at various time points. The data are representative of two independent experiments from different donors.

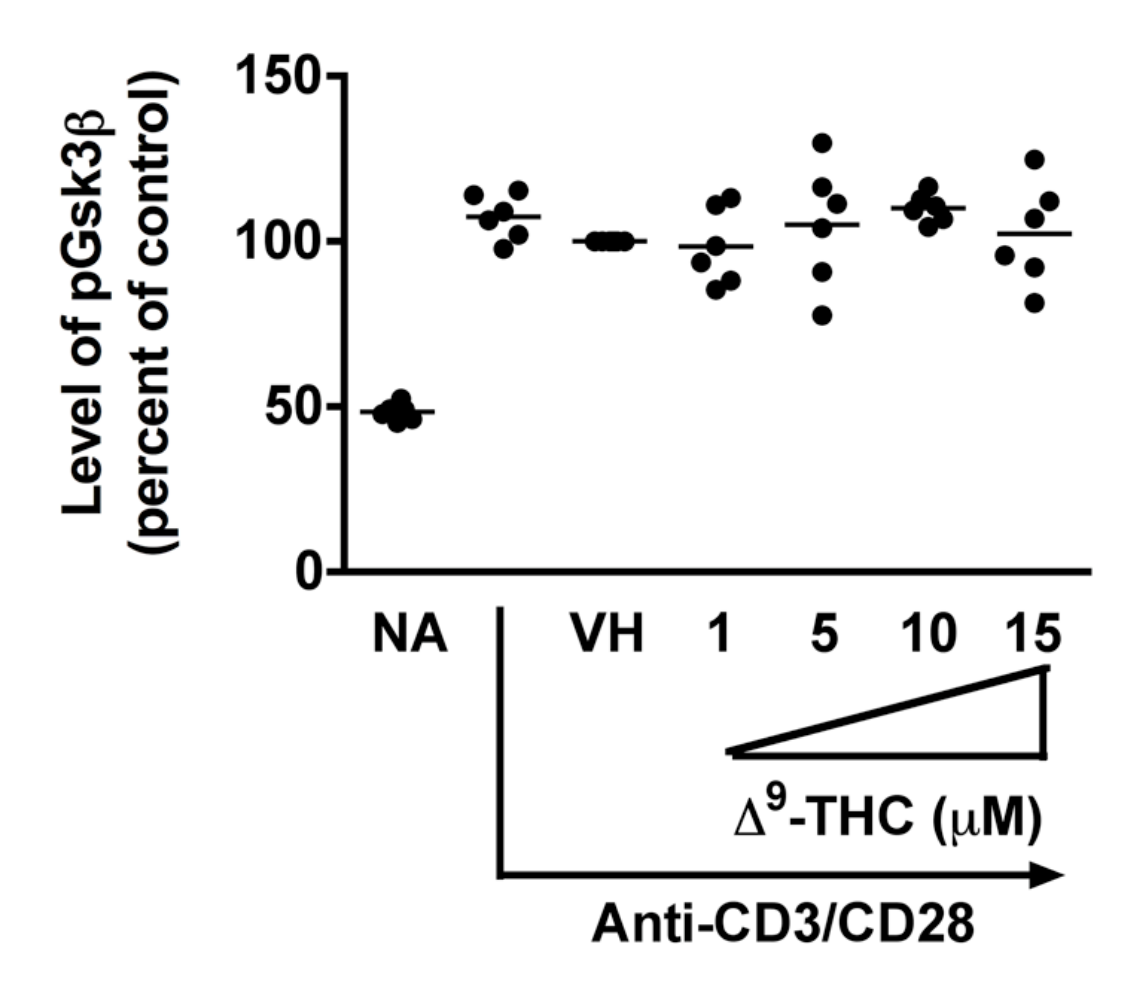


Figure 24. Effect of Δ^9 -THC on the activity of GSK3 β in activated human CD4⁺ T cells.

PBMC (1x10⁶ cells/100 μ L) were equilibrated at 37°C in 5% CO₂ for 3 h, treated with Δ^9 -THC (1, 5, 10, and 15 μ M) and/or VH for 30 min, and then incubated with anti-CD3, anti-CD28, and IgG crosslinker on ice. T cell activation was initiated by transferring to 37°C water bath for 5 min. Cells were fixed with 1.5% paraformaldehyde and permeabilized with ice-cold 100% methanol, followed by staining with anti-CD4 and anti-pGSK3 β . The intracellular expression of pGSK3 β in CD4⁺ T cells was assessed by flow cytometry. Results depicted are MFI of pGSK3 β gated on CD4⁺ T cells. Data were normalized to the VH-treated group and presented as percent of control. Each dot represents data from one individual donor.

D. Δ^9 -THC attenuates anti-CD3/CD28-induced elevated intracellular Ca $^{2+}$, but does not impair PLC γ activation.

The inhibitory effect of Δ^9 -THC on the DNA binding activity of both NFAT and NFkB strongly implicated altered intracellular Ca²⁺ regulation in the presence of Δ^9 -THC. To investigate the effects of Δ^9 -THC on anti-CD3/CD28-induced Ca²⁺ elevation in human CD4⁺ T cells, naïve CD4⁺ T cells were incubated with the Ca²⁺ indicator dyes fluo-3 and fura-red for 60 min, following by treatment with Δ^9 -THC for 30 min. Cells were then incubated with anti-CD3/CD28 on ice. Upon TCR stimulation with an IgG crosslinker, there was a pronounced rise in intracellular Ca^{2+} (Figure 25). Pretreatment with Δ^{9} -THC resulted in a concentration-dependent attenuation of elevated Ca²⁺ following anti-CD3/CD28 crosslinking in activated human CD4+ T cells with nearly complete loss of the response at 15 μ M Δ^9 -THC (Figure 25). The increase in intracellular Ca²⁺ following TCR stimulation is mainly regulated by the activation of PLCy (reviewed in [50]). Furthermore, PLC_γ also controls NFκB activation though the PKCθ pathway (reviewed in [334]). We next tested whether Δ^9 -THC affects the activation of PLCy. The phosphorylation status of PLCy1/2 (pPLCy1/2), which corresponds to its active state, was determined by flow cytometry at 5 min post

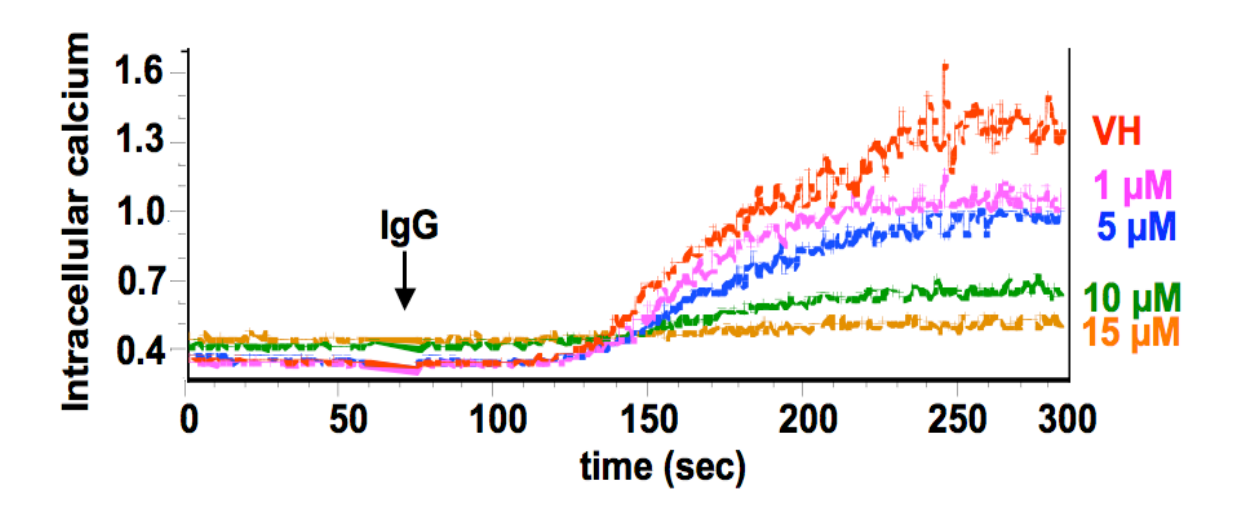


Figure 25. Δ^9 -THC suppressed TCR-induced elevation of intracellular Ca²⁺ in activated human CD4⁺ T cells.

Naïve CD4 $^+$ T cells (1x10 6 cells/mL) were incubated with the indicator dyes Fura-3 and Fluo-red for 60 min. Cells were treated with Δ^9 -THC (1, 5, 10, and 15 μ M) and/or VH for 30 min before incubating with anti-CD3 and anti-CD28. Intracellular Ca $^{2+}$ mobilization was observed by flow cytometry. After 60 sec of data acquisition, TCR activation was initiated by adding IgG crosslinker followed by measuring the intracellular Ca $^{2+}$ mobilization for the total of 300 sec. Kinetic plots are expressed as median of the FL1:FL3 ratio. Results represent two separate experiments. Data are presented in arbitrary units as a function of fluorescence (relative intracellular Ca $^{2+}$) versus time.

stimulation with anti-CD3/CD28 crosslinking. Upon activation, there was a robust increase in the amount of pPLC γ 1/2 as demonstrating by the increase of MFI in activated human CD4 $^+$ T cells. However, pretreatment with Δ^9 -THC did not significantly affect anti-CD3/CD28-mediated increase of pPLC γ 1/2 in activated human CD4 $^+$ T cells (Figure 26). These results suggest that suppression of anti-CD3/CD28-induced elevation of Ca $^{2+}$ influx by Δ^9 -THC in human CD4 $^+$ T cells is not mediated through the activation of PLC γ 1/2.

E. Δ^9 -THC does not modulate anti-CD3/CD28-mediated phosphorylation of ZAP70 or Akt in activated human CD4⁺ T cells.

The previous study using mouse splenocytes suggested that Δ^9 -THC affected the proximal signaling of TCR, based on the fact that Δ^9 -THC-mediated suppression of CD40L expression occurred following T cell activation by anti-CD3/CD28 antibodies, but not PMA/Io [333]. Along the same line, a study reported by Borner *et. al.* demonstrated that the T-cell inhibitory effect of Δ^9 -THC is due, in part, to the impairment of proximal TCR signaling cascades [308]. To test this hypothesis, the effect of Δ^9 -THC on proximal TCR signaling cascades was investigated. To identify the peak time induction, the level of phosphorylated ZAP70 (pZAP70), which is mediated though CD3 activation, and the level of phosphorylated Akt (pAkt), which is mediated though CD28 activation, were

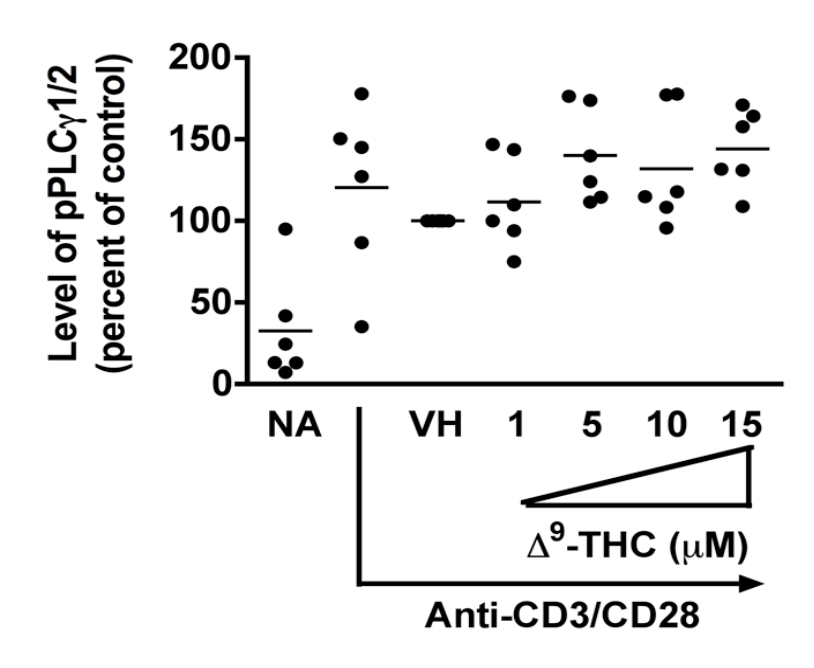


Figure 26. Effect of Δ^9 -THC on the activation of PLC γ in activated human CD4⁺ T cells.

PBMC (1x10⁶ cells/100 μ L) were equilibrated at 37°C in 5% CO₂ for 3 h, treated with Δ^9 -THC (1, 5, 10, and 15 μ M) and/or VH for 30 min, and then incubated with anti-CD3, anti-CD28, and IgG crosslinker on ice. T cells activation was initiated by transferring to 37°C water bath for 5 min. Cells were fixed with 1.5% paraformaldehyde and permeabilized with ice-cold 100% methanol, followed by staining with anti-CD4 and anti-pPLC γ . The intracellular expression of pPLC γ 1/2 in CD4⁺ T cells was assessed by flow cytometry. Results depicted are MFI of pPLC γ 1/2 gated on CD4⁺ T cells. Data were normalized to the VH-treated group and presented as percent of control. Each dot represents data from one individual donor.

measured by flow cytometry at the indicated time points post activation with anti-CD3/CD28 crosslinking. Upon activation, there was an increase in the amount of both pZAP70 (Figure 27) and pAkt (Figure 28) in activated human CD4⁺ T cells as early as 2 min, maximal at 5 min, and was declining to the background level by 15 min. Pretreatment with Δ^9 -THC did not significantly affect anti-CD3/CD28induced phosphorylation of either ZAP70 or Akt in activated human CD4⁺ T cells (Figure 29a and 29b, respectively). Interestingly, pretreatment with Δ^9 -THC increased the variability in the phosphorylation of ZAP70 among the human subjects (Figure 29a). Thus, a comparable mouse model was used to investigate the effect of Δ^9 -THC on the activation of ZAP70. We found that Δ^9 -THC did not affect the phosphorylation level of Zap70 in activated mouse CD4⁺ T cells (Figure Collectively, these results demonstrate that $\Delta^9\text{-THC}$ does not impair 30). proximal TCR-associated signaling in activated human CD4⁺ T cells.

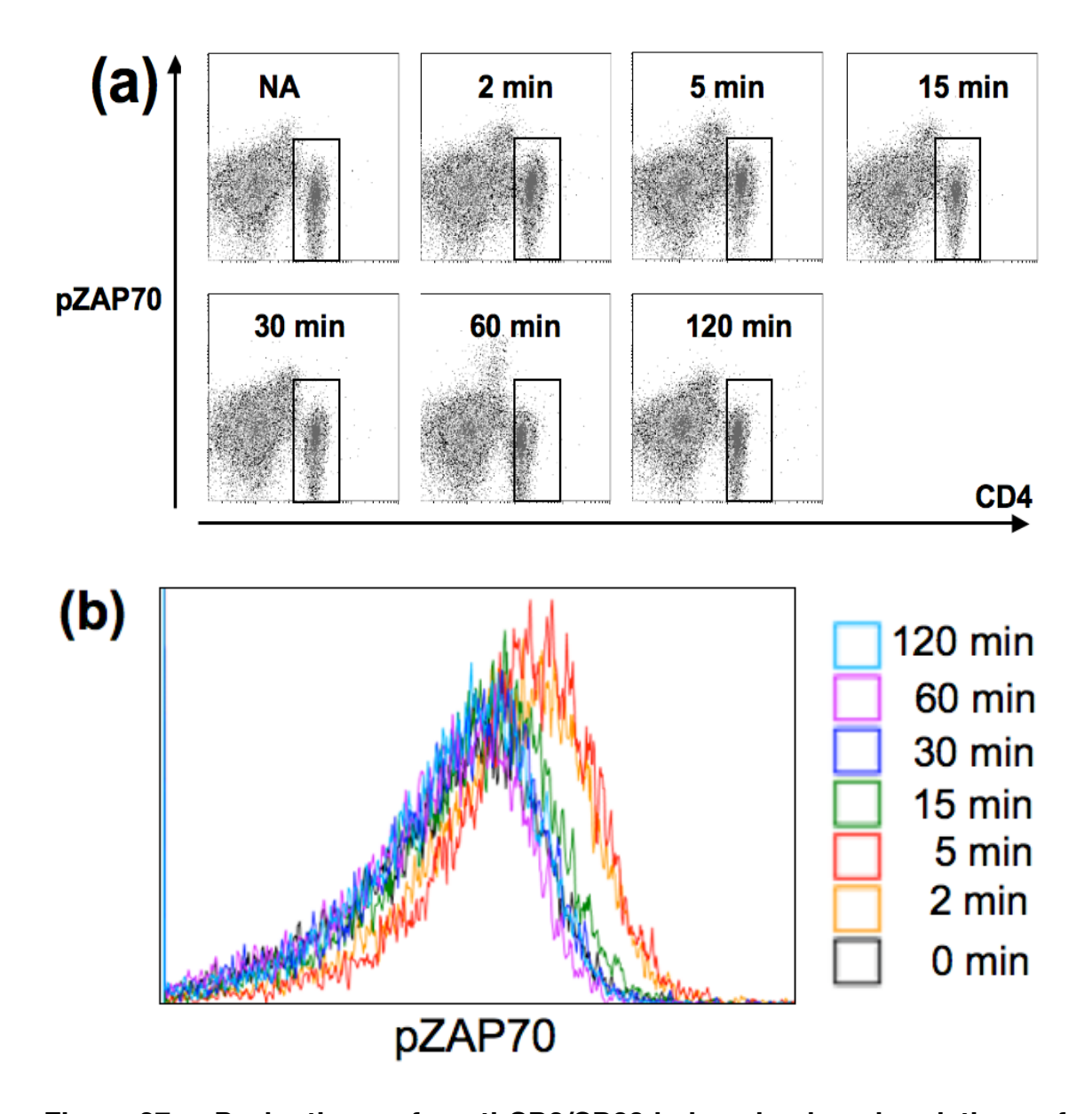


Figure 27. Peak time of anti-CD3/CD28-induced phosphorylation of ZAP70 in activated human T cells.

PBMC ($1x10^6$ cells/ $100~\mu$ L) were equilibrated at 37° C in 5% CO $_2$ for 3 h, followed by incubation with anti-CD3, anti-CD28, and IgG crosslinker on ice. T cell activation was initiated by transferring to 37° C water bath. Cells were fixed with 1.5% paraformaldehyde at indicated time points. Cells were permeabilized with ice-cold 100% methanol, followed by staining with anti-CD4 and anti-pZAP70. The intracellular expression of pZAP70 in CD4 $^+$ T cells was assessed by flow cytometry. (a) Dot plot represents CD4 $^+$ pZAP70 $^+$ cell population at various time points (b) Histogram plot represents MFI of pZAP70 gated on CD4 $^+$ T cells at various time points. The data are representative of two independent experiments from different donors.

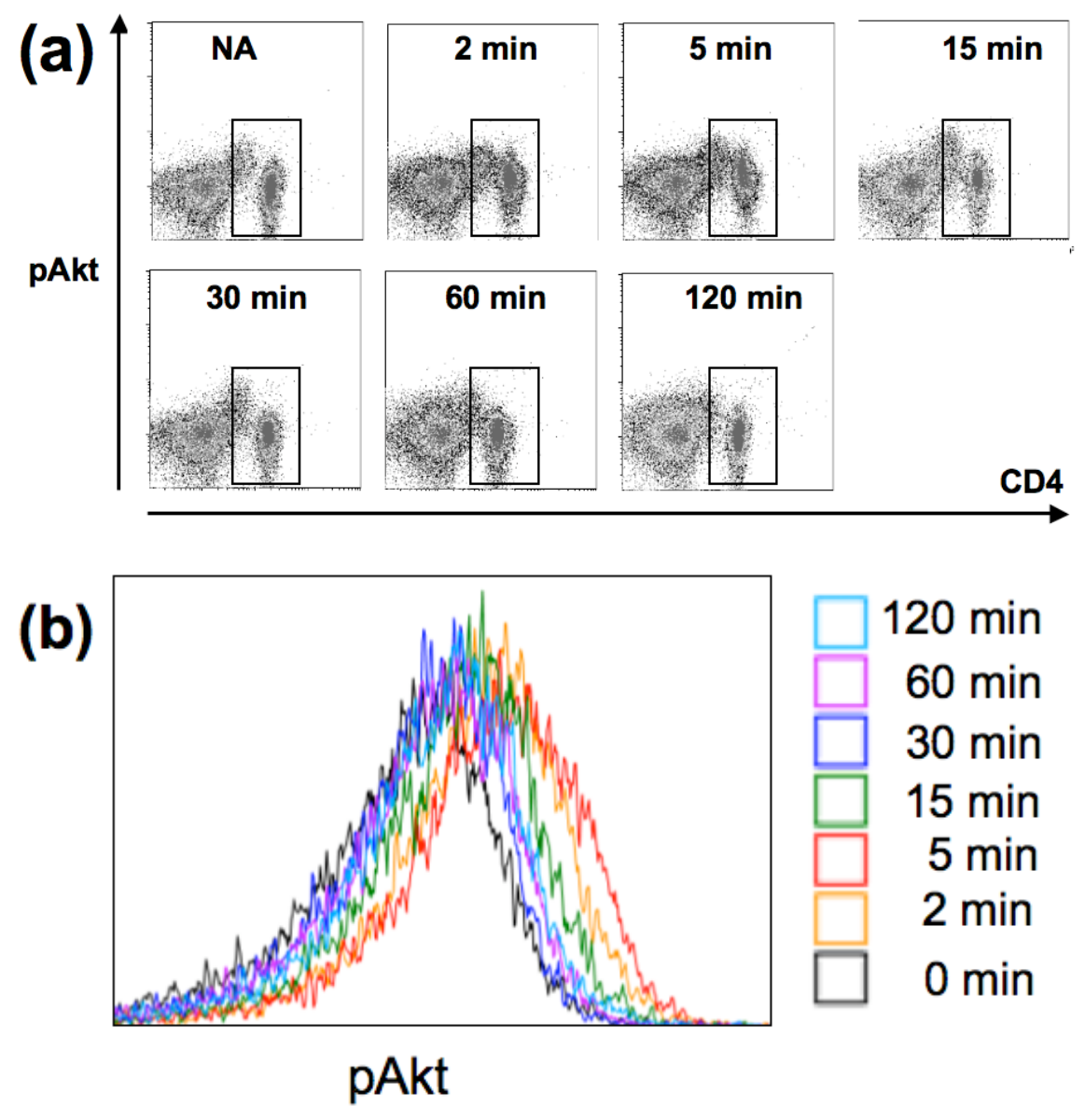


Figure 28. Peak time of anti-CD3/CD28-induced phosphorylation of Akt in activated human T cells.

PBMC ($1x10^6$ cells/ $100~\mu$ L) were equilibrated at 37° C in 5% CO $_2$ for 3 h, followed by incubation with anti-CD3, anti-CD28, and IgG crosslinker on ice. T cell activation was initiated by transferring to 37° C water bath. Cells were fixed with 1.5% paraformaldehyde at indicated time points. Cells were permeabilized with ice-cold 100% methanol, followed by staining with anti-CD4 and anti-pAkt. The intracellular expression of pAkt in CD4 $^+$ T cells was assessed by flow cytometry. (a) Dot plot represents CD4 $^+$ pAkt $^+$ cell population at various time points (b) Histogram plot represents MFI of pAkt gated on CD4 $^+$ T cells at various time points. The data are representative of two independent experiments from different donors.

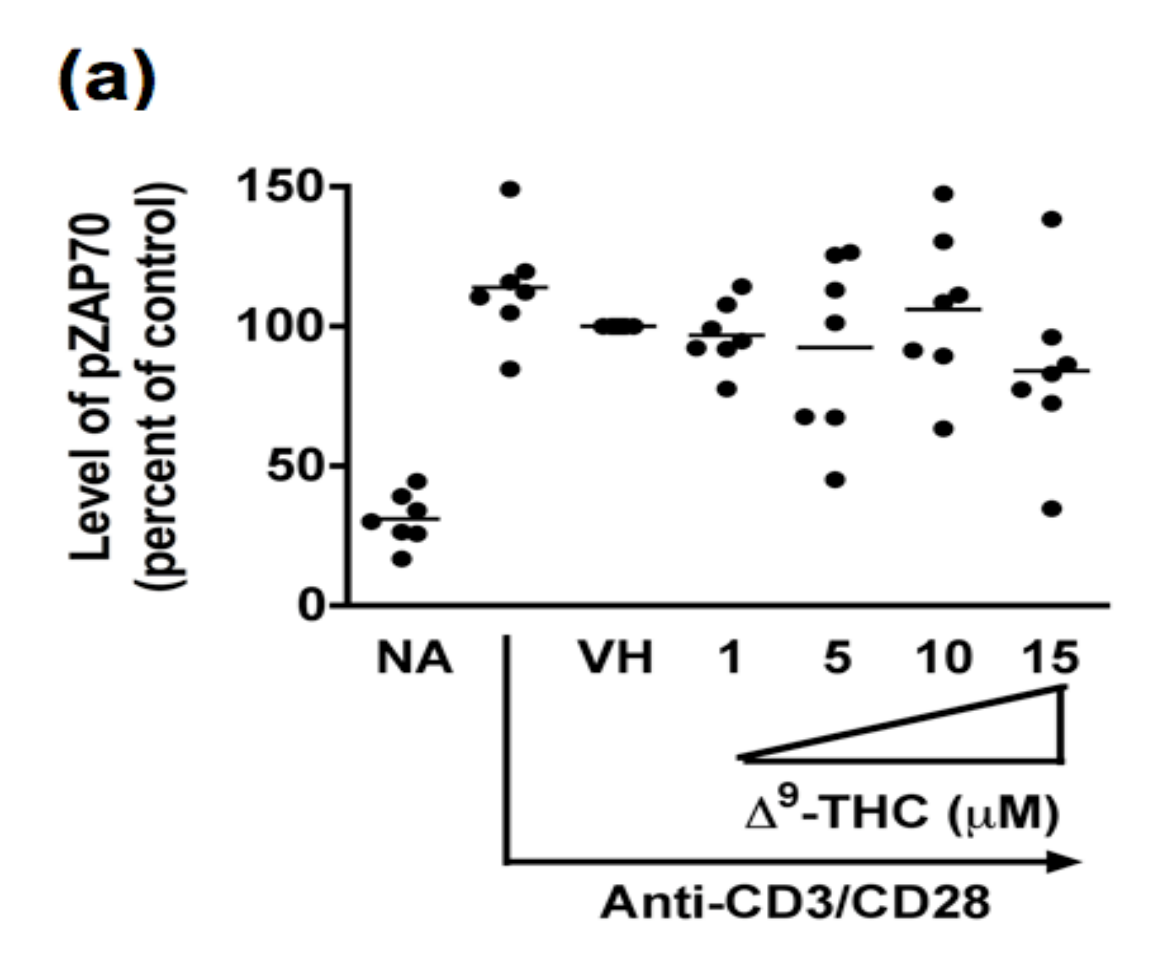
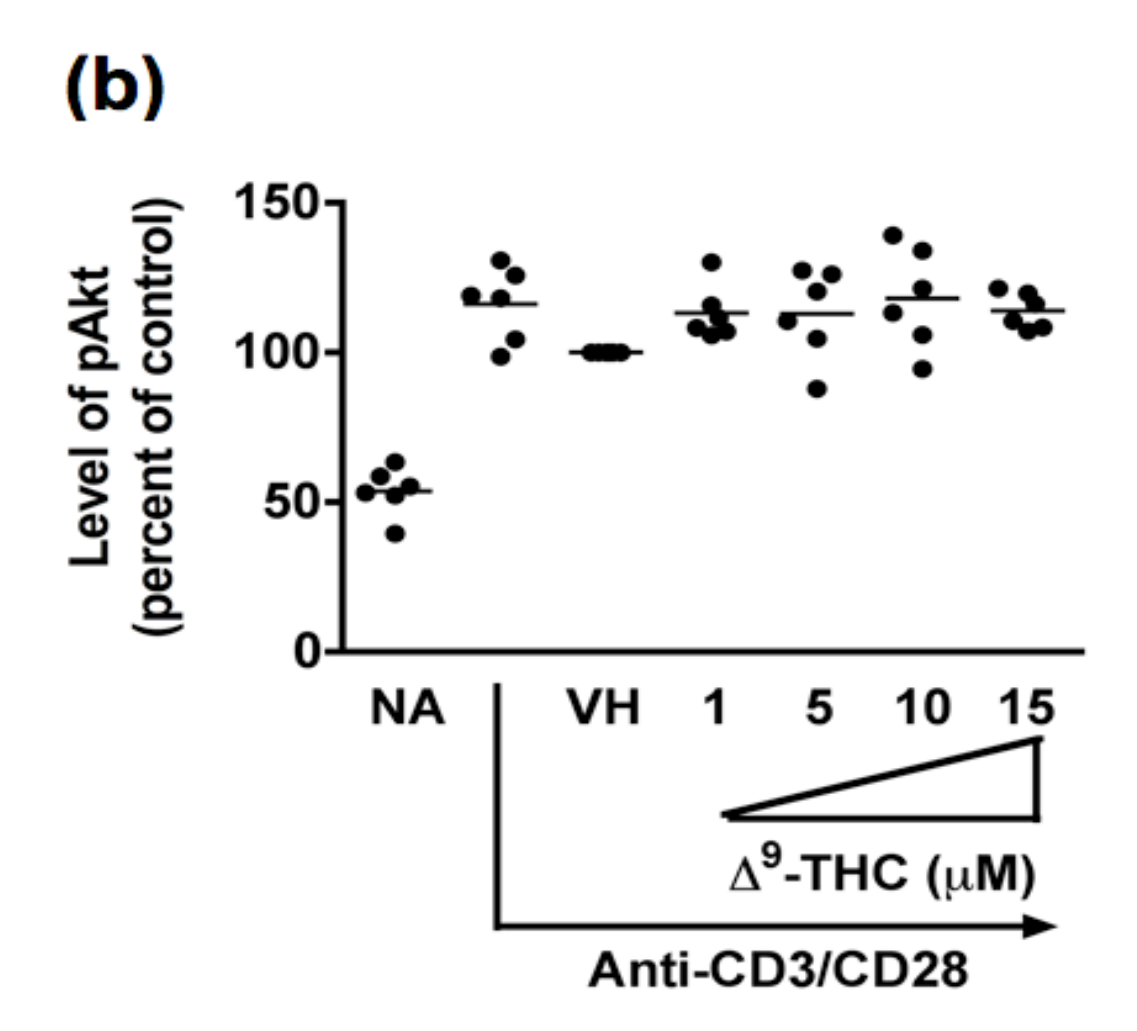


Figure 29. Effect of Δ^9 -THC on the proximal T cell receptor signaling molecules in activated human CD4⁺T cells.

PBMC (1x10⁶ cells/100 μ L) were equilibrated at 37°C in 5% CO₂ for 3 h, treated with Δ^9 -THC (1, 5, 10, and 15 μ M) and/or VH for 30 min, and then incubated with anti-CD3, anti-CD28, and IgG crosslinker on ice. T cell activation was initiated by transferring to 37°C water bath for 5 min. Cells were fixed with 1.5% paraformaldehyde and permeabilized with ice-cold 100% methanol, followed by staining with anti-CD4, anti-pZAP70, and anti-pAKT. The intracellular expression of pZAP70 or pAkt in CD4⁺ T cells was assessed by flow cytometry. (a) Scatter plot represents the level of pZAP70 in CD4⁺ T cells. (b) Scatter plot represents the level of pAkt. Results depicted are MFI of pZAP70 or pAkt gated on CD4⁺ T cells. Data were normalized to the VH-treated group and presented as percent of control. Each dot represents data from one individual donor.

Figure 29 (cont'd)



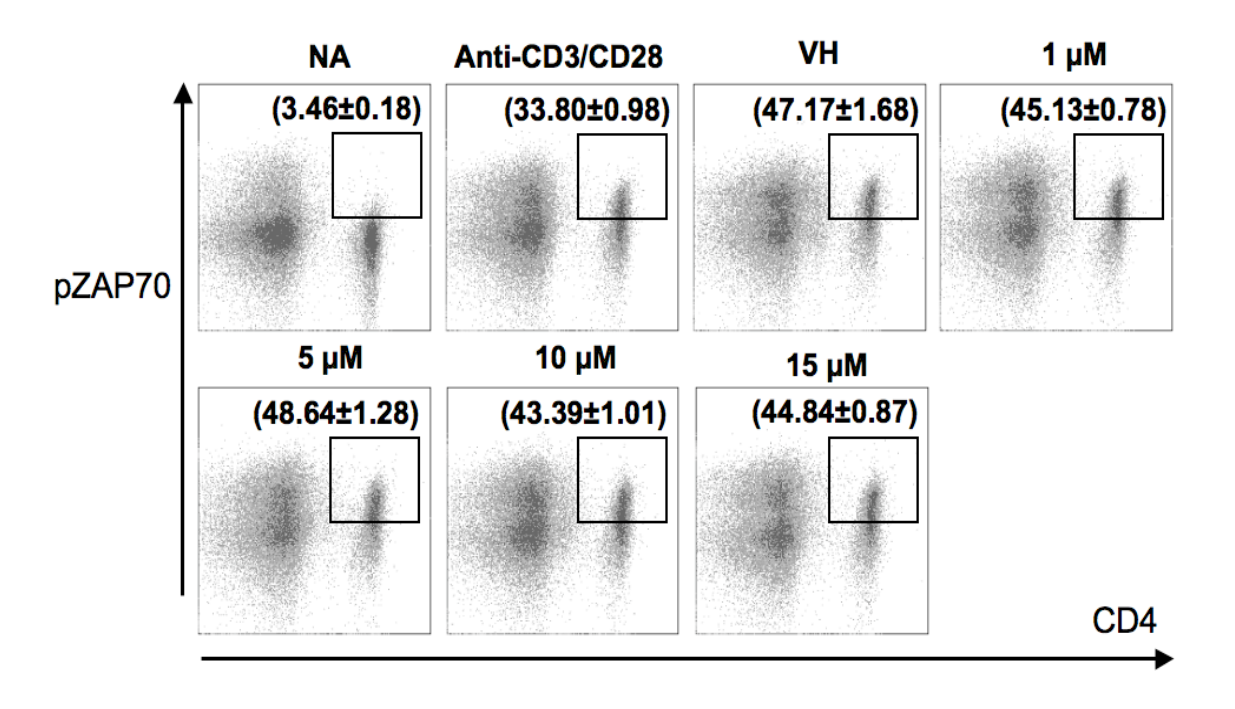


Figure 30. Effect of Δ^9 -THC on anti-CD3/CD28-induced phosphorylation of ZAP70 in activated mouse CD4⁺ T cells.

SPLC (1x10⁶ cells/100 μ L) were equilibrated at 37°C in 5% CO₂ for 3 h, treated with Δ^9 -THC (1, 5, 10, and 15 μ M) and/or VH for 30 min, and then incubated with anti-CD3, anti-CD28, and IgG crosslinker on ice. T cell activation was initiated by transferring to 37°C water bath for 5 min. Cells were fixed with 1.5% paraformaldehyde and permeabilized with ice-cold 100% methanol, followed by staining with anti-CD4 and anti-pZAP70. The intracellular expression of pZAP70 in CD4⁺ T cells was assessed by flow cytometry. Dot plot represents the level of pZAP70 in CD4⁺ T cells.

- III. Effect of Δ^9 -THC on CD40 plus cytokine-induced primary IgM response by HPB B cells.
- A. Δ^9 -THC attenuates CD40L plus cytokine-induced primary IgM responses of HPB B cells.

This laboratory previously demonstrated a marked suppression of in vitro T cell-dependent antibody response by Δ^9 -THC in mouse was due in part to a direct effect on B cells [294]. Further, our lab established a polyclonal in vitro activation model of primary human B cell differentiation to generate primary antibody secreting cells, which mainly produce IgM [320]. Thus, the effect of Δ^9 -THC on the primary antibody response in humans was investigated. Naïve B cells were co-cultured with irradiated CD40L-L cells in the presence of recombinant cytokines IL-2, -6, and -10 (CD40L plus cytokine) and IgM secreting cells were enumerated by ELISPOT on day 7. The effect of Δ^9 -THC on IqM responses was assessed from 6 donors and the data are presented as percentage of control (VH-treated group). Pretreatment with Δ^9 -THC significantly decreased the percentage of IgM secreting cells induced by CD40L plus cytokine (Figure 31a), but not the total viable cells (Figure 31b). These results suggested that Δ^9 -THC-mediated suppression of primary IgM response in humans involves perturbation of differentiation of naïve B cells into plasma cells rather than direct cytotoxicity.

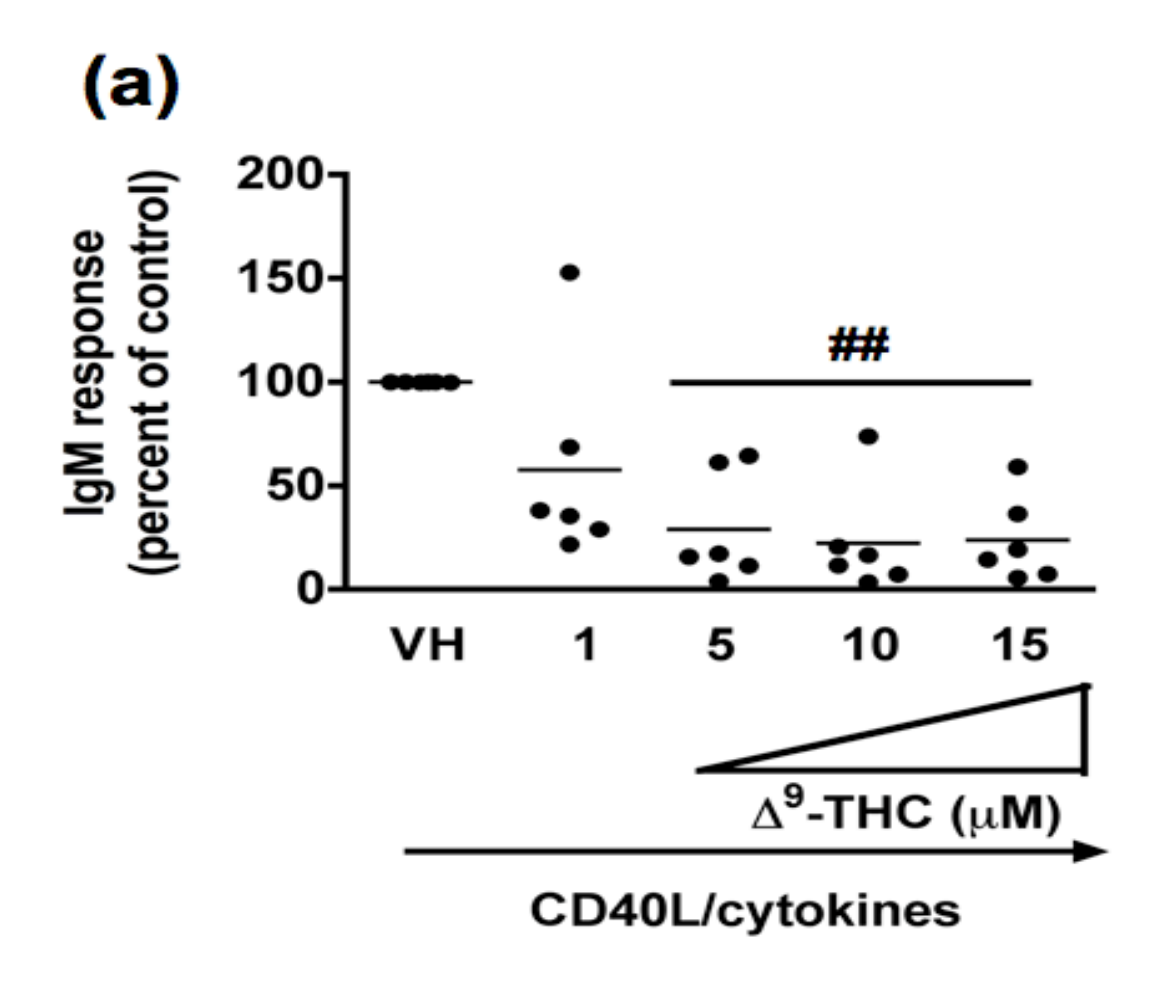
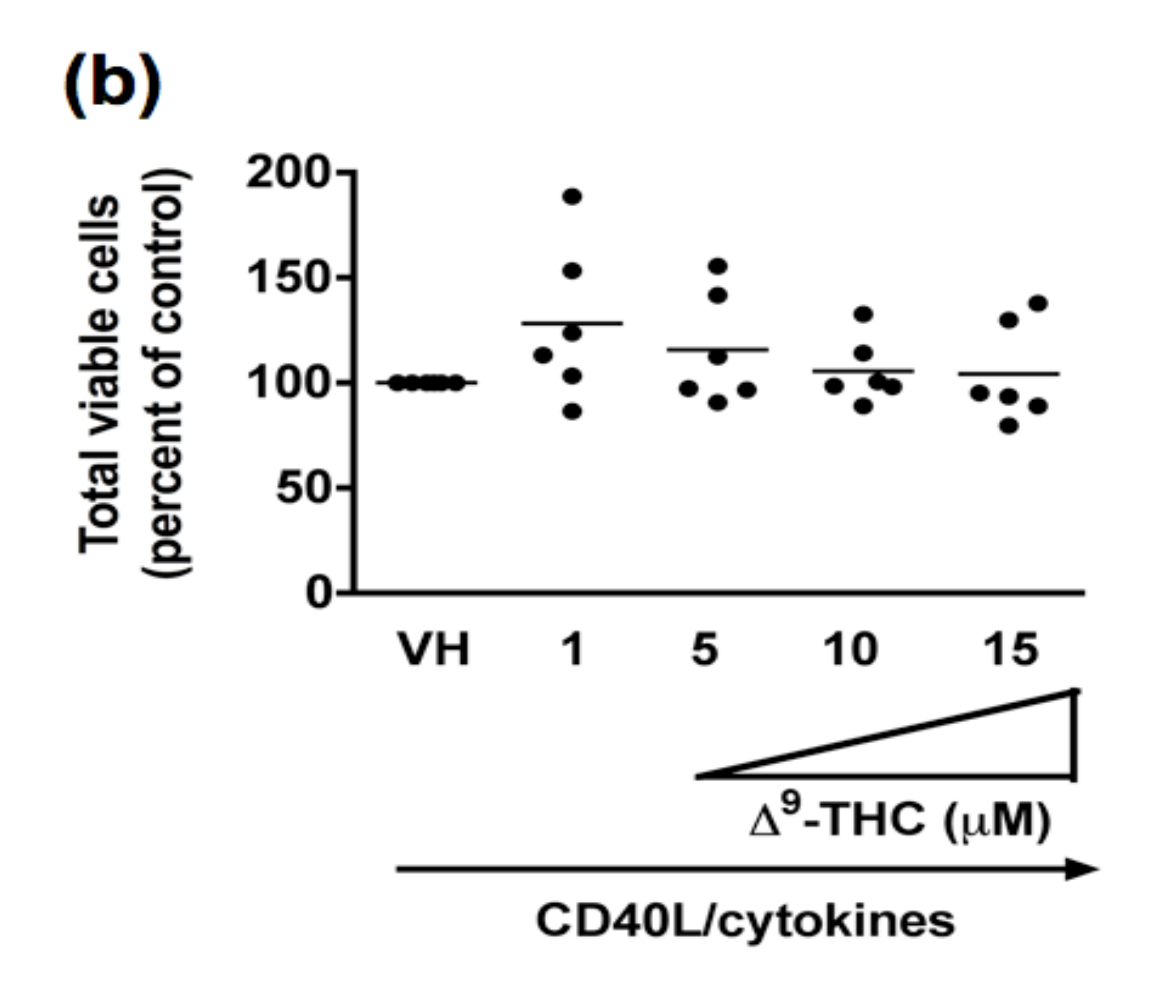


Figure 31. Effect of Δ^9 -THC on CD40L plus cytokine-induced IgM secreting cell response in humans.

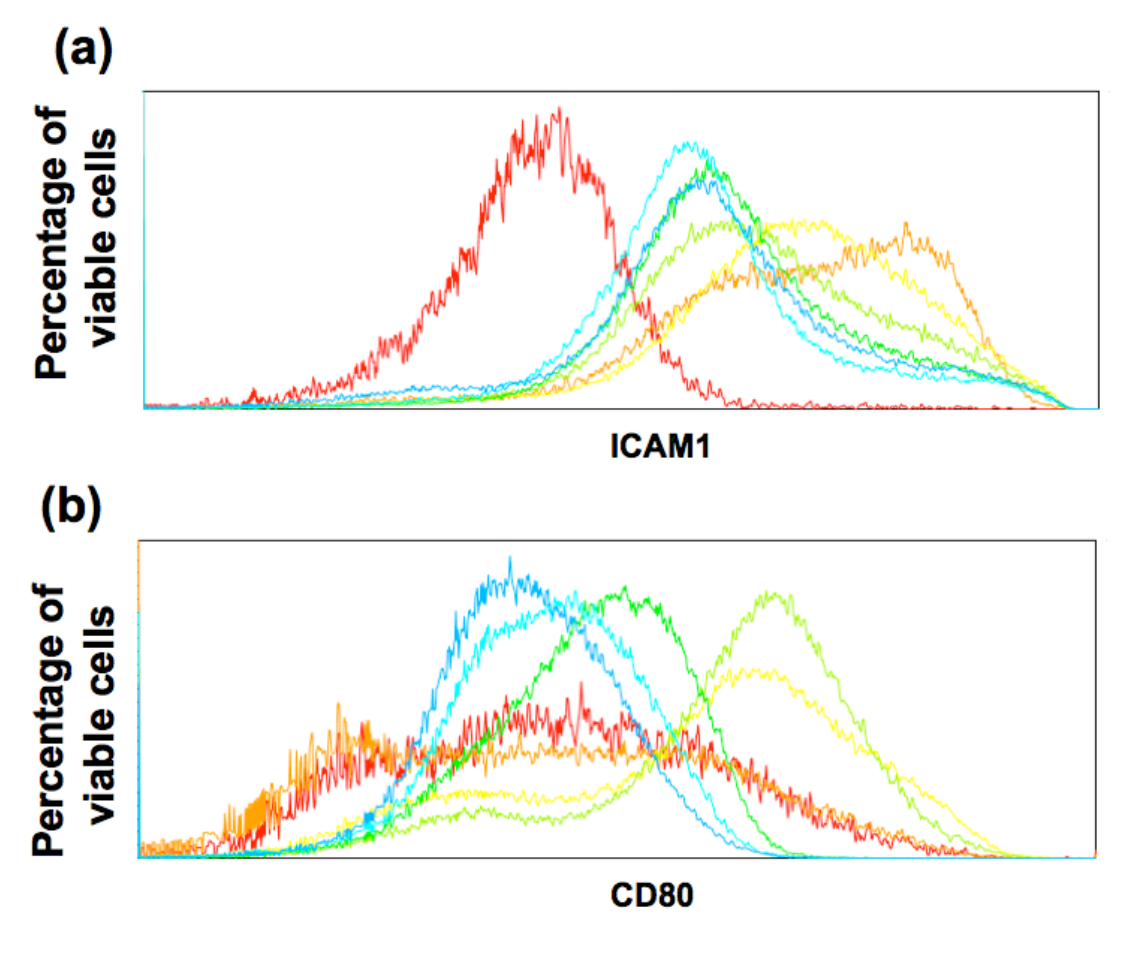
HPB naïve B cells $(1x10^6 \text{ cells})$ were treated with $\Delta^9\text{-THC}$ at indicated concentrations or VH (0.02% DMSO) for 30 min and then cultured with irradiated CD40L-L cells $(1.5 \times 10^3 \text{ cells/well})$ in the presence of recombinant human IL-2 (10 U/mL), IL-6 (100 U/mL), and IL-10 (20 ng/mL). Cells were transferred to new culture plates without CD40L-L cells on Day 4 and cultured for additional 3 days. IgM secreting cells were enumerated by ELISPOT on day 7. The total viable cells were counted by Z1 Coulter Counter following pronase treatment. Data were normalized to the VH-treated group and presented as percent of control with at least three replicates per groups. (a) Scatter plot represents the number of IgM secreting cells. (b) Scatter plot represents the total viable cells. The ## indicates significant effect compared to VH-treated group at p \leq 0.01. Each dot represents data from one individual donor.

Figure 31 (cont'd)



B. Δ^9 -THC suppresses CD40L plus cytokine-induced surface expression of CD80, but not CD69, CD86, and ICAM1 in HPB B cells.

To identify which stages in plasma cell differentiation are modulated by Δ^9 -THC, we first examined whether Δ^9 -THC affects B cell activation by assessing surface expression of CD80, CD86, CD69, and ICAM1 on activated B cells by flow cytometry. Kinetic studies showed that surface expression of ICAM1 peaked on day 1, whereas peak expression of surface CD80 was on day 3 post activation (Figure 32a and 32b respectively). The magnitude of surface expression for both CD69 and CD86 by HPB B cells was highest on day 4 post activation [320]. Thus, the effect of Δ^9 -THC was investigated either on day 1 and/or day 3 post activation. Pretreatment with Δ^9 -THC did not affect the upregulation of ICAM1 (Fig 33a), CD69 (Fig 33b), and CD86 (Fig 33c), but significantly suppressed the upregulation of surface CD80 (Fig 33d). As the induction of surface CD80 by CD40 ligation in B cells is primarily regulated at the level of transcription [335,336], we next investigated whether Δ^9 -THC affects the steady-state level of *CD80* mRNA by RT-PCR. Pretreatment with Δ^9 -THC did not affect CD80 mRNA expression induced by CD40 plus cytokine in activated HPB B cells (Fig 34). These data demonstrated that Δ^9 -THC impaired CD40L plus cytokine-induced B-cell activation, at least in part, through the downregulation of surface CD80.



Day 0, Day 1, Day 2, Day 3, Day 4, Day 5, Day 6

Figure 32. Peak time of CD40L plus cytokine-induced surface expression of ICAM1 and CD80 on HPB B cells.

HPB naïve B cells (1x10⁶ cells) were cultured with irradiated CD40L-L cells (1.5 x 10³ cells/well) in the presence of recombinant human IL-2 (10 U/mL), IL-6 (100 U/mL), and IL-10 (20 ng/mL). Cells were transferred to new culture plates without CD40L-L cells on Day 4 and cultured for additional 3 days. Cells were harvested everyday from day 0 to day 6. Dead cells were identified by staining with Live/Dead near-infrared Staining Kit, and are excluded. Surface expression of ICAM1 and CD80 induced by CD40L plus cytokine were assessed by flow cytometric analysis. (a) Histogram plot represents the MFI of ICAM1 gated on live population. (b) Histogram plot represents the MFI of CD80 gated on live population. Results represent two different donors with three replicates per treatment group.

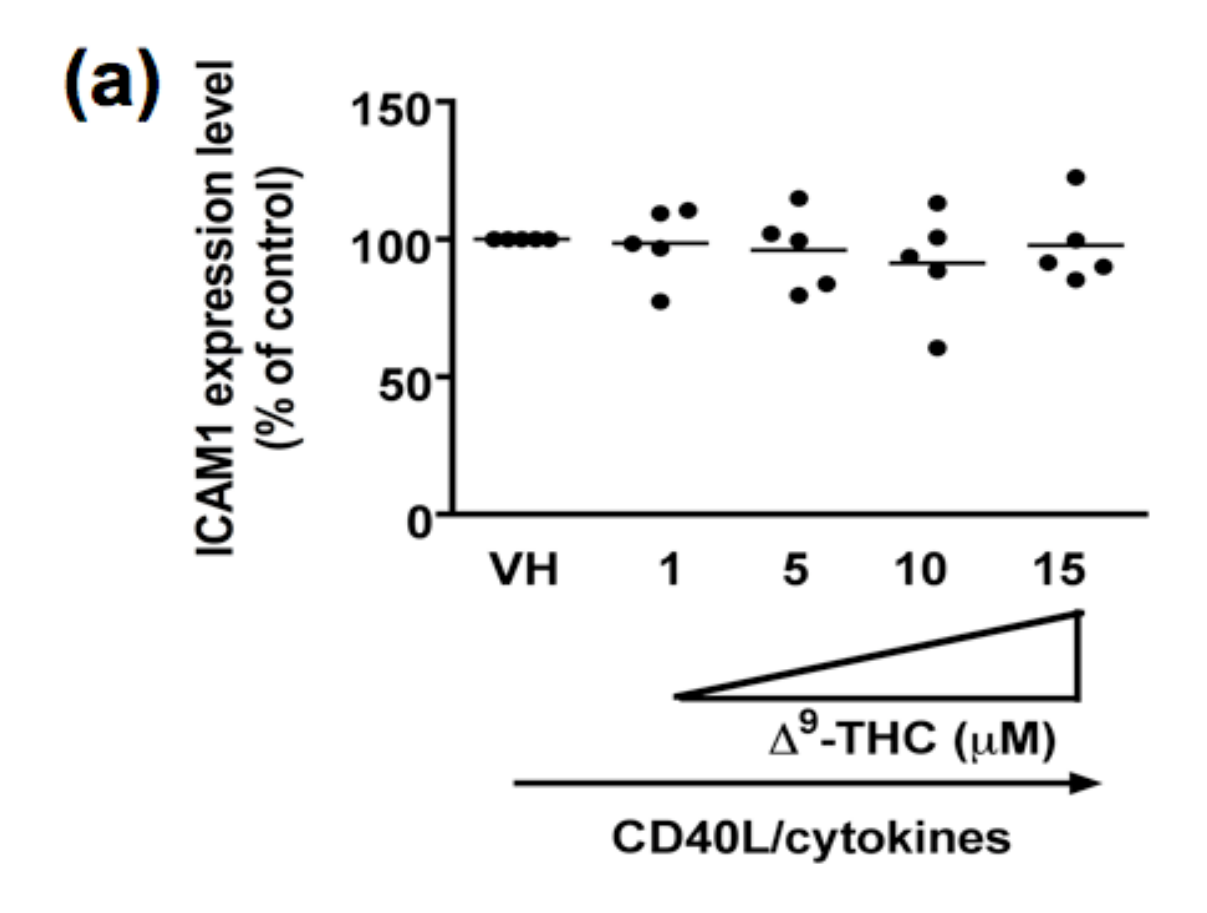
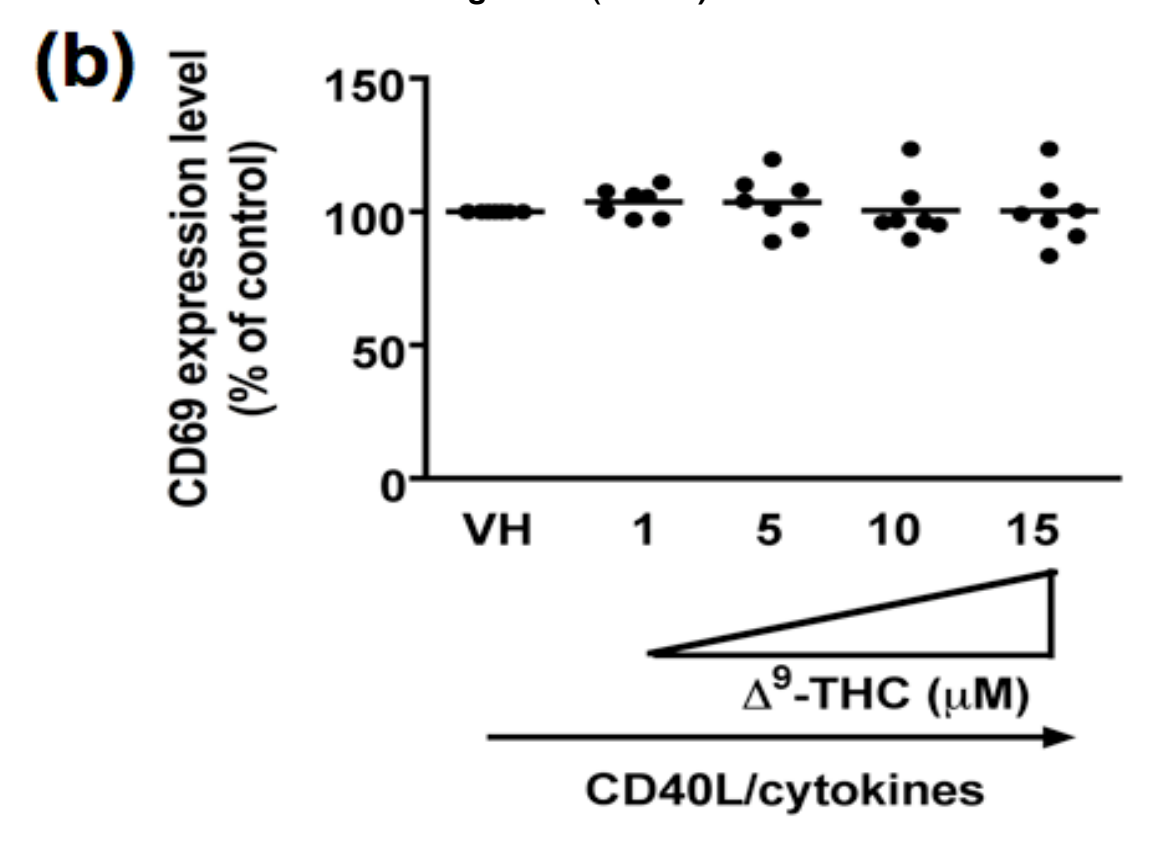


Figure 33. Effect of Δ^9 -THC on surface expression of activation markers in activated HPB B cells.

HPB naïve B cells $(1x10^6 \text{ cells})$ were treated with Δ^9 -THC at indicated concentrations or VH (0.02% DMSO) for 30 min and then cultured with irradiated CD40L-L cells $(1.5 \text{ x } 10^3 \text{ cells/well})$ in the presence of recombinant human IL-2 (10 U/mL), IL-6 (100 U/mL), and IL-10 (20 ng/mL). Surface expression of B-cell activation markers induced by CD40L plus cytokine were assessed by flow cytometric analysis on day 1 for expression of ICAM1 (a) or day 3 for expression of CD69 (b), CD86 (c), and CD80 (d). Dead cells were identified by staining with Live/Dead near-infrared Staining Kit, and are excluded. Results depicted are mean fluorescent intensity of each surface marker. Data were normalized to the VH-treated group and presented as percent of control. The unstimulated B cells express each surface marker with the average less than 3%. The ## indicates significant effect compared to VH-treated group at p \leq 0.01. Each dot represents data from one individual donor.

Figure 33 (cont'd)



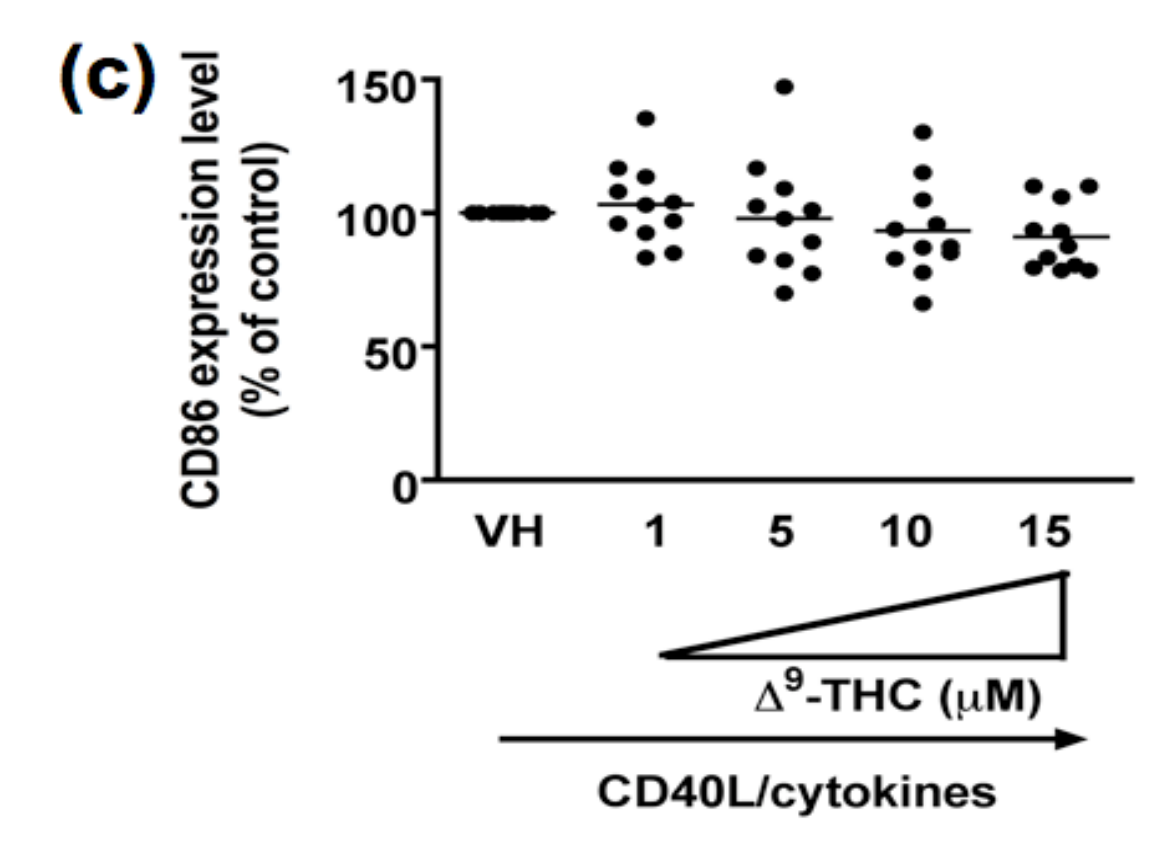
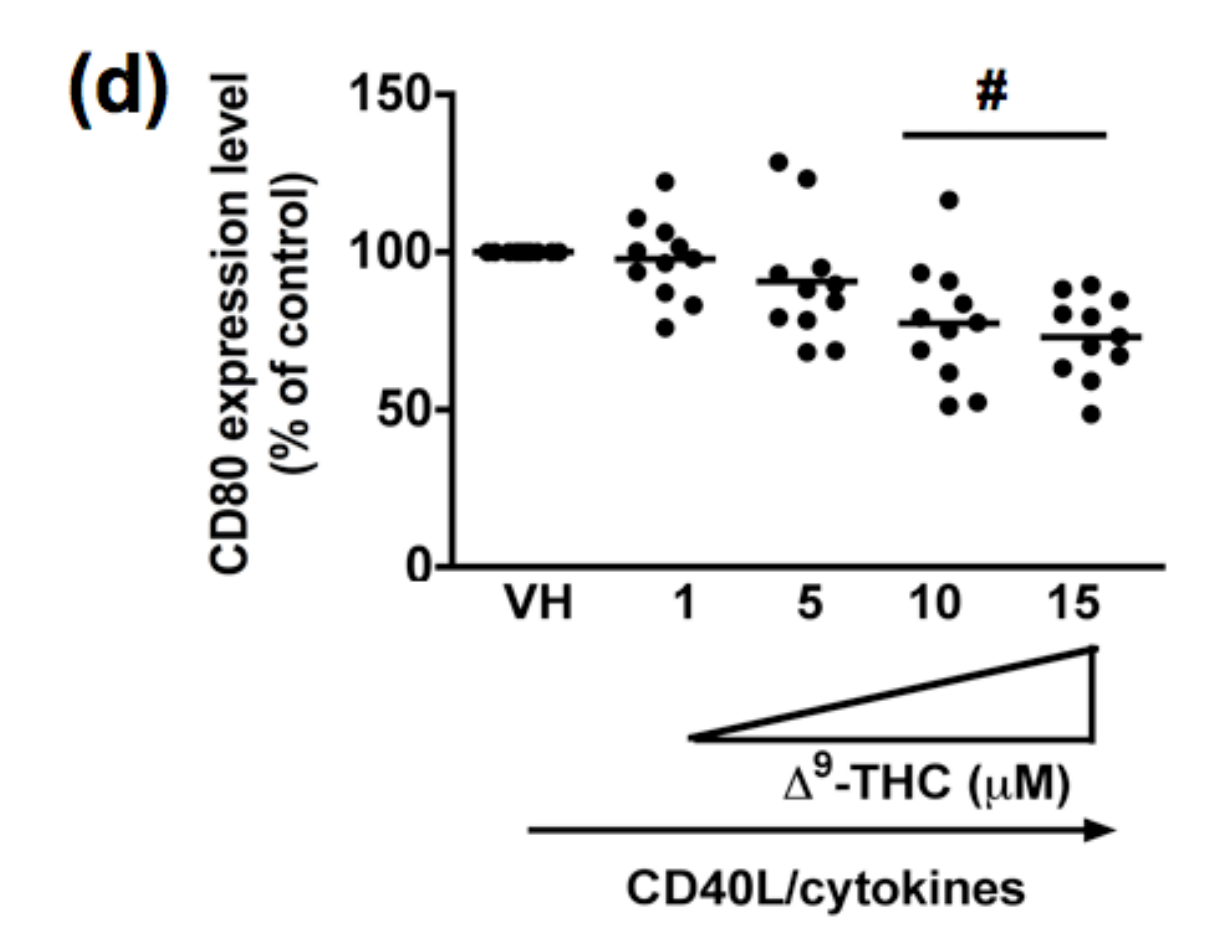


Figure 33 (cont'd)



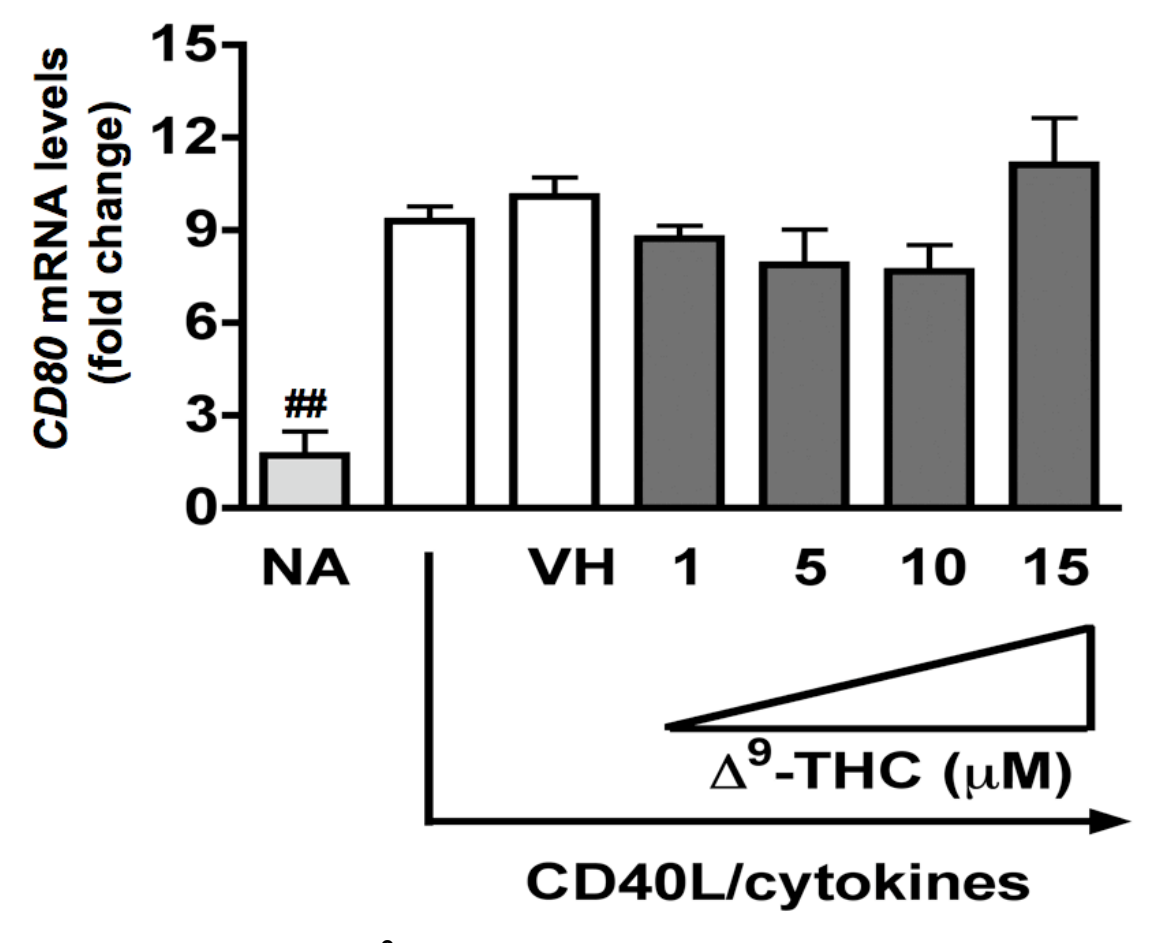


Figure 34 Effect of Δ^9 -THC on *CD80* mRNA levels in activated HPB B cells.

Human naïve B cells $(1x10^6 \text{ cells})$ were treated with Δ^9 -THC at the indicated concentrations or VH (0.02% DMSO) for 30 min and then cultured with irradiated CD40L-L cells $(1.5 \text{ x } 10^3 \text{ cells/well})$ in the presence of recombinant human IL-2 (10 U/mL), IL-6 (100 U/mL), and IL-10 (20 ng/mL). Cells were harvested for RNA isolation on day 2. Steady-state *CD80* mRNA levels were determined by real-time PCR. The fold difference of *CD80* mRNA molecules relative to nonactivated resting cells (naïve, NA) was normalized using the endogenous reference, 18s rRNA. The ## indicates significant effect compared to VH-treated group at p \leq 0.01. Results represent three different donors with four replicates per treatment group.

C. Δ^9 -THC impairs CD40L plus cytokine-induced proliferation of HPB B cells.

Survival and proliferation of activated B cells are required and linked to plasma cell differentiation (reviewed in [337]). We therefore examined the effect of Δ^9 -THC on CD40L plus cytokine-induced proliferation of activated B cells by flow cytometry on day 7. Naïve B cells were labeled with CFSE dye before pretreatment with Δ^9 -THC. As shown in Figure 35, stimulation with CD40L plus cytokine induced B cells to undergo multiple divisions, as revealed by the dilution of CFSE signal. In general, Δ^9 -THC did not affect the number of cell divisions, but rather significantly decreased the number of cells that progressed to the latest division, thereby retaining B cells in earlier cell divisions (Table 1). These results suggest that attenuation of B-cell proliferation plays a role in Δ^9 -THC-mediated suppression of CD40 plus cytokine-induced IgM response in humans.

D. Δ^9 -THC suppresses CD40L plus cytokine-induced mRNA expression of *IGJ* in HPB B cells.

To investigate whether Δ^9 -THC perturbs the transcriptional regulatory network of terminally differentiated plasma cells, the steady-state mRNA expression of genes critical in plasmacytic differentiation including, but not limited to, *PRDM1* (encoding for Blimp-1), *PAX5*, and *IGJ* was assessed by RT-PCR on day 6 post activation, which is the peak time of induction [338]

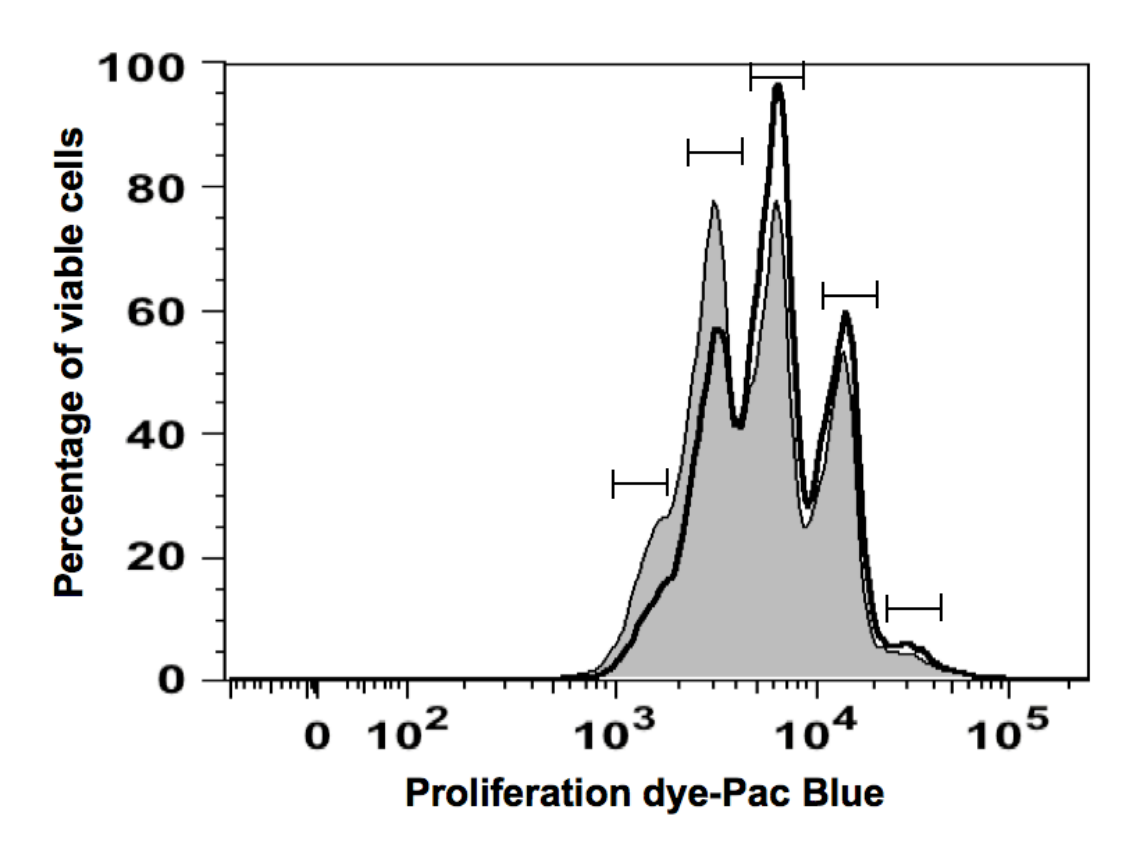


Figure 35. Δ^9 -THC impaires CD40L plus cytokine-induced proliferation of HPB B cells.

HPB naïve B cells ($5x10^6$ cells/mL) were labeled with the proliferation dye prior to treatment with Δ^9 -THC at indicated concentrations or VH (0.02% DMSO) for 30 min and then cultured with irradiated CD40L-L cells (1.5 x 10^3 cells/well) in the presence of recombinant human IL-2 (10 U/mL), IL-6 (100 U/mL), and IL-10 (20 ng/mL). Cells were transferred to new plates without CD40L-L cells on Day 4 and cultured for additional 3 days. Dead cells were excluded from the analysis using the Live/Dead Near-Infrared Dead Cell Staining Kit and flow cytometry analysis were performed on day 7. The concatenated data from three replicates per treatment groups were used. Histogram plot represents proliferation profile compared between groups treated with either VH (shaded) or 15 μ M Δ^9 -THC (open). Data are representative of 5 donors.

Table 1. Δ^9 -THC impairs CD40L plus cytokine-induced proliferation of HPB B cells.

Percentage of viable cells at each cell division upon traeatment with Δ^9 -THC at indicated concentrations or VH (0.02% DMSO).

Groups	CD40L	VH	Δ ⁹ -THC (μM)			
Cell division			1	5	10	15
0	1.9±0.1	1.9±0.1	2.2±0.2	2.4±0.1	2.4±0.1	2.6±0.2*
1	15.6±0.9	15.0±0.4	15.3±0.4	17.0±0.8	18.0±0.3	17.8±1.3
2	15.4±0.6	12.3±0.6	13.5±0.7	14.6±0.6	16.0±0.3**	15.3±1.0*
3	26.5±0.7	24.3±0.8	26.6±0.6	28.9±0.6**	30.9±0.5**	30.1±0.4**
4	24.3±0.4	24.7±0.3	23.8±0.3	21.2±0.2**	20.0±0.6**	19.8±0.7**

Pretreatment with Δ^9 -THC did not affect the upregulation of *PRDM1* mRNA levels (Figure 36) or the downregulation of *PAX5* mRNA levels (Figure 37), but significantly suppressed the upregulation of *IGJ* mRNA levels in activated B cells (Figure 38). These results demonstrated that attenuation of plasmacytic differentiation in human B cells by Δ^9 -THC is mediated, at least in part, through impairment of IgJ expression.

E. Δ^9 -THC suppresses CD40L plus cytokine-induced phosphorylation of STAT3, but not p65 NF $_K$ B, in HPB B cells.

The mechanism by which normal human B cells proliferate to external signals is not entirely clear, but inhibition of NF κ B pathways has a profound effect on CD40-mediated B-cell proliferation and differentiation [98]. In addition, STAT signaling is involved in cell survival, proliferation and differentiation [reviewed in [116]]. Specifically, STAT3 induced by IL-6 promotes both B cell proliferation and differentiation into plasma cells [339]. In light of the above, we further investigated the effect of Δ^9 -THC on the immediate activation of p65 NF κ B and STAT3. Due to the dynamic changes in phosphorylation status, we selected an early time point after activation to increase sensitivity of detection, and therefore, the phosphorylation status of p65 NF κ B and STAT3 in activated HPB B cells was assessed by flow cytometry at 10 min post activation. The soluble recombinant human CD40L in combination with IL-2, -6, and -10 were utilized to promote rapid activation of the signaling pathway of interests. Stimulation of naïve B cells with

recombinant CD40L plus cytokine for 10 min induced phosphorylation of p65 and STAT3 (Figure 39a and 39b). Pretreatment with Δ^9 -THC did not alter the level of phosphorylated p65 (pp65) (Figure 39a), but significantly suppressed the level of phosphorylated STAT3 (pSTAT3) in a concentration-dependent manner (Figure 39b). These results demonstrated that STAT3 is one possible target of Δ^9 -THC.

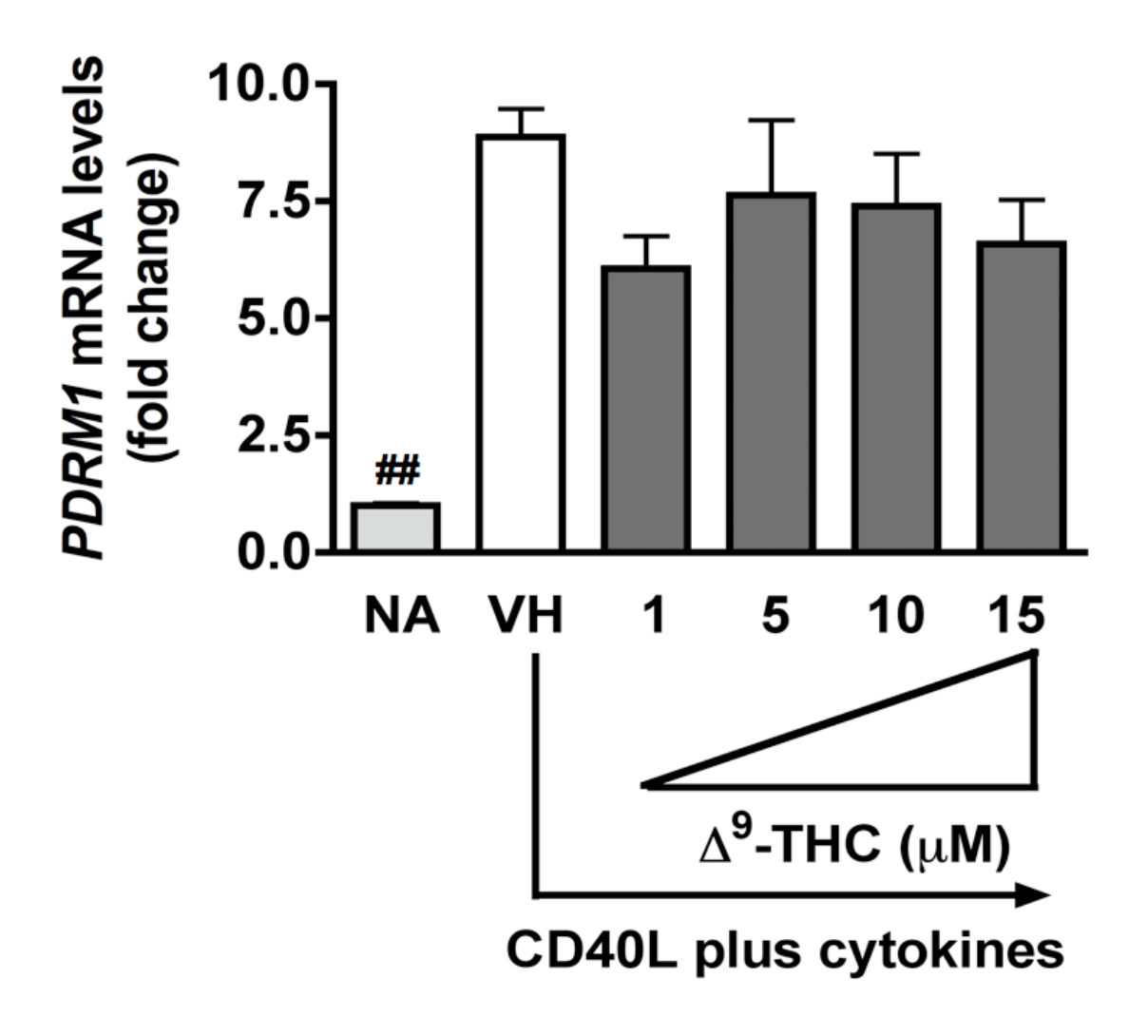


Figure 36. Effect of Δ^9 -THC on *PRDM1* mRNA levels in activated HPB B cells.

Human naïve B cells $(1x10^6 \text{ cells})$ were treated with Δ^9 -THC at indicated concentrations or VH (0.02% DMSO) for 30 min and then cultured with irradiated CD40L-L cells $(1.5 \text{ x } 10^3 \text{ cells/well})$ in the presence of recombinant human IL-2 (10 U/mL), IL-6 (100 U/mL), and IL-10 (20 ng/mL). Cells were transferred to new plates without CD40L-L cells on Day 4 and cultured for 2 additional days. Steady-state *PRDM1* mRNA levels were determined by real-time PCR on day 6. The fold difference of *PRDM1* mRNA molecules relative to nonactivated resting cells (naïve, NA) was normalized using the endogenous reference, 18s rRNA. Results represent three different donors with four replicates per treatment group.

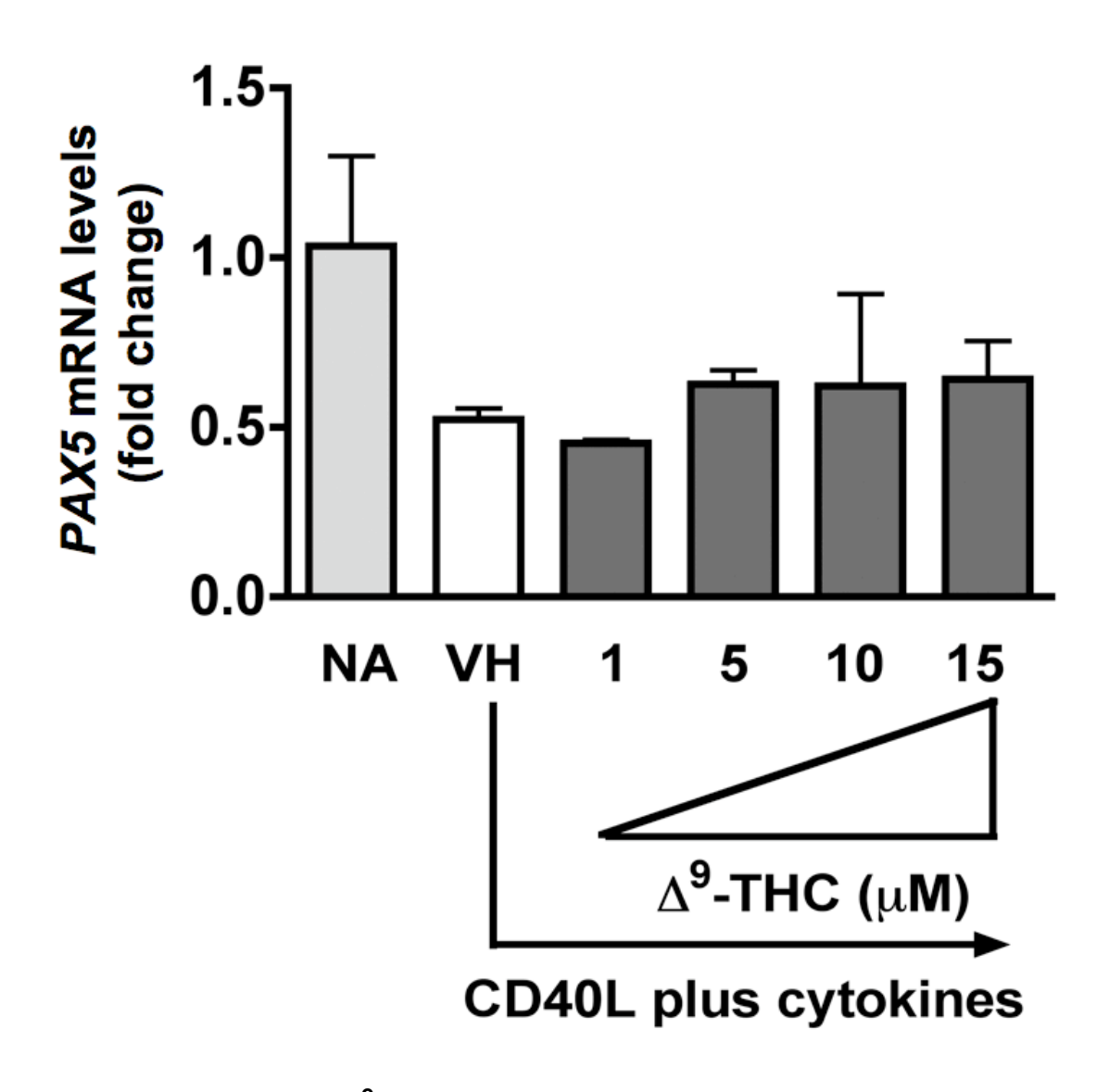


Figure 37. Effect of Δ^9 -THC on *PAX5* mRNA levels in activated HPB B cells

Human naïve B cells $(1x10^6 \text{ cells})$ were treated with Δ^9 -THC at indicated concentrations or VH (0.02% DMSO) for 30 min and then cultured with irradiated CD40L-L cells $(1.5 \times 10^3 \text{ cells/well})$ in the presence of recombinant human IL-2 (10 U/mL), IL-6 (100 U/mL), and IL-10 (20 ng/mL). Cells were transferred to new plates without CD40L-L cells on Day 4 and cultured for 2 additional days. Steady-state *PAX5* mRNA levels were determined by real-time PCR on day 6. The fold difference of *PAX5* mRNA molecules relative to nonactivated resting cells (naïve, NA) was normalized using the endogenous reference, 18s rRNA. Results represent three different donors with four replicates per treatment group.

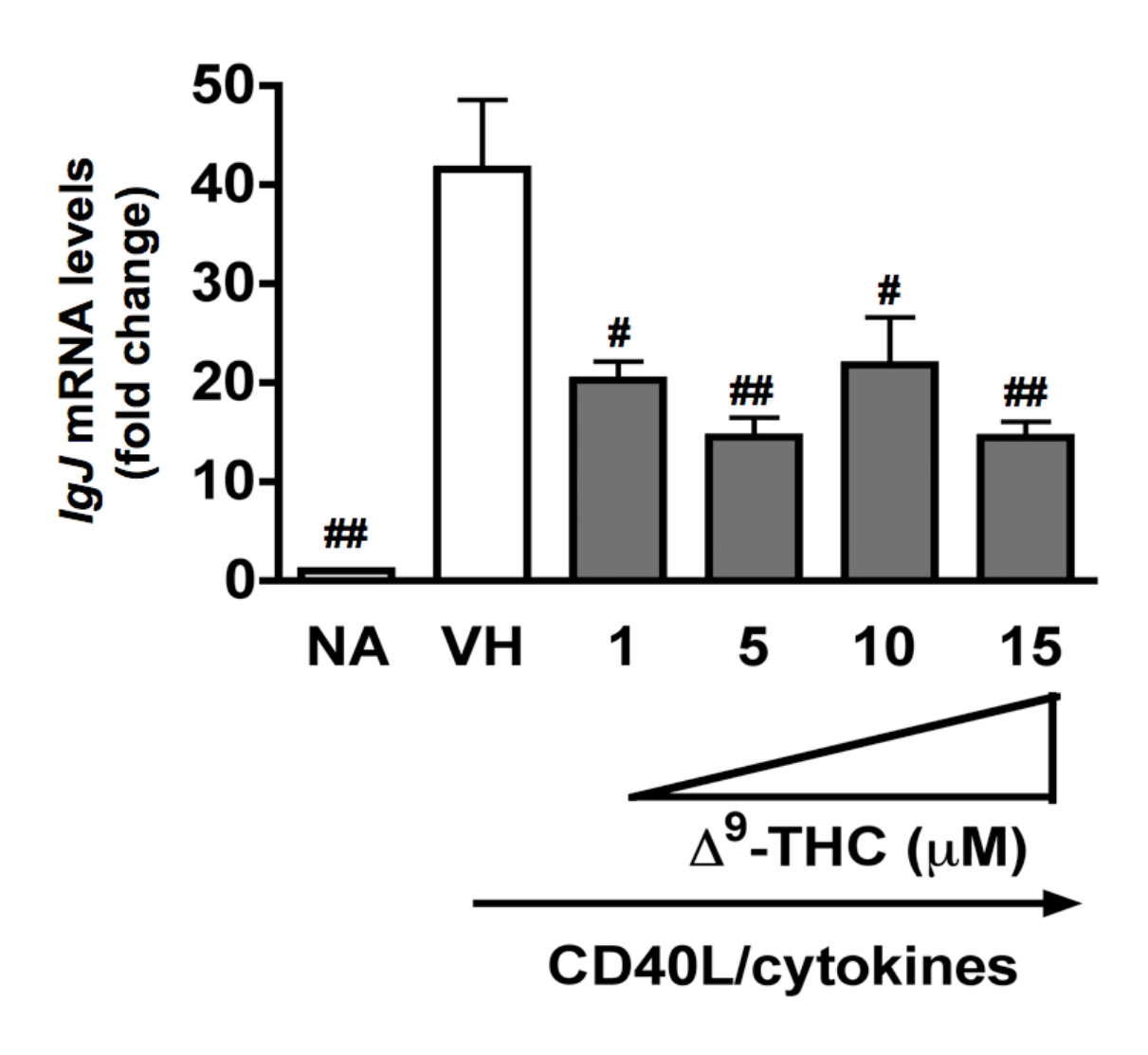


Figure 38. Δ^9 -THC suppresses CD40L plus cytokine-induced *IGJ* mRNA levels in activated HPB B cells.

Human naïve B cells $(1x10^6 \text{ cells})$ were treated with $\Delta^9\text{-THC}$ at indicated concentrations or VH (0.02% DMSO) for 30 min and then cultured with irradiated CD40L-L cells $(1.5 \text{ x } 10^3 \text{ cells/well})$ in the presence of recombinant human IL-2 (10 U/mL), IL-6 (100 U/mL), and IL-10 (20 ng/mL). Cells were transferred to new plates without CD40L-L cells on Day 4 and cultured for 2 additional days. Steady-state IGJ mRNA levels were determined by real-time PCR on day 6. The fold difference of IGJ mRNA molecules relative to nonactivated resting cells $(na\"{i}ve, NA)$ was normalized using the endogenous reference, 18s rRNA. The # or ## indicates significant effect compared to VH-treated group at p ≤ 0.05 or ≤ 0.01 , respectively. Results represent three different donors with four replicates per treatment group.

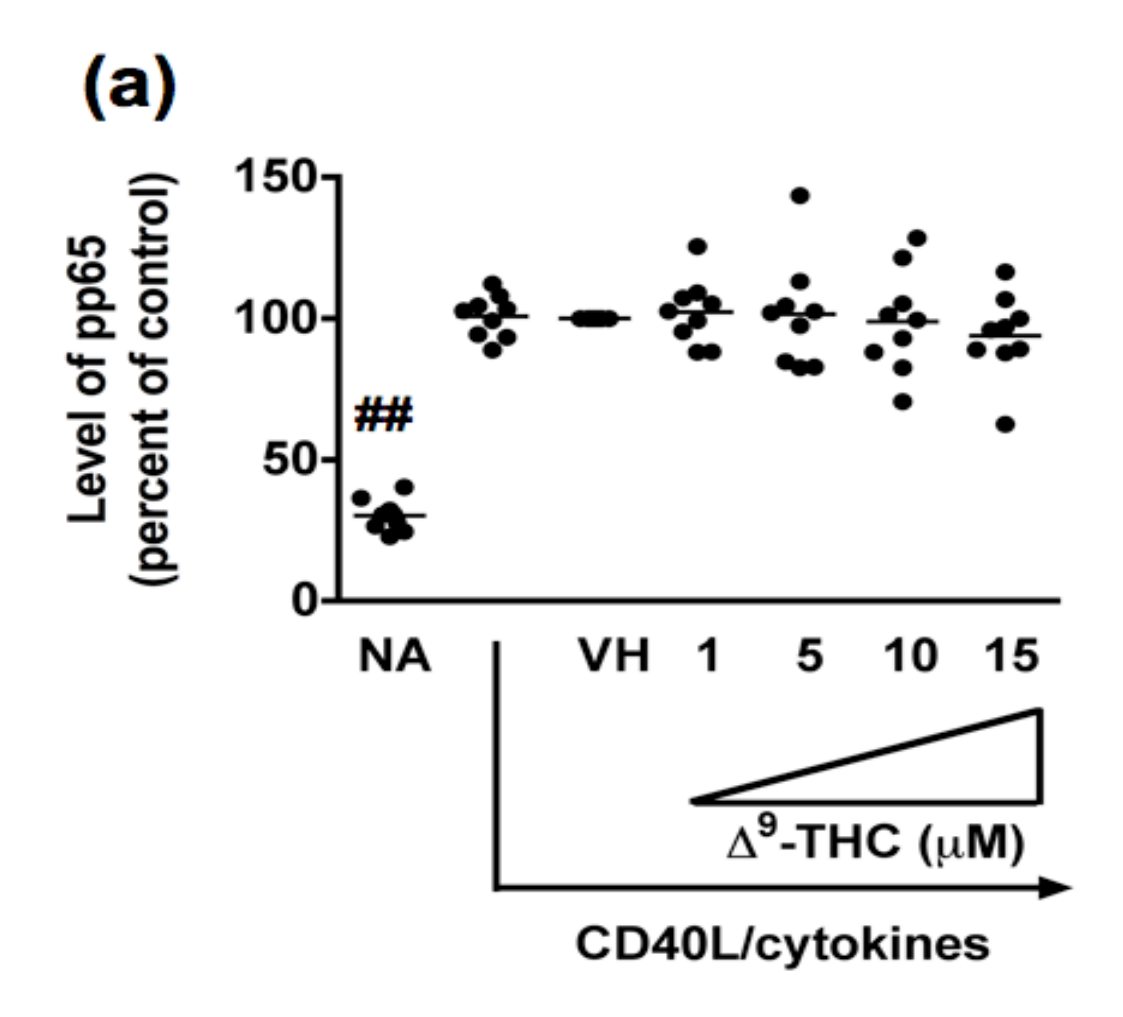
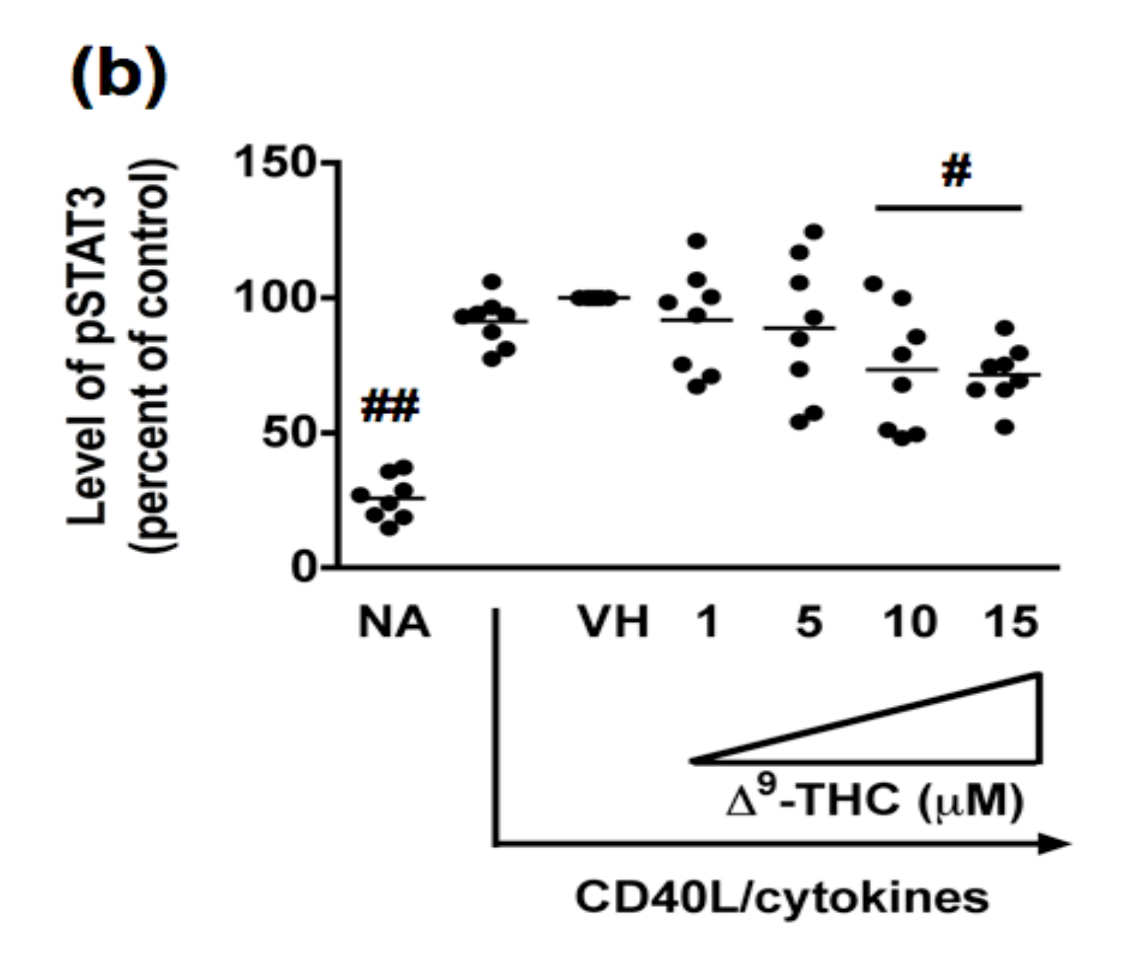


Figure 39. Effect of Δ^9 -THC on the phosphorylation of p65 NF_KB and STAT3 in activated HPB B cells.

HPB naïve B cells (1x10⁶ cells) were equilibrated at 37°C in 5% CO₂ for 3 h prior treated with Δ^9 -THC at indicated concentrations or VH (0.02% DMSO) for 30 min. B cells were activated with recombinant human CD40L (200 nM), human IL-2 (10 U/mL), IL-6 (100 U/mL), and IL-10 (20 ng/mL) for 10 min at 37°C. Cells were fixed with 1.5% paraformaldehyde and permeabilized with ice-cold 100% methanol. The intracellular expression of pSTAT3 and pp65 NFκB was assessed by phosflow cytometry. (a) Scatter plot represents the level of pp65 NFκB. (b) Scatter plot represents the level of pSTAT3. Results depicted are mean fluorescent intensity of each surface marker. Data were normalized to the VH-treated group and presented as percent of control. The # or ## indicates significant effect compared to VH-treated group at p ≤ 0.05 or ≤ 0.01. Each dot represents data from one individual donor.

Figure 39 (cont'd)



DISCUSSION

This dissertation research aimed to investigate the role of CD40-CD40L interaction in Δ^9 -THC-mediated suppression of the T cell-dependent IgM response. Toward this end, the effect of Δ^9 -THC on both T and B cells were determined. The first section focused on characterizing the effect of Δ^9 -THC on the upregulation of CD40L expression in activated mouse and human T cells. The second section focused on how Δ^9 -THC suppresses CD40L-induced primary antibody response in primary human B cells.

I. Effect of Δ^9 -THC on the upregulation of CD40L on activated CD4⁺ T cells

The strength and duration of CD40 signaling is crucial in initiating adaptive immune responses mainly involved in inflammation and is controlled by the presence of its cognate ligand, CD40L, which is mainly expressed on the surface of activated CD4⁺ T cells. Δ^9 -THC impairs multiple aspects of T cell action, including activation, accessory, and effector functions [294,303]. Thus, the influence of Δ^9 -THC on the upregulation of CD40L on activated mouse CD4⁺ T cells was initially investigated, followed by extensive characterization of critical molecular events that are involved in primary human T cells.

In studies investigating the effect of Δ^9 -THC on the upregulation of surface CD40L on activated mouse CD4⁺ T cells, two modes of in vitro T cells activation were used. In concordance with prior reports, similar CD40L expression kinetics were observed with splenic CD4+ T cells activated by either PMA/Io or anti-CD3/CD28 (reviewed in [69]). It is noteworthy that while we observed a similar kinetic profile, the magnitude of surface CD40L expression induced by both stimuli under our experimental condition was modest compared to published reports and could be due to several factors including differences in culture conditions, mouse strain, and species (human versus mouse). Another possibility that might contribute to the modest CD40L induction is the internalization of CD40L after binding to its receptor, CD40, on B cells [75]. Although this possibility seems plausible since we utilized splenocytes, which are heterogeneous and contain B cells, we excluded this possibility, as T cell enrichment did not increase the magnitude of surface CD40L expression. We also found that the kinetics of CD40L mRNA upregulation induced by these two stimuli were quite different. PMA/lo induced steady-state CD40L mRNA levels rapidly, but transiently, while steady-state CD40L mRNA levels induced by anti-CD3/CD28 were slow, but sustained. These differences might be explained by the observation that the CD28 costimulatory signal promoted mRNA stability for many T cell-derived cytokines [340]. However, CD40L mRNA is still very unstable, with a $t_{1/2}$ of approximately 23 min in mouse [341].

We show here that Δ^9 -THC distinctly modulated the upregulation of surface CD40L induced by different T cell activation stimuli. Δ^9 -THC suppressed the upregulation of both surface CD40L expression and steady-state CD40L mRNA levels induced by anti-CD3/CD28 in a concentration-dependent manner. Δ^9 -THC did not affect the upregulation of surface CD40L induced by PMA/Io. This is in contrast to our previous reports showing that Δ^9 -THC suppressed PMA/Io-induced cytokines (such as IL-2 and IFN_γ), and co-stimulatory molecules (such as ICOS) [294,303]. Unlike other proteins that are induced by T cell activation, the expression of CD40L on activated T cells largely depends on an increase in $[Ca^{2+}]_i$ though the activation of calcineurin and $Ca^{2+}/Calmodulin$ kinase Type IV [327,342]. This correlates well with numerous reports showing that NFAT, the activation of which requires calcineurin, is a critical transcription factor in regulating CD40L expression [323,343,344]. The importance of NFAT is also evidenced by a marked decrease in CD40L expression in the presence of CsA, an immunosuppressive drug that blocks NFAT activation and nuclear translocation [325]. As stated previously, our laboratory has demonstrated marked suppression by Δ^9 -THC of NFAT activation [303] and leads us to speculate that impaired NFAT likely also contributes to suppression of CD40L by Δ^9 -THC. It is also noteworthy that the downregulation of surface CD4, a coreceptor on helper T cells, after PMA/Io treatment as observed here is a common phenomenon [345-348], but did not affect the upregulation of CD40L.

Based on the fact that PMA/Io activates T cells by bypassing the proximal TCR signaling, it is possible that Δ^9 -THC might target one or more signaling molecules between the T cell receptor and the activation of PKC-θ and/or This is in accordance with a study induction of intracellular calcium. demonstrating that Δ^9 -THC suppressed the activation of proximal TCR signaling components, partly due to the stabilization of Lck, the kinase responsible for initiating TCR signaling, when present in its inactive form [308]. Borner and coworkers also demonstrated the involvement of CB1 and CB2 in $\Delta^9\text{-THC-}$ mediated impairment of proximal TCR signaling, as evidenced by reversion of the suppressive effect of Δ^9 -THC, in the presence of CB1 and CB2 antagonists. This is in contrast to the results reported here, in which the suppressive effect of Δ^9 -THC on anti-CD3/CD28-induced CD40L expression occurred in the presence and absence of CB1 and CB2 in mice. It is noteworthy that Borner and coworkers studied the involvement of CB1 and CB2 by using IL-4 stimulated Jurkat or primary human T cells to induce CB1 expression (prestimulated cells) together with CB1 and CB2 selective antagonists (AM281 and AM630, respectively). In contrast, in our experiments, splenocytes from CB1/CB2 null mice (CB1-/-CB2-/mice) were used eliminating the need for cannabinoid receptor antagonists, which are known to have inverse agonist activity as well as off-target effects.

particularly in case of AM281 [349]. These differences in experimental conditions might account for the discrepancy between our findings and that of Borner and coworkers. At this time, we cannot exclude the possibility that cannabinoids target various orphan G protein-coupled receptors (e.g. GPR55 and GPR119), nuclear hormone receptors (e.g. the PPAR α and γ), or ion channels (e.g. the TRPV1 and 2, and the TRPC1 (reviewed in [349,350]). However, we have ruled out the possible involvement of GR in suppression of CD40L by Δ^9 -THC. Finally, although less likely, the CB1/CB2-independent mechanism may also be explained by the fact that Δ^9 -THC, which is very lipophilic, preferentially aligns its hydrophobic portion parallel with the membrane phospholipid chain (reviewed in [351]). This perpendicular orientation results in alteration of plasma membrane's thermodynamic properties [352] and may disrupt the migration and interaction of TCR/co-receptors in the plasma membrane during activation. Thus, it is possible that Δ^9 -THC may exert its suppressive effect by interfering the formation of TCR microcluster, which has been shown to be important in T cell activation [reviewed in (Yukosuka and Saito, 2010)].

In studies characterizing the involved mechanism in human, we first investigated whether Δ^9 -THC suppresses CD40L expression by activated primary human CD4⁺ T cells. Consistent with our previous study demonstrating the suppression of CD40L upregulation by Δ^9 -THC in mouse splenic T cells [333],

 Δ^9 -THC attenuated anti-CD3/CD28-induced CD40L expression in human T cells at both the protein and mRNA level. It is notable that the kinetics of CD40L upregulation in human that we observed here is different from our observations in mouse T cells and several previous reports, in which the peak induction was early, approximately 6-8 h post stimulation [324-327,333]. Although the rapid induction of CD40L on activated CD4⁺ T cells is well-established, more recent studies support a biphasic kinetic profile of CD40L induction in both mouse and human activated CD4⁺ T cells [71-74]. Here we report that the peak time of induction of surface CD40L expression on activated human CD4⁺ T cells was 48 h post activation with anti-CD3/CD28. This is in accordance with reports showing that the second peak occurred at 48 h. However we did not observe the biphasic kinetics, which could possibly be due to differences in the *in vitro* culture model. Although our study and the studies conducted by McDyer et al. and Snyder et al. used PBMCs as the source of T cells, the clones and concentrations of antibodies directed against CD3 and CD28 were different from those used here [73,74].

Mechanistically, we demonstrate that Δ^9 -THC impaired the DNA-binding activity of both NFAT and NF κ B, two critical transcription factors involved in regulating CD40L expression [76,78-80]. Consistent with several reports demonstrating that there are two specific complexes formed at the proximal NFAT site, we also observed two specific NFAT-DNA complexes, which are likely

composed of NFATc (NFATc1) and NFATp (NFATc2) [323,353]. Δ⁹-THCmediated suppression of NFAT-DNA complexes observed here was consistent with our previous mouse study in which we demonstrated that the mechanism of T cell suppression by Δ^9 -THC involves, at least in part, the impairment of NFAT activity [303]. In addition, CBN, another immunomodulatory plant-derived cannabinoid compound, 2-AG, an endogenous cannabinoid, and 15-deoxy-Δ^{12,14}-PGJ₂-alverol ester, a putative metabolite of 2-AG, were all found to inhibit the DNA-binding activity of NFAT in activated T cells [354-357]. 2-AG also inhibited the nuclear translocation of both NFATc1 and NFATc2 [358]. In order to characterize the molecular target responsible for Δ^9 -THC-mediated suppression of NFAT, the possible involvement of GSK3β, a kinase regulating NFAT activation, was investigated, but was found not to be affected by Δ^9 -THC. These results clearly demonstrated that GSK3\beta is not involved in cannabinoidsmediated suppression of NFAT activity. For NF κ B, we observed thee complexes, of which only one complex exhibited specific NFκB-DNA binding activity, which is consistent with a report by Shena et. al., who also identified p65 containing NFκB-DNA binding complexes in the absence of p50 [80]. Again, these results are consistent with another study from our laboratory demonstrating that CBN primarily suppressed the DNA binding of p65 and c-Rel in mouse T cells [311]. Overall, these results demonstrate that suppression of NFAT and

NF_KB DNA binding activity are common mechanisms underlying the impairment of T cell activity by cannabinoids.

Part of the mechanism by which NFAT and NFκB DNA binding activity are suppressed by Δ^9 -THC involves dysregulation of Ca²⁺ since we demonstrate for the first time that Δ^9 -THC significantly impaired anti-CD3/CD28-induced Ca²⁺ elevation in activated primary human CD4⁺ T cells. This observation is somewhat in contrast to our prior finding that immunomodulatory cannabinoids, Δ^9 -THC, CBN, and HU-210 robustly increased the influx of extracellular Ca²⁺ in resting T cells [239,240]. It is noteworthy that although this study investigated the effect of Δ^9 -THC on Ca²⁺ signaling in response to anti-CD3/CD28 activation, pretreatment with Δ^9 -THC and/or preincubation with anti-CD3 and anti-CD28 in the absence of the IgG crosslinker did not increase [Ca²⁺]_i. The previous studies were performed using either purified mouse splenic T cells and/or the human peripheral blood acute lymphoid leukemia (HPB-ALL) T cell line, and therefore, these differences might account for the differential effect of Δ^9 -THC on Ca²⁺ elevation. However, our results are consistent with a report demonstrating that pretreatment with Δ^9 -THC suppressed the increase of $[Ca^{2+}]_i$ induced by concanavalin A in mouse thymocytes [359]. The exact mechanism by which Δ^9 -THC exerts its suppressive effect on anti-CD3/CD28-induced Ca²⁺ elevation in

primary human CD4⁺ T cells has not been fully elucidated. In the present study, demonstrated that Δ^9 -THC did not affect anti-CD3/CD28-induced phosphorylation of PLC_γ1/2, the active forms of PLC_γ that generate IP₃ to release Ca²⁺ from intracellular stores. To date, the activation of PLC_Y is the major pathway responsible for the IP $_3$ production; therefore it is unlikely that $\Delta^9\text{-THC}$ affects IP₃ production without changes in the activation of PLC_γ. In contrast, if $\Delta^9\text{-THC}$ altered the capacity of IP $_3$ receptors to bind IP $_3$, a similar profile of activity could be observed. Another possibility is that Δ^9 -THC may affect distal steps in receptor-mediated Ca²⁺ mobilization. Indeed, not only Ca²⁺ channels, but voltage- and Ca²⁺-dependent potassium channels, play critical roles in promoting the sustained increase of $[Ca^{2+}]_i$ (reviewed in [360]). Therefore, Δ^9 -THC might directly or indirectly target one of the aforementioned ion channels in T cells. Additional studies are required to decipher the detailed molecular mechanisms of Ca^{2+} regulation by Δ^{9} -THC in T cells.

In conjunction with the absence of an inhibitory effect of Δ^9 -THC on phosphorylation of PLC γ 1/2, Δ^9 -THC did not attenuate anti-CD3/CD28-induced phosphorylation of pZAP70 and Akt, key regulators in early events of TCR and CD28 signaling, respectively. These results clearly demonstrated that Δ^9 -THC

does not interfere with the proximal events of TCR signaling in primary human CD4⁺ T cells. This is contrasted with a study utilizing the human Jurkat T cell line in which Δ^9 -THC suppressed TCR-induced phosphorylation of ZAP70 [308]. The divergent results might be due to the differences in the cell model and/or experimental conditions. The Jurkat E6.1 T cell line likely has aberrant signaling pathways that facilitate its immortalized state. For instance, Jurkat E6.1 T cells exhibit lower phosphorylation of ZAP70, but have higher phosphorylation of PLCy upon TCR stimulation [361]. In addition, here we demonstrated that 30 min pretreatment with Δ^9 -THC significantly suppressed TCR-induced CD40L expression; whereas Borner et al. did not observe any effect of Δ^9 -THC in any measurement unless the cells were pretreated with Δ^9 -THC for 2 h. Differences in clones and concentration of anti-CD3 and anti-CD28, as well as the differences in concentration of Δ^9 -THC, might also account for the differential effect of Δ^9 -THC on proximal TCR signaling [308].

II. Effect of Δ^9 -THC on CD40L plus cytokine-induced primary antibody response in primary human B cells.

This section focused primarily on the effect of Δ^9 -THC on primary antibody responses, the effector functions of B cells. We demonstrated here that Δ^9 -THC

significantly attenuated the primary antibody response by HPB B cells stimulated with CD40L plus cytokine. This finding is contrast to previous reports describing B cell is not a sensitive target for Δ^9 -THC-mediated suppression of IgM response against sRBC as Δ^9 -THC did not alter the number of IgM antibody forming cells induced either by LPS, the polyclonal B cell activator, both in vivo [298] and in vitro [294]. However, our result is consistent with a previous study using mouse splenic B cells in which treatment with Δ^9 -THC decreased the numbers of IgM secreting cells induced by CD40L plus cytokine [294]. These results clearly demonstrate that the B cell is a direct cellular target of Δ^9 -THC in the suppression of T-cell dependent antibody response in both mouse and humans. Furthermore, we extended our initial investigation of direct Δ^9 -THC effects on B cells to elucidate key molecular events that contribute to the mechanism by which Δ^9 -THC suppressed B cell differentiation.

We demonstrated that Δ^9 -THC selectively alters the initial activation of B cells as evidenced by significant suppression of surface CD80 expression induced by CD40L plus cytokine. However, the expression of other B cell surface molecules, CD69, CD86, or ICAM1, remained unaffected upon treatment with Δ^9 -THC. These aforementioned molecules play critical roles in the T cell-B cell interaction, especially CD80 and CD86 [reviewed in [362]]. Both CD80 and CD86 serve as ligands for CD28 or CTLA4 expressed on activated CD4⁺ T cells,

thereby increasing or decreasing, respectively, the T cell activation signal [363]. Therefore, the attenuation of surface CD80 expression on activated B cells by Δ^9 -THC could play an important role in the initial phase of plasma cell differentiation by disrupting the antigen presentation capacity of B cells. A recent study suggested that CD80 plays important role in formation and/or maintenance of long-live plasma cells, in which the antibody production from long-live plasma cells, but not plasmablasts, was impaired in CD80-deficient mice [364]. Therefore, it is possible that the selective inhibitory effect of Δ^9 -THC on the upregulation of CD80 may impair the production of high-affinity long-lived plasma cells and memory B cells. The exact mechanism(s) by which Δ^9 -THC mediates suppression of surface CD80 expression is still unknown and warrant further investigation, but our observation that Δ^9 -THC did not affect the steady-state level of *CD80* mRNA suggests that Δ^9 -THC regulates the expression of surface CD80 at the post-transcriptional level. One possibility is Δ^9 -THC increases internalization and degradation of surface CD80. Although regulation of CD80 degradation is not understood, the ubiquitin-dependent degradation of surface CD86 has been shown to be mediated, in part, by ubiquitin ligase membraneassociated RING-CH-1 (MARCH1) [365]. Although overexpression of MARCH1 did not affect the surface expression of CD80 [365], the possibility that Δ^9 -THC

may facilitate the internalization and/or degradation of CD80 by altering a yetunknown ubiquitin ligase cannot be ruled out.

Our finding that Δ^9 -THC impaired the ability of activated B cells to divide correlates well with the suppressive effect on the generation of IgM secreting cells since differentiation into Ig-secreting cells is also linked to cell division [366,367]. It is noteworthy that the anti-proliferative effect of Δ^9 -THC on activated B cells, at least in this model, did not affect the number of total viable cells. Although Δ^9 -THC and other cannabinoids have been shown to induce apoptosis in immune cells (reviewed in [368]), we did not find any evidence of cell loss. Next we investigated whether Δ^9 -THC impaired the transcriptional regulatory network involved in plasmacytic differentiation and demonstrated that $\Delta^9\text{-THC}$ significantly suppressed IGJ mRNA expression, but did not alter the mRNA level of PRDM1, "the master regulator" of plasma cell differentiation, or PAX5, one of critical transcription factors in maintaining B cell identity (reviewed in [3]). Taken together, these results suggested that suppression by Δ^9 -THC of the primary IgM response in human primary B cells is, at least in part, mediated through the impairment of IgJ expression.

At the molecular level we demonstrated that treatment with Δ^9 -THC attenuated the phosphorylation of STAT3, but not p65 NF κ B, in response to recombinant CD40L and cytokine. It is well established that CD40 signals mainly

through NF κ B, whereas cytokines signal mainly through STAT pathways; in particular IL-10 induces phosphorylation of STAT3 [134]. STAT3 is necessary for the generation of plasma cells by promoting B cell survival *in vitro* [151,369] and increasing the upregulation of Blimp1 [149]. Further, mutations of STAT3 resulted in a reduction of DNA-binding activity and was associated with decreasing the induction of Blimp1 in response to recombinant CD40L plus IL-10 or IL-21 [161]. Taken together, this finding suggests that IL-10-mediated induction of STAT3 could be another putative target of suppression by Δ^9 -THC and likely contributes to Δ^9 -THC-mediated impairment of IgM response in humans.

The inability of Δ^9 -THC to modulate the phosphorylation of p65 NF κ B is in contrast to previous studies from our laboratory demonstrating as mentioned earlier, that CBN suppressed the DNA binding of p65 and c-Rel in mouse T cells [311] and our finding here that Δ^9 -THC suppresses the DNA-binding activity of NF κ B in activated human T cells. These findings suggest that Δ^9 -THC exhibits stimulation- and/or cell type-specific selectivity in NF κ B inhibition. It is noteworthy that NF κ B is one of the critical transcription factor involved in the regulation of genes encoding for CD69, CD80, CD86, and ICAM1 [100,370-372]. Therefore, the lack of an effect of Δ^9 -THC on CD40-mediated phosphorylation of

p65 NF κ B supports our findings that Δ^9 -THC did not affect cell surface expression of CD86, CD69 and ICAM1 or gene transcription of *CD80*.

III. Concluding remarks

The studies reported in this dissertation demonstrated that suppression of primary IgM response in humans by Δ^9 -THC involves the perturbation of CD40-CD40L interactions, in particular the upregulation of CD40L in activated CD4⁺ T cells. Moreover, these studies show that the mode of T cell activation leading to the induction of surface CD40L plays an important role in determining the magnitude of sensitivity to Δ^9 -THC. While Δ^9 -THC impaired CD40L expression induced by anti-CD3/CD28, it did not appear to alter the PMA/Io-induced CD40L expression in mouse splenic CD4 $^+$ T cells. These findings suggested that Δ^9 -THC targets proximal TCR-associated signaling. However, the demonstration that Δ^9 -THC did not interrupt proximal TCR signaling events (e.g. tyrosine phosphorylation of ZAP70, Akt, and PLCy1/2) in primary human CD4⁺ T cells suggested that the aforementioned membrane-proximal effectors were not targeted by Δ^9 -THC, at least in human primary T cells.

The precise role of CB1 and/or CB2 in cannabinoid-mediated immune modulation remains elusive. Both receptor-dependent and receptor-independent mechanisms are involved depending on cell type and the response being

measured [294,309,373], suggesting the existence of additional receptors beyond CB1/CB2 (reviewed in [350]). With the demonstration that Δ^9 -THC attenuated anti-CD3/CD28-induced CD40L expression in a CB1/CB2 receptor independent manner, another potential target, GR, was examined. In fact, dexamethasone, a potent GR agonist, suppresses T-cell dependent humoral immune responses, shares structural similarity with Δ^9 -THC and also suppresses anti-CD3/CD28-induced CD40L expression in mouse splenic CD4⁺ T cells [374,375]. However, none of the measurements used in this present study were able to demonstrate the potential interaction between Δ^9 -THC and GR. Collectively, suppression of anti-CD3/CD28-induced CD40L expression in mouse splenic CD4⁺ T cells by Δ^9 -THC likely occurs independently of CB1, CB2 and GR.

 Δ^9 -THC was shown to impair the DNA binding activity of both NFAT and NF $_{\rm K}$ B to their response elements derived from CD40L promoter, thereby attenuating the transcription of *CD40L* gene and resulting in reduction of steady-state *CD40L* mRNA levels in activated human primary T cells. The inhibitory effects of Δ^9 -THC on NFAT are likely mediated through impairment of T cell activation, rather than retention of inactive cytoplasmic NFAT, as evidenced by a lack of change in the phosphorylation status of GSK3 β , a NFAT kinase that regulates cytoplasmic-nuclear localization (reviewed in [59]). Importantly, Δ^9 -

THC impaired anti-CD3/CD28-induced Ca²⁺ elevation, the major mechanism involved in NFAT activation, and to a certain extent is also involved in NF κ B activation (reviewed in [31]). These findings identify perturbation of the calcium-NFAT and NF κ B signaling cascade as a key event in the mode of action by which Δ^9 -THC exerts a suppressive effect on human T cell function. Future studies are needed to elucidate the exact mechanism by which Δ^9 -THC exerts its suppressive effect on anti-CD3/CD28-induced Ca²⁺ elevation in primary human CD4⁺ T cells.

In addition to suppression of CD40L upregulation on activated CD4 $^+$ T cells, Δ^9 -THC attenuated B-cell function involved in the generation of IgM secreting cells in humans. Δ^9 -THC was found to impair the initial activation stage of B cells as demonstrated by significant suppression of surface CD80 expression induced by CD40L plus cytokine. Further, Δ^9 -THC did not affect the steady-state levels of *CD80* mRNA, suggesting that suppression of surface CD80 expression by Δ^9 -THC regulates the expression of CD80 at the post-transcriptional level. Importantly, no change in the expression of CD69, CD86, and ICAM1 was observed in the presence of Δ^9 -THC. These results suggest that Δ^9 -THC did not affect the common transcription factors regulating expression of

the genes encoding for all aforementioned molecules. Indeed, this notion is well supported by the demonstration that Δ^9 -THC did not perturb CD40-induced activation of NF κ B, as evidence by the absence of alterations in the phosphorylation status of p65 NF κ B in activated human B cells. An avenue for future research in this area would be to investigate the biological consequence of Δ^9 -THC-mediated specific suppression of surface CD80 on T cell activation, as CD80 is one of co-stimulatory molecules that can provide either positive or negative signals to T cells during T cell-B cell interaction [363].

Proliferation of activated human B cells also attenuated by Δ^9 -THC. Further, Δ^9 -THC was shown to impair transcription of the genes involved in plasmacytic differentiation, as evidenced by decreased mRNA levels of *IGJ*. With the demonstration that Δ^9 -THC impairs B cell function, the immediate downstream signaling molecules in B cell activation were examined. These studies showed that Δ^9 -THC attenuated the phosphorylation of STAT3 but not p65 NF κ B. Collectively, these findings demonstrated that suppression by Δ^9 -THC of the IgM response by human primary B cells is mediated, at least in part, through impairment of STAT3 activation, proliferation and plasmacytic differentiation. Future studies are required to 1) elucidate the molecular mechanism underlying suppression of *IGJ* mRNA, which may be mediated

through alterations in STAT5 [376] and 2) investigate how suppression of STAT3 activation may lead to impaired B cell proliferation and plasmacytic differentiation.

In summary, this dissertation research advances the current state of the science in this area in several ways. First, the demonstration that Δ^9 -THC attenuates CD40L expression on T cells is a novel observation, and potentially one of the key events in the mechanism by which Δ^9 -THC suppresses T-cell dependent humoral immune response in humans. Second, the demonstration that suppression of CD40L by Δ^9 -THC occurs independently of CB1 and CB2 emphasizes that cannabinoid receptors are not involved in all aspects of immune modulation by cannabinoid compounds. Further, this study is the first to show that there is no potential interaction between Δ^9 -THC and GR. This finding is also significant as it rules out the possible involvement of GR in the immune suppression mediated by Δ^9 -THC. Third, the demonstration that Δ^9 -THC impaired Ca²⁺ elevation in activated human T cells resulting in suppression of NFAT-and NFkB-DNA binding activity is also important. This finding not only supports the notion that immediate perturbation of intracellular Ca²⁺ levels by cannabinoids, including Δ^9 -THC, is central to the initiation of signaling cascades responsible for impairment of T cell function, but also challenges previous findings demonstrating that Δ^9 -THC and CBD enhanced Ca²⁺ elevation in both

resting and PMA/lo-stimulating lymphocytes [239,240,299]. Fourth. dysregulation of CD40 plus cytokine-induced B-cell activation, proliferation and differentiation into IgM secreting cells by Δ^9 -THC further provides mechanistic insights by which Δ^9 -THC suppresses T-cell dependent humoral immune response in humans. Finally, we provided the first conclusive evidence that Δ^9 -THC selectively suppresses surface expression of CD80 in activated human B cells, which may provide a new therapeutic strategy for diseases mediated by excess CD80 activation, such as Minimal Change Disease, the most common nephrotic syndrome in children (reviewed in [377]). Additionally, the novel identification that inactivation of STAT3, but not p65 NFκB, serves as one possible target of Δ^9 -THC in activated human primary B cells and underscores the direct effect of Δ^9 -THC on intrinsic signaling in B cells. The differential effect of Δ^9 -THC on NF_KB signaling also emphasizes the multi-faceted mechanisms involved in immune suppression by Δ^9 -THC, which most likely depend on cell types. Figure 40 summarized the possible mechanisms involved in suppression of T cell-dependent humoral immune response by Δ^9 -THC. Despite the predominant role of CD40-CD40L interaction in the T cell-dependent humoral immune response, the aberrant CD40L expression on activated T cells was demonstrated in the pathogenesis of many autoimmune and inflammatory diseases (reviewed in [378]). In addition, constitutively activated STAT3 was

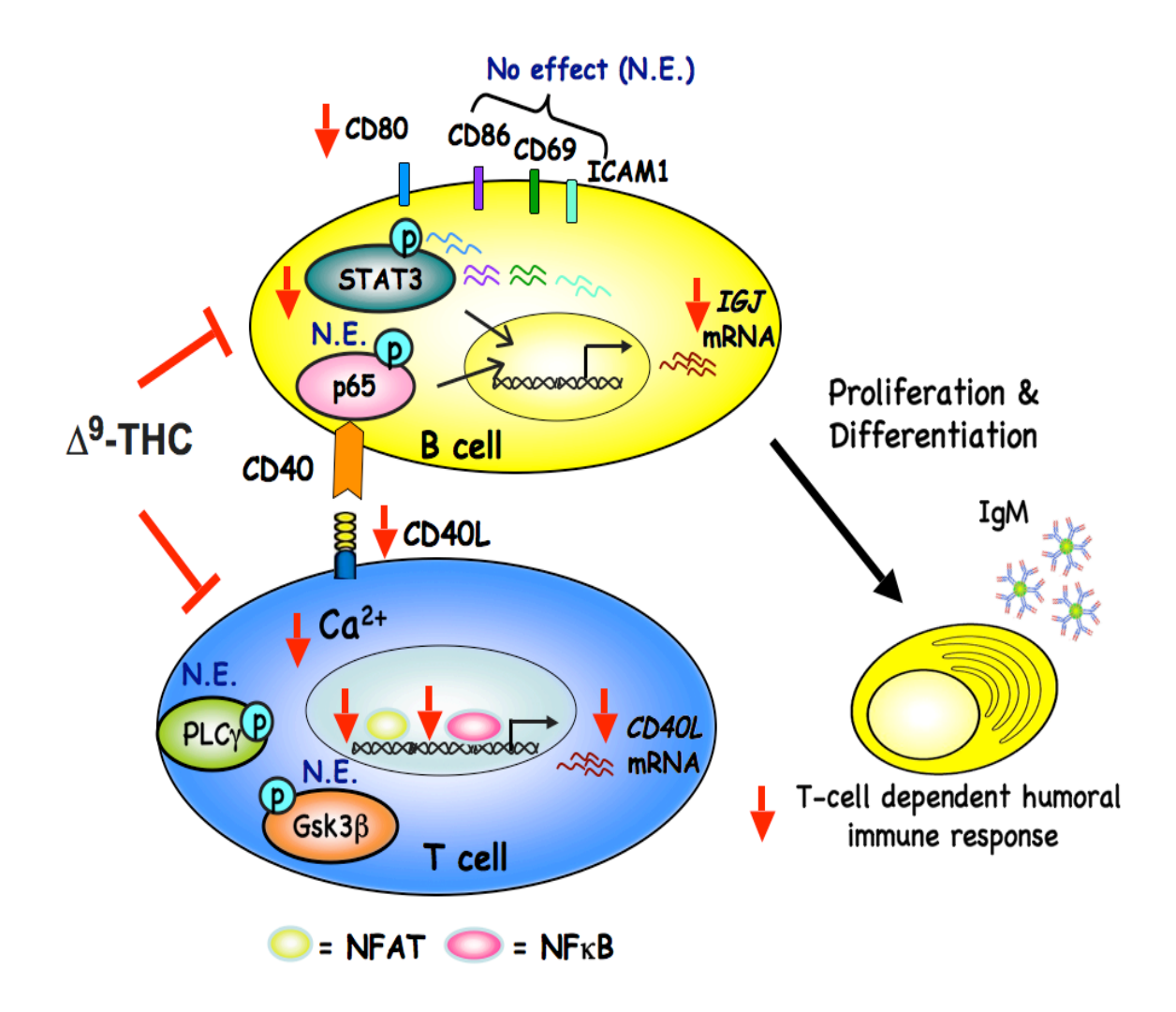


Figure 40. Schematic diagram summarizing the possible mechanisms involved in suppression of T cell-dependent humoral immune response by Δ^9 -THC.

 $\Delta^9\text{-THC}$ suppressed both T cells and B cells, which are the major play in T-cell dependent humoral immune response. The suppression of CD40L expression on activated CD4 $^+$ T cells by $\Delta^9\text{-THC}$ is mediated at least by perturbation of the calcium-NFAT and NF $_\kappa$ B signaling cascade without affected the activation of proximal kinases in TCR signaling. The suppression of B cell function by $\Delta^9\text{-THC}$ is mediated at least by impariment of STAT3 activation without affected the acitvation of p65 NF $_\kappa$ B subunit.

shown to promote cell proliferation and survival of the activated B-cell subtype of diffuse large B-cell lymphoma [379]. Hence, these critical observations may be of practical importance in future efforts to develop effective and safer therapeutic strategies in the treatment of inflammatory related and/or autoimmune diseases as well as cancer, especially for B-cell lymphomas. Collectively, an understanding of the mechanisms by which Δ^9 -THC, and structurally-related cannabinoids, affect T and B cell function might allow for the development of cannabinoid-based therapeutic strategies and also provide important information when weighing benefit to risk in immunocompromised patients such as those undergoing cancer chemotherapy or suffering from HIV/AIDS.

APPENDICES

APPENDIX A. Antibodies

Table 2. List of antibodies used in this dissertation research.

<u>Target</u>	Fluoro- phore	<u>-</u>	Clone	<u>Host</u>	Reactivity	<u>Supplier</u>
CD4 Per	CP-Cy5	.5	OKT4	Mouse	Human	Biolegend
CD4	APC		RPA-T4	Mouse	Human	BD Biosciences
CD4	FITC		OKT4	Hamster	Human	BD Biosciences
CD4	V450		RPA-T4	Mouse	Human	BD Biosciences
CD4	V450		RM4-5	Rat	Mouse	BD Biosciences
CD16/32	None		2.4G2	Rat	Mouse	BD Biosciences
CD40L	PE		24-31	Mouse	Human	Biolegend
CD40L	APC		RM1	Hamster	Mouse	eBiosciences
CD69	PE/Cy7	•	FN 50	Mouse	Human	Biolegend
CD80	PE/Cy5	•	2D10	Mouse	Human	Biolegend
CD86	PE		IT2.2	Mouse	Human	Biolegend
ICAM1 (CD54)	APC		HCD54	Mouse	Human	Biolegend
Akt (pS473)	PE		N/A	Mouse	Human	BD Biosciences
GSK3β (pS9)	FITC		N/A	Mouse	Human	R&D
p65 NFκB (pS529)	FITC	K10	0-895.12.50	Mouse	Human	BD Biosciences
PLC-γ2 (pY759)	PE	K86	6-689.37	Mouse	Human	BD Biosciences

Table 2 (cont'd)

STAT3 (pY705)	AF647 4/P	-STAT3	Mouse	Human	BD Biosciences
ZAP70 (pY319)/Sy	AF647 k (pY352)	N/A	Mouse	Mouse /Human	BD Biosciences

APPENDIX B. TaqMan Primers

Table 3. List of Tagman primers used in this dissertation research.

<u>Gene</u>	Catalog number	RefSeq
18s	4319413E	X03205.1
Human CD40L	Hs99999102_m1	NM_000074.2
Human CD80	Hs00175478_m1	NM_005191.3
Human IgJ	Hs00376160_m1	NM_144646.3
Human PAX5	Hs00277134_m1	NM_016743.1
Human PRDM1	Hs00153357_m1	NM_001189.

BIBLIOGRAPHY

BIBLIOGRAPHY

- 1. Kishimoto T, Hirano T. Molecular regulation of B lymphocyte response. *Annu Rev Immunol*, 6, 485-512 (1988).
- 2. Howard M, Paul WE. Regulation of B-cell growth and differentiation by soluble factors. *Annu Rev Immunol*, 1, 307-333 (1983).
- 3. Alinikula J, Lassila O. Gene interaction network regulates plasma cell differentiation. *Scand J Immunol*, 73(6), 512-519 (2011).
- 4. Cobaleda C, Schebesta A, Delogu A, Busslinger M. Pax5: the guardian of B cell identity and function. *Nat Immunol*, 8(5), 463-470 (2007).
- 5. Pridans C, Holmes ML, Polli M *et al.* Identification of Pax5 target genes in early B cell differentiation. *J Immunol*, 180(3), 1719-1728 (2008).
- 6. Schebesta A, McManus S, Salvagiotto G, Delogu A, Busslinger GA, Busslinger M. Transcription factor Pax5 activates the chromatin of key genes involved in B cell signaling, adhesion, migration, and immune function. *Immunity*, 27(1), 49-63 (2007).
- 7. Rinkenberger JL, Wallin JJ, Johnson KW, Koshland ME. An interleukin-2 signal relieves BSAP (Pax5)-mediated repression of the immunoglobulin J chain gene. *Immunity*, 5(4), 377-386 (1996).
- 8. Cattoretti G, Chang CC, Cechova K *et al.* BCL-6 protein is expressed in germinal-center B cells. *Blood*, 86(1), 45-53 (1995).
- 9. Basso K, Dalla-Favera R. BCL6: master regulator of the germinal center reaction and key oncogene in B cell lymphomagenesis. *Adv Immunol*, 105, 193-210 (2010).
- 10. Martins G, Calame K. Regulation and functions of Blimp-1 in T and B lymphocytes. *Annu Rev Immunol*, 26, 133-169 (2008).

- 11. Shaffer AL, Lin KI, Kuo TC *et al.* Blimp-1 orchestrates plasma cell differentiation by extinguishing the mature B cell gene expression program. *Immunity*, 17(1), 51-62 (2002).
- 12. Reimold AM, Iwakoshi NN, Manis J *et al.* Plasma cell differentiation requires the transcription factor XBP-1. *Nature*, 412(6844), 300-307 (2001).
- 13. Lee AH, Iwakoshi NN, Glimcher LH. XBP-1 regulates a subset of endoplasmic reticulum resident chaperone genes in the unfolded protein response. *Mol Cell Biol*, 23(21), 7448-7459 (2003).
- 14. Kwon H, Thierry-Mieg D, Thierry-Mieg J *et al.* Analysis of interleukin-21-induced Prdm1 gene regulation reveals functional cooperation of STAT3 and IRF4 transcription factors. *Immunity*, 31(6), 941-952 (2009).
- 15. Frauwirth KA, Thompson CB. Activation and inhibition of lymphocytes by costimulation. *J Clin Invest*, 109(3), 295-299 (2002).
- 16. Boomer JS, Green JM. An enigmatic tail of CD28 signaling. *Cold Spring Harb Perspect Biol*, 2(8), a002436 (2010).
- 17. Williams BL, Irvin BJ, Sutor SL *et al.* Phosphorylation of Tyr319 in ZAP-70 is required for T-cell antigen receptor-dependent phospholipase C-gamma1 and Ras activation. *Embo J*, 18(7), 1832-1844 (1999).
- 18. Bromley SK, Burack WR, Johnson KG *et al.* The immunological synapse. *Annu Rev Immunol*, 19, 375-396 (2001).
- 19. Feske S. Calcium signalling in lymphocyte activation and disease. *Nat Rev Immunol*, 7(9), 690-702 (2007).
- 20. Hogan PG, Lewis RS, Rao A. Molecular basis of calcium signaling in lymphocytes: STIM and ORAI. *Annu Rev Immunol*, 28, 491-533 (2010).
- 21. Putney JW. Origins of the concept of store-operated calcium entry. *Front Biosci (Schol Ed)*, 3, 980-984 (2011).

- 22. Shaw PJ, Qu B, Hoth M, Feske S. Molecular regulation of CRAC channels and their role in lymphocyte function. *Cell Mol Life Sci*, (2012).
- 23. Spassova MA, Soboloff J, He LP, Xu W, Dziadek MA, Gill DL. STIM1 has a plasma membrane role in the activation of store-operated Ca(2+) channels. *Proc Natl Acad Sci U S A*, 103(11), 4040-4045 (2006).
- 24. Wu MM, Buchanan J, Luik RM, Lewis RS. Ca2+ store depletion causes STIM1 to accumulate in ER regions closely associated with the plasma membrane. *J Cell Biol*, 174(6), 803-813 (2006).
- 25. Xu P, Lu J, Li Z, Yu X, Chen L, Xu T. Aggregation of STIM1 underneath the plasma membrane induces clustering of Orai1. *Biochem Biophys Res Commun*, 350(4), 969-976 (2006).
- 26. Zhang SL, Yu Y, Roos J *et al.* STIM1 is a Ca2+ sensor that activates CRAC channels and migrates from the Ca2+ store to the plasma membrane. *Nature*, 437(7060), 902-905 (2005).
- 27. Nicolaou SA, Neumeier L, Steckly A, Kucher V, Takimoto K, Conforti L. Localization of Kv1.3 channels in the immunological synapse modulates the calcium response to antigen stimulation in T lymphocytes. *J Immunol*, 183(10), 6296-6302 (2009).
- 28. Ghanshani S, Wulff H, Miller MJ *et al.* Up-regulation of the IKCa1 potassium channel during T-cell activation. Molecular mechanism and functional consequences. *J Biol Chem*, 275(47), 37137-37149 (2000).
- 29. Bautista DM, Hoth M, Lewis RS. Enhancement of calcium signalling dynamics and stability by delayed modulation of the plasma-membrane calcium-ATPase in human T cells. *J Physiol*, 541(Pt 3), 877-894 (2002).
- 30. Cahalan MD, Chandy KG. The functional network of ion channels in T lymphocytes. *Immunol Rev*, 231(1), 59-87 (2009).
- 31. Quintana A, Griesemer D, Schwarz EC, Hoth M. Calcium-dependent activation of T-lymphocytes. *Pflugers Arch*, 450(1), 1-12 (2005).

- 32. Macian F. NFAT proteins: key regulators of T-cell development and function. *Nat Rev Immunol*, 5(6), 472-484 (2005).
- 33. Lyakh L, Ghosh P, Rice NR. Expression of NFAT-family proteins in normal human T cells. *Mol Cell Biol*, 17(5), 2475-2484 (1997).
- 34. Trama J, Lu Q, Hawley RG, Ho SN. The NFAT-related protein NFATL1 (TonEBP/NFAT5) is induced upon T cell activation in a calcineurin-dependent manner. *J Immunol*, 165(9), 4884-4894 (2000).
- 35. Lopez-Rodriguez C, Aramburu J, Rakeman AS, Rao A. NFAT5, a constitutively nuclear NFAT protein that does not cooperate with Fos and Jun. *Proc Natl Acad Sci U S A*, 96(13), 7214-7219 (1999).
- 36. James P, Vorherr T, Carafoli E. Calmodulin-binding domains: just two faced or multi-faceted? *Trends Biochem Sci*, 20(1), 38-42 (1995).
- 37. Loh C, Shaw KT, Carew J *et al.* Calcineurin binds the transcription factor NFAT1 and reversibly regulates its activity. *J Biol Chem*, 271(18), 10884-10891 (1996).
- 38. Wesselborg S, Fruman DA, Sagoo JK, Bierer BE, Burakoff SJ. Identification of a physical interaction between calcineurin and nuclear factor of activated T cells (NFATp). *J Biol Chem*, 271(3), 1274-1277 (1996).
- 39. Kiani A, Rao A, Aramburu J. Manipulating immune responses with immunosuppressive agents that target NFAT. *Immunity*, 12(4), 359-372 (2000).
- 40. Beals CR, Sheridan CM, Turck CW, Gardner P, Crabtree GR. Nuclear export of NF-ATc enhanced by glycogen synthase kinase-3. *Science*, 275(5308), 1930-1934 (1997).
- 41. Gwack Y, Sharma S, Nardone J *et al.* A genome-wide Drosophila RNAi screen identifies DYRK-family kinases as regulators of NFAT. *Nature*, 441(7093), 646-650 (2006).

- 42. Okamura H, Garcia-Rodriguez C, Martinson H, Qin J, Virshup DM, Rao A. A conserved docking motif for CK1 binding controls the nuclear localization of NFAT1. *Mol Cell Biol*, 24(10), 4184-4195 (2004).
- 43. May MJ, Ghosh S. Rel/NF-kappa B and I kappa B proteins: an overview. *Semin Cancer Biol*, 8(2), 63-73 (1997).
- 44. Li Q, Verma IM. NF-kappaB regulation in the immune system. *Nat Rev Immunol*, 2(10), 725-734 (2002).
- 45. Ghosh S, Karin M. Missing pieces in the NF-kappaB puzzle. *Cell*, 109 Suppl, S81-96 (2002).
- 46. Chen LF, Greene WC. Shaping the nuclear action of NF-kappaB. *Nat Rev Mol Cell Biol*, 5(5), 392-401 (2004).
- 47. Thome M, Tschopp J. TCR-induced NF-kappaB activation: a crucial role for Carma1, Bcl10 and MALT1. *Trends Immunol*, 24(8), 419-424 (2003).
- 48. Thome M, Weil R. Post-translational modifications regulate distinct functions of CARMA1 and BCL10. *Trends Immunol*, 28(6), 281-288 (2007).
- 49. Matsumoto R, Wang D, Blonska M *et al.* Phosphorylation of CARMA1 plays a critical role in T Cell receptor-mediated NF-kappaB activation. *Immunity*, 23(6), 575-585 (2005).
- 50. Feske S, Okamura H, Hogan PG, Rao A. Ca2+/calcineurin signalling in cells of the immune system. *Biochem Biophys Res Commun*, 311(4), 1117-1132 (2003).
- 51. Hughes K, Edin S, Antonsson A, Grundstrom T. Calmodulin-dependent kinase II mediates T cell receptor/CD3- and phorbol ester-induced activation of IkappaB kinase. *J Biol Chem*, 276(38), 36008-36013 (2001).
- 52. Palkowitsch L, Marienfeld U, Brunner C, Eitelhuber A, Krappmann D, Marienfeld RB. The Ca2+-dependent phosphatase calcineurin controls the formation of the Carma1-Bcl10-Malt1 complex during T cell receptor-induced NF-kappaB activation. *J Biol Chem*, 286(9), 7522-7534).

- 53. Ishiguro K, Green T, Rapley J *et al.* Ca2+/calmodulin-dependent protein kinase II is a modulator of CARMA1-mediated NF-kappaB activation. *Mol Cell Biol*, 26(14), 5497-5508 (2006).
- 54. Ishiguro K, Ando T, Goto H, Xavier R. Bcl10 is phosphorylated on Ser138 by Ca2+/calmodulin-dependent protein kinase II. *Mol Immunol*, 44(8), 2095-2100 (2007).
- 55. Woodgett JR. Molecular cloning and expression of glycogen synthase kinase-3/factor A. *Embo J*, 9(8), 2431-2438 (1990).
- 56. Wang H, Brown J, Martin M. Glycogen synthase kinase 3: a point of convergence for the host inflammatory response. *Cytokine*, 53(2), 130-140 (2011).
- 57. Garcia CA, Benakanakere MR, Alard P, Kosiewicz MM, Kinane DF, Martin M. Antigenic experience dictates functional role of glycogen synthase kinase-3 in human CD4+ T cell responses. *J Immunol*, 181(12), 8363-8371 (2008).
- 58. Ohteki T, Parsons M, Zakarian A *et al.* Negative regulation of T cell proliferation and interleukin 2 production by the serine threonine kinase GSK-3. *J Exp Med*, 192(1), 99-104 (2000).
- 59. Grimes CA, Jope RS. The multifaceted roles of glycogen synthase kinase 3beta in cellular signaling. *Prog Neurobiol*, 65(4), 391-426 (2001).
- 60. Chen K, Huang J, Gong W, Zhang L, Yu P, Wang JM. CD40/CD40L dyad in the inflammatory and immune responses in the central nervous system. *Cell Mol Immunol*, 3(3), 163-169 (2006).
- 61. Schonbeck U, Libby P. The CD40/CD154 receptor/ligand dyad. *Cell Mol Life Sci*, 58(1), 4-43 (2001).
- 62. van Kooten C, Banchereau J. CD40-CD40 ligand. *J Leukoc Biol*, 67(1), 2-17 (2000).
- 63. Schonbeck U, Mach F, Libby P. CD154 (CD40 ligand). *Int J Biochem Cell Biol*, 32(7), 687-693 (2000).

- 64. Lutgens E, Lievens D, Beckers L, Donners M, Daemen M. CD40 and its ligand in atherosclerosis. *Trends Cardiovasc Med*, 17(4), 118-123 (2007).
- 65. Schonbeck U, Libby P. CD40 signaling and plaque instability. *Circ Res*, 89(12), 1092-1103 (2001).
- 66. Smola-Hess S, Schnitzler R, Hadaschik D *et al.* CD40L induces matrix-metalloproteinase-9 but not tissue inhibitor of metalloproteinases-1 in cervical carcinoma cells: imbalance between NF-kappaB and STAT3 activation. *Exp Cell Res*, 267(2), 205-215 (2001).
- 67. Chatzigeorgiou A, Lyberi M, Chatzilymperis G, Nezos A, Kamper E. CD40/CD40L signaling and its implication in health and disease. *Biofactors*, 35(6), 474-483 (2009).
- 68. Daoussis D, Andonopoulos AP, Liossis SN. Targeting CD40L: a promising therapeutic approach. *Clin Diagn Lab Immunol*, 11(4), 635-641 (2004).
- 69. Cron RQ. CD154 transcriptional regulation in primary human CD4 T cells. *Immunol Res*, 27(2-3), 185-202 (2003).
- 70. Blair PJ, Riley JL, Harlan DM *et al.* CD40 ligand (CD154) triggers a short-term CD4(+) T cell activation response that results in secretion of immunomodulatory cytokines and apoptosis. *J Exp Med*, 191(4), 651-660 (2000).
- 71. Kaminski DA, Lee BO, Eaton SM, Haynes L, Randall TD. CD28 and inducible costimulator (ICOS) signalling can sustain CD154 expression on activated T cells. *Immunology*, 127(3), 373-385 (2009).
- 72. Lee BO, Haynes L, Eaton SM, Swain SL, Randall TD. The biological outcome of CD40 signaling is dependent on the duration of CD40 ligand expression: reciprocal regulation by interleukin (IL)-4 and IL-12. *J Exp Med*, 196(5), 693-704 (2002).
- 73. McDyer JF, Li Z, John S, Yu X, Wu CY, Ragheb JA. IL-2 receptor blockade inhibits late, but not early, IFN-gamma and CD40 ligand expression in human T cells: disruption of both IL-12-dependent and independent pathways of IFN-gamma production. *J Immunol*, 169(5), 2736-2746 (2002).

- 74. Snyder JT, Shen J, Azmi H, Hou J, Fowler DH, Ragheb JA. Direct inhibition of CD40L expression can contribute to the clinical efficacy of daclizumab independently of its effects on cell division and Th1/Th2 cytokine production. *Blood*, 109(12), 5399-5406 (2007).
- 75. Yellin MJ, Sippel K, Inghirami G *et al.* CD40 molecules induce down-modulation and endocytosis of T cell surface T cell-B cell activating molecule/CD40-L. Potential role in regulating helper effector function. *J Immunol*, 152(2), 598-608 (1994).
- 76. Schubert LA, King G, Cron RQ, Lewis DB, Aruffo A, Hollenbaugh D. The human gp39 promoter. Two distinct nuclear factors of activated T cell protein-binding elements contribute independently to transcriptional activation. *J Biol Chem*, 270(50), 29624-29627 (1995).
- 77. Steiper ME, Parikh SJ, Zichello JM. Phylogenetic analysis of the promoter region of the CD40L gene in primates and other mammals. *Infect Genet Evol*, 8(4), 406-413 (2008).
- 78. Mendez-Samperio P, Ayala H, Vazquez A. NF-kappaB is involved in regulation of CD40 ligand expression on Mycobacterium bovis bacillus Calmette-Guerin-activated human T cells. *Clin Diagn Lab Immunol*, 10(3), 376-382 (2003).
- 79. Smiley ST, Csizmadia V, Gao W, Turka LA, Hancock WW. Differential effects of cyclosporine A, methylprednisolone, mycophenolate, and rapamycin on CD154 induction and requirement for NFkappaB: implications for tolerance induction. *Transplantation*, 70(3), 415-419 (2000).
- 80. Srahna M, Remacle JE, Annamalai K *et al.* NF-kappaB is involved in the regulation of CD154 (CD40 ligand) expression in primary human T cells. *Clin Exp Immunol*, 125(2), 229-236 (2001).
- 81. Loughnan MS, Nossal GJ. Interleukins 4 and 5 control expression of IL-2 receptor on murine B cells through independent induction of its two chains. *Nature*, 340(6228), 76-79 (1989).
- 82. Bartlett WC, McCann J, Shepherd DM, Roy M, Noelle RJ. Cognate interactions between helper T cells and B cells. IV. Requirements for the

- expression of effector phase activity by helper T cells. *J Immunol*, 145(12), 3956-3962 (1990).
- 83. Hodgkin PD, Yamashita LC, Coffman RL, Kehry MR. Separation of events mediating B cell proliferation and Ig production by using T cell membranes and lymphokines. *J Immunol*, 145(7), 2025-2034 (1990).
- 84. Noelle R, Krammer PH, Ohara J, Uhr JW, Vitetta ES. Increased expression of la antigens on resting B cells: an additional role for B-cell growth factor. *Proc Natl Acad Sci U S A*, 81(19), 6149-6153 (1984).
- 85. Oliver K, Noelle RJ, Uhr JW, Krammer PH, Vitetta ES. B-cell growth factor (B-cell growth factor I or B-cell-stimulating factor, provisional 1) is a differentiation factor for resting B cells and may not induce cell growth. *Proc Natl Acad Sci U S A*, 82(8), 2465-2467 (1985).
- 86. Brian AA. Stimulation of B-cell proliferation by membrane-associated molecules from activated T cells. *Proc Natl Acad Sci U S A*, 85(2), 564-568 (1988).
- 87. Noelle RJ, Roy M, Shepherd DM, Stamenkovic I, Ledbetter JA, Aruffo A. A 39-kDa protein on activated helper T cells binds CD40 and transduces the signal for cognate activation of B cells. *Proc Natl Acad Sci U S A*, 89(14), 6550-6554 (1992).
- 88. Clark EA, Ledbetter JA. Activation of human B cells mediated through two distinct cell surface differentiation antigens, Bp35 and Bp50. *Proc Natl Acad Sci U S A*, 83(12), 4494-4498 (1986).
- 89. Fuleihan R, Ramesh N, Loh R *et al.* Defective expression of the CD40 ligand in X chromosome-linked immunoglobulin deficiency with normal or elevated IgM. *Proc Natl Acad Sci U S A*, 90(6), 2170-2173 (1993).
- 90. Korthauer U, Graf D, Mages HW *et al.* Defective expression of T-cell CD40 ligand causes X-linked immunodeficiency with hyper-lgM. *Nature*, 361(6412), 539-541 (1993).
- 91. DiSanto JP, Bonnefoy JY, Gauchat JF, Fischer A, de Saint Basile G. CD40 ligand mutations in x-linked immunodeficiency with hyper-IgM. *Nature*, 361(6412), 541-543 (1993).

- 92. Callard RE, Armitage RJ, Fanslow WC, Spriggs MK. CD40 ligand and its role in X-linked hyper-IgM syndrome. *Immunol Today*, 14(11), 559-564 (1993).
- 93. Foy TM, Shepherd DM, Durie FH, Aruffo A, Ledbetter JA, Noelle RJ. In vivo CD40-gp39 interactions are essential for thymus-dependent humoral immunity. II. Prolonged suppression of the humoral immune response by an antibody to the ligand for CD40, gp39. *J Exp Med*, 178(5), 1567-1575 (1993).
- 94. Xu J, Foy TM, Laman JD *et al.* Mice deficient for the CD40 ligand. *Immunity*, 1(5), 423-431 (1994).
- 95. Bishop GA, Moore CR, Xie P, Stunz LL, Kraus ZJ. TRAF proteins in CD40 signaling. *Adv Exp Med Biol*, 597, 131-151 (2007).
- 96. Bishop GA, Hostager BS. The CD40-CD154 interaction in B cell-T cell liaisons. *Cytokine Growth Factor Rev*, 14(3-4), 297-309 (2003).
- 97. Elgueta R, Benson MJ, de Vries VC, Wasiuk A, Guo Y, Noelle RJ. Molecular mechanism and function of CD40/CD40L engagement in the immune system. *Immunol Rev*, 229(1), 152-172 (2009).
- 98. Lu LF, Ahonen CL, Lind EF *et al.* The in vivo function of a noncanonical TRAF2-binding domain in the C-terminus of CD40 in driving B-cell growth and differentiation. *Blood*, 110(1), 193-200 (2007).
- 99. Hsing Y, Bishop GA. Requirement for nuclear factor-kappaB activation by a distinct subset of CD40-mediated effector functions in B lymphocytes. *J Immunol*, 162(5), 2804-2811 (1999).
- 100. Craxton A, Shu G, Graves JD, Saklatvala J, Krebs EG, Clark EA. p38 MAPK is required for CD40-induced gene expression and proliferation in B lymphocytes. *J Immunol*, 161(7), 3225-3236 (1998).
- 101. Pullen SS, Miller HG, Everdeen DS, Dang TT, Crute JJ, Kehry MR. CD40-tumor necrosis factor receptor-associated factor (TRAF) interactions: regulation of CD40 signaling through multiple TRAF binding sites and TRAF hetero-oligomerization. *Biochemistry*, 37(34), 11836-11845 (1998).

- Lu LF, Cook WJ, Lin LL, Noelle RJ. CD40 signaling through a newly identified tumor necrosis factor receptor-associated factor 2 (TRAF2) binding site. J Biol Chem, 278(46), 45414-45418 (2003).
- 103. Hanissian SH, Geha RS. Jak3 is associated with CD40 and is critical for CD40 induction of gene expression in B cells. *Immunity*, 6(4), 379-387 (1997).
- 104. Horvath CM, Darnell JE. The state of the STATs: recent developments in the study of signal transduction to the nucleus. *Curr Opin Cell Biol*, 9(2), 233-239 (1997).
- 105. Leonard WJ, O'Shea JJ. Jaks and STATs: biological implications. *Annu Rev Immunol*, 16, 293-322 (1998).
- 106. Imada K, Leonard WJ. The Jak-STAT pathway. *Mol Immunol*, 37(1-2), 1-11 (2000).
- 107. Jabara HH, Buckley RH, Roberts JL *et al.* Role of JAK3 in CD40-mediated signaling. *Blood*, 92(7), 2435-2440 (1998).
- 108. Karras JG, Wang Z, Huo L, Frank DA, Rothstein TL. Induction of STAT protein signaling through the CD40 receptor in B lymphocytes: distinct STAT activation following surface Ig and CD40 receptor engagement. *J Immunol*, 159(9), 4350-4355 (1997).
- 109. Arpin C, Dechanet J, Van Kooten C *et al.* Generation of memory B cells and plasma cells in vitro. *Science*, 268(5211), 720-722 (1995).
- 110. Randall TD, Heath AW, Santos-Argumedo L, Howard MC, Weissman IL, Lund FE. Arrest of B lymphocyte terminal differentiation by CD40 signaling: mechanism for lack of antibody-secreting cells in germinal centers. *Immunity*, 8(6), 733-742 (1998).
- 111. Burdin N, Van Kooten C, Galibert L *et al.* Endogenous IL-6 and IL-10 contribute to the differentiation of CD40-activated human B lymphocytes. *J Immunol*, 154(6), 2533-2544 (1995).

- 112. Rousset F, Garcia E, Defrance T *et al.* Interleukin 10 is a potent growth and differentiation factor for activated human B lymphocytes. *Proc Natl Acad Sci U S A*, 89(5), 1890-1893 (1992).
- 113. Jego G, Bataille R, Pellat-Deceunynck C. Interleukin-6 is a growth factor for nonmalignant human plasmablasts. *Blood*, 97(6), 1817-1822 (2001).
- 114. Tarte K, De Vos J, Thykjaer T *et al.* Generation of polyclonal plasmablasts from peripheral blood B cells: a normal counterpart of malignant plasmablasts. *Blood*, 100(4), 1113-1122 (2002).
- 115. Kindler V, Zubler RH. Memory, but not naive, peripheral blood B lymphocytes differentiate into Ig-secreting cells after CD40 ligation and costimulation with IL-4 and the differentiation factors IL-2, IL-10, and IL-3. *J Immunol*, 159(5), 2085-2090 (1997).
- 116. Chen E, Staudt LM, Green AR. Janus kinase deregulation in leukemia and lymphoma. *Immunity*, 36(4), 529-541 (2012).
- 117. Nakagawa N, Nakagawa T, Volkman DJ, Ambrus JL, Jr., Fauci AS. The role of interleukin 2 in inducing Ig production in a pokeweed mitogenstimulated mononuclear cell system. *J Immunol*, 138(3), 795-801 (1987).
- 118. Muraguchi A, Kehrl JH, Longo DL, Volkman DJ, Smith KA, Fauci AS. Interleukin 2 receptors on human B cells. Implications for the role of interleukin 2 in human B cell function. *J Exp Med*, 161(1), 181-197 (1985).
- 119. Jelinek DF, Splawski JB, Lipsky PE. The roles of interleukin 2 and interferon-gamma in human B cell activation, growth and differentiation. *Eur J Immunol*, 16(8), 925-932 (1986).
- 120. Callard RE, Smith SH, Shields JG, Levinsky RJ. T cell help in human antigen-specific antibody responses can be replaced by interleukin 2. *Eur J Immunol*, 16(9), 1037-1042 (1986).
- 121. Litjens NH, Huisman M, Hijdra D, Lambrecht BM, Stittelaar KJ, Betjes MG. IL-2 producing memory CD4+ T lymphocytes are closely associated with the generation of IgG-secreting plasma cells. *J Immunol*, 181(5), 3665-3673 (2008).

- 122. Kim HP, Imbert J, Leonard WJ. Both integrated and differential regulation of components of the IL-2/IL-2 receptor system. *Cytokine Growth Factor Rev*, 17(5), 349-366 (2006).
- 123. Mittler R, Rao P, Olini G *et al.* Activated human B cells display a functional IL 2 receptor. *J Immunol*, 134(4), 2393-2399 (1985).
- 124. Waldmann TA, Goldman CK, Robb RJ *et al.* Expression of interleukin 2 receptors on activated human B cells. *J Exp Med*, 160(5), 1450-1466 (1984).
- 125. Le Gallou S, Caron G, Delaloy C, Rossille D, Tarte K, Fest T. IL-2 requirement for human plasma cell generation: coupling differentiation and proliferation by enhancing MAPK-ERK signaling. *J Immunol*, 189(1), 161-173 (2012).
- 126. Nakanishi K, Cohen DI, Blackman M *et al.* Ig RNA expression in normal B cells stimulated with anti-IgM antibody and T cell-derived growth and differentiation factors. *J Exp Med*, 160(6), 1736-1751 (1984).
- 127. Matsui K, Nakanishi K, Cohen DI *et al.* B cell response pathways regulated by IL-5 and IL-2. Secretory microH chain-mRNA and J chain mRNA expression are separately controlled events. *J Immunol*, 142(8), 2918-2923 (1989).
- 128. Hirano T, Taga T, Nakano N *et al.* Purification to homogeneity and characterization of human B-cell differentiation factor (BCDF or BSFp-2). *Proc Natl Acad Sci U S A*, 82(16), 5490-5494 (1985).
- 129. Hirano T, Yasukawa K, Harada H *et al.* Complementary DNA for a novel human interleukin (BSF-2) that induces B lymphocytes to produce immunoglobulin. *Nature*, 324(6092), 73-76 (1986).
- 130. Kopf M, Baumann H, Freer G *et al.* Impaired immune and acute-phase responses in interleukin-6-deficient mice. *Nature*, 368(6469), 339-342 (1994).
- 131. Suematsu S, Matsuda T, Aozasa K *et al.* IgG1 plasmacytosis in interleukin 6 transgenic mice. *Proc Natl Acad Sci U S A*, 86(19), 7547-7551 (1989).

- 132. Hilbert DM, Kopf M, Mock BA, Kohler G, Rudikoff S. Interleukin 6 is essential for in vivo development of B lineage neoplasms. *J Exp Med*, 182(1), 243-248 (1995).
- 133. Hibi M, Murakami M, Saito M, Hirano T, Taga T, Kishimoto T. Molecular cloning and expression of an IL-6 signal transducer, gp130. *Cell*, 63(6), 1149-1157 (1990).
- 134. Lafarge S, Hamzeh-Cognasse H, Richard Y *et al.* Complexes between nuclear factor-kappaB p65 and signal transducer and activator of transcription 3 are key actors in inducing activation-induced cytidine deaminase expression and immunoglobulin A production in CD40L plus interleukin-10-treated human blood B cells. *Clin Exp Immunol*, 166(2), 171-183 (2011).
- 135. Daeipour M, Kumar G, Amaral MC, Nel AE. Recombinant IL-6 activates p42 and p44 mitogen-activated protein kinases in the IL-6 responsive B cell line, AF-10. *J Immunol*, 150(11), 4743-4753 (1993).
- 136. Berger LC, Hawley TS, Lust JA, Goldman SJ, Hawley RG. Tyrosine phosphorylation of JAK-TYK kinases in malignant plasma cell lines growth-stimulated by interleukins 6 and 11. *Biochem Biophys Res Commun*, 202(1), 596-605 (1994).
- 137. Guschin D, Rogers N, Briscoe J *et al.* A major role for the protein tyrosine kinase JAK1 in the JAK/STAT signal transduction pathway in response to interleukin-6. *Embo J*, 14(7), 1421-1429 (1995).
- 138. Kumar G, Gupta S, Wang S, Nel AE. Involvement of Janus kinases, p52shc, Raf-1, and MEK-1 in the IL-6-induced mitogen-activated protein kinase cascade of a growth-responsive B cell line. *J Immunol*, 153(10), 4436-4447 (1994).
- 139. Matsuda T, Yamanaka Y, Hirano T. Interleukin-6-induced tyrosine phosphorylation of multiple proteins in murine hematopoietic lineage cells. *Biochem Biophys Res Commun*, 200(2), 821-828 (1994).
- 140. Narazaki M, Witthuhn BA, Yoshida K *et al.* Activation of JAK2 kinase mediated by the interleukin 6 signal transducer gp130. *Proc Natl Acad Sci U S A*, 91(6), 2285-2289 (1994).

- 141. Stahl N, Boulton TG, Farruggella T *et al.* Association and activation of Jak-Tyk kinases by CNTF-LIF-OSM-IL-6 beta receptor components. *Science*, 263(5143), 92-95 (1994).
- 142. Fukada T, Hibi M, Yamanaka Y *et al.* Two signals are necessary for cell proliferation induced by a cytokine receptor gp130: involvement of STAT3 in anti-apoptosis. *Immunity*, 5(5), 449-460 (1996).
- 143. Takahashi-Tezuka M, Yoshida Y, Fukada T *et al.* Gab1 acts as an adapter molecule linking the cytokine receptor gp130 to ERK mitogen-activated protein kinase. *Mol Cell Biol*, 18(7), 4109-4117 (1998).
- 144. Nishida K, Yoshida Y, Itoh M *et al.* Gab-family adapter proteins act downstream of cytokine and growth factor receptors and T- and B-cell antigen receptors. *Blood*, 93(6), 1809-1816 (1999).
- 145. Hirano T, Ishihara K, Hibi M. Roles of STAT3 in mediating the cell growth, differentiation and survival signals relayed through the IL-6 family of cytokine receptors. *Oncogene*, 19(21), 2548-2556 (2000).
- 146. Shirogane T, Fukada T, Muller JM, Shima DT, Hibi M, Hirano T. Synergistic roles for Pim-1 and c-Myc in STAT3-mediated cell cycle progression and antiapoptosis. *Immunity*, 11(6), 709-719 (1999).
- 147. Zushi S, Shinomura Y, Kiyohara T *et al.* STAT3 mediates the survival signal in oncogenic ras-transfected intestinal epithelial cells. *Int J Cancer*, 78(3), 326-330 (1998).
- 148. Rahaman SO, Harbor PC, Chernova O, Barnett GH, Vogelbaum MA, Haque SJ. Inhibition of constitutively active Stat3 suppresses proliferation and induces apoptosis in glioblastoma multiforme cells. *Oncogene*, 21(55), 8404-8413 (2002).
- 149. Diehl SA, Schmidlin H, Nagasawa M *et al.* STAT3-mediated up-regulation of BLIMP1 Is coordinated with BCL6 down-regulation to control human plasma cell differentiation. *J Immunol*, 180(7), 4805-4815 (2008).
- 150. Saeland S, Duvert V, Moreau I, Banchereau J. Human B cell precursors proliferate and express CD23 after CD40 ligation. *J Exp Med*, 178(1), 113-120 (1993).

- 151. Levy Y, Brouet JC. Interleukin-10 prevents spontaneous death of germinal center B cells by induction of the bcl-2 protein. *J Clin Invest*, 93(1), 424-428 (1994).
- 152. Rousset F, Peyrol S, Garcia E *et al.* Long-term cultured CD40-activated B lymphocytes differentiate into plasma cells in response to IL-10 but not IL-4. *Int Immunol*, 7(8), 1243-1253 (1995).
- 153. Merville P, Dechanet J, Grouard G, Durand I, Banchereau J. T cell-induced B cell blasts differentiate into plasma cells when cultured on bone marrow stroma with IL-3 and IL-10. *Int Immunol*, 7(4), 635-643 (1995).
- 154. Choe J, Choi YS. IL-10 interrupts memory B cell expansion in the germinal center by inducing differentiation into plasma cells. *Eur J Immunol*, 28(2), 508-515 (1998).
- 155. Moore KW, de Waal Malefyt R, Coffman RL, O'Garra A. Interleukin-10 and the interleukin-10 receptor. *Annu Rev Immunol*, 19, 683-765 (2001).
- 156. Ho AS, Wei SH, Mui AL, Miyajima A, Moore KW. Functional regions of the mouse interleukin-10 receptor cytoplasmic domain. *Mol Cell Biol*, 15(9), 5043-5053 (1995).
- 157. Wehinger J, Gouilleux F, Groner B, Finke J, Mertelsmann R, Weber-Nordt RM. IL-10 induces DNA binding activity of three STAT proteins (Stat1, Stat3, and Stat5) and their distinct combinatorial assembly in the promoters of selected genes. *FEBS Lett*, 394(3), 365-370 (1996).
- 158. Lai CF, Ripperger J, Morella KK *et al.* Receptors for interleukin (IL)-10 and IL-6-type cytokines use similar signaling mechanisms for inducing transcription through IL-6 response elements. *J Biol Chem*, 271(24), 13968-13975 (1996).
- 159. Bonig H, Korholz D, Pafferath B, Mauz-Korholz C, Burdach S. Interleukin 10 induced c-fos expression in human B cells by activation of divergent protein kinases. *Immunol Invest*, 25(1-2), 115-128 (1996).
- 160. Itoh K, Hirohata S. The role of IL-10 in human B cell activation, proliferation, and differentiation. *J Immunol*, 154(9), 4341-4350 (1995).

- 161. Avery DT, Deenick EK, Ma CS *et al.* B cell-intrinsic signaling through IL-21 receptor and STAT3 is required for establishing long-lived antibody responses in humans. *J Exp Med*, 207(1), 155-171 (2010).
- 162. Gaoni Y, Mechoulam R. Isoaltion, structure, and partial synthesis of an active constituent of harnish. *Journal of the American Chemical Society*, 86, 1646-1647 (1964).
- 163. Turner CE, Elsohly MA, Boeren EG. Constituents of Cannabis sativa L. XVII. A review of the natural constituents. *J Nat Prod*, 43(2), 169-234 (1980).
- 164. De Petrocellis L, Di Marzo V. An introduction to the endocannabinoid system: from the early to the latest concepts. *Best Pract Res Clin Endocrinol Metab*, 23(1), 1-15 (2009).
- 165. Pertwee RG, Howlett AC, Abood ME *et al.* International Union of Basic and Clinical Pharmacology. LXXIX. Cannabinoid receptors and their ligands: beyond CB and CB. *Pharmacol Rev*, 62(4), 588-631 (2010).
- 166. Guzman M. Cannabinoids: potential anticancer agents. *Nat Rev Cancer*, 3(10), 745-755 (2003).
- 167. Musto DF. The Marihuana Tax Act of 1937. *Arch Gen Psychiatry*, 26(2), 101-108 (1972).
- 168. UNODC. World Drug Report 2012. (Ed.^(Eds) (United Nations publication, Sales No. E.12.XI.1, 2012)
- 169. Klein TW. Cannabinoid-based drugs as anti-inflammatory therapeutics. *Nat Rev Immunol*, 5(5), 400-411 (2005).
- 170. NIDA. Marijuana-An Update from the National Institute on Drug Abuse. Services, USDoHaH (Ed.^(Eds) (Public Information and Liaison Branch, 2011)
- 171. Karschner EL, Darwin WD, Goodwin RS, Wright S, Huestis MA. Plasma cannabinoid pharmacokinetics following controlled oral delta9-

- tetrahydrocannabinol and oromucosal cannabis extract administration. *Clin Chem*, 57(1), 66-75 (2011).
- 172. Matsuda LA, Lolait SJ, Brownstein MJ, Young AC, Bonner TI. Structure of a cannabinoid receptor and functional expression of the cloned cDNA. *Nature*, 346(6284), 561-564 (1990).
- 173. Munro S, Thomas KL, Abu-Shaar M. Molecular characterization of a peripheral receptor for cannabinoids. *Nature*, 365(6441), 61-65 (1993).
- 174. Stella N. Cannabinoid and cannabinoid-like receptors in microglia, astrocytes, and astrocytomas. *Glia*, 58(9), 1017-1030 (2010).
- 175. Pertwee RG, Howlett AC, Abood ME *et al.* International Union of Basic and Clinical Pharmacology. LXXIX. Cannabinoid receptors and their ligands: beyond CB(1) and CB(2). *Pharmacol Rev*, 62(4), 588-631).
- 176. Shire D, Calandra B, Bouaboula M *et al.* Cannabinoid receptor interactions with the antagonists SR 141716A and SR 144528. *Life Sci*, 65(6-7), 627-635 (1999).
- 177. Brown SM, Wager-Miller J, Mackie K. Cloning and molecular characterization of the rat CB2 cannabinoid receptor. *Biochim Biophys Acta*, 1576(3), 255-264 (2002).
- 178. Chakrabarti A, Onaivi ES, Chaudhuri G. Cloning and sequencing of a cDNA encoding the mouse brain-type cannabinoid receptor protein. *DNA Seg*, 5(6), 385-388 (1995).
- 179. Shire D, Calandra B, Rinaldi-Carmona M *et al.* Molecular cloning, expression and function of the murine CB2 peripheral cannabinoid receptor. *Biochim Biophys Acta*, 1307(2), 132-136 (1996).
- 180. Galiegue S, Mary S, Marchand J *et al.* Expression of central and peripheral cannabinoid receptors in human immune tissues and leukocyte subpopulations. *Eur J Biochem*, 232(1), 54-61 (1995).
- 181. Herkenham M, Lynn AB, Little MD *et al.* Cannabinoid receptor localization in brain. *Proc Natl Acad Sci U S A*, 87(5), 1932-1936 (1990).

- 182. Miller LK, Devi LA. The highs and lows of cannabinoid receptor expression in disease: mechanisms and their therapeutic implications. *Pharmacol Rev*, 63(3), 461-470 (2012).
- 183. Borner C, Hollt V, Kraus J. Activation of human T cells induces upregulation of cannabinoid receptor type 1 transcription. *Neuroimmunomodulation*, 14(6), 281-286 (2007).
- 184. Wang D, Wang H, Ning W, Backlund MG, Dey SK, DuBois RN. Loss of cannabinoid receptor 1 accelerates intestinal tumor growth. *Cancer Res*, 68(15), 6468-6476 (2008).
- 185. Wright K, Rooney N, Feeney M *et al.* Differential expression of cannabinoid receptors in the human colon: cannabinoids promote epithelial wound healing. *Gastroenterology*, 129(2), 437-453 (2005).
- 186. Nong L, Newton C, Cheng Q, Friedman H, Roth MD, Klein TW. Altered cannabinoid receptor mRNA expression in peripheral blood mononuclear cells from marijuana smokers. *J Neuroimmunol*, 127(1-2), 169-176 (2002).
- 187. Zhang PW, Ishiguro H, Ohtsuki T *et al.* Human cannabinoid receptor 1: 5' exons, candidate regulatory regions, polymorphisms, haplotypes and association with polysubstance abuse. *Mol Psychiatry*, 9(10), 916-931 (2004).
- Ryberg E, Vu HK, Larsson N et al. Identification and characterisation of a novel splice variant of the human CB1 receptor. FEBS Lett, 579(1), 259-264 (2005).
- 189. Comings DE, Muhleman D, Gade R *et al.* Cannabinoid receptor gene (CNR1): association with i.v. drug use. *Mol Psychiatry*, 2(2), 161-168 (1997).
- 190. Karsak M, Malkin I, Toliat MR *et al.* The cannabinoid receptor type 2 (CNR2) gene is associated with hand bone strength phenotypes in an ethnically homogeneous family sample. *Hum Genet*, 126(5), 629-636 (2009).

- 191. Karsak M, Cohen-Solal M, Freudenberg J *et al.* Cannabinoid receptor type 2 gene is associated with human osteoporosis. *Hum Mol Genet*, 14(22), 3389-3396 (2005).
- 192. Sipe JC, Arbour N, Gerber A, Beutler E. Reduced endocannabinoid immune modulation by a common cannabinoid 2 (CB2) receptor gene polymorphism: possible risk for autoimmune disorders. *J Leukoc Biol*, 78(1), 231-238 (2005).
- 193. Bayewitch M, Avidor-Reiss T, Levy R, Barg J, Mechoulam R, Vogel Z. The peripheral cannabinoid receptor: adenylate cyclase inhibition and G protein coupling. *FEBS Lett*, 375(1-2), 143-147 (1995).
- 194. Slipetz DM, O'Neill GP, Favreau L *et al.* Activation of the human peripheral cannabinoid receptor results in inhibition of adenylyl cyclase. *Mol Pharmacol*, 48(2), 352-361 (1995).
- 195. Howlett AC, Qualy JM, Khachatrian LL. Involvement of Gi in the inhibition of adenylate cyclase by cannabimimetic drugs. *Mol Pharmacol*, 29(3), 307-313 (1986).
- 196. Felder CC, Briley EM, Axelrod J, Simpson JT, Mackie K, Devane WA. Anandamide, an endogenous cannabimimetic eicosanoid, binds to the cloned human cannabinoid receptor and stimulates receptor-mediated signal transduction. *Proc Natl Acad Sci U S A*, 90(16), 7656-7660 (1993).
- 197. Hillard CJ, Manna S, Greenberg MJ et al. Synthesis and characterization of potent and selective agonists of the neuronal cannabinoid receptor (CB1). J Pharmacol Exp Ther, 289(3), 1427-1433 (1999).
- 198. Howlett AC, Fleming RM. Cannabinoid inhibition of adenylate cyclase. Pharmacology of the response in neuroblastoma cell membranes. *Mol Pharmacol*, 26(3), 532-538 (1984).
- 199. Bidaut-Russell M, Devane WA, Howlett AC. Cannabinoid receptors and modulation of cyclic AMP accumulation in the rat brain. *J Neurochem*, 55(1), 21-26 (1990).

- 200. Childers SR, Sexton T, Roy MB. Effects of anandamide on cannabinoid receptors in rat brain membranes. *Biochem Pharmacol*, 47(4), 711-715 (1994).
- 201. Wade MR, Tzavara ET, Nomikos GG. Cannabinoids reduce cAMP levels in the striatum of freely moving rats: an in vivo microdialysis study. *Brain Res*, 1005(1-2), 117-123 (2004).
- 202. Glass M, Felder CC. Concurrent stimulation of cannabinoid CB1 and dopamine D2 receptors augments cAMP accumulation in striatal neurons: evidence for a Gs linkage to the CB1 receptor. *J Neurosci*, 17(14), 5327-5333 (1997).
- 203. Calandra B, Portier M, Kerneis A *et al.* Dual intracellular signaling pathways mediated by the human cannabinoid CB1 receptor. *Eur J Pharmacol*, 374(3), 445-455 (1999).
- 204. Bonhaus DW, Chang LK, Kwan J, Martin GR. Dual activation and inhibition of adenylyl cyclase by cannabinoid receptor agonists: evidence for agonist-specific trafficking of intracellular responses. *J Pharmacol Exp Ther*, 287(3), 884-888 (1998).
- 205. Busch L, Sterin-Borda L, Borda E. Expression and biological effects of CB1 cannabinoid receptor in rat parotid gland. *Biochem Pharmacol*, 68(9), 1767-1774 (2004).
- 206. Felder CC, Joyce KE, Briley EM *et al.* LY320135, a novel cannabinoid CB1 receptor antagonist, unmasks coupling of the CB1 receptor to stimulation of cAMP accumulation. *J Pharmacol Exp Ther*, 284(1), 291-297 (1998).
- 207. Maneuf YP, Brotchie JM. Paradoxical action of the cannabinoid WIN 55,212-2 in stimulated and basal cyclic AMP accumulation in rat globus pallidus slices. *Br J Pharmacol*, 120(8), 1397-1398 (1997).
- 208. Rhee MH, Bayewitch M, Avidor-Reiss T, Levy R, Vogel Z. Cannabinoid receptor activation differentially regulates the various adenylyl cyclase isozymes. *J Neurochem*, 71(4), 1525-1534 (1998).

- Bouaboula M, Poinot-Chazel C, Bourrie B et al. Activation of mitogenactivated protein kinases by stimulation of the central cannabinoid receptor CB1. Biochem J, 312 (Pt 2), 637-641 (1995).
- 210. Bouaboula M, Poinot-Chazel C, Marchand J *et al.* Signaling pathway associated with stimulation of CB2 peripheral cannabinoid receptor. Involvement of both mitogen-activated protein kinase and induction of Krox-24 expression. *Eur J Biochem*, 237(3), 704-711 (1996).
- 211. Kobayashi Y, Arai S, Waku K, Sugiura T. Activation by 2-arachidonoylglycerol, an endogenous cannabinoid receptor ligand, of p42/44 mitogen-activated protein kinase in HL-60 cells. *J Biochem*, 129(5), 665-669 (2001).
- 212. Sanchez MG, Ruiz-Llorente L, Sanchez AM, Diaz-Laviada I. Activation of phosphoinositide 3-kinase/PKB pathway by CB(1) and CB(2) cannabinoid receptors expressed in prostate PC-3 cells. Involvement in Raf-1 stimulation and NGF induction. *Cell Signal*, 15(9), 851-859 (2003).
- 213. Faubert Kaplan BL, Kaminski NE. Cannabinoids inhibit the activation of ERK MAPK in PMA/lo-stimulated mouse splenocytes. *Int Immunopharmacol*, 3(10-11), 1503-1510 (2003).
- 214. Gomez del Pulgar T, Velasco G, Guzman M. The CB1 cannabinoid receptor is coupled to the activation of protein kinase B/Akt. *Biochem J*, 347(Pt 2), 369-373 (2000).
- 215. Galve-Roperh I, Rueda D, Gomez del Pulgar T, Velasco G, Guzman M. Mechanism of extracellular signal-regulated kinase activation by the CB(1) cannabinoid receptor. *Mol Pharmacol*, 62(6), 1385-1392 (2002).
- 216. Melck D, Rueda D, Galve-Roperh I, De Petrocellis L, Guzman M, Di Marzo V. Involvement of the cAMP/protein kinase A pathway and of mitogen-activated protein kinase in the anti-proliferative effects of anandamide in human breast cancer cells. FEBS Lett, 463(3), 235-240 (1999).
- 217. Davis MI, Ronesi J, Lovinger DM. A predominant role for inhibition of the adenylate cyclase/protein kinase A pathway in ERK activation by cannabinoid receptor 1 in N1E-115 neuroblastoma cells. *J Biol Chem*, 278(49), 48973-48980 (2003).

- 218. Derkinderen P, Valjent E, Toutant M *et al.* Regulation of extracellular signal-regulated kinase by cannabinoids in hippocampus. *J Neurosci*, 23(6), 2371-2382 (2003).
- 219. Mackie K, Hille B. Cannabinoids inhibit N-type calcium channels in neuroblastoma-glioma cells. *Proc Natl Acad Sci U S A*, 89(9), 3825-3829 (1992).
- 220. Mackie K, Devane WA, Hille B. Anandamide, an endogenous cannabinoid, inhibits calcium currents as a partial agonist in N18 neuroblastoma cells. *Mol Pharmacol*, 44(3), 498-503 (1993).
- 221. Pan X, Ikeda SR, Lewis DL. Rat brain cannabinoid receptor modulates N-type Ca2+ channels in a neuronal expression system. *Mol Pharmacol*, 49(4), 707-714 (1996).
- 222. Wilson RI, Kunos G, Nicoll RA. Presynaptic specificity of endocannabinoid signaling in the hippocampus. *Neuron*, 31(3), 453-462 (2001).
- 223. Mackie K, Lai Y, Westenbroek R, Mitchell R. Cannabinoids activate an inwardly rectifying potassium conductance and inhibit Q-type calcium currents in AtT20 cells transfected with rat brain cannabinoid receptor. *J Neurosci*, 15(10), 6552-6561 (1995).
- 224. Hampson AJ, Bornheim LM, Scanziani M *et al.* Dual effects of anandamide on NMDA receptor-mediated responses and neurotransmission. *J Neurochem*, 70(2), 671-676 (1998).
- 225. Gebremedhin D, Lange AR, Campbell WB, Hillard CJ, Harder DR. Cannabinoid CB1 receptor of cat cerebral arterial muscle functions to inhibit L-type Ca2+ channel current. *Am J Physiol*, 276(6 Pt 2), H2085-2093 (1999).
- 226. Straiker A, Stella N, Piomelli D, Mackie K, Karten HJ, Maguire G. Cannabinoid CB1 receptors and ligands in vertebrate retina: localization and function of an endogenous signaling system. *Proc Natl Acad Sci U S A*, 96(25), 14565-14570 (1999).
- 227. Schweitzer P. Cannabinoids decrease the K(+) M-current in hippocampal CA1 neurons. *J Neurosci*, 20(1), 51-58 (2000).

- 228. Deadwyler SA, Hampson RE, Mu J, Whyte A, Childers S. Cannabinoids modulate voltage sensitive potassium A-current in hippocampal neurons via a cAMP-dependent process. *J Pharmacol Exp Ther*, 273(2), 734-743 (1995).
- 229. McAllister SD, Griffin G, Satin LS, Abood ME. Cannabinoid receptors can activate and inhibit G protein-coupled inwardly rectifying potassium channels in a xenopus oocyte expression system. *J Pharmacol Exp Ther*, 291(2), 618-626 (1999).
- 230. Vasquez C, Navarro-Polanco RA, Huerta M *et al.* Effects of cannabinoids on endogenous K+ and Ca2+ currents in HEK293 cells. *Can J Physiol Pharmacol*, 81(5), 436-442 (2003).
- 231. Felder CC, Joyce KE, Briley EM *et al.* Comparison of the pharmacology and signal transduction of the human cannabinoid CB1 and CB2 receptors. *Mol Pharmacol*, 48(3), 443-450 (1995).
- 232. Sugiura T, Kodaka T, Kondo S *et al.* 2-Arachidonoylglycerol, a putative endogenous cannabinoid receptor ligand, induces rapid, transient elevation of intracellular free Ca2+ in neuroblastoma x glioma hybrid NG108-15 cells. *Biochem Biophys Res Commun*, 229(1), 58-64 (1996).
- 233. Venance L, Sagan S, Giaume C. (R)-methanandamide inhibits receptor-induced calcium responses by depleting internal calcium stores in cultured astrocytes. *Pflugers Arch*, 434(1), 147-149 (1997).
- 234. Fimiani C, Mattocks D, Cavani F *et al.* Morphine and anandamide stimulate intracellular calcium transients in human arterial endothelial cells: coupling to nitric oxide release. *Cell Signal*, 11(3), 189-193 (1999).
- 235. Chou KJ, Tseng LL, Cheng JS *et al.* CP55,940 increases intracellular Ca2+ levels in Madin-Darby canine kidney cells. *Life Sci*, 69(13), 1541-1548 (2001).
- 236. Filipeanu CM, de Zeeuw D, Nelemans SA. Delta9-tetrahydrocannabinol activates [Ca2+]i increases partly sensitive to capacitative store refilling. *Eur J Pharmacol*, 336(1), R1-3 (1997).

- 237. Zoratti C, Kipmen-Korgun D, Osibow K, Malli R, Graier WF. Anandamide initiates Ca(2+) signaling via CB2 receptor linked to phospholipase C in calf pulmonary endothelial cells. *Br J Pharmacol*, 140(8), 1351-1362 (2003).
- 238. Sugiura T, Kondo S, Kishimoto S et al. Evidence that 2arachidonoylglycerol but not N-palmitoylethanolamine or anandamide is the physiological ligand for the cannabinoid CB2 receptor. Comparison of the agonistic activities of various cannabinoid receptor ligands in HL-60 cells. J Biol Chem, 275(1), 605-612 (2000).
- 239. Rao GK, Kaminski NE. Cannabinoid-mediated elevation of intracellular calcium: a structure-activity relationship. *J Pharmacol Exp Ther*, 317(2), 820-829 (2006).
- 240. Rao GK, Zhang W, Kaminski NE. Cannabinoid receptor-mediated regulation of intracellular calcium by delta(9)-tetrahydrocannabinol in resting T cells. *J Leukoc Biol*, 75(5), 884-892 (2004).
- 241. Grotenhermen F. Pharmacokinetics and pharmacodynamics of cannabinoids. *Clin Pharmacokinet*, 42(4), 327-360 (2003).
- 242. Huestis MA, Henningfield JE, Cone EJ. Blood cannabinoids. I. Absorption of THC and formation of 11-OH-THC and THCCOOH during and after smoking marijuana. *J Anal Toxicol*, 16(5), 276-282 (1992).
- 243. Kelly P, Jones RT. Metabolism of tetrahydrocannabinol in frequent and infrequent marijuana users. *J Anal Toxicol*, 16(4), 228-235 (1992).
- 244. Wall ME, Sadler BM, Brine D, Taylor H, Perez-Reyes M. Metabolism, disposition, and kinetics of delta-9-tetrahydrocannabinol in men and women. Clin Pharmacol Ther, 34(3), 352-363 (1983).
- 245. Blackard C, Tennes K. Human placental transfer of cannabinoids. *N Engl J Med*, 311(12), 797 (1984).
- 246. Perez-Reyes M, Wall ME. Presence of delta9-tetrahydrocannabinol in human milk. *N Engl J Med*, 307(13), 819-820 (1982).

- 247. Matsunaga T, Iwawaki Y, Watanabe K, Yamamoto I, Kageyama T, Yoshimura H. Metabolism of delta 9-tetrahydrocannabinol by cytochrome P450 isozymes purified from hepatic microsomes of monkeys. *Life Sci*, 56(23-24), 2089-2095 (1995).
- 248. Narimatsu S, Watanabe K, Matsunaga T *et al.* Cytochrome P-450 isozymes involved in the oxidative metabolism of delta 9-tetrahydrocannabinol by liver microsomes of adult female rats. *Drug Metab Dispos*, 20(1), 79-83 (1992).
- 249. Watanabe K, Matsunaga T, Yamamoto I, Funae Y, Yoshimura H. Involvement of CYP2C in the metabolism of cannabinoids by human hepatic microsomes from an old woman. *Biol Pharm Bull*, 18(8), 1138-1141 (1995).
- 250. Burstein SH. The cannabinoid acids: nonpsychoactive derivatives with therapeutic potential. *Pharmacol Ther*, 82(1), 87-96 (1999).
- 251. Perez-Reyes M, Timmons MC, Lipton MA, Davis KH, Wall ME. Intravenous injection in man of 9 -tetrahydrocannabinol and 11-OH- 9 -tetrahydrocannabinol. *Science*, 177(4049), 633-635 (1972).
- 252. Hunt CA, Jones RT. Tolerance and disposition of tetrahydrocannabinol in man. *J Pharmacol Exp Ther*, 215(1), 35-44 (1980).
- 253. Alburges ME, Peat MA. Profiles of delta 9-tetrahydrocannabinol metabolites in urine of marijuana users: preliminary observations by high performance liquid chromatography-radioimmunoassay. *J Forensic Sci*, 31(2), 695-706 (1986).
- 254. Manno JE, Manno BR, Kemp PM *et al.* Temporal indication of marijuana use can be estimated from plasma and urine concentrations of delta9-tetrahydrocannabinol, 11-hydroxy-delta9-tetrahydrocannabinol, and 11-nor-delta9-tetrahydrocannabinol-9-carboxylic acid. *J Anal Toxicol*, 25(7), 538-549 (2001).
- 255. Williams PL, Moffat AC. Identification in human urine of delta 9-tetrahydrocannabinol-11-oic acid glucuronide: a tetrahydrocannabinol metabolite. *J Pharm Pharmacol*, 32(7), 445-448 (1980).

- 256. Pertwee RG. Pharmacology of cannabinoid receptor ligands. *Curr Med Chem*, 6(8), 635-664 (1999).
- 257. Pertwee RG. The diverse CB1 and CB2 receptor pharmacology of three plant cannabinoids: delta9-tetrahydrocannabinol, cannabidiol and delta9-tetrahydrocannabivarin. *Br J Pharmacol*, 153(2), 199-215 (2008).
- 258. Acquas E, Pisanu A, Marrocu P, Goldberg SR, Di Chiara G. Delta9-tetrahydrocannabinol enhances cortical and hippocampal acetylcholine release in vivo: a microdialysis study. *Eur J Pharmacol*, 419(2-3), 155-161 (2001).
- 259. Nagai H, Egashira N, Sano K *et al.* Antipsychotics improve Delta9-tetrahydrocannabinol-induced impairment of the prepulse inhibition of the startle reflex in mice. *Pharmacol Biochem Behav*, 84(2), 330-336 (2006).
- 260. Pistis M, Ferraro L, Pira L *et al.* Delta(9)-tetrahydrocannabinol decreases extracellular GABA and increases extracellular glutamate and dopamine levels in the rat prefrontal cortex: an in vivo microdialysis study. *Brain Res*, 948(1-2), 155-158 (2002).
- Tanda G, Pontieri FE, Di Chiara G. Cannabinoid and heroin activation of mesolimbic dopamine transmission by a common mu1 opioid receptor mechanism. *Science*, 276(5321), 2048-2050 (1997).
- 262. Verrico CD, Jentsch JD, Dazzi L, Roth RH. Systemic, but not local, administration of cannabinoid CB1 receptor agonists modulate prefrontal cortical acetylcholine efflux in the rat. *Synapse*, 48(4), 178-183 (2003).
- 263. Maneuf YP, Crossman AR, Brotchie JM. Modulation of GABAergic transmission in the globus pallidus by the synthetic cannabinoid WIN 55,212-2. *Synapse*, 22(4), 382-385 (1996).
- 264. Little PJ, Compton DR, Johnson MR, Melvin LS, Martin BR. Pharmacology and stereoselectivity of structurally novel cannabinoids in mice. *J Pharmacol Exp Ther*, 247(3), 1046-1051 (1988).
- 265. Hampson RE, Deadwyler SA. Cannabinoids, hippocampal function and memory. *Life Sci*, 65(6-7), 715-723 (1999).

- 266. Heyser CJ, Hampson RE, Deadwyler SA. Effects of delta-9-tetrahydrocannabinol on delayed match to sample performance in rats: alterations in short-term memory associated with changes in task specific firing of hippocampal cells. *J Pharmacol Exp Ther*, 264(1), 294-307 (1993).
- Leirer VO, Yesavage JA, Morrow DG. Marijuana carry-over effects on aircraft pilot performance. Aviat Space Environ Med, 62(3), 221-227 (1991).
- 268. Hartman RL, Huestis MA. Cannabis Effects on Driving Skills. *Clin Chem*, (2012).
- 269. Hunault CC, Mensinga TT, Bocker KB *et al.* Cognitive and psychomotor effects in males after smoking a combination of tobacco and cannabis containing up to 69 mg delta-9-tetrahydrocannabinol (THC). *Psychopharmacology (Berl)*, 204(1), 85-94 (2009).
- Benowitz NL, Jones RT. Cardiovascular effects of prolonged delta-9tetrahydrocannabinol ingestion. *Clin Pharmacol Ther*, 18(3), 287-297 (1975).
- 271. Tashkin DP, Levisman JA, Abbasi AS, Shapiro BJ, Ellis NM. Short-term effects of smoked marihuana on left ventricular function in man. *Chest*, 72(1), 20-26 (1977).
- 272. Formukong EA, Evans AT, Evans FJ. The inhibitory effects of cannabinoids, the active constituents of Cannabis sativa L. on human and rabbit platelet aggregation. *J Pharm Pharmacol*, 41(10), 705-709 (1989).
- 273. Dewey WL. Cannabinoid pharmacology. *Pharmacol Rev*, 38(2), 151-178 (1986).
- 274. Asch RH, Smith CG. Effects of delta 9-THC, the principal psychoactive component of marijuana, during pregnancy in the rhesus monkey. *J Reprod Med*, 31(12), 1071-1081 (1986).
- 275. Darmani NA, Johnson JC. Central and peripheral mechanisms contribute to the antiemetic actions of delta-9-tetrahydrocannabinol against 5-

- hydroxytryptophan-induced emesis. *Eur J Pharmacol*, 488(1-3), 201-212 (2004).
- 276. Van Sickle MD, Oland LD, Mackie K, Davison JS, Sharkey KA. Delta9-tetrahydrocannabinol selectively acts on CB1 receptors in specific regions of dorsal vagal complex to inhibit emesis in ferrets. *Am J Physiol Gastrointest Liver Physiol*, 285(3), G566-576 (2003).
- 277. Shook JE, Burks TF. Psychoactive cannabinoids reduce gastrointestinal propulsion and motility in rodents. *J Pharmacol Exp Ther*, 249(2), 444-449 (1989).
- 278. Hinds NM, Ullrich K, Smid SD. Cannabinoid 1 (CB1) receptors coupled to cholinergic motorneurones inhibit neurogenic circular muscle contractility in the human colon. *Br J Pharmacol*, 148(2), 191-199 (2006).
- 279. McCallum RW, Soykan I, Sridhar KR, Ricci DA, Lange RC, Plankey MW. Delta-9-tetrahydrocannabinol delays the gastric emptying of solid food in humans: a double-blind, randomized study. *Aliment Pharmacol Ther*, 13(1), 77-80 (1999).
- 280. Thompson GR, Rosenkrantz H, Schaeppi UH, Braude MC. Comparison of acute oral toxicity of cannabinoids in rats, dogs and monkeys. *Toxicol Appl Pharmacol*, 25(3), 363-372 (1973).
- 281. Bachs L, Morland H. Acute cardiovascular fatalities following cannabis use. *Forensic Sci Int*, 124(2-3), 200-203 (2001).
- 282. Mittleman MA, Lewis RA, Maclure M, Sherwood JB, Muller JE. Triggering myocardial infarction by marijuana. *Circulation*, 103(23), 2805-2809 (2001).
- 283. Clark SC. Marihuana and the cardiovascular system. *Pharmacol Biochem Behav*, 3(2), 299-306 (1975).
- 284. Huestis MA. Cannabis (Marijuan) Effect in human behavior and performance. *Forensic Sci Rev*, 14(15), 15-60 (2002).

- 285. Pope HG, Jr., Gruber AJ, Hudson JI, Huestis MA, Yurgelun-Todd D. Cognitive measures in long-term cannabis users. *J Clin Pharmacol*, 42(11 Suppl), 41S-47S (2002).
- 286. Renault PF, Schuster CR, Heinrich R, Freeman DX. Marihuana: standardized smoke administration and dose effect curves on heart rate in humans. *Science*, 174(4009), 589-591 (1971).
- 287. Jones RT, Benowitz N, Bachman J. Clinical studies of cannabis tolerance and dependence. *Ann N Y Acad Sci*, 282, 221-239 (1976).
- 288. Buchweitz JP, Karmaus PW, Harkema JR, Williams KJ, Kaminski NE. Modulation of airway responses to influenza A/PR/8/34 by Delta9-tetrahydrocannabinol in C57BL/6 mice. *J Pharmacol Exp Ther*, 323(2), 675-683 (2007).
- 289. Arata S, Newton C, Klein T, Friedman H. Enhanced growth of Legionella pneumophila in tetrahydrocannabinol-treated macrophages. *Proc Soc Exp Biol Med*, 199(1), 65-67 (1992).
- 290. Klein TW, Newton CA, Nakachi N, Friedman H. Delta 9-tetrahydrocannabinol treatment suppresses immunity and early IFN-gamma, IL-12, and IL-12 receptor beta 2 responses to Legionella pneumophila infection. *J Immunol*, 164(12), 6461-6466 (2000).
- 291. Karmaus PW, Chen W, Kaplan BL, Kaminski NE. Delta9tetrahydrocannabinol suppresses cytotoxic T lymphocyte function independent of CB1 and CB 2, disrupting early activation events. *J Neuroimmune Pharmacol*, 7(4), 843-855 (2012).
- 292. Croxford JL, Yamamura T. Cannabinoids and the immune system: potential for the treatment of inflammatory diseases? *J Neuroimmunol*, 166(1-2), 3-18 (2005).
- 293. Lu T, Newton C, Perkins I, Friedman H, Klein TW. Cannabinoid treatment suppresses the T-helper cell-polarizing function of mouse dendritic cells stimulated with Legionella pneumophila infection. *J Pharmacol Exp Ther*, 319(1), 269-276 (2006).

- 294. Springs AE, Karmaus PW, Crawford RB, Kaplan BL, Kaminski NE. Effects of targeted deletion of cannabinoid receptors CB1 and CB2 on immune competence and sensitivity to immune modulation by Delta9-tetrahydrocannabinol. *J Leukoc Biol*, 84(6), 1574-1584 (2008).
- 295. Luo YD, Patel MK, Wiederhold MD, Ou DW. Effects of cannabinoids and cocaine on the mitogen-induced transformations of lymphocytes of human and mouse origins. *Int J Immunopharmacol*, 14(1), 49-56 (1992).
- 296. Pross SH, Nakano Y, McHugh S, Widen R, Klein TW, Friedman H. Contrasting effects of THC on adult murine lymph node and spleen cell populations stimulated with mitogen or anti-CD3 antibody. *Immunopharmacol Immunotoxicol*, 14(3), 675-687 (1992).
- 297. Pross SH, Nakano Y, Widen R *et al.* Differing effects of delta-9-tetrahydrocannabinol (THC) on murine spleen cell populations dependent upon stimulators. *Int J Immunopharmacol*, 14(6), 1019-1027 (1992).
- 298. Schatz AR, Koh WS, Kaminski NE. Delta 9-tetrahydrocannabinol selectively inhibits T-cell dependent humoral immune responses through direct inhibition of accessory T-cell function. *Immunopharmacology*, 26(2), 129-137 (1993).
- 299. Chen W, Kaplan BL, Pike ST *et al.* Magnitude of stimulation dictates the cannabinoid-mediated differential T cell response to HIVgp120. *J Leukoc Biol*, 92(5), 1093-1102 (2012).
- 300. Mosmann TR, Coffman RL. TH1 and TH2 cells: different patterns of lymphokine secretion lead to different functional properties. *Annu Rev Immunol*, 7, 145-173 (1989).
- 301. Massi P, Sacerdote P, Ponti W *et al.* Immune function alterations in mice tolerant to delta9-tetrahydrocannabinol: functional and biochemical parameters. *J Neuroimmunol*, 92(1-2), 60-66 (1998).
- 302. Yuan M, Kiertscher SM, Cheng Q, Zoumalan R, Tashkin DP, Roth MD. Delta 9-Tetrahydrocannabinol regulates Th1/Th2 cytokine balance in activated human T cells. *J Neuroimmunol*, 133(1-2), 124-131 (2002).

- Lu H, Kaplan BL, Ngaotepprutaram T, Kaminski NE. Suppression of T cell costimulator ICOS by Delta9-tetrahydrocannabinol. *J Leukoc Biol*, 85(2), 322-329 (2009).
- 304. Klein TW, Kawakami Y, Newton C, Friedman H. Marijuana components suppress induction and cytolytic function of murine cytotoxic T cells in vitro and in vivo. *J Toxicol Environ Health*, 32(4), 465-477 (1991).
- Fischer-Stenger K, Updegrove AW, Cabral GA. Delta 9tetrahydrocannabinol decreases cytotoxic T lymphocyte activity to herpes simplex virus type 1-infected cells. *Proc Soc Exp Biol Med*, 200(3), 422-430 (1992).
- 306. Karmaus PW, Chen W, Kaplan BL, Kaminski NE. Delta(9)-Tetrahydrocannabinol Suppresses Cytotoxic T Lymphocyte Function Independent of CB(1) and CB (2), Disrupting Early Activation Events. *J Neuroimmune Pharmacol*, 7(4), 843-855 (2012).
- 307. Schatz AR, Kessler FK, Kaminski NE. Inhibition of adenylate cyclase by delta 9-tetrahydrocannabinol in mouse spleen cells: a potential mechanism for cannabinoid-mediated immunosuppression. *Life Sci*, 51(6), PL25-30 (1992).
- 308. Borner C, Smida M, Hollt V, Schraven B, Kraus J. Cannabinoid receptor type 1- and 2-mediated increase in cyclic AMP inhibits T cell receptor-triggered signaling. *J Biol Chem*, 284(51), 35450-35460 (2009).
- 309. Kaplan BL, Rockwell CE, Kaminski NE. Evidence for cannabinoid receptor-dependent and -independent mechanisms of action in leukocytes. *J Pharmacol Exp Ther*, 306(3), 1077-1085 (2003).
- 310. Rao GK, Kaminski NE. Induction of intracellular calcium elevation by Delta9-tetrahydrocannabinol in T cells involves TRPC1 channels. *J Leukoc Biol*, 79(1), 202-213 (2006).
- 311. Herring AC, Kaminski NE. Cannabinol-mediated inhibition of nuclear factor-kappaB, cAMP response element-binding protein, and interleukin-2 secretion by activated thymocytes. *J Pharmacol Exp Ther*, 291(3), 1156-1163 (1999).

- 312. Klein TW, Newton CA, Widen R, Friedman H. The effect of delta-9-tetrahydrocannabinol and 11-hydroxy-delta-9-tetrahydrocannabinol on T-lymphocyte and B-lymphocyte mitogen responses. *J Immunopharmacol*, 7(4), 451-466 (1985).
- 313. Derocq JM, Segui M, Marchand J, Le Fur G, Casellas P. Cannabinoids enhance human B-cell growth at low nanomolar concentrations. *FEBS Lett*, 369(2-3), 177-182 (1995).
- 314. Carayon P, Marchand J, Dussossoy D *et al.* Modulation and functional involvement of CB2 peripheral cannabinoid receptors during B-cell differentiation. *Blood*, 92(10), 3605-3615 (1998).
- 315. Kaminski NE, Abood ME, Kessler FK, Martin BR, Schatz AR. Identification of a functionally relevant cannabinoid receptor on mouse spleen cells that is involved in cannabinoid-mediated immune modulation. *Mol Pharmacol*, 42(5), 736-742 (1992).
- 316. Rachelefsky GS, Opelz G, Mickey MR *et al.* Intact humoral and cell-mediated immunity in chronic marijuana smoking. *J Allergy Clin Immunol*, 58(4), 483-490 (1976).
- 317. Nahas GG, Osserman EF. Altered serum immunoglobulin concentration in chronic marijuana smokers. *Adv Exp Med Biol*, 288, 25-32 (1991).
- 318. El-Gohary M, Eid MA. Effect of cannabinoid ingestion (in the form of bhang) on the immune system of high school and university students. *Hum Exp Toxicol*, 23(3), 149-156 (2004).
- 319. Basu S, Ray A, Dittel BN. Cannabinoid receptor 2 is critical for the homing and retention of marginal zone B lineage cells and for efficient T-independent immune responses. *J Immunol*, 187(11), 5720-5732 (2011).
- 320. Lu H, Crawford RB, North CM, Kaplan BL, Kaminski NE. Establishment of an immunoglobulin m antibody-forming cell response model for characterizing immunotoxicity in primary human B cells. *Toxicol Sci*, 112(2), 363-373 (2009).

- 321. Livak KJ, Schmittgen TD. Analysis of relative gene expression data using real-time quantitative PCR and the 2(-Delta Delta C(T)) Method. *Methods*, 25(4), 402-408 (2001).
- 322. Condie R, Herring A, Koh WS, Lee M, Kaminski NE. Cannabinoid inhibition of adenylate cyclase-mediated signal transduction and interleukin 2 (IL-2) expression in the murine T-cell line, EL4.IL-2. *J Biol Chem*, 271(22), 13175-13183 (1996).
- 323. Lindgren H, Axcrona K, Leanderson T. Regulation of transcriptional activity of the murine CD40 ligand promoter in response to signals through TCR and the costimulatory molecules CD28 and CD2. *J Immunol*, 166(7), 4578-4585 (2001).
- 324. Roy M, Waldschmidt T, Aruffo A, Ledbetter JA, Noelle RJ. The regulation of the expression of gp39, the CD40 ligand, on normal and cloned CD4+ T cells. *J Immunol*, 151(5), 2497-2510 (1993).
- 325. Fuleihan R, Ramesh N, Horner A *et al.* Cyclosporin A inhibits CD40 ligand expression in T lymphocytes. *J Clin Invest*, 93(3), 1315-1320 (1994).
- 326. Ford GS, Barnhart B, Shone S, Covey LR. Regulation of CD154 (CD40 ligand) mRNA stability during T cell activation. *J Immunol*, 162(7), 4037-4044 (1999).
- 327. Nusslein HG, Frosch KH, Woith W, Lane P, Kalden JR, Manger B. Increase of intracellular calcium is the essential signal for the expression of CD40 ligand. *Eur J Immunol*, 26(4), 846-850 (1996).
- 328. Van den Eertwegh AJ, Noelle RJ, Roy M *et al.* In vivo CD40-gp39 interactions are essential for thymus-dependent humoral immunity. I. In vivo expression of CD40 ligand, cytokines, and antibody production delineates sites of cognate T-B cell interactions. *J Exp Med*, 178(5), 1555-1565 (1993).
- 329. Klaus SJ, Pinchuk LM, Ochs HD *et al.* Costimulation through CD28 enhances T cell-dependent B cell activation via CD40-CD40L interaction. *J Immunol*, 152(12), 5643-5652 (1994).

- 330. Vavassori S, Covey LR. Post-transcriptional regulation in lymphocytes: the case of CD154. *RNA Biol*, 6(3), 259-265 (2009).
- 331. Eldridge JC, Landfield PW. Cannabinoid interactions with glucocorticoid receptors in rat hippocampus. *Brain Res*, 534(1-2), 135-141 (1990).
- 332. Baschant U, Tuckermann J. The role of the glucocorticoid receptor in inflammation and immunity. *J Steroid Biochem Mol Biol*, 120(2-3), 69-75 (2010).
- 333. Ngaotepprutaram T, Kaplan BL, Crawford RB, Kaminski NE. Differential Modulation by Delta(9)-Tetrahydrocannabinol ((9)-THC) of CD40 Ligand (CD40L) Expression in Activated Mouse Splenic CD4(+) T cells. *J Neuroimmune Pharmacol*, 7(4), 969-980 (2012).
- 334. Schmitz ML, Bacher S, Dienz O. NF-kappaB activation pathways induced by T cell costimulation. *Faseb J*, 17(15), 2187-2193 (2003).
- 335. Ishikawa F, Nakano H, Seo A *et al.* Irradiation up-regulates CD80 expression through induction of tumour necrosis factor-alpha and CD40 ligand expression on B lymphoma cells. *Immunology*, 106(3), 354-362 (2002).
- 336. Niu H, Cattoretti G, Dalla-Favera R. BCL6 controls the expression of the B7-1/CD80 costimulatory receptor in germinal center B cells. *J Exp Med*, 198(2), 211-221 (2003).
- 337. Shapiro-Shelef M, Calame K. Regulation of plasma-cell development. *Nat Rev Immunol*, 5(3), 230-242 (2005).
- 338. Lu H, Crawford RB, Kaplan BL, Kaminski NE. 2,3,7,8-Tetrachlorodibenzo-p-dioxin-mediated disruption of the CD40 ligand-induced activation of primary human B cells. *Toxicol Appl Pharmacol*, 255(3), 251-260 (2011).
- Faris M, Kokot N, Stahl N, Nel AE. Involvement of Stat3 in interleukin-6induced IgM production in a human B-cell line. *Immunology*, 90(3), 350-357 (1997).

- 340. Lindstein T, June CH, Ledbetter JA, Stella G, Thompson CB. Regulation of lymphokine messenger RNA stability by a surface-mediated T cell activation pathway. *Science*, 244(4902), 339-343 (1989).
- 341. Vavassori S, Shi Y, Chen CC, Ron Y, Covey LR. In vivo post-transcriptional regulation of CD154 in mouse CD4+ T cells. *Eur J Immunol*, 39(8), 2224-2232 (2009).
- 342. Lobo FM, Zanjani R, Ho N, Chatila TA, Fuleihan RL. Calcium-dependent activation of TNF family gene expression by Ca2+/calmodulin kinase type IV/Gr and calcineurin. *J Immunol*, 162(4), 2057-2063 (1999).
- 343. Crist SA, Sprague DL, Ratliff TL. Nuclear factor of activated T cells (NFAT) mediates CD154 expression in megakaryocytes. *Blood*, 111(7), 3553-3561 (2008).
- 344. Lobo FM, Xu S, Lee C, Fuleihan RL. Transcriptional activity of the distal CD40 ligand promoter. *Biochem Biophys Res Commun*, 279(1), 245-250 (2000).
- 345. Kaldjian E, McCarthy SA, Sharrow SO, Littman DR, Klausner RD, Singer A. Nonequivalent effects of PKC activation by PMA on murine CD4 and CD8 cell-surface expression. *Faseb J*, 2(12), 2801-2806 (1988).
- 346. Martinez-Valdez H, Madrid-Marina V, Cohen A. Phorbol esters and cAMP differentially regulate the expression of CD4 and CD8 in human thymocytes. *BMC Immunol*, 3, 1 (2002).
- 347. Pelchen-Matthews A, Parsons IJ, Marsh M. Phorbol ester-induced downregulation of CD4 is a multistep process involving dissociation from p56lck, increased association with clathrin-coated pits, and altered endosomal sorting. *J Exp Med*, 178(4), 1209-1222 (1993).
- 348. Weyand CM, Goronzy J, Fathman CG. Modulation of CD4 by antigenic activation. *J Immunol*, 138(5), 1351-1354 (1987).
- 349. Pertwee RG. Receptors and channels targeted by synthetic cannabinoid receptor agonists and antagonists. *Curr Med Chem*, 17(14), 1360-1381 (2010).

- 350. Brown AJ. Novel cannabinoid receptors. *Br J Pharmacol*, 152(5), 567-575 (2007).
- 351. Makriyannis A, Tian X, Guo J. How lipophilic cannabinergic ligands reach their receptor sites. *Prostaglandins Other Lipid Mediat*, 77(1-4), 210-218 (2005).
- 352. Makriyannis A, Yang DP, Griffin RG, Das Gupta SK. The perturbation of model membranes by (-)-delta 9-tetrahydrocannabinol. Studies using solid-state 2H- and 13C-NMR. *Biochim Biophys Acta*, 1028(1), 31-42 (1990).
- 353. Tsytsykova AV, Tsitsikov EN, Geha RS. The CD40L promoter contains nuclear factor of activated T cells-binding motifs which require AP-1 binding for activation of transcription. *J Biol Chem*, 271(7), 3763-3770 (1996).
- 354. Faubert BL, Kaminski NE. AP-1 activity is negatively regulated by cannabinol through inhibition of its protein components, c-fos and c-jun. *J Leukoc Biol*, 67(2), 259-266 (2000).
- 355. Ouyang Y, Kaminski NE. Phospholipase A2 inhibitors p-bromophenacyl bromide and arachidonyl trifluoromethyl ketone suppressed interleukin-2 (IL-2) expression in murine primary splenocytes. *Arch Toxicol*, 73(1), 1-6 (1999).
- 356. Raman P, Kaplan BL, Kaminski NE. 15-Deoxy-Delta(1)(2),(1)(4)-prostaglandin J(2)-glycerol, a putative metabolite of 2-arachidonyl glycerol and a peroxisome proliferator-activated receptor gamma ligand, modulates nuclear factor of activated T cells. *J Pharmacol Exp Ther*, 342(3), 816-826 (2012).
- 357. Yea SS, Yang KH, Kaminski NE. Role of nuclear factor of activated T-cells and activator protein-1 in the inhibition of interleukin-2 gene transcription by cannabinol in EL4 T-cells. *J Pharmacol Exp Ther*, 292(2), 597-605 (2000).
- 358. Kaplan BL, Ouyang Y, Rockwell CE, Rao GK, Kaminski NE. 2-Arachidonoyl-glycerol suppresses interferon-gamma production in phorbol ester/ionomycin-activated mouse splenocytes independent of CB1 or CB2. *J Leukoc Biol*, 77(6), 966-974 (2005).

- 359. Yebra M, Klein TW, Friedman H. Delta 9-tetrahydrocannabinol suppresses concanavalin A induced increase in cytoplasmic free calcium in mouse thymocytes. *Life Sci*, 51(2), 151-160 (1992).
- 360. Lewis RS, Cahalan MD. Potassium and calcium channels in lymphocytes. *Annu Rev Immunol*, 13, 623-653 (1995).
- 361. Bartelt RR, Cruz-Orcutt N, Collins M, Houtman JC. Comparison of T cell receptor-induced proximal signaling and downstream functions in immortalized and primary T cells. *PLoS One*, 4(5), e5430 (2009).
- 362. Greenwald RJ, Freeman GJ, Sharpe AH. The B7 family revisited. *Annu Rev Immunol*, 23, 515-548 (2005).
- 363. Collins AV, Brodie DW, Gilbert RJ *et al.* The interaction properties of costimulatory molecules revisited. *Immunity*, 17(2), 201-210 (2002).
- 364. Good-Jacobson KL, Song E, Anderson S, Sharpe AH, Shlomchik MJ. CD80 expression on B cells regulates murine T follicular helper development, germinal center B cell survival, and plasma cell generation. *J Immunol*, 188(9), 4217-4225 (2012).
- 365. Corcoran K, Jabbour M, Bhagwandin C, Deymier MJ, Theisen DL, Lybarger L. Ubiquitin-mediated regulation of CD86 protein expression by the ubiquitin ligase membrane-associated RING-CH-1 (MARCH1). *J Biol Chem*, 286(43), 37168-37180).
- 366. Hodgkin PD, Lee JH, Lyons AB. B cell differentiation and isotype switching is related to division cycle number. *J Exp Med*, 184(1), 277-281 (1996).
- 367. Tangye SG, Avery DT, Hodgkin PD. A division-linked mechanism for the rapid generation of Ig-secreting cells from human memory B cells. *J Immunol*, 170(1), 261-269 (2003).
- 368. Rieder SA, Chauhan A, Singh U, Nagarkatti M, Nagarkatti P. Cannabinoid-induced apoptosis in immune cells as a pathway to immunosuppression. *Immunobiology*, 215(8), 598-605 (2009).

- 369. Otero DC, Poli V, David M, Rickert RC. Cutting edge: inherent and acquired resistance to radiation-induced apoptosis in B cells: a pivotal role for STAT3. *J Immunol*, 177(10), 6593-6597 (2006).
- 370. Lopez-Cabrera M, Munoz E, Blazquez MV, Ursa MA, Santis AG, Sanchez-Madrid F. Transcriptional regulation of the gene encoding the human C-type lectin leukocyte receptor AIM/CD69 and functional characterization of its tumor necrosis factor-alpha-responsive elements. *J Biol Chem*, 270(37), 21545-21551 (1995).
- 371. Zhao J, Freeman GJ, Gray GS, Nadler LM, Glimcher LH. A cell type-specific enhancer in the human B7.1 gene regulated by NF-kappaB. *J Exp Med*, 183(3), 777-789 (1996).
- 372. Zou GM, Hu WY. LIGHT regulates CD86 expression on dendritic cells through NF-kappaB, but not JNK/AP-1 signal transduction pathway. *J Cell Physiol*, 205(3), 437-443 (2005).
- 373. Newton CA, Chou PJ, Perkins I, Klein TW. CB(1) and CB(2) cannabinoid receptors mediate different aspects of delta-9-tetrahydrocannabinol (THC)-induced T helper cell shift following immune activation by Legionella pneumophila infection. *J Neuroimmune Pharmacol*, 4(1), 92-102 (2009).
- 374. Silberman DM, Ayelli-Edgar V, Zorrilla-Zubilete M, Zieher LM, Genaro AM. Impaired T-cell dependent humoral response and its relationship with T lymphocyte sensitivity to stress hormones in a chronic mild stress model of depression. *Brain Behav Immun*, 18(1), 81-90 (2004).
- 375. Wilckens T, De Rijk R. Glucocorticoids and immune function: unknown dimensions and new frontiers. *Immunol Today*, 18(9), 418-424 (1997).
- 376. Cho SJ, Kang CJ. A Stat5-overlapping site is critical for the IgJ enhancer activity in the plasma cells and bound by a ubiquitous protein. *Biochem Biophys Res Commun*, 338(4), 1897-1905 (2005).
- 377. Ishimoto T, Shimada M, Araya CE, Huskey J, Garin EH, Johnson RJ. Minimal change disease: a CD80 podocytopathy? *Semin Nephrol*, 31(4), 320-325 (2011).

- 378. Law CL, Grewal IS. Therapeutic interventions targeting CD40L (CD154) and CD40: the opportunities and challenges. *Adv Exp Med Biol*, 647, 8-36 (2009).
- 379. Ding BB, Yu JJ, Yu RY *et al.* Constitutively activated STAT3 promotes cell proliferation and survival in the activated B-cell subtype of diffuse large B-cell lymphomas. *Blood*, 111(3), 1515-1523 (2008).